Natural variation in heat tolerance of corals on the Great Barrier Reef

Thesis submitted by

Josephine Jacoba Valentin Nielsen

BSc (Hons1A)

April 2023

For the degree of Doctor of Philosophy in Marine Biology, within the College of Public Health, Medicine, and Veterinary Sciences, James Cook University, Townsville, Queensland, Australia

Acknowledgements

First and foremost, I wish to thank my supervisors Dr Line Bay (AIMS), Dr Ira Cooke (JCU), Dr Kate Quigley (Minderoo, JCU), Prof Jan Strugnell (JCU) and Prof David Suggett (KAUST) for enabling the project and entrusting me to complete it. I thank Prof David Suggett for taking such a large interest in the project despite only having met in person twice, both times in Cairns. Prof Jan Strugnell and Dr Kate Quigley for their continued guidance throughout the project. I am grateful to Dr Ira Cooke for his never-ending patience in guiding me through the bioinformatics and HPC aspects of my thesis, and I sincerely hope that I have not inflected permanent damage to the systems. Finally, I wish the acknowledge and thank Dr Line Bay for the important role she has played through most of my academic career, inspiring me to keep on going and thank her for her continued support.

I also wish to thank the Bay lab group and colleagues at the Australian Institute of Marine Science for embracing me for the duration of the project and longer. Without the exceptional assistance of Veronique Mocellin in the field, this thesis would not exist. Thanks also goes to Magena Marzonie, who has always been available for idea brainstorming, and has lent a patient ear to troubles and complaints for the last four years.

I wish to thank my parents for always supporting my curiosity as a child, enabled by countless visits to any and all aquariums we drove past, hours upon hours in the cold waters around Denmark, and the introduction to SCUBA diving. If not for their love and support, pursuing my dreams across the world would not have been feasible, and I am forever grateful to them and for their sacrifices to make this happen for me.

And finally, this thesis is a testament to the unwavering support I have received from my partner, Lee. Not only has he had to deal with the break-downs, the disappointments of failing experiments and sequencing outcomes one might expect during a PhD, along with acting the occasional research/experimental assistant and night-watch but he, and the rest of my family, has also dealt with the added emotional instability and general uncertainty that COVID-19 introduced into our lives. Not only with respect to project progression and timeline impacts of which there were a few, but more importantly with respect to the uncertainty and at times incomprehensible despair of border-closures, having to postpone our wedding, and not knowing when we got to see our families again.

"Shoot for the moon, even if you miss, you'll land among the stars." – Les Brown

Statement of the Contributions of Others

Nature of support	Contribution	Contributors (affiliation)
Intellectual support	Supervision	Line K Bay (AIMS) Ira R Cooke (JCU) David J Suggett (KAUST) Kate M. Quigley (Minderoo Foundation, JCU) Jan M Strugnell (JCU)
	Editorial assistance	Line K Bay (AIMS) Ira R Cooke (JCU) David J Suggett (KAUST) Kate M. Quigley (Minderoo Foundation, JCU) Jan M Strugnell (JCU) Christian R Voolstra (UKON) Magena R Marzonie (JCU) Hugo B Harrison (UOB) Samantha Goyen (AIMS)
	Methodological advice	Christian R Voolstra (UKON) Luke Thomas (AIMS) Lesa Peplow (AIMS) Magena R Marzonie (JCU) Sara Bell (AIMS) Samantha Goyen (AIMS)
	Statistical advice	Murray Logan (AIMS) Hugo B Harrison (UOB) Matthew Nitschke (AIMS)
Data collection	Fieldwork	Georgina Matthews Line Bay (AIMS) Kirsty Frith Darren Anderson Magena R Marzonie (JCU) Veronique Mocellin (AIMS) Johnston Davidson (AIMS) Alyssa Budd (JCU) Rebecca Forster (AIMS) AIMS LTMP team RV Solander RV Cape Fergusson
	Laboratory work	Georgina Matthews Romain Pry Rachael Collins Kirsty Frith Kate Slaughter Ebba Dahlstrøm Chloe Parish Sasha Faul
	Aquarium work	Lee Bastin (AIMS)

		AIMS National Sea Simulator and staff Andrea Severati (AIMS) Tom Barker (AIMS) Steven Green (AIMS) Justin Hochen (AIMS)
	Sequencing	Ramaciotti Centre for Genomics (UNSW) NovoGene (Hong Kong)
	Bioinformatics	SymPortal Ira R Cooke (JCU) Luke Thomas (AIMS)
	Logistical support	AIMS Stores Peter Davern† Pia Wimmer Veronique Mocellin
Financial support	Stipend and tuition fee	James Cook University Postgraduate Research Scholarship Australian Government
	Project infrastructure	AIMS AIMS@JCU JCU
	Research funding	AIMS AIMS@JCU PADI Foundation CPHMVS HDRES JCU Auguron
	Conference travel/attendance	AIMS@JCU AMSA-NQ CPHMVS HDRES JCU

Thesis title	Natural variation in heat tolerance and underlying genetic and physiological mechanisms of corals on the Great Barrier Reef		
Name of Candidate	Josephine Jacoba Valentin Nielsen		
Chapter No	Details of publication(s) on which the chapter is based	Nature and extent of the intellectual input of each author, including the candidate	I confirm the candidate's contribution to this paper and consent to the inclusion of the paper in the thesis
2	**Nielsen, JJV***., Matthews, G., Frith, KR., Harrison, HB., Marzonie, MR., Slaughter, KL., Suggett, DJ., & Bay, LK. (2022). Experimental considerations of acute heat stress assays to quantify coral thermal tolerance. *Scientific Reports*, *12*(16831), 1–13. https://doi.org/10.1038/s41598-022-20138-2	Authors JJVN, DJS, and LKB developed the research questions and experimental design. JJVN, GM, and LKB conducted the field work and experiments. JJVN, GM, KRF, and KS conducted the laboratory assays. KS and JJVN performed preliminary data visualisations. JJVN and HBH analysed the data with advice from DJS. JJVN produced the manuscript figures and tables. MM, HBH, LBK, JJVN, and DJS contributed to data interpretation. JJVN wrote the manuscript and all authors contributed to manuscript editing.	Name: Gina Matthews Signature Name: Kirsty R Frith Signature Name: Hugo B Harrison Signature Name: Magena R Marzonie Signature Name: Kate L Slaughter Signature Name: David J Suggett Signature Name: Line K Bay Signature

Research output related to PhD thesis

Peer-reviewed publications:

Nielsen, J. J. V., Matthews, G., Frith, K. R., Harrison, H. B., Marzonie, M. R., Slaughter, K. L., Suggett, D. J., & Bay, L. K. (2022). Experimental considerations of acute heat stress assays to quantify coral thermal tolerance. *Scientific Reports*, *12*(16831), 1–13. https://doi.org/10.1038/s41598-022-20138-2

Conference/workshop presentations:

(1) AIMS@JCU Student Seminar Day, Townsville, QLD, Dec 2nd 2022. "Large-scale patterns of thermal tolerance in two species of *Pocillopora* on the Great Barrier Reef", **JJV Nielsen***, KM Quigley, IR Cooke, JM Strugnell, DJ Suggett, & LK Bay.

(2) Australian Marine Science Association (AMSA), Cairns, Queensland, Australia, Aug 7th – 11th 2022. "Spatial distribution of Symbiodiniaceae communities across the Great Barrier Reef in two species of Pocilloporids." **JJV Nielsen***, KM Quigley, IR Cooke, JM Strugnell, DJ Suggett, & LK Bay.

(3) International Society for Coral Reef Studies (ICRS), Bremen, Germany, July 3rd – 8th 2022. "Effects of symbiont community and environmental history on acute heat tolerance in two common coral species across the Great Barrier Reef". **JJV Nielsen***, KM Quigley, IR Cooke, JM Strugnell, DJ Suggett & LK Bay.

(4) AIMS@JCU Student Seminar Day, Townsville, QLD, Nov 26th 2021 - "Reef-level threshold temperatures appear highly correlated to annual temperature variability", Poster, **JJV Nielsen***, E Dahlstroem, C Parish, KM Quigley, J Strugnell, I Cooke, DJ Suggett & LK Bay.

(5) Three Minute Thesis Competition, College of Public Health, Medicine, and Veterinary Sciences, James Cook University, Townsville, QLD, Sep 13th 2021. "Temperature variability impacts coral performance". **JJV Nielsen*.** University-Final Runner-Up. $500 research grant. JJVN_3MT_2021 (vimeo.com).

(6) International Society for Coral Reef Studies (ICRS), Bremen, Germany, July 23rd 2021. "Physiological correlates of coral thermal tolerance across latitudinal gradients on the Great Barrier Reef". **JJV Nielsen***, KM Quigley, IR Cooke, G Matthews, JM Strugnell, DJ Suggett & LK Bay.

(7) ECT-CAD program meeting, Australian Institute of Marine Science: "Travelling the Great Barrier Reef with SeaSim-in-a-Box; the evolution of acute heat stress assays in the field", Townsville, June 3rd 2021.

(8) Acute heat stress workshop, Australian Institute of Marine Science and James Cook University: "Developing and testing mobile acute heat stress assays on the Great Barrier Reef", Magnetic Island, QLD, Nov 26th 2020.

(9) Torres Strait Regional Authority meeting, Australian Institute of Marine Science: "Exploring the genetic variability of adaptation through the 1000 coral genome project", Townsville, QLD, March 13th 2020.

(10) Townsville Local Marine Advisory Committee meeting, Great Barrier Reef Marine Park Authority: "Exploring the genetic variability of adaptation through the 1000 coral genome project", Townsville, QLD, Feb 13th 2020.

Research output during Candidature

Peer-reviewed publications:

Nielsen, J. J. V., Kenkel, C. D., Bourne, D. G., Despringhere, L., Mocellin, V. J. L., & Bay, L. K. (2020). Physiological effects of heat and cold exposure in the common reef coral Acropora millepora. *Coral Reefs*, *39*(2), 259–269. https://doi.org/10.1007/s00338-019-01881-x

Marzonie, M. R., Bay, L. K., Bourne, D. G., Hoey, A. S., Matthews, S., **Nielsen, J. J. V**, & Harrison, H. B. (2022). *The effects of marine heatwaves on acute heat tolerance in corals*. *August*, 1–13. https://doi.org/10.1111/gcb.16473

Thesis Abstract

Coral reefs are threatened globally from anthropogenic climate change with current and future rates of warming driving catastrophic loss of coral reefs. This is highlighted by the increasing frequency and severity of mass bleaching-induced coral mortality. The Great Barrier Reef (GBR) has experienced three mass bleaching events in six years. Corals already live at or near their upper thermal tolerance limits and further temperature increases, both committed to already and projected, will require that corals either move or adapt to survive.

Bleaching thresholds have been used to quantify coral thermal tolerance and explore the capacity for thermal adaptation to warming. Typically, bleaching thresholds are resolved experimentally *ex situ* (in aquarium-based experiments) through quantification of visual and/or physiological traits or *in situ* via survival observations measured in the field during a "natural" bleaching event. However, such approaches are slow and laborious. Reef management under rapid environmental change requires urgent and deep knowledge of variation in thermal tolerance, thereby necessitating the development of fast, standardised, and highly scalable protocols. Designing systems, protocols, or assays with mobility would allow researchers to test bleaching thresholds and other proxies of temperature tolerance onboard research vessels, on islands, or in isolated mainland communities thus reaching areas that have previously been excluded or less studied due to logistical challenges. This thesis explored the utility of rapid heat stress assays (18-24 h) and examined ways in which this data can be scaled and standardised. Applying such rapid and standardised approaches widespread provides an opportunity for the coral research community to generate information quickly and share results across species and geographic scales to address the urgency of the climate change challenge.

Coral restoration and adaptation approaches are currently being investigated globally as mitigation strategies for the effects of global warming. Efforts such as assisted migration and assisted gene flow rely on thermally tolerant source populations and require baseline knowledge on the drivers of differential thermal tolerance within and between coral populations, potentially across expansive spatial scales. Locating tolerant populations requires a rapid tolerance metric coupled with an understanding of other critical components of coral thermal tolerance, like disturbance history and their endosymbiotic community composition. The rapid assays investigated here meet this accelerating global need for deep knowledge of coral thermal tolerance and how it varies within and between populations.

In **chapter 2**, I focused on testing the experimental approach and methodological framework of applying rapid, acute heat stress assays on corals from the GBR. I show that sampling time post heat stress was an important driver of observed heat stress responses and document the cost and sample processing time requirements associated with quantifying multiple physiological traits. Finally, photosynthetic performance was stable across both experimental design decisions (sampling time and fragment size), making this trait more robust as a metric to quantify acute coral heat tolerance across large spatial scales.

In **chapter 3**, I employed these standardised acute heat stress assays across the latitudinal extent of the GBR to document patterns of upper heat tolerance in key coral species. Of the three species examined, *Pocillopora verrucosa* was the most tolerant compared to *Pocillopora meandrina* and *Acropora tenuis* as measured by photosynthetic threshold temperatures (ED50) following acute heat stress. These differences were largely found at the reef sector-level, potentially driven by variation in thermal disturbance histories between sectors and inter-species differences in acute heat tolerance. Another explanation could be species-level differences in the dominant symbiont types harboured within *P. verrucosa* versus *P. meandrina.*

In **chapter 4**, I investigated the role of coral host gene expression in differential thermal tolerance within a single population of *A. tenuis*, exposed to an acute heat stress. I found high intra-population differences in acute heat tolerance (ED50 range = 0.94ºC) and differential physiological responses to heat stress in tissue colour change and photosynthetic efficiency. Interestingly, weighted gene co-expression network analysis (WGCNA) found two gene modules to be significantly associated with high acute heat tolerance (ED50) and nine genes were identified as potential gene expression markers of high heat tolerance. These results support the role of the coral genotype in holobiont thermal tolerance and provide a transcriptomic background to variability in coral thermal tolerance.

Overall, this thesis demonstrates the utility of applying rapid, experimental quantification of coral acute heat tolerance across large spatial scales. This approach allowed the identification of tolerant species and populations across the GBR and examined extrinsic (environment) and intrinsic (host genetics and symbionts) drivers of thermal tolerance. This thesis generated data relevant to reef management in multiple ways, including 1) by identifying reefs with high thermal tolerance for spatial protection; 2) by locating coral populations with high thermal tolerance to serve as brood and source stock for genetic management interventions such as

assisted gene flow and assisted migration and 3) by providing a measure of heat tolerance in populations which can be utilised to improve demographic and forecast modelling of coral persistence under future climate change scenarios. However, further exploration of the acute heat stress framework as well as determining the temporal stability of acute heat tolerance, is necessary to understand acute heat stress responses in relation to natural bleaching resistance.

Table of Contents

List of Figures

List of Tables

Chapter 1 General Introduction

1.1 Coral reefs and climate change

Coral reefs are some of the most diverse ecosystems on the planet, harbouring up to 25% of all described marine species (Knowlton, 2001; Thornton & Richardson, 2022). The reefs support nearly a billion people globally (Sing Wong et al., 2022) and in Australia alone contribute $6.4 billion annually to the economy (Costanza et al., 2014; Deloitte Access Economics, 2017). Global sea surface temperatures (SSTs) have increased by 0.65°C since 1880 (Lough et al., 2018) and unless there is immediate global action to completely eliminate greenhouse gas emissions, warming of a further 2°C is likely within this century (Raftery et al., 2017). However, climate change has placed coral reef ecosystems under threat globally with total reef area declining by 14% since 2009 (Souter et al., 2020). Continued warming will increase the severity of cyclones, the frequency and intensity of weather anomalies, heighten the deleterious effects of ocean acidification and, in general, make the climate more unpredictable (Crabbe, 2012; Hoegh-Guldberg et al., 2019). Increasing SSTs by 1.5°C will reduce global thermal refuges (areas likely to experience less impacts of climate change) on coral reefs to 0.2% of their overall area (Ashcroft, 2010; Osman et al., 2018), while 2°C of warming will effectively erode away thermal refuges (0% of coral reef pixels, Dixon et al., 2022).

1.2 Coral bleaching is a major threat under continued climate change

Corals are complex animals, living in symbiosis with a wide range of microorganisms and threatened by climate change. Corals associate with photosynthetic endosymbiotic dinoflagellates in the family Symbiodiniaceae (Abrego et al., 2008; Coles & Brown, 2003; Cunning et al., 2015). When temperature increases, the symbiosis between the coral host and Symbiodiniaceae is disrupted (Baker et al., 2008; Gates et al., 1992; Weis, 2008). As the density of symbiont cells decreases in the coral tissues, colour is lost, and corals appear white; this phenomenon is referred to as bleaching. While bleaching is a complex response to many stressors (Suggett & Smith, 2020), it is most commonly witnessed as the result of corals suffering thermal stress (Baker, 2001; Gates et al., 1992; Lirman et al., 2011). If the

perturbations which caused bleaching (for example thermal stress and/or solar irradiance) persist, the coral eventually dies (Suggett & Smith, 2011). As such, the mounting pressure from climate change on the persistence of coral reefs has prompted a need to understand the mechanistic underpinnings of coral resilience to environmental disturbances, and particularly to gradual and acute heat stress.

Bleaching is a global issue. Since 2003, 10% of all Caribbean reefs have experienced heat stress annually with that year identified as a tipping point (Muñiz-Castillo et al., 2019). Additionally, Kalmus et al., (2022) projects that as of 2021, 79% of coral reefs globally are likely to experience severe bleaching events at least once every five years with 91% of reefs to experience severe bleaching once every 10 years. As predicted by Hoegh-Guldberg, (1999) these observations support projections that reefs will continue to experience more frequent bleaching as thermal refuges decrease under continued climate change (Dixon et al., 2022; Kalmus et al., 2022; McManus et al., 2021). Severe thermal disturbances leading to widespread bleaching and subsequent coral mortality are now recognised as drivers of natural selection (Drury, 2020; Genevier et al., 2019). The Great Barrier Reef (GBR) has experienced three major bleaching events in just six years (2016/2017, 2020, and 2022, Fig 1.1). As evidenced by the 2016/17 events on the GBR, bleaching events are heterogenous in trajectory, intensity, duration, and spatial footprint. For example, in 2016/17, the southern sector of the GBR experienced relatively less heat stress while the northern sector recorded coral cover losses of upwards of 50.3%, resulting in a reef-wide coral decline of 30% (Hughes et al., 2017; Hughes et al., 2018). In contrast, during the 2020 event, the entire latitudinal extent of the GBR experienced bleaching to some level, indicating that the southern regions are not immune to thermal stress (Nolan et al., 2021; Page et al., 2023). These recurrent, extensive, and severe bleaching events pose a significant challenge to the persistence of coral reefs and corals will need to adapt to the oceans of the future either through natural processes or through active management approaches.

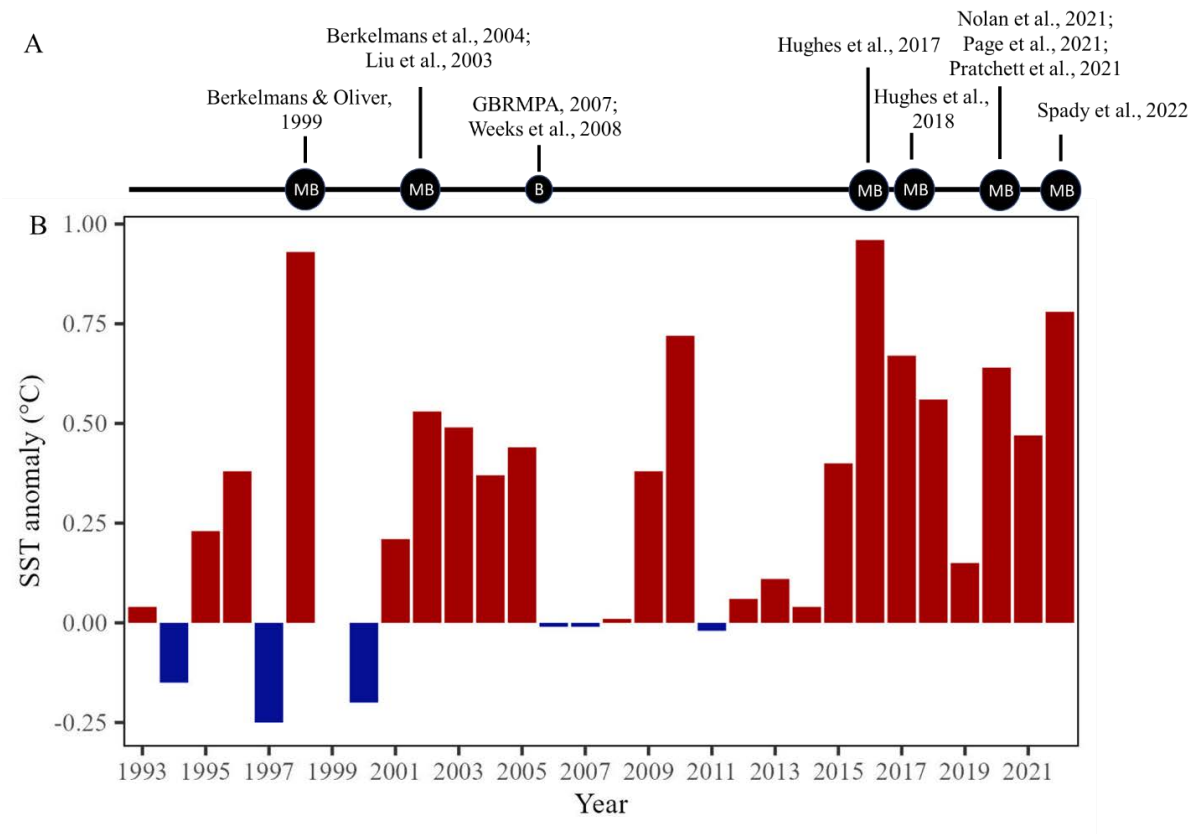

Figure 1.1 Timeline of bleaching events on the Great Barrier Reef since 1992. A) Mass bleaching events on record are denoted as "MB" in large black circles while local-scale bleaching events are noted as "B" in smaller black circles. References are associated with each bleaching event. B) SST anomalies on the GBR from 1992 to 2022 based on a 30-year climatology (1961-1990). Data obtained from the Australian Bureau of Meteorology and based on the NOAA ERSST v5 2°-2° grid data (Australian climate variability & change - Time series graphs (bom.gov.au)).

1.3 The capacity for genetic adaptation to increasing heat stress in corals

Genetic adaptation is required for current coral populations to persist under continued climate change (Bay et al., 2017; Rose et al., 2018). Adaptation works through selective pressures which alter the frequency of better-suited genotypes within populations across multiple generations. Therefore, to increase coral thermal tolerance by means of adaptation requires either genome mutations, genetic drift, and/or gene flow leading to increased standing genetic variation within populations (Pavlova et al., 2017; Petit & Excoffier, 2009; van Oppen et al., 2011). Corals can have high genetic diversity (Drury et al., 2016; Matias et al., 2022) and evidence from laboratory (Humanes et al., 2022; Quigley et al., 2020; Wright et al., 2019), field (Cooke et al., 2020; D'Angelo et al., 2015; Howells et al., 2011), and modelling studies (Matz

et al., 2020; McManus et al., 2021) have demonstrated that corals have some capacity to adapt to changing thermal environments and that this capacity is (partly) heritable (reviewed in Bairos-Novak et al., 2021; Howells et al., 2022). This heritable capacity for local adaptation is an important requirement for the development and implementation of new genetic conservation efforts (van Oppen et al., 2015; Voolstra et al., 2021a).

Due to the mounting pressure from climate change, coral reef managers are now looking beyond traditional conservation methods such as Marine Protected Areas (MPAs), restricted use zones, coral predator control, and steps to improve water quality (Mellin et al., 2019). On the GBR, several types of novel interventions are under investigation (Anthony et al., 2020; Boström-Einarsson et al., 2020; McLeod et al., 2022). Genetic interventions such as assisted gene flow, selective breeding and managed translocation of target individuals have been used successfully in terrestrial and aquatic management (Aitken & Bemmels, 2016; Aitken & Whitlock, 2013; Pavlova et al., 2017) and are now being applied on the GBR (McLeod et al., 2022; van Oppen & Quigley, 2022). However, these genetic conservation approaches all rely on understanding the adaptive potential along with the occurrence of thermally tolerant corals but the mechanisms of genetic adaptation in corals is not fully understood (Baums et al., 2022) and there is a lack of a full appreciation of the level and occurrence of local adaptation to thermal regimes on the GBR.

1.4 The challenges associated with estimating coral thermal tolerance

Thermal tolerance, and the variation herein, is key to understanding coral survival under continued climate change and has received significant scientific attention. Traditionally, the majority of coral thermal tolerance studies were undertaken *in situ* in the field, either during natural thermal stress events (Guest et al., 2012; Hoey et al., 2016), or using common garden/transplantation studies (Bay & Palumbi, 2017; Kenkel et al., 2015) or under experimental conditions *ex situ* in aquaria (Coles & Jokiel, 1977; Middlebrook et al., 2010; Pratchett et al., 2020). Long-term monitoring of coral communities has enabled the detection of community-level patterns of thermal tolerance (AIMS, 2022; McClanahan et al., 2007) and serves to identify relative tolerance between species (Loya et al., 2001). However, the pressing need to further our understanding of coral thermal tolerance requires multiple sources of evidence spanning spatial, temporal and biological scales (van Woesik et al., 2022).

Variability in coral thermal tolerance can be investigated with common garden and reciprocal transplant experiments in which colonies are moved along an environmental gradient (Howells et al., 2013; Kenkel et al., 2015), hence removing the requirement of a natural bleaching event to occur. The experimental transplantation of corals along such gradients has been used to examine physiological responses to projected future environments (Sampayo et al., 2016; Tisthammer et al., 2021). However, under natural conditions, it is challenging to confirm if the observed patterns are the result of a single driver such as differential thermal tolerance or potentially due to interactions of multiple environmental variables (McClanahan et al., 2007). Aquarium-based experiments can offer highly controlled conditions under which drivers of differential thermal tolerance can be examined by isolating multiple factors simultaneously (D'Angelo & Wiedenmann, 2012). This was recently exemplified by Cleves et al., (2020c) who utilised aquarium-based thermal stress experiments to document specific gene function (gene HSF1) in thermal tolerance of coral larvae. Despite the usefulness and increasing potential of *ex situ*, aquarium-based assessments of coral thermal tolerance, undertaking such experiments carry limitations, particularly around logistics, husbandry, and costs (Orejas et al., 2019) which may reduce the scope of such experiments with regards to sample volume and accessible study locations. Additionally, target species must be able to be maintained in aquaria successfully long-term. However, not all species can be easily maintained in aquaria (Delbeek 2001). This has resulted in an under-representation of species in thermal tolerance studies which predominantly rely on *Pocillopora damicornis*, *Stylophora pistillata*, and *Acropora millepora* (McLachlan et al., 2020). To further our understanding of coral thermal tolerance, it is therefore important to broaden the scope of species assessed as well as developing standardised experimental methods for this purpose.

1.5 Acute heat stress assays as a tool to quantify coral thermal tolerance at scale

Acute heat stress assays have been widely used across scientific disciplines, including in human medicine (Gianrossi et al., 1989), caterpillars and insects (Kingsolver et al., 2013; Kingsolver & Gomulkiewicz, 2003), as well as aquatic and marine invertebrates (Kim et al., 2017; Pallarés et al., 2012; Qin et al., 2018) to obtain fitness measurements rapidly. In this thesis, acute heat stress assays refer to rapid (<24h) experimental *ex-situ* exposures to high levels of thermal stress above the site-specific max monthly mean (MMM) climatology). These assays expose

corals to heating challenges lasting six hours, followed by a short recovery period. These methods were originally developed by Palumbi and colleagues working along the thermally variable reef areas in American Samoa (Bay & Palumbi, 2015; Oliver & Palumbi, 2011). They showed that these assays provide a valuable, valid, and fast way of assessing coral thermal tolerance across spatial scales (Cunning et al., 2021; Voolstra et al., 2020). Voolstra et al., (2020) further showed that thermal performance results obtained from these acute heat stress assays were comparable to standard, long-term (3-week) thermal exposure studies. Additionally, coral genotypes that had performed well under acute heat stress exposure also fared well through a natural bleaching event in Samoa (Morikawa & Palumbi, 2019; Rose et al., 2018), demonstrating the ability of the experimental framework to identify thermally tolerant individuals within a population. The assays have further allowed for large sample sizes across spatial scales (Cunning et al., 2021; Marzonie et al., 2022; Nielsen et al., 2022) that would not be feasible with traditional, land-based aquarium experiments. For example, Cunning et al., (2021) surveyed 229 colonies of *Acropora cervicornis* along a 2° latitudinal gradient in Florida, USA, while Marzonie et al., (2022) quantified thermal tolerance of 376 colonies of three coral species across 6.7^{o} latitude in the Coral Sea, Australia.

Previous efforts to compare results from the substantial literature of coral thermal tolerance has in part been hindered by the lack of a common experimental framework and shared variables and traits quantified (Grottoli et al., 2020; McLachlan et al., 2020). For example, McLachlan et al., (2020) highlights that even different methods of standardisation (such as chlorophyll concentration per cm^{-2} vs g^{-1} dry weight) hinder comparisons between studies. Additionally, Kellermann et al., (2019) found that exposure duration significantly influenced thermal performance of multiple traits, making sampling time an important consideration for heat stress studies. Finally, Leggat et al., (2022) recommended that the amount of heat stress applied during experiments should be reported to enable cross-comparisons between studies. Globally, there is now a push to adopt a standardised protocol and treatment temperatures relative to the local thermal environment to allow direct comparisons of relative heat tolerance between studies and populations.

1.6 Multiple metrics are required to capture coral responses to thermal stress

After identifying a suitable experimental framework for quantifying coral thermal tolerance, choosing how to measure thermal tolerance is a challenging task as this trait spans multiple levels of biological organisation. Macro-physiological measures such as survival, growth, and reproductive output are ideal fitness traits to quantify coral thermal tolerance (Barott et al., 2021; Hazraty-Kari et al., 2022; Madin et al., 2014). However, quantifying size changes or reproductive output in corals is challenging and highly time dependent. Reproductive studies are confined to once per year for most species (Baird et al., 2021) while substantial time is required for size changes to be detectable (Harriott, 1998; Smith et al., 2007). To overcome these challenges, tissue and cellular responses to thermal stress have been used as proxies of thermal tolerance. For example, common markers of coral health such as changes in photosynthetic efficiency, chlorophyll, protein, and lipid content all show a general decrease with increasing temperatures (Al-Moghrabi et al., 1995; Barshis et al., 2013; Conlan et al., 2014; Fitt et al., 2009; Nielsen et al., 2020; Roth et al., 2012; Thomas et al., 2018) while other metrics like antioxidative enzyme activities are generally increased under thermal stress (Gardner et al., 2017b; Krueger et al., 2015; Lutz et al., 2015). However, how these common physiological indicators respond to acute heating has received little attention.

While photosynthesis is paramount to coral productivity (Anthony & Hoegh-Guldberg, 2003; Lohr et al., 2019), it also contributes to the symbiosis break-down between coral and algae symbionts due to high production of harmful reactive oxygen species (ROS) during stress (Gardner et al., 2017b). Therefore, declines in photosynthetic efficiency, and in particular in maximum photochemical yield (F_v/F_m), are considered an early sign of thermal stress (Jones & Berkelmans, 2012) and detecting such responses can be achieved relatively easily and non-destructively. Maximum photochemical yield of Photosystem II (F_v/F_m) has been used widely in the literature to document thermal stress in multiple organisms (González-Guerrero et al., 2021; Jones & Berkelmans, 2012; Lohr et al., 2019). Obtaining photo-physiological data is also rapid and allows researchers to fully capitalise on the high experimental throughput of acute heat stress assays (see **chapter 2**; Nielsen et al., 2022). Additionally, coral tissue colour has been used as a rapid indicator of colony health (Chow et al., 2016; Siebeck et al., 2006) with visible paling indicating bleaching and therefore thermal stress (Jones & Berkelmans, 2011; Tsang & Ang, 2015). Tissue colour has been shown to correlate to chlorophyll content (Nielsen

et al., 2020; Winters et al., 2009) and symbiont cell density (Siebeck et al. 2006). Importantly, given that photographic assessments of tissue colour can scale rapidly with the advance of automated image processing (Macadam et al., 2021), this trait could serve as a rapid indicator of thermal stress.

Coral thermal tolerance is governed through multiple physiological and transcriptional pathways (Cleves et al., 2020c; Kenkel et al., 2013). Therefore, holobiont thermal tolerance is rarely captured by measuring only one fitness trait as tolerance is a complex and multivariate trait prone to physiological trade-offs (Day et al., 2008; Jones & Berkelmans, 2010; Precoda et al., 2020; Quigley et al., 2021), although the extent of such trade-offs in thermally tolerant corals is still under investigation (Lachs et al., 2023). Importantly, candidate traits should show a clear, direct relationship between temperature and the trait response and the trait should ideally be clearly linked to the overall fitness of the organism (Angilletta et al., 2003; Kingsolver & Woods, 2016; Wikelski & Cooke, 2006). As a minimum, it has been recommended that studies focus on quantifying at least one symbiont and one host trait (Grottoli et al., 2021). Additionally, the concept of a cascading network response to heat stress supports the capture of multiple tolerance measures (Gardner et al., 2017a; Suggett & Smith, 2020). Further, responses to disturbance are time-dependent and initial reactions to thermal stress may happen rapidly as part of physiological acclimatization but these costly mechanisms are quickly replaced by long-term processes which maintain homeostasis under thermal stress (Borowitzka, 2018), making the sampling time point an important consideration for the experimental outcomes.

1.6.1 Transcriptional mechanisms of heat tolerance

The molecular common stress responses (CSRs) following thermal disturbances have been well studied in corals exposed to long-term thermal stress (Cleves et al., 2020b; Cziesielski et al., 2019; Dixon et al., 2020; Louis et al., 2017). The genes or clusters involved with these responses in corals generally involve upregulation of heat shock proteins (*hsp*) and antioxidative enzymes at the early onset of heat stress (Louis et al., 2017; Meyer et al., 2011) followed by upregulation of genes involved in apoptosis and protein folding (Cleves et al., 2020b; Maor-Landaw & Levy, 2016). Although some processes such as protein expression changes are known to show rapid transcriptional responses to heat stress (Traylor-Knowles et al., 2017), little is currently known about the wider molecular responses to acute heat exposure. Recently, Voolstra et al., (2021b) documented contrasting patterns of gene expression

strategies between two populations of *Stylophora pistillata* with one showing a large shift in expression levels of a suite of genes while the other population recorded almost no differentially expressed genes across three different temperatures (30, 33, and 36ºC, respectively). Following on, Savary et al., (2021) tracked gene expression responses to acute heat stress through time; immediately after heat stress and at 18h post heating, following a recovery period. They found that corals exposed to the most extreme temperature (34.5º) under acute heat stress assays failed to return to baseline expression profiles at the recovery sampling point and highlighted significant genotypic variation in transcriptional responses (despite the study only including five genotypes). Transcriptional responses to thermal stress can not only be early indicators of coral stress (Bay et al., 2013) but through biomarkers, can also be used to predict how corals fare through a disturbance (Bay & Palumbi, 2017). Additionally, capacity for phenotypic plasticity may originate from increased gene expression plasticity (Kenkel & Matz, 2016). Therefore, documenting the transcriptional diversity and plasticity (Granados-Cifuentes et al., 2013) of corals in response to thermal challenges will further inform genetic adaptive capacity.

1.7 Symbionts

Corals are symbiotic animals and their thermal tolerance is influenced by the community composition of their photosynthetic endosymbionts of the family Symbiodiniaceae (Baker et al., 2004; Berkelmans & van Oppen, 2006; LaJeunesse et al., 2018; Wall et al., 2020). Some Symbiodiniaceae taxa, such as representatives in the genus *Durusdinium,* are capable of increasing holobiont bleaching thresholds by 1ºC or more (Berkelmans & van Oppen, 2006; Cunning et al., 2015; Quigley et al., 2020). Studies previously focussed on the role of the dominant symbiont taxa (Berkelmans & van Oppen, 2006; Jones & Berkelmans, 2010) but in the last decade, the importance of low-abundance, background strains has been recognised (Cunning et al., 2015; Quigley et al., 2014), driven in part by advances in sequencing technology and cost reductions. Environmental factors also affect symbiont communities given their establishment is regulated by both environmental and genetic influences (Quigley et al., 2018). However, the extent appears to be highly host-species specific, likely due to these genetic influences. For example, *Pocillopora verrucosa* in the Red Sea (Sawall et al., 2014; Ziegler et al., 2014) and *Acropora tenuis* on the GBR (Cooke et al., 2020; Matias et al., 2022)

tend to show very conserved Symbiodiniaceae communities across significant environmental (thermal and depth) gradients (Cooke et al., 2020; Matias et al., 2022; Sawall et al., 2014; Ziegler et al., 2014) whereas *A. millepora* (Cantin et al., 2009; van Oppen et al., 2001) and *Platygyra daedalea* are more flexible in their associations (Howells et al., 2016). However, we do not currently have a good understanding of the distribution of tolerant symbionts within coral species with potentially highly conserved communities, like the species studies here. Further, environmental factors associated with different symbiont communities are not well understood. Therefore, we need to document and describe the symbiont communities of thermally tolerant corals at the level of intra- and interpopulation, across spatial scales and identify potential environmental drivers of community differences.

1.8 Environmental factors

Past environmental history is a major driver of local adaptation to temperature in coral populations. Classical thermal adaptation theory predicts that higher tolerance is found in heterogenous environments (Angilletta, 2009; Gilchrist, 1995; Magozzi & Calosi, 2015; Nilsson-Örtman et al., 2012) and this has been experimentally validated in corals (for example Barott et al., 2021; Palumbi et al., 2014; Quigley & van Oppen, 2022) where thermal variability promotes a wider thermal tolerance breadth than what is expected in homogenous thermal environments (Oliver & Palumbi, 2011; Richter-Boix et al., 2015; Safaie et al., 2018; Schoepf et al., 2015b). However, the optimal trait temperature is often lower in variable environments compared to homogenous ones which favour the evolution of thermal specialists (Seebacher et al., 2015). Corals' thermal strategies on the GBR can be ambiguous with species or populations not adhering to a strictly generalist-specialist trade-off (Jurriaans & Hoogenboom, 2019) whereby generalists maintain higher performance across a wide thermal spectrum and specialists record greater performance but over a narrow thermal spectrum (Gilchrist, 1995; Seebacher et al., 2015).

Recent studies have further showed that coral thermal tolerance is correlated to site-specific Maximum Monthly Mean (MMM) temperatures and Degree Heating Weeks (DHW) (Mason et al., 2020) while Marzonie et al., (2022) reported a strong positive relationship between the exposure to mild (DHW>4) heatwaves and acute thermal tolerance. As other environmental variables such as salinity (D'Angelo et al., 2015), water quality (Wooldridge,

2009), oxygen content (Alderdice et al., 2021) and nutrients (Béraud et al., 2013; Rosset et al., 2017; Wiedenmann et al., 2013) also impact the metabolic and physiological pathways of coral, these variables have also been shown to impact holobiont thermal tolerance. To identify areas or coral populations characterised by increased temperature tolerance, it is therefore important to investigate the impacts of thermal history and other environmental covariates across large spatial scales on the Great Barrier Reef. This knowledge will help identify specific conditions conducive to high thermal tolerance which could have wider implications for restoration initiatives on the reef. Incorporation of site-specific thermal disturbance history has previously highlighted differences in bleaching susceptibilities within species; both on a smaller scale (~15 ha, Drury et al., (2022b) and across ocean basins (Kenya vs GBR; McClanahan et al., 2004). Further, large-scale gradients of SSTs have been shown to impact coral thermal tolerance (Carilli et al., 2012), and understanding the drivers or environmental covariates of high heat tolerance can therefore be furthered by increasing the spatial footprint of such investigations. Finally, to successfully implement assisted translocation approaches as considered under genetic management interventions (Baums et al., 2019; McLeod et al., 2022), it is important to first understand both upper and lower tolerance limits. For example, corals from the central GBR experienced significant winter bleaching when transplanted to the southern region (Howells et al., 2013). Therefore, patterns of coral thermal tolerance must be examined across latitudinal and thermal gradients.

1.9 Thesis aims and objectives.

To increase our understanding of the drivers of coral thermal tolerance at scale and the need for foundational knowledge for genetic management approaches under climate change, in this thesis I aimed to **document and describe the distribution of thermally tolerant coral (populations) across the Great Barrier Reef (GBR) and investigate the underlying drivers and co-variates of enhanced tolerance**. This thesis demonstrates the first application of acute heat stress assays to quantify thermal tolerance in multiple coral species across the latitudinal extent of the GBR. Mapping thermally tolerant corals will provide benefits to conservation and restoration activities by not only documenting occurrence but could also serve as the basis for modelling thermal tolerance capacity based on information on the drivers of this differential tolerance.

In **chapter 2*: Experimental considerations of acute heat stress assays to quantify coral thermal tolerance***, I completed multiple field tests using the acute heat stress assay system across the far northern reaches of the GBR. Specifically, I aimed to:

- Field test, assess and resolve multiple experimental design and methodological decisions.
- Provide a cost analysis for the acquisition of data on common coral thermal tolerance traits.
- Examine the use of rapidly quantifiable proxy traits to guide trait choice for future studies.

I show how experimental and methodology decisions such as coral fragment size and sampling time point influence the responses to heat stress across multiple physiological traits. I also provide a cost-benefit analysis of common coral health physiological traits to inform downstream analyses for other chapters in this project. Finally, I show how rapid measures of heat stress (photosynthetic efficiency and tissue colour change) may be used as proxies of acute heat tolerance when studies need to scale up investigations and traditional laboratory-based assays become too time- and labour-consuming, creating a bottleneck.

This chapter was published in *Scientific Reports* and the version in the thesis is the same as the published version:

Nielsen, J. J. V., Matthews, G., Frith, K. R., Harrison, H. B., Marzonie, M. R., Slaughter, K. L., Suggett, D. J., & Bay, L. K. (2022). Experimental considerations of acute heat stress assays to quantify coral thermal tolerance. *Scientific Reports*, *12*(16831), 1–13. https://doi.org/10.1038/s41598-022-20138-2

In **Chapter 3: *Patterns of upper thermal performance in reef-building corals on the Great Barrier Reef are dictated by sector-level differences in thermal disturbance history,*** I deployed acute heat stress assays across 11.5° latitude along the GBR with the aims to:

- Quantify acute heat tolerance in multiple coral species across the latitudinal extent of the Great Barrier Reef.
- Document and describe spatial patterns of symbiont communities on the Great Barrier Reef.
- Examine environmental and thermal history covariates of high and low acute heat tolerance.

This chapter utilised the experimental design decisions and cost-benefit framework identified in **Chapter 2** to provide the largest experimental assessment of heat tolerance on the GBR to date. Here, I incorporate the importance of the dominant Symbiodiniaceae community in two species of *Pocillopora* in recognition of its contribution to holobiont tolerance. I also perform an environmental covariate analysis in which I combine 19 thermal history variables to identify the maximum SST and the number of mild heating events (where heat stress > 3 DHW) as factors that explained the greatest amount of variation in differences in upper acute heat tolerance within three coral species on the GBR.

In C**hapter 4:** ***Does gene expression plasticity underpin acute heat tolerance in a population of reef-building coral?*** I performed acute heat stress assays to focus on intra-population variation in physiological and transcriptomic responses to acute heat stress. Focusing on a single population allowed me to interrogate the genetic mechanisms underlying host responses to acute heat tolerance more closely. Specifically, I aimed to:

- Identify thermally tolerant and intolerant individuals from within a population using acute heat stress and multiple physiological traits.
- Identify gene expression patterns and potential biomarkers of thermal tolerance between thermally tolerant and intolerant colonies.

This chapter combined high-throughput heat tolerance phenotyping with transcriptomic analyses to identify host drivers of increased heat tolerance within a population. I describe significant effects of acute heat stress exposure on gene expression profiles 24 h after heat stress and find a small number of genes which were significantly upregulated in the heat tolerant colonies in the absence of heat stress and propose these could serve as gene expression markers of acute heat tolerance.

Finally, I combine the results from chapters 2-4 in C**hapter 5:** ***General Discussion*** where the major context of the thesis and its wider implications are interrogated. I highlight future directions and opportunities for this research, including how this data can contribute towards coral management initiatives through identification of areas of exceptional heat tolerance for spatial protection but also through the identification of thermally tolerant brood- and source-stock for genetic interventions. I describe how these data can feed into coral demographic modelling to improve forecasts of survival and recovery following heat stress. Finally, I discuss the limitations of acute heat stress assays and highlight the need for further ground-truthing of

the experimental framework to ensure that acute heat stress tolerance is indeed indicative of long-term, natural bleaching and mortality resilience under natural marine heat wave events.

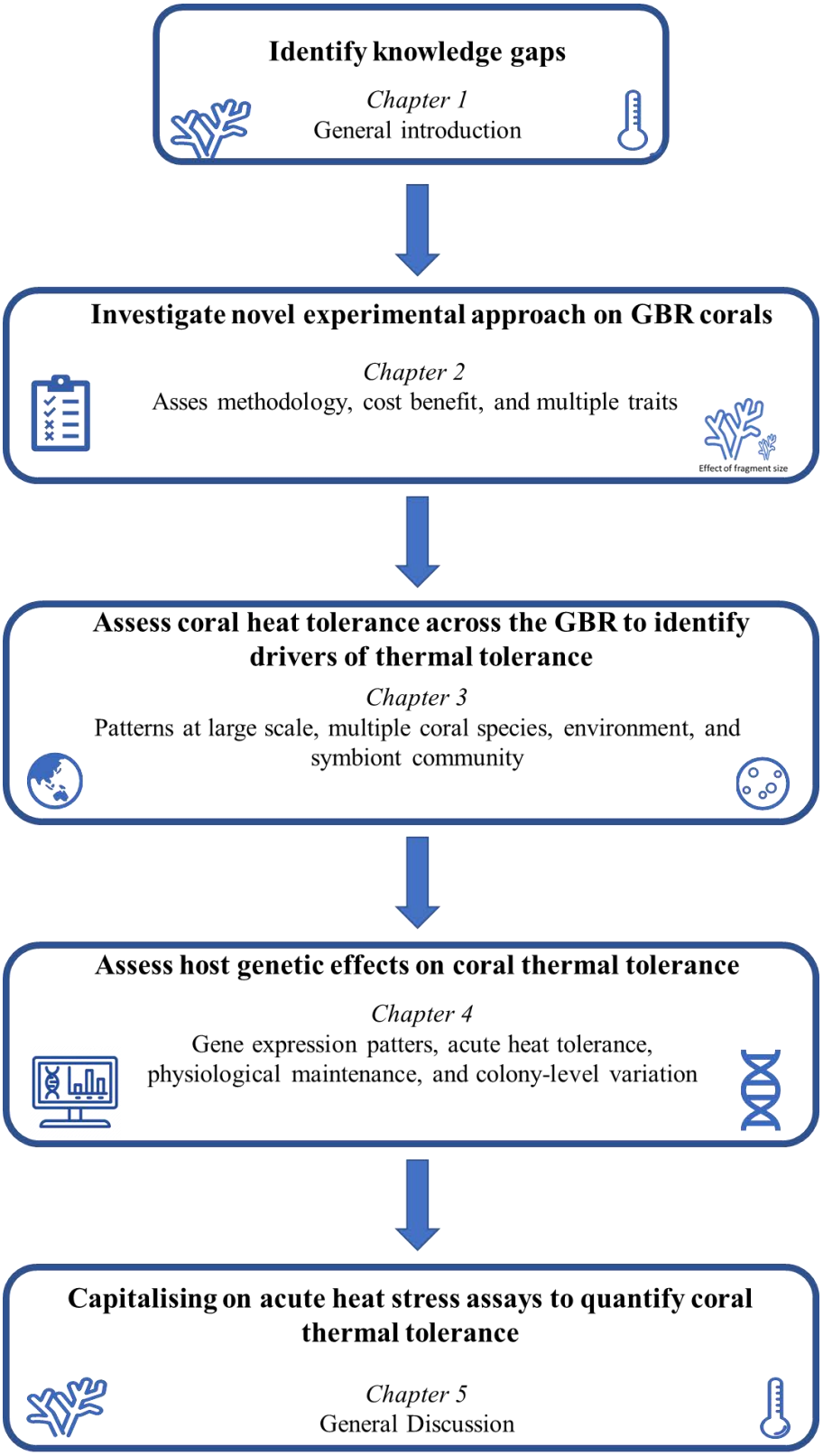

Figure 1.2 Thesis summary.

Chapter 2 Experimental considerations of acute heat stress assays to quantify coral thermal tolerance.

This paper was published and the text has only been altered with respect to formating but otherwise appears as in the published version.

Nielsen, J. J. V., Matthews, G., Frith, K. R., Harrison, H. B., Marzonie, M. R., Slaughter, K. L., Suggett, D. J., & Bay, L. K. (2022). Experimental considerations of acute heat stress assays to quantify coral thermal tolerance. *Scientific Reports*, *12*(16831), 1–13. https://doi.org/10.1038/s41598-022-20138-2

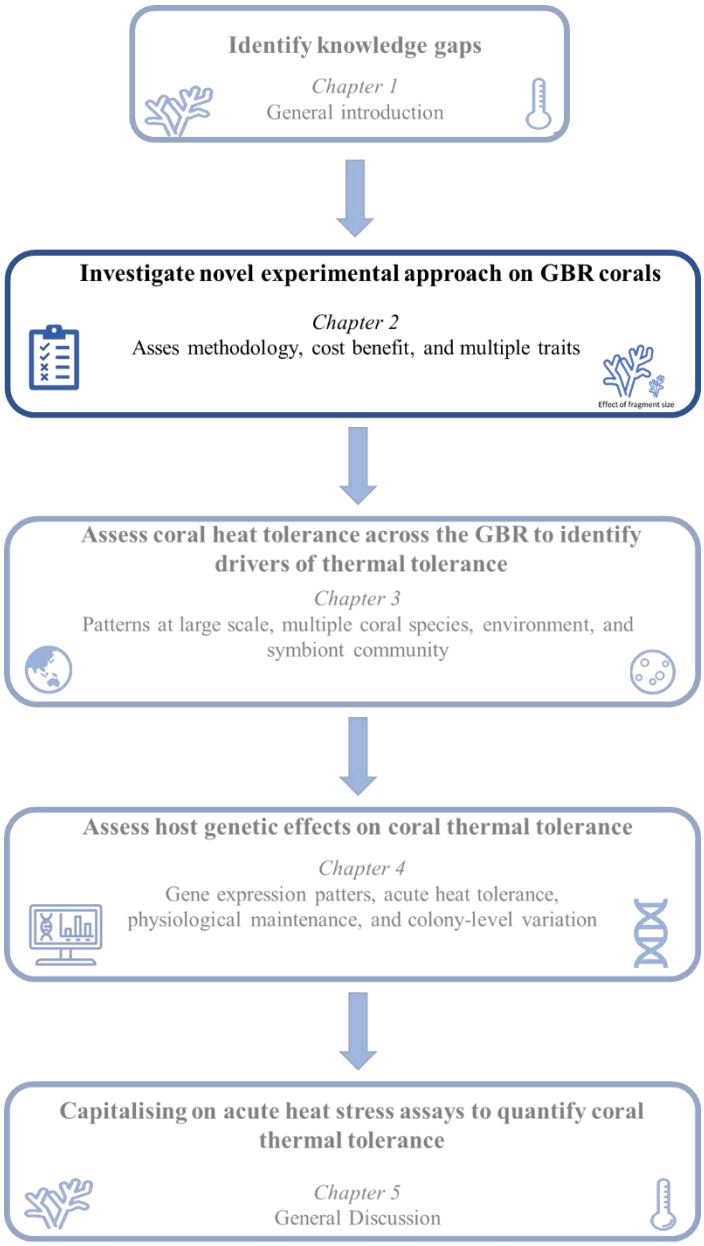

2.1 Abstract

Understanding the distribution and abundance of heat tolerant corals across seascapes is imperative for predicting responses to climate change and to support novel management actions. Thermal tolerance is variable in corals and intrinsic and extrinsic drivers of tolerance are not well understood. Traditional experimental evaluations of coral heat and bleaching tolerance typically involve ramp-and-hold experiments run across days to weeks within aquarium facilities with limits to colony replication. Field-based acute heat stress assays have emerged as an alternative experimental approach to rapidly quantify heat tolerance in many samples yet the role of key methodological considerations on the stress response measured remains unresolved. Here, I quantify the effects of coral fragment size, sampling time point, and physiological measures on the acute heat stress response in adult corals. The effect of fragment size differed between species (*Acropora tenuis* and *Pocillopora damicornis*). Most physiological parameters measured here declined over time (tissue colour, chlorophyll-*a* and protein content) from the onset of heating, with the exception of maximum photosynthetic efficiency (F_v/F_m) which was surprisingly stable over this time scale. Based on these experiments, I identified photosynthetic efficiency, tissue colour change, and host-specific assays such as catalase activity as key physiological measures for rapid quantification of thermal tolerance. I recommend that future applications of acute heat stress assays include larger fragments (>9 cm^2) where possible and sample between 10 – 24 h after the end of heat stress. A validated high-throughput experimental approach combined with cost-effective genomic and physiological measurements underpins the development of markers and maps of heat tolerance across seascapes and ocean warming scenarios.

2.2 Introduction

Coral reefs are under increasing threat from climate change with strong and direct impacts from the interaction of chronic ocean warming (Pörtner et al., 2019) and the increasing frequency of acute heat waves driving episodes of mass coral bleaching (Genevier et al., 2019; Hughes et al., 2018). The process of bleaching is a well-described physiological response to the interaction of temperature and light, resulting in nutritional (Morris et al., 2019) and oxidative stress in the coral holobiont (reviewed in Suggett & Smith, 2020). It is recognised as the loss of coral colour due to expulsion of symbiotic algae and/or photosynthetic pigments (Baker et al., 2008; Brown et al., 1994; Suggett & Smith, 2011). When environmental stressors persist and/or events are extreme, bleaching may be followed by coral mortality (Maynard et al., 2008; Weis, 2010). Therefore, the ability of populations and species to cope with increasing temperature extremes is likely to define the structure and function of coral reefs into the future. Until recently, high throughput approaches capable of measuring and comparing heat tolerance within and between populations had only been applied to coral larvae (Dixon et al., 2015; Meyer et al., 2011) and not to adult colonies (Grottoli et al., 2021).

Acute thermal stress experiments provide a tool to identify and predict tolerance to stress using large sample sizes across environmental gradients (Evensen et al., 2022). In the marine environment, such experiments have been used to investigate heat stress thresholds in metabolic (Song et al., 2019), molecular (Juárez et al., 2018; Kim et al., 2017), and/or behavioural (Pallarés et al., 2012; Qin et al., 2018; Zanuzzo et al., 2019) traits across a variety of marine vertebrates and invertebrates. These various approaches have identified heat-tolerant corals after exposure to acute thermal stress (Cunning et al., 2021; Evensen et al., 2021; Morikawa & Palumbi, 2019; Rose et al., 2018; Thomas et al., 2018; Voolstra et al., 2020). For example, Morikawa et al., (2019) showed that nursery corals which survived a natural bleaching event (American Samoa) all originated from top-performing colonies under acute heat stress assays. Further work in the Red Sea has demonstrated that physiological responses (including photosynthetic efficiency) from such acute assays could be differentiated among four species (Evensen et al., 2022) and were consistent with those from more traditional, longer-term heating experiments (Evensen et al., 2021; Voolstra et al., 2020). Consequently, acute heat stress assays are highly applicable to quantify how corals respond to different temperature treatments across broad spatial and temporal scales in the field (Cunning et al.,

2021; Klepac & Barshis, 2022). However, specific experimental considerations have not been resolved for these assays.

As acute heat stress assays increase the extent of sampling possible, the processing times of ever more extensive coral phenotypic data creates an increasing bottleneck (Gardner et al., 2017a; Madin et al., 2016; Suggett et al., 2022). Existing physiological metrics of bleaching sensitivity, such as quantification of pigment (chlorophyll-*a*), protein, and antioxidative enzyme activity assays (e.g. catalase; Krueger et al., 2015) are invasive and labour-intensive to obtain. High-throughput assessment often relies on real time, non-invasive, and active fluorescence-based measures of the photo-physiological performance of coral endosymbionts – notably the maximum photochemical yield of photosystem II (PSII), F_v/F_m (dimensionless; Leggat et al., 2011; Nitschke et al., 2018) – as a first order proxy for other physiological metrics. F_v/F_m is long evidenced in quantifying declining endosymbiont function as corals bleach under heat stress (Nitschke et al., 2018; Warner et al., 1999), and correlates to other heat-response characteristics such as declining chlorophyll-*a* content (Fitt et al., 2001), protein content (Tolosa et al., 2011), and changes to the microbial community composition (Grottoli et al., 2018). Other studies have employed image-based measures of colour to rapidly assay bleaching (Chow et al., 2016); for example, Nielsen et al., (2020) showed a strong relationship between tissue colour and chlorophyll-*a* content. Thus, coupling readily quantifiable, cost-effective parameters and their relationship to thermal tolerance with acute heat stress assays allows faster quantification of the coral bleaching response and provides a platform for developing a deeper insight into patterns of thermal tolerance across time and space.

To ensure that growing acute heat stress data sets (Cunning et al., 2021; Evensen et al., 2022; Voolstra et al., 2020) are comparable among studies to support robust reconciliation through cross-study meta-analyses, a consistent set of guidelines will be required. A common standardised framework is required to resolve drivers of bleaching susceptibility between species and regions spanning different geographical (habitat, reef, region) and biological (colony, population, species) scales (McLachlan et al., 2020). Basic operational factors that can potentially influence measures of thermal tolerance remain largely untested (Edmunds & Burgess, 2018; Madin et al., 2014). The size of the sampled fragment has been shown to affect thermal tolerance and bleaching resistance in some corals (Pausch et al., 2018; Shenkar et al., 2005). Similarly, it is unknown whether physiological changes occur linearly or non-linearly over time, and by extension, whether studies measuring at different time points can be compared (Hoey et al., 2016; Middlebrook et al., 2010).

I examined how the understanding of heat tolerance based on acute assays is affected by fundamental methodological considerations. I firstly investigate the effect of experimental fragment size using two common coral species of varying thermal sensitivities, *Acropora tenuis* and *Pocillopora damicornis*. Since published studies of acute thermal tolerance have sampled at slightly different time-points, I then examined the effect of sampling time on the resulting acute heat stress phenotypes of *A. tenuis* over 48 h. Due to the high-throughput potential of these acute heat stress assays, I provide a cost analysis of the physiological metrics included here and finally I investigate how rapid, non-invasive measures of coral thermal tolerance (F_v/F_m and colour change) compare to more time-consuming and labour-intensive measures using evidence from multiple physiological traits. I discuss experimental considerations and cost effectiveness of physiological measurements for future applications of high throughput acute heat stress assays to measure thermal tolerance of corals and identify rapidly quantifiable descriptors of physiological responses to heat stress. This study benefits the development of cost-effective and rapid descriptors of (heat) stress tolerance amongst coral populations for targeted protection or propagation.

2.3 Materials and Methods

2.3.1 Study region, species, and collection

Acute heat stress assays on *Acropora tenuis* and *Pocillopora damicornis* were conducted in the Far Northern Great Barrier Reef (FNGBR) in January 2019 (Fig 2.1A). This region of the Reef is characterised by high summer temperatures and irradiance (Bainbridge, 2017; Smith & Spillman, 2019) and experienced consecutive bleaching events in the austral summers of 2016 and 2017 (18-82 % bleaching, n = 15 reefs (Hughes et al., 2018). All coral samples were collected on SCUBA (3 – 6 m) under Great Barrier Reef Marine Park permit G16/38488. Colony colour was assessed against the Coral Watch reference chart at the time of collection (Siebeck et al., 2006). Fragments were placed in perforated zip-lock bags for no more than two h, and further fragmented for experiments. Fragments were placed in aquaria (60 L) on the vessel deck, supplied with ambient flow-through seawater, and shaded with cloth prior to being moved into the experimental tanks. Seven separate experimental runs were conducted no later than 24 h after collection across three experiments (Table 2.1). The two species were selected to represent two abundant genera and for their ease of collection with hand tools. Collection, transport, and fragmentation are likely stressful for corals and the protocol did not allow for recovery time prior to experimental exposure, hence heated fragments were compared to ambient-held fragments.

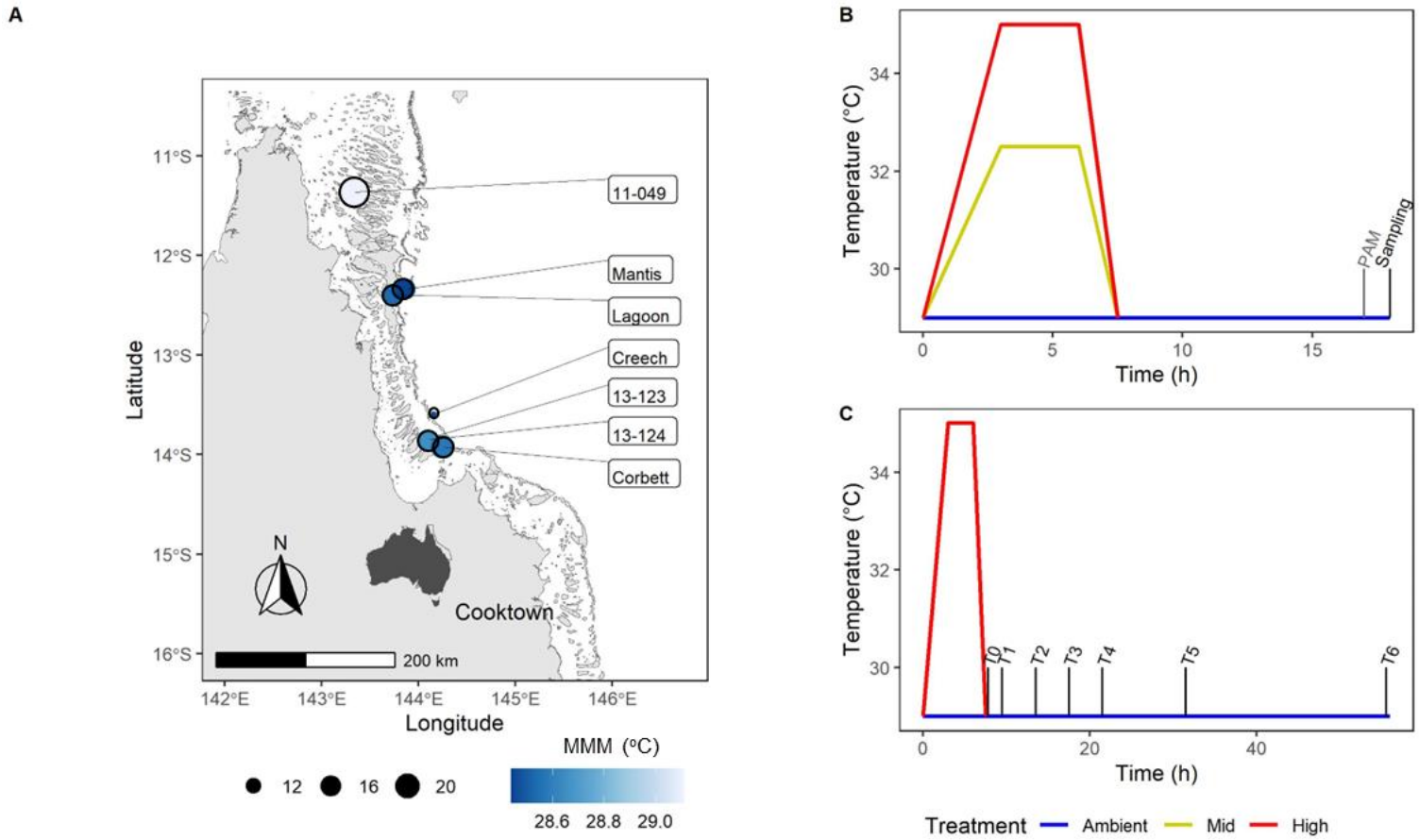

Figure 2.1 Collection and experimental designs used to examine the influence of fragment size on two species (*A. tenuis* and *P. damicornis*) and time of sampling on multiple physiological measures. A: Map of sampling locations, size of dot indicates number of colonies sampled per site and colour shows Max Monthly Mean (MMM) temperature of each site. Map generated in R version 4.1.3. B: Temperature profiles used to test for size effects in *A. tenuis* and *P. damicornis* (ambient and high treatments only, experiment 1) and to investigate multiple physiological measures across five reefs in *A. tenuis* (all three treatments, experiment 3). C: Temperature profile and sampling time points for assessing changes in physiological metrics through time (experiment 2).

Table 2.1 Coral collection and experiment details. Collection dates are given as day of January 2019.

Purpose of experiment	Reef	Coordinates	Species collected	Colonies sampled	Treatments	MMM °C	Collection date	Experiment date
1.Fragment Size effect	13-123	144.1348 °E, 13.8552 °S	*A. tenuis*	9	Ambient and +6°C	28.6	14/01	15/01
			P. damicornis	9				
2.Time effect	Creech	144.1071 °E, 13.6447 °S	*A. tenuis*	9	Ambient and +6°C	28.46	15/01	16/01
3.Alternative physiological measurements	Corbett	144.2405°E, 13.9227°S	*A. tenuis*	18	Ambient, +3°C, +6°C	28.58	10-11/01	11/01
	13-124	144.0906°E, 13.8517°S	*A. tenuis*	15	Ambient, +3°C, +6°C	28.66	12-13/01	13/01
	Lagoon	143.7394°E, 12.3922°S	*A. tenuis*	15	Ambient, +3°C, +6°C	28.54	18/01	19/01
	Mantis	143.8808°E, 12.3041°S	*A. tenuis*	15	Ambient, +3°C, +6°C	28.44	20/01	21/01
	11-049	143.3262°E, 11.3637°S	*A. tenuis*	23	Ambient and +6°C	29.11	28/01	28/01

2.3.2 Temperature treatments and experimental design

Heat treatment profiles were designed following Palumbi et al., (2014) and Voolstra et al., (2020) using a new delivery system designed by the National Sea Simulator Facility at the Australian Institute of Marine Science (AIMS). The tank-based heat stress assay system was specifically designed for mobility and flexibility of application following the CBASS (Coral Bleaching Automated Stress System) principle outlined by Voolstra et al. (2020). The system used here consisted of two sets of three tanks, one set with temperature control capability (temperature manipulation system, Fig 2.2) and the other without (ambient system, Fig 2.2). The temperature manipulation system consisted of three independent acrylic tanks (55 L), each supplied with heated flow-through seawater (55 L h^{-1}). Tanks were placed in water jackets to aid in temperature control and stability. The jackets were supplied with recirculating, warm seawater, heated with a titanium heating element (Omega 2 kW) held in a separate jacket (sump, Fig 2.2) and pumped between jackets using a submersible pump (Reefe RP2400LV 24v). The sump also held a heat exchange coil (Wateco 56") to heat seawater delivered to the tanks. Temperature was controlled with a programmable logic controller (Siemens S7 15-11-1 PN). For the ambient system, both the jackets and experimental tanks were supplied with flow-through seawater pumped from the ocean (55 L h^{-1}). Every tank was fitted with a circulation pump (Turbelle® nanostream® 6055, Tunze, Penzburg, Germany). The temperature manipulation system was run indoors onboard a research vessel and treatments consisted of an initial ramp up over three h from ambient incoming seawater to the desired treatment temperature. Treatment temperature was held for three h, followed by ramp down to ambient within 1.5 h. Once returned to ambient temperature, corals were maintained for 11 h in the dark before data collection and sampling (Fig 2.1B). The control treatment was held at ambient temperature for the duration of the experiment and ambient temperatures ranged between 29.5 - 30.9°C across the sampling duration. Treatments used were ambient, mid (approx. +3°C) and high (+6°C). Experimental temperatures and Max Monthly Mean (MMM) temperatures are presented in Appendix A.1. Lighting profiles followed summer, mid-day light levels at Lizard Island in the northern GBR (450 µmol photons m^{-2} s^{-1}, no ramping, 7h:11h light:dark, 60% blue, 20% white, 10% green, and 10% red, 10 m, Lizard Island Light From 26 Feb 2012 | AIMS metadata | aims.gov.au). I conducted three separate experiment to test the effects of 1) fragment size, 2) timing of measurements and 3) physiological proxies for heat tolerance. In experiment 2 (time-effect), ambient-treated corals experienced reductions in most physiological measures

and thus responses were expressed as % change in physiological measures (colour change, F_v/F_m, chlorophyll-α and protein content, and catalase activity) in heated corals relative to their ambient counterparts.

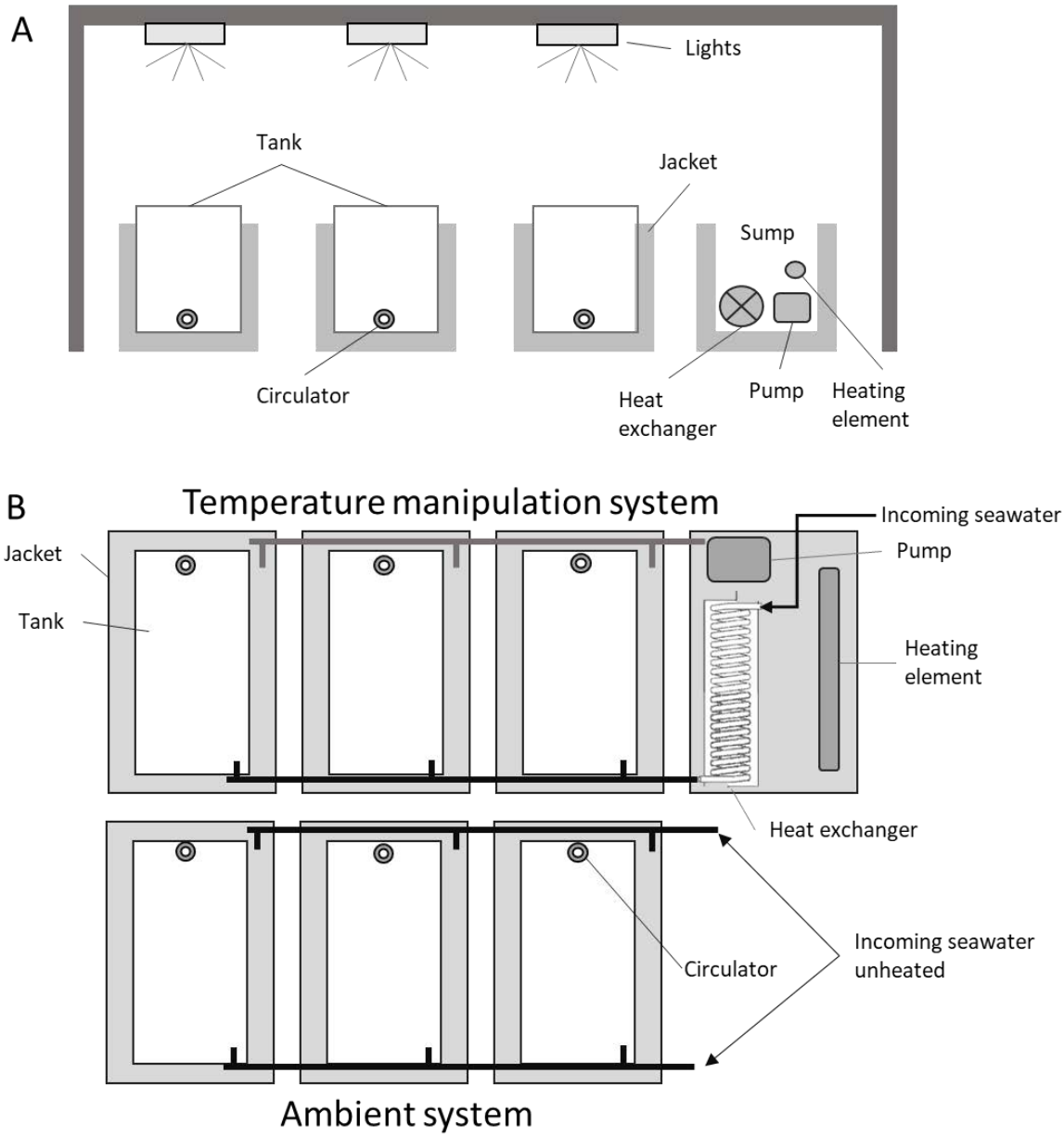

Figure 2.2 Schematic overview of the experimental tank set-up. (A) Side view of the temperature manipulation system, with three experimental tanks in water jackets and a fourth jacket acting as sump for heating water for both tanks and jackets. The sump contained the heating element, heat exchange coil, and a submersible pump to pump recirculating water to the jackets while the tanks were supplied

with warm water from the heating coil. (B) Top-down view of the temperature manipulation and ambient systems. The ambient system was supplied unheated seawater to both jackets and tanks.

2.3.3 Experiment 1 - Size effect

Nine colonies each of *A. tenuis* and *P. damicornis* (Table 2.1) from reef 13-123 were fragmented into six large (9.05 ± 0.44 cm^2, 12.45 ± 0.7 cm^2, *A. tenuis* and *P. damicornis*, respectively) and six small fragments (3.51 ± 0.19 cm^2, 7.13 ± 0.34 cm^2, *A. tenuis* and *P. damicornis*, respectively). Three large and three small fragments from each colony were assigned to the two treatments (ambient and +6ºC, 1 size pair per tank per treatment, n = 216 for both species, Appendix A.1). The fragments were wrapped in aluminium foil and snap frozen in liquid N_2 11 h after the end of heat stress for further analysis (Fig 2.1B).

2.3.4 Experiment 2 - Time effect

Samples of *A. tenuis* were collected from nine individual colonies at Creech reef (Table 2.1). Samples were further fragmented (18 per colony, ~5 cm in length), and distributed across treatments (ambient and +6ºC, n = 3 fragments per colony per tank, total = 162 fragments, Appendix A.1). Sampling occurred immediately after the end of heat stress (T_0), and then at two h (T_1), six h (T_2), 10 h (T_3), 14 h (T_4), 24 h (T_5), and 48 h (T_6) after the end of heat stress (Fig 2.1C). At each sampling point, one fragment per colony per treatment was sampled apart from T_6 (48 h) when all remaining fragments were sampled and preserved (Fig 2.1C).

2.3.5 Experiment 3 – Alternative physiological measurements

Collections of *A. tenuis* to evaluate physiological metrics (including chlorophyll-*a* and protein content, catalase activity, tissue colour change, and photosynthetic efficiency) took place across five reefs and included 86 colonies (Table 2.1, Appendix A.1). Four fragments were made per colony except for reef 11-049 where only two fragments per colony were made. Fragments were distributed between treatments (n = 1 per colony per treatment) and sampled after an 11 h recovery period at ambient temperature (Fig 2.1B).

2.3.6 Photosynthetic efficiency

Photo-physiological status is a common diagnostic to measure effects of heat exposure and coral bleaching (Fitt et al., 2001; Suggett & Smith, 2011) and thus I also quantified photosystem II (PSII) maximum photochemical efficiency *(F_v/F_m*, dimensionless*)* using Pulse Amplitude Modulated Fluorometry of chlorophyll-*a* (PAM, Diving-PAM, Heinz Walz GmbH, Effeltrich, Germany, MI = 8, SI = 8, saturation width = 0.8, Gain = 3, Damp = 2; Nitschke et

al., 2018; Saxby et al., 2003). A clear piece of PVC tubing was used to maintain a constant distance (2 mm) between the glass fibre-optic probe (6 mm Ø) and the coral fragment. Samples were dark acclimated for 30 min before measurements were taken. Each fragment was measured twice at different spots approx. 1/3 distance from the apical corallite. For experiments 1 (size) and 3 (physiological measures), values of F_v/F_m were determined 10 h after the end of heat stress (Fig 2.1B). For experiment 2 (time) F_v/F_m was measured at each sampling time point (T_0 – T_6, Fig 2.1C).

2.3.7 Visual signs of bleaching

For experiments 1 (size) and 3 (physiological measures), samples were photographed prior to, and after, heat treatment with a digital SLR camera (Nikon D300, F stop = 4, shutter speed = 100, ISO = 400). For experiment 2 (time), samples were also photographed at each time point (T_0 – T_6, Fig 2.1C). Photographs were taken at a distance of 25 cm against a dark background, which included the *Coral Watch* colour reference chart (Siebeck et al., 2006). Tissue colour was assessed as per Nielsen et al. (2020).

2.3.8 Sampling and sample preparation for physiological assays

A pressurized air gun and 0.02 µm filtered seawater (FSW) was used to remove tissue from coral skeletons (Deschaseaux et al., 2013). The resulting slurry was homogenised (30 s, 40% power, Pro200, Bio-gen Series, ProScientific, USA) and aliquots were removed for chlorophyll-*a* quantification (1 mL), centrifuged (5 min, 4ºC, 1500 rpm) and the supernatant discarded. The resulting symbiont pellet was stored dry at -80ºC. Remaining tissue slurry was centrifuged (5 min, 4ºC, 1500 rpm) to separate host tissues from Symbiodiniaceae cells. Host tissue was aliquoted (500 µL) into 96-well tissue culture plates for protein analysis. For catalase activity, 1 mL of host tissue was aliquoted into Eppendorf tubes.

2.3.9 Surface area quantification

Surface area of each blasted coral skeleton was quantified according to the double wax dipping method (Holmes et al., 2008), which has been shown to accurately calculate the surface area of branching species (Naumann et al., 2009). Skeletons were bleached (10%), rinsed, dried, and stored at room temperature prior to dipping. Cylindrical shapes of known sizes were used to produce a standard curve of surface area. Skeletons and standards were immersed (4 s) into hot wax (65ºC), removed, swirled to air-dry and left to dry for a further 15 min before weighing.

The dipping procedure was repeated, and surface area calculated as the weight difference between the first and second dip.

2.3.10 Chlorophyll-a quantification

Pre-chilled ethanol (0.8 mL, EtOH, 95%) was added to each frozen sample and vortexed until the pellet was fully resuspended then sonicated (3 min, 40% power, Sonic Power® MU-600, Mirae Ultrasonic Tech Co, Korea), vortexed, and incubated on ice in the dark to extract pigments (20 min). Triplicate aliquots (200 µL) were loaded onto a 96 microwell plate (Immulon® 4, HBX) using EtOH (95%) as a blank and absorbance was read immediately at 664 nm and 649 nm. Chlorophyll-*a* content was calculated following Equation 1 (Licthenthaler, 1987; Ritchie, 2006), corrected for absorbance in the blanks and normalised to surface area of the coral fragment.

$$((13.36*Abs_{664nm})-(5.19*Abs_{649nm}))/0.794 \quad (1)$$

2.3.11 Protein content

Water-soluble protein content was determined using the Bio-Rad *DC* Protein Assay following the manufacturer's guidelines. Protein samples were thawed on ice, homogenised and diluted 1:1 in NaOH (200 µL, 1M). Samples were sonicated using an ultrasound water bath for 5 min (40% amplitude, Sonic Power® MU-600, Mirae Ultrasonic Tech Co, Korea) before being digested in an oven for 1 h at 90ºC. Samples were then centrifuged (10 min, 2000 rpm) before loading 10 µL per replicate into a microtiter plate (96-well, 300 µL, Immulon® 4, HBX). Reagent A (25 µL) was added and allowed to stand for 5 min before adding 200 µL of Reagent B. The plate was covered and incubated in the dark at room temperature for 15 min. After incubation, the plate was loaded into the spectrophotometer (Synergy H4 Hybrid Reader®, Bio-Tek, Winooski, VT, USA) and absorbance read at 750 nm (25ºC). Protein content was normalised to surface area and reported as mg cm^{-2}.

2.3.12 Catalase activity

Catalase activity was quantified as the change in H_2O_2 concentration over time (Krueger et al., 2015). Samples were thawed on ice, vortexed (40 s) and 30 µL were added to a UV-transparent micro-well plate (UV-Star®, 96 wells, Greiner Bio-One, Monroe, NC, USA) in triplicate with FSW as blanks. 60 µL of PBS (50 mM, pH 7) and 20 µL of EDTA (10 mM) were added to the plate before adding 120 µL of H_2O_2 (50 mM) as substrate for the reaction. The plate was

immediately loaded into the spectrophotometer (Synergy H4 Hybrid Reader®) and absorbance was read at 240 nm every 30 s for 15 min. Catalase activity (U) was assessed over the linear portion of the curve and expressed as specific activities (U mg^{-1} protein).

2.3.13 Cost-benefit of alternative physiological measurements

A qualitative cost-benefit analysis was conducted to contrast the data returned relative to resource and time investment across the various physiological measurements. I identified the consumables and (capital) equipment required for each physiological measurement (Appendix A.7-10). Cost of consumables per 100 samples was calculated from pricing available online or via direct quotes. No shipping or GST costs were included. The cost of equipment use per 100 samples was based on an approximation of how many samples were likely to be processed over a conservative lifespan of the respective item. Time estimates were based on in-laboratory experiences processing the samples for this study (n = 779 fragments). Chlorophyll, protein, and catalase assays according to methods presented here, require the samples to be tissue blasted. Therefore, the cost and time requirement of tissue blasting should be accounted for if planning to conduct any of these. Similarly, these assays are standardised to fragment surface area, and the costs associated with this assay are therefore also included. No sample preservation costs were included in these estimates.

2.3.14 Statistical analyses

All statistical analyses were conducted in R (R Core Team, 2020). The effects of fragment size were investigated by generalised linear mixed effects models. I assumed a Gaussian distribution of all dependent variables and checked for normality of modelled residuals and homoscedasticity of plotted residuals (package DHARMa; Hartig & Lohse, 2021). The models were fitted by restricted maximum likelihood and generated using the *glmmTMB* function in the R package glmmTMB (Brooks et al., 2017), where treatment (ambient vs high) and fragment size (large vs small) were used as fixed effects. Colony identity was fitted as a random effect with a random intercept (Harrison et al., 2018). Model fit was evaluated by assumption fit and R^2 (Nakagawa & Schielzeth, 2013). Adjusted p-values for the Post-hoc Tukey HSD tests were calculated using the single-step method.

Because of the decline in coral condition in the ambient treatment evident in the time effect experiment, data were transformed to percent change in the heated treatment relative to ambient and modelled against a gaussian distribution using a linear mixed effects model using the glmmTMB R package (Brooks et al., 2017). Assumptions and homoscedasticity were

confirmed as above. Time was modelled as a categorical variable rather than a continuous to allow direct, post-hoc comparisons between specific sampling times. Post-hoc comparisons were investigated with Tukey's HSD tests.

The relative importance of multiple physiological metrics driving observed differences in thermal responses to acute heat stress was assessed by Principal Component Analysis (PCA) performed in R, using the package vegan (Oksanen et al., 2020). Based on Eigenvalues (>1), I used two principal components (PCs) to account for the variability within the data. PC1 (43%) and PC2 (21%) cumulatively accounted for 64% of the variance. Additionally, each physiological trait was correlated to each other and a heatmap produced using the lattice R package (Sarkar, 2008).

2.4 Results

2.4.1 Experiment 1: Effect of fragment size

Effect of fragment size differed between species and physiological metrics investigated. Collectively, fragment size affected nearly all examined physiological measures in *P. damicornis* except photosynthetic efficiency while an effect of fragment size was largely absent in *A. tenuis* samples. Treatment at high temperatures resulted in significant declines across all measures relative to treatment at ambient temperatures.Tissue colour change was affected by the interaction of treatment and fragment size in both species (*A. tenuis*, df = 106, z = -3.26, p = 0.001; *P. damicornis*, df = 106, z = 2.50, p = 0.023). In *A. tenuis*, large fragments (-0.34 ± 0.05 colour units) exhibited nearly twice the colour loss of small fragments (-0.19 ± 0.07 colour unit, df = 106, t = -4.231, p < 0.0001, Fig 2.3A) while in *P. damicornis*, large fragments (-0.40 ±0.06 colour unit) exhibited less colour loss relative to the small fragments (-0.91 ±0.06 colour unit, Fig 2.3F, df = 106, t = 5.745, p <0.0001). See statistical outputs in Appendix A.2 and A.3.

Chlorophyll-*a* content and catalase activity (U) in *P. damicornis* were both affected by the interaction of treatment and fragment size (Chl-α; df = 96, z = -1.975, p = 0.048, Fig 2.3H; catalase; df = 86, z = 2.82, p = 0.005, Fig 2.3J, respectively). Catalase activity (U) varied within heat-treated corals between fragment sizes (df = 86, t = -2.146, p = 0.035; large = 0.286 ± 0.1 U; small = 0.03 ±0.01) but not for ambient corals (df = 86, t = 1.851, p = 0.068). In *A. tenuis*, chlorophyll-*a* content and catalase activity were only affected by temperature (chlorophyll-*a* df = 104, z = -6.24, p < 0.001, Fig 2.3C; catalase activity df = 93, z = 2.38, p = 0.017, Fig 2.3E) but not fragment size, or their interaction.

Photosynthetic efficiency was only affected by treatment in both species, but not fragment size or their interaction (Fig 2.3B and 2.3G). Finally, *P. damicornis* protein content was affected by both treatment and fragment size, but not by their interaction (Treatment; df = 102, z = -3.173, p = 0.002; Size df = 102, z = -2.761, p = 0.0058, Fig 2.3I). In *A. tenuis*, protein content was only impacted by treatments (df = 91, z = -5.112, p < 0.0001, Fig 2.3D).

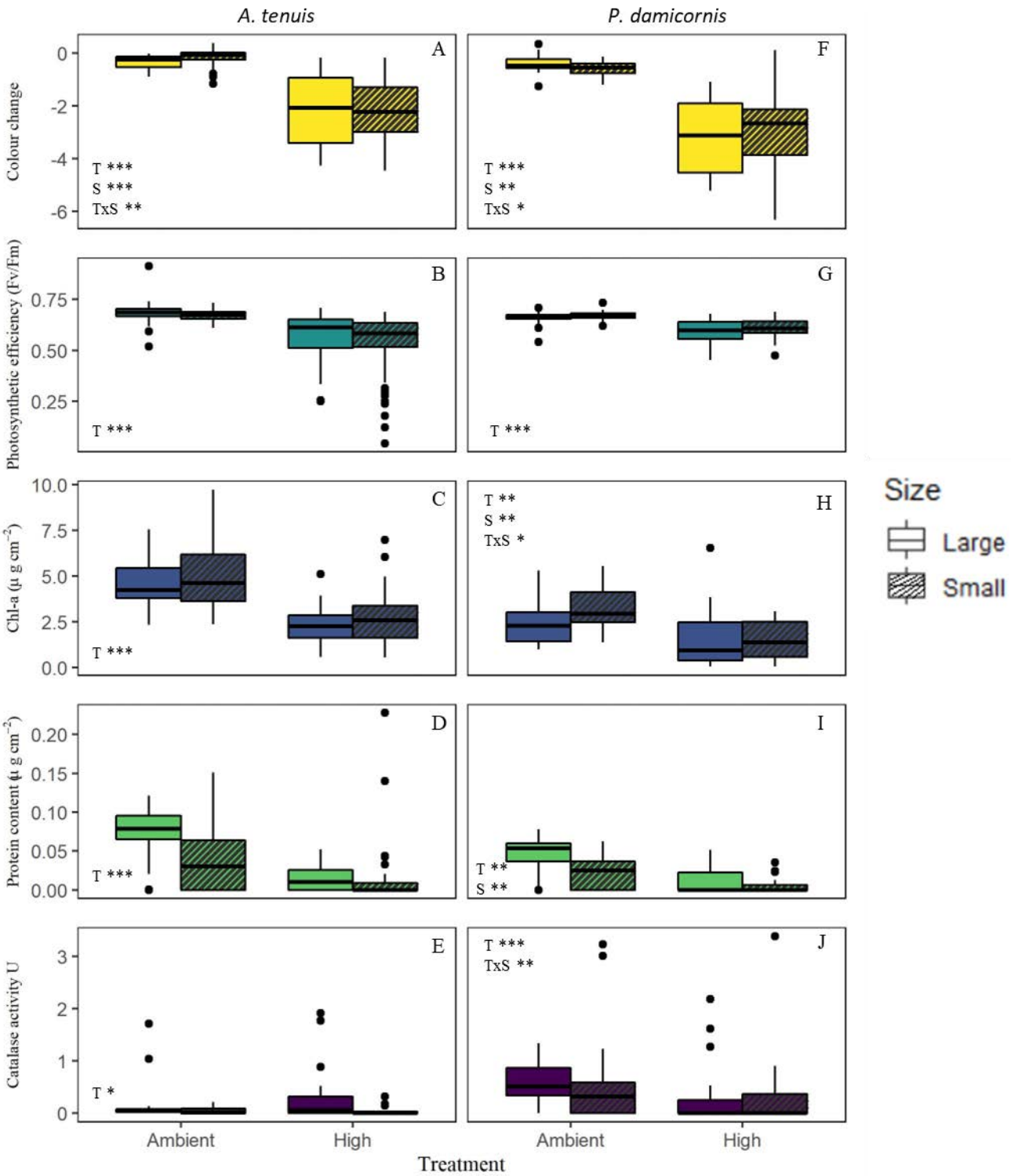

Figure 2.3 Physiological responses of large (full) and small (hatched) coral fragments to temperature treatment in *A. tenuis* (left panels) and *P. damicornis* (right panels). Bold line inside boxes shows the median, boxes indicate the interquartile range and dots represent data outliers. Significant effects are indicated for treatment (T), size (S) and their interaction (T x S) by asterisk where * $p < 0.05$, ** $p < 0.005$, *** $p < 0.0005$.

2.4.2 Experiment 2: Time effect

All physiological metrics except catalase experienced a significant initial decline immediately following heat stress (Appendix A.4). Most metrics then continued to decline through time before reaching a steady-state between 10 to 24 h after heat stress. However, photosynthetic efficiency was stable until the final sampling point at 48 h (Fig 2.4). Coral tissue colour recorded an initial decrease immediately following the exposure to heat stress (0h, T_0, -9.98%, z = -3.18, p = 0.0015), and remained stable until six h and then declined steadily until 24 h (T_5; post hoc T_2-T_5 t =7.57 p < 0.001) before stabilising again and remaining unchanged until 48 h (T_6, Fig 2.4A, T_5-T_6 t = 2.51, p = 0.18). Similarly, chlorophyll-*a* content declined at 0 h (T_0, -24.18%, z = -2.44, p = 0.015) before stabilising at 10 h (T_3, Fig 2.4A). In contrast, photosynthetic efficiency (F_v/F_m) declined by 5.8% immediately following the experiment (z = -2.4, p = 0.016) and remained stable until the 24-hour sampling point (T_5, Fig 2.4A) before declining again after 48 h (T_6, Fig 2.4A).

Antioxidative catalase activity did not change initially following exposure to heat stress but recorded a significant increase six h after heat stress (T_0-T_2, t = -3.24, p = 0.037). Catalase activity then decreased towards the end of the experiment and was nearly absent by 24 h (T_5, -88.38%, Fig 2.4B). Finally, protein content recorded an initial decrease immediately following heat exposure (26.44%, z = -2.35, p = 0.019) and then declined in the first 10 h (T_0-T_3 t = 3.48, p = 0.02) before stabilising (-58.1%, Fig 2.4B). All statistical outcomes from post-hoc comparisons are presented in Appendix A.5.

2.4.3 Experiment 3: Physiological measures comparisons

To investigate how rapid, non-invasive measures of coral thermal tolerance (F_v/F_m and colour change) compared to more time-consuming and labour-intensive measures, I performed a Principal Component Analysis. The PCA identified response patterns of multiple physiological measures to acute thermal exposure in *A. tenuis* (Fig 2.5). Four of the five physiological response measurements (colour change, protein and chlorophyll content, and F_v/F_m) were correlated to and accounted for variation along PC1 (43% variation explained), while only catalase activity separated data along PC2 (21% variation explained). All physiological metrics analysed were significant in driving the separation among samples (Fig 2.5A, Appendix A.6).

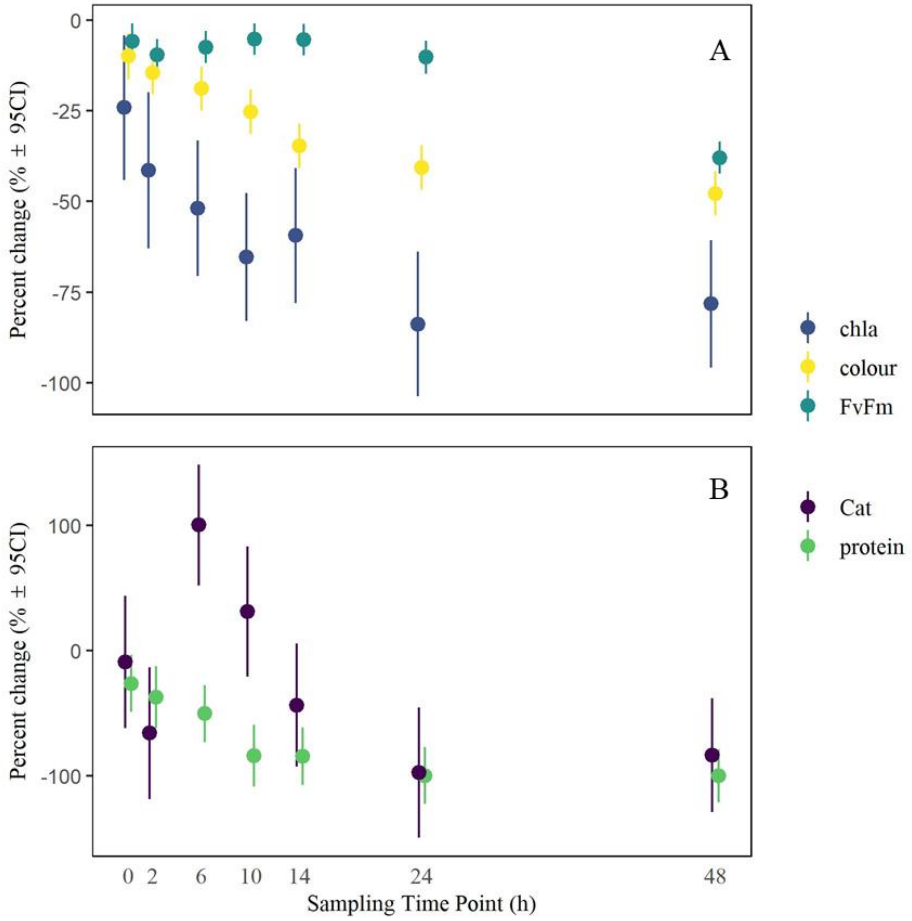

Figure 2.4 Percent change in physiological metrics over time in heat-treated relative to ambient corals. Fragments from nine colonies were sampled through time at 0 – 48 h(T_0-T_6) after the end of heat stress from both an ambient (29.6 °C) and heated treatment (34.6 °C). (A) Fluorometric and colour assays. (B) Biochemical assays. Points represent the estimated marginal means of physiological metrics at each sampling time point (T_1-T_6). Error bars indicate the upper and lower 95% confidence intervals.

To identify which metrics were driving data variability I examined correlations among the physiological metrics (Fig 2.5B). Both tissue colour change and maximum photochemical yield (F_v/F_m) showed a significantly positive correlation to the three laboratory-derived metrics (catalase, protein, and chlorophyll-α content). Both tissue colour change and F_v/F_m were most strongly correlated with host protein content. As such, both non-invasive physiological measures of tolerance describe overall patterns observed.

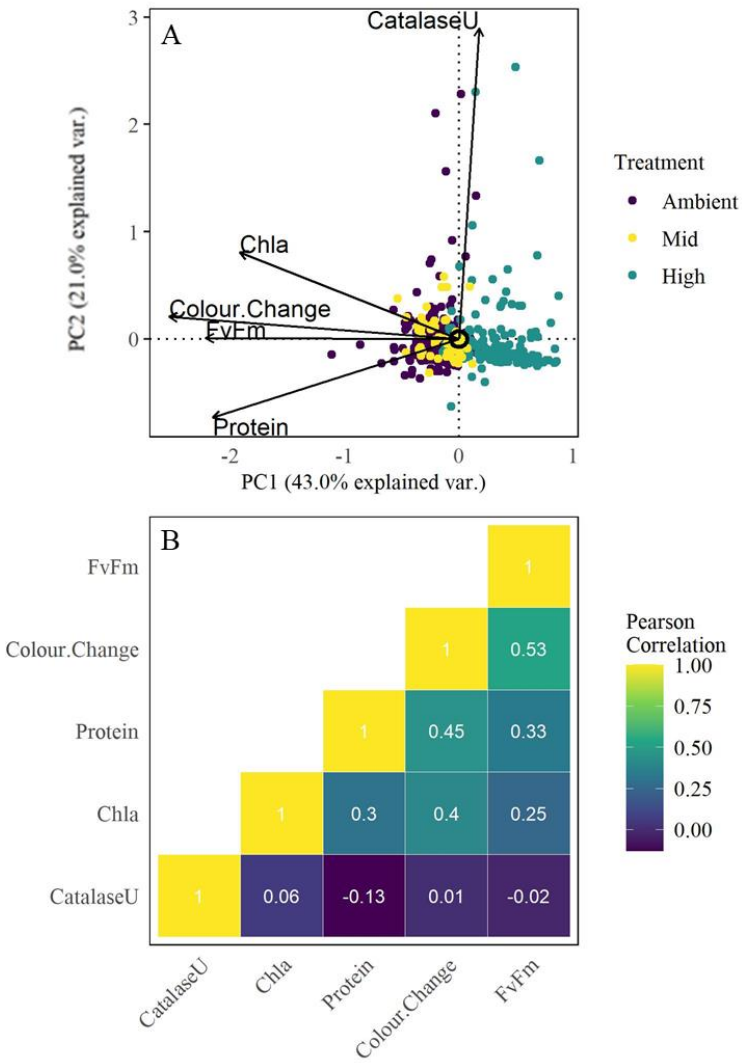

Figure 2.5 Relationships between multiple physiological responses to heat stress in *A. tenuis*. (A) Principal Component Analysis (PCA) of five physiological traits in response to acute heat stress in *A.tenuis* (n reefs = 7, n samples = 423) and (B) correlation heatmap between all traits. Yellow diagonal are self-comparisons.

2.4.4 Cost-benefit analysis

Of all physiological measurements utilised here, the more rapid field-based measures of maximum photochemical yield (F_v/F_m) and tissue colour change carried the lowest associated costs (including labour) and were also the most time-efficient (Tables 2.2 and 2.3, Appendix A.7). Based on 100 samples, I estimated a time of ~ 45 min to gather and a further 45 min to analyse maximum photochemical yield data and ~100 min to gather and analyse tissue colour changes. In comparison, > 28 h was required to quantify protein content in the laboratory with catalase and chlorophyll assays each requiring approximately 25 h to complete.

Table 2.2 Cost of consumables and time requirements for each assay to process 100 samples.

Assay	Consumable cost 100 samples ($AUD)	Time requirement 100 samples (min)	Time cost $33 h^{-1}	Total
Photosynthesis efficiency (PAM)	NA	90	$49.5	$49.5
Tissue colour change	NA	102	$56.1	$56.1
Tissue blasting	$156	1210	$665.5	$821.5
Chlorophyll	$27	305	$167.75	$194.75
Protein	$49	463	$254.65	$303.65
Catalase	$85	480	$264	$349
Surface area	$4.2	585	$321.75	$325.95
Total for 100 samples	$321.2	54h	$1,782	
			Grand total	**$2,103.2**

Table 2.3 Costs and benefits of measures of coral thermal tolerance. Benefit classification used based on 100 samples; financial; Cheap < $200, Moderate $200-$600, Expensive > $600. Time; Effective < 5h, Moderate 5 -10 h, Intensive >10 h per 100 samples. Level of training required; low = little to no instruction required, easy to do from protocol, no specialised laboratory skills required; Moderate = some basic laboratory skills required, operator generally supervised a couple of times then works from protocol, special instruction in equipment use. Hourly rate used for time cost is $33 AUD per hour. See Appendices A.7 and A.8 for an overview and price-guideline for the equipment required for each of these assays. Cell colours reflect coding for high (red; expensive, intensive), medium (yellow; moderate) and low (green; cheap, effective, low) across categories.

Assay	Location	Cost	Time	Level of training required
F_v/F_m	Field	Cheap	Effective	Moderate
Colour change	Field	Cheap	Effective	Low
Tissue blasting	Lab	Expensive	Intensive	Low
Chlorophyll	Lab	Moderate	Moderate	Moderate
Protein	Lab	Moderate	Moderate	Moderate
Catalase	Lab	Moderate	Moderate	Moderate
Surface area	Lab	Moderate	Moderate	Low

2.5 Discussion

Variation in coral thermal tolerance both within-(Cornwell et al., 2021; Marhoefer et al., 2021) and between-(McClanahan et al., 2020) reef systems is likely key to their continued survival under further ocean warming (Drury et al., 2017; Magozzi & Calosi, 2015; Morikawa & Palumbi, 2019). To date, aquarium-based ramp-and-hold experiments have been widely applied to investigate variation in thermal tolerance but are limited logistically in terms of how many samples can be included and the sampling areas they can cover. Recently, acute heat stress assays have increased the capacity to quantify heat tolerance in adult corals (e.g. Cunning et al., 2021; Voolstra et al., 2020) through field-deployments with rapid experimental turnover. However, efforts to scale towards higher throughput both within studies and through comparisons among studies must be based on solid methodologies that control technical sources of variance and utilise common measures of coral thermal tolerance (Grottoli et al., 2021; McLachlan et al., 2020).

This study investigated the effect of fragment size and sampling timing on coral acute thermal tolerance. I presented a cost analysis of all physiological measures analysed herein to provide planning background to other users of acute thermal stress assays and finally, I showed how rapid, non-invasive measures of coral thermal tolerance (F_v/F_m and tissue colour change) compared to more time-consuming and labour-intensive measures using evidence from multiple physiological traits. Together, these results highlight the need to consider fundamental experimental design criteria of these assays to ensure that results are repeatable and comparable among studies.

2.5.1 Fragment size affected P. damicornis more than A. tenuis

There are currently no guidelines on appropriate fragment sizes for experimental examination of coral thermal tolerance (Grottoli et al., 2021) and this metric is rarely reported (McLachlan et al., 2021). The coral restoration literature has suggested that larger fragments may result in greater survival (Okubo et al., 2007) although this is not always the case (Bruno, 1998; Howlett et al., 2021; Suggett et al., 2019). With the advance of acute heat stress assays, fragment size could therefore be a source of technical variability. In this study, effect of fragment size differed between species; one out of five physiological responses of *A. tenuis* were significantly affected by fragment size while in *P. damicornis* four out of five measures showed significant fragment size effects. In *A. tenuis*, large fragments showed greater colour loss than the small fragments

in the ambient treatment. Similarly, fragments of *Acropora palmata* have recorded differential bleaching resistance during a natural thermal stress event where small fragments recorded less bleaching than larger ones (Pausch et al., 2018). Additionally, corallite formation differs between the two species where *A. tenuis* produces an apical corallite characteristic for the *Acroporids* while *P. damicornis* does not. The presence of an apical corallite in the absence of Symbiodiniaceae-rich tissues could potentially skew the colour change metric. Whilst I did not test this factor explicitly, it would be important in the future to consider species-specific morphology when designing data-gathering protocols that span diverse taxa.

Changes in protein content and catalase enzyme activity were more pronounced in large relative to small fragments in *P. damicornis*. Protein and catalase assays from small fragments may be nearing the detection limits of the instrument (spectrophotometer), and the issue is further compounded by quantifying surface area by wax dipping as uncertainty increases when used on small fragments (Veal et al., 2010). To avoid potential detection limits of assays and instruments, I recommend using larger fragments (~ 9 cm^2 for *A. tenuis* and ~ 12 cm^2 for *P. damicornis*). Ultimately, properties that require normalisation – and therefore introduce error propagation from >1 measurement – may be less suitable to detect more subtle changes through acute stress experimentation. Interestingly, size effects primarily occurred in ambient-treated corals and were absent in heat-treated fragments, suggesting that a fragment size effect is introduced to the experiments initially, but that this effect is insignificant compared to the applied heat exposure. While this is important to consider when comparing heated to non-heated coral fragments, I demonstrate no size effect on physiological responses in either species in the heated treatment, highlighting that any initial size effects are not likely to influence thermal tolerance results obtained by this approach.

2.5.2 Choosing when to sample post heat stress impacts conclusions drawn

Responses to heat stress varies with exposure duration and sampling time. Sampling variation may therefore limit how different combinations of measurements can ultimately be used to reconcile large-scale heat stress assay data sets. Therefore, sampling time is a critical component of experimental design. Here I observed that physiological responses decreased up to 24 h post heating with the notable exception of photosynthetic efficiency which was stable up to 24 h. I therefore recommend sampling between 10 – 24 h post heating. Sampling prior to 10 h post heating could fail to detect a response while sampling post 24 h may result in sampling

of mortality or severe tissue necrosis, particularly at higher temperatures (see Voolstra et al., 2021b). I did not sample past two days post heating (48 h) to maintain the rapidity of these acute heat stress assays. Other studies have also reported rapid changes in response to acute heat stress; for example, Dove et al., (2006) found significantly reduced protein and chlorophyll content following a six-hour temperature exposure while Traylor-Knowles et al., (2017) found upregulated heat shock protein expression in response to heat stress after only 2 h 30 min and evidence of protein degradation after 5 h. The decline through time observed in most traits in the present study may complicate direct comparisons of results between studies depending on the traits quantified and the sampling time point.

2.5.3 Time- and cost- efficient physiological measures to capture coral thermal tolerance variability

Capitalising on the rapid throughput of acute heat stress assays requires the adoption of standardised phenotyping measures which can be quantified rapidly in the field at minimal cost. Maximum photochemical yield (F_v/F_m) and tissue colour change are both time- and cost-efficient to capture, making them ideal candidate measurements for rapid tests of coral thermal tolerance. While photosynthetic efficiency was the fastest measure quantified in this study, the capital outlay for a fluorometer such as the one used here (~$50,000 AUD) may be beyond the scope of some groups. However, cheaper alternatives exist (for example AquaPen®, ~$4,050 AUD) and the costings presented here are highly conservative. While fluorometric data is fast to gather and has a low cost per sample when considering the lifespan of the instrument, it is not currently possible to calibrate fluorometric data between studies due to the lack of universal standards, multiple sensor types, and diverse sampling protocols used (Schuback et al., 2021; Suggett et al., 2022). This makes direct comparisons between studies challenging.

When considering capital costs and accessibility, tissue colour change is by far the most cost-effective measure captured, further reducing processing and analysis time investment through the development of automated approaches (Macadam et al., 2021). Recent technological advances also allow scaling of automated bleaching assessments with the implementation of new technologies such as hyperspectral imaging (Teague et al., 2019), despite additional and significant capital costs. If these rapid measures (tissue colour change and F_v/F_m) are to be used at a large scale, it is important to keep their relationship to coral thermal tolerance in mind and carefully consider which measures best address the research question.

2.5.4 Selecting physiological measures of coral thermal tolerance for acute heat stress assays

Photosynthetic efficiency and tissue colour change are higher-order traits, derived from multiple other measures. For example, changes in tissue colour can result from a loss of Symbiodiniaceae cells, loss of chlorophyll pigmentation within those cells (Chow et al., 2016), or the loss of coral tissue itself. Photosynthetic efficiency, on the other hand, is a direct measure of viability of the symbiont partners and only an indirect indicator of thermal tolerance of the coral holobiont (Middlebrook et al., 2010; Suggett & Smith, 2011). I therefore examined whether tissue colour change and photosynthetic efficiency captured differences in other physiological measures of thermal tolerance in *A. tenuis*. I found that both photosynthetic efficiency and tissue colour change showed similar responses to heat stress as chlorophyll-*a* and protein content but not catalase activity. Similarly, acute heat stress studies of *Stylophora pistillata* (Evensen et al., 2021) found that changes in F_v/F_m values correspond well to other physiological measures quantified and a high correlation between F_v/F_m and tissue colour change was reported in *Siderastrea sidereal* (Davies et al., 2018). Coral host catalase activity showed an opposite trend to all other measures as catalase was correlated to PC2 rather than PC1 (Fig 2.5A). The opposing trend displayed by the catalase vector in the PCA is expected as catalase generally increases during heat stress (Krueger et al., 2015; Tang et al., 2020), while all other measures quantified here are expected to decrease. As a mechanistic measure of heat tolerance, catalase activity or other antioxidative enzymes provide valuable insight into the host responses to acute heat stress (Krueger et al., 2015) but are impractical and time-consuming for 'routine' use of high throughput assays. Due to the scalability of acute heat stress assays, it is also possible to utilise these experiments for higher throughput mechanistic studies including metabolomics, proteomics and gene expression analyses (Sweet et al., 2021; Voolstra et al., 2021b).

Finally, when selecting which physiology traits to measure for acute heat stress assays, it is important to consider the data variability that appears inherent with this experimental approach. I document large standard errors in all responses despite sampling > 110 colonies. However, this is also the case for other acute heat stress assays (Klepac & Barshis, 2022; Voolstra et al., 2020). As such, alternate indicators of thermal tolerance may have different capacities to resolve subtle differences in temperature thresholds (Evensen et al., 2022).

Acute stress experiments have resolved thermal tolerances of many organisms including fish (Newton et al., 2010; Waltham & Sheaves, 2017), intertidal invertebrates (Iwabuchi & Gosselin, 2020), extremophiles (Cox et al., 2010), and coral; both in adult life stages (Voolstra et al., 2020) and larvae (Dixon et al., 2015; Quigley et al., 2017). Here, I assess aspects of experimental design for acute heat stress assays and their applicability to coral studies. I suggest that sampling occurs more than 10 h after the end of heat stress but before the 24 h mark. I conclude that by adopting standardised approaches, these experiments have the capacity to address the yet unresolved mechanisms of thermal tolerance and provide a means to obtain information spanning emergent physiological responses and thermal thresholds to underlying transcriptional regulation (Voolstra et al., 2021a) and form the basis in moving towards a systems biology approach (Cocciardi et al., 2019). If large datasets are collected across spatial and temporal scales, insights such as environmental and genomic drivers of tolerance and thermal adaptation could be identified. Scaling efforts to quantify thermal tolerance is becoming increasingly important due to the continued threat to coral reefs globally from climate change.

Data availability statement

Data and associated code to produce the statistical and graphical components of this manuscript are available on JJVN's GitHub (https://github.com/josephinenielsen/AcuteHeatStressMethods_SciReps.git).

Chapter 3 Patterns of upper thermal performance in reef-building corals on the Great Barrier Reef are influenced by sector-level differences in thermal disturbance history

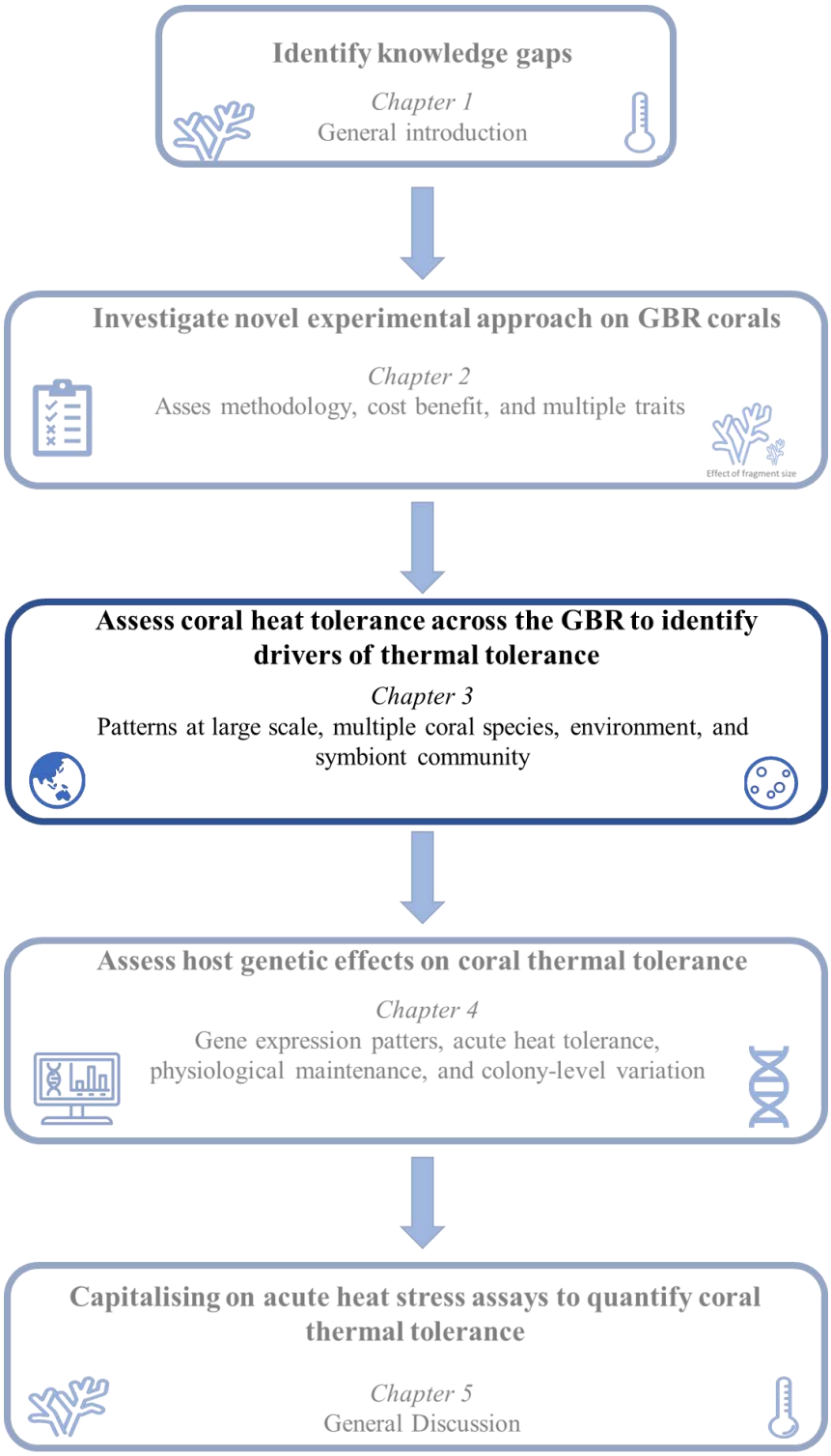

3.1 Abstract

Mortality from coral bleaching is a significant threat to reefs worldwide. The capacity of corals to acclimate and/or adapt is important for their continued survival under all projected global emission scenarios. Variation in the susceptibility of different coral species and individuals to thermal stress varies greatly, and large-scale studies of coral thermal tolerance provide an opportunity to investigate the potential for both acclimation and adaptation across individuals, populations, and environmental gradients. Here, I deployed acute heat stress assays across 11.5° latitude to quantify and describe patterns of acute heat tolerance in multiple coral species and populations. I show that the number of mild heat stress events (DHW >3) were highly negatively correlated while maximum sea surface temperature (max_SST) were highly positively correlated with acute heat tolerance (represented here by ED50) across three common reef-building coral species along the latitudinal extent of the Great Barrier Reef. I also show that *Pocillopora verrucosa* has a higher acute heat tolerance (36.21°C) compared to both *P. meandrina* (35.22°C) and *Acropora tenuis* (35.31°C). The high acute heat tolerance observed in the northern GBR and in *P. verrucosa* is likely influenced by recent severe warming events while the acute heat tolerance of both *P. meandrina* and *A. tenuis* were more strongly correlated with longer-term trends in SST. Differences in acute heat tolerance between species likely reflect their spatial distribution patterns on the GBR and the differences in recent thermal disturbance histories within reef sectors. Symbiont community composition varied significantly across environmental gradients within each species. Specifically, differences within symbiont community composition in *P. meandrina* were associated with variable acute heat tolerance between colonies, with the dominant symbiont taxa differing between *P. meandrina* and *P. verrucosa.* Finally, I show that the relationship between acute heat tolerance (ED50) and coral physiology (catalase activity, protein, and chlorophyll-*a* content) differed between the two *Pocillopora* species. When ED50 was modelled as a function of all co-variates investigated, maximum SST was the strongest driver of acute heat tolerance. Taken together, these results highlight the need to consider drivers of thermal tolerance within the coral holobiont across scales. Understanding the distribution of thermally tolerant coral individuals and their associated symbiont communities is important for future projections of coral demographics and a necessary first step in developing targeted management approaches to optimize the return on effort of coral restoration.

3.2 Introduction

Coral bleaching is a sign of poor reef health that results in fitness reductions (Leuzinger et al., 2012), increased disease susceptibility (Pinzón et al., 2014) and ultimately drives mortality of reef-building corals (Maynard et al., 2008). While bleaching can result from multiple environmental disturbances, it is most widely recorded as a response to thermal stress, typically elicited when water temperatures exceed long-term mean maximum temperatures by 1 - 2ºC (LaJeunesse et al., 2007; Smith & Spillman, 2019). If elevated temperatures are extreme or prolonged, bleaching can rapidly lead to widespread coral mortality (Hughes et al., 2018). Bleaching events have occurred throughout the tropics with three mass bleaching events (2016/17, 2020, and 2022) recorded since 2016 on the Great Barrier Reef (GBR) of varying spatial extent, duration, and severity (Fig 1.1; Hughes et al., 2017; Page et al., 2023; Spady et al., 2022). Studies relying on reciprocal transplant experiments have shown that local adaptation to thermal regimes can occur (Howells et al., 2013; Palumbi et al., 2014; Schoepf et al., 2015a) with corals exhibiting significant capacity for plasticity and genetic adaptation (Marhoefer et al., 2021). However, the adaptive component and extent of this tolerance is not well-understood.

Quantification of thermal and bleaching tolerance requires the use of traits across multiple scales of biological organisation (Cziesielski et al., 2018; Gardner et al., 2017a). Growth and reproductive output are key fitness traits (Edmunds & Putnam, 2020; Madin et al., 2016); however, both are temporally-intensive to measure robustly, making them less feasible to quantify for large-scale, high-throughput studies of coral thermal tolerance. As such, the use of proxy traits is required (Carturan et al., 2018; Muller et al., 2018). Photosynthetic performance is considered a key indicator of early-onset thermal stress due to its importance in coral productivity but also due to its role in the symbiosis breakdown between the coral host and the endosymbionts (Warner et al., 1996). Photosynthetic performance is quick and relatively cost-effective to quantify in the field (Nielsen et al., 2022) and has been widely used in acute high-throughput heat stress assessments of coral thermal tolerance (Cunning et al., 2021; Evensen et al., 2022; Marzonie et al., 2022; Voolstra et al., 2020). Such studies have employed an Effective Dose 50 (ED50) measurement as a proxy of coral thermal tolerance. ED50 is a widely used concept in pharmacology and ecotoxicology to describe the medicinal dose required to induce a specific response in 50% of the population subjected to the dose

(Kenny et al., 2022; Tallarida, 1992). In the case of coral thermal tolerance research, ED50 values represent the temperature required to reduce the maximum photochemical yield (F_v/F_m) by 50% relative to a control (Evensen et al., 2022; Marzonie et al., 2022), and where ED50 temperature can be expressed either in absolute terms, typically around ~33-36ºC (Cunning et al., 2021; Evensen et al., 2022) or in relative terms as ºC above local maximum monthly mean (MMM) temperatures (Marzonie et al., 2022).

Whilst coral heat and bleaching tolerance is shaped by thermal histories (McClanahan et al., 2007; Scheufen et al., 2017), the main driver remains highly debated. Some studies highlight the importance of the maximum temperature and deviation from MMMs (Berkelmans & Willis, 1999; Claar et al., 2018; Glynn & D'Croz, 1990), whereas others emphasise the critical role of temperature variability enhancing thermal tolerance (Marhoefer et al., 2021; Palumbi et al., 2014; Schoepf et al., 2015b). For example, in a review of observed bleaching patterns, Baumann et al., (2016) found that number of days above the bleaching threshold (MMM+1ºC) was the main determinant of coral community composition on reefs in Belize. In contrast, multiple studies have shown that average thermal variability appears to predominantly determine coral thermal tolerance across multiple physiological (growth, F_v/F_m) and demographic (population-level) traits (Barshis et al., 2018; Cornwell et al., 2021; Sully et al., 2019). Safaie et al., (2018) further demonstrated that high frequency (daily temperature range) thermal variability best predicted coral bleaching severity out of 27 thermal metrics, and that only a 1ºC increase in daily temperature range reduced the likelihood of severe bleaching by a factor of 33. Such daily fluctuations also appear significant in aposymbiotic corals (*Platygyra verweyi* in Taiwan; (Wang et al., 2019), where corals from thermally variable environments recorded much higher threshold temperatures relative to corals from a more homogeneous site. As such, the heterogeneous environments of coral reefs has likely given rise to differential thermal tolerances between populations, species, and even individuals (Quigley & van Oppen, 2022). Along with the highly heterogenous thermal environment of coral reefs, local-scale environments are also impacted by a range of oceanographic processes (wave energy, upwelling, etc) promoting environments that may reduce local heat stress (Eakin et al., 2009; Wyatt et al., 2023), further confounding the partitioning of differential thermal tolerance to any one metric/environment characteristic.

Corals exist in symbiosis with a wide range of micro-organisms – comprising a microbial community – that can also impact the thermal tolerance of the host (Voolstra et al., 2021a; Ziegler et al., 2017). In particular, the type of endosymbiotic dinoflagellates (Family:

Symbiodiniaceae; LaJeunesse et al., 2018) affects the coral holobiont thermal tolerance (Berkelmans & van Oppen, 2006; Cunning & Baker, 2020; Silverstein et al., 2015). The symbiosis between the coral animal and the endosymbiotic Symbiodiniaceae can be either highly conserved or flexible. Some genera, such as *Porites* are known to associate with only a few symbiont types (Cunning et al., 2015; Edmunds et al., 2012) while other coral taxa associate more freely with multiple types (Abrego et al., 2008; Quigley et al., 2022b). Different symbionts can confer alternate thermal tolerance limits to their coral hosts with some types known to increase holobiont tolerance by 1°C (Berkelmans & van Oppen, 2006); for example, *Durusdinium* (LaJeunesse et al., 2018) is often associated with corals living in warmer environments (Cunning et al., 2015; Rowan, 2004). Evidence has shown that symbiont communities can be either stable across large spatial scales (Sawall et al., 2014) or exhibit extensive variation across even small spatial scales (<1 km; De Souza et al., 2022; Ros et al., 2021). Therefore, it is important to resolve spatial distribution patterns of thermally tolerant symbionts as well as the genetic and community-level diversity harboured by corals. Such a step is essential to identify coral populations for targeted spatial management and understand large-scale patterns of symbiont communities.

To better understand the drivers of variation in coral thermal tolerance, I determined proxies for the upper thermal tolerance in three common corals species *Pocillopora verrucosa*, *P. meandrina*, and *Acropora tenuis* across 11.5^{o} of latitude on the Great Barrier Reef, Australia. Specifically, I quantified four physiological proxies for bleaching tolerance (F_v/F_m for all species; and changes in chlorophyll-*a* and protein content along with catalase activity in the two *Pocillopora* species) to acute heat stress exposure and examined the extent to which variation could be explained by thermal environment characteristics across 19 reefs. I further analysed differences in Symbiodiniaceae community composition within the *Pocillopora* species to resolve the extent to which observed variations in acute heat tolerance could be explained by changes in symbiont association. *P. verrucosa* showed higher acute heat tolerance than *P. meandrina* and *A. tenuis,* which likely reflected both sector-wide thermal disturbance histories and differences in symbiont communities. Overall, the variation found in this study highlights the need to consider drivers of heat tolerance in multiple coral species across large spatial scales.

3.3 Materials and Methods

3.3.1 Collections and field experiments

This study was conducted at 19 reefs across the GBR. Collections were made under GBRMPA Permits # G16/38488, G19/43423.1, and G19/43148.1 (Fig. 3.1; Appendix B.1). Field collections and experimental protocols followed those in **Chapter 2** (Nielsen et al., 2022). In brief, coral fragments were collected on SCUBA, stored in perforated plastic zip-lock bags for no more than two h before being further fragmented onboard the research vessel and then distributed through all treatments such that each colony was present in all treatments. In total, 17 runs of the heat stress system were completed. All fragments were secured upright on PVC racks and photographed within 30 min prior to treatment. Temperature started at 11am for each run and was ramped from local maximum monthly means (MMM) to target treatment temperatures over a three-hour period, held for three h, before being ramped down over 1.5 – 2 h. One hour after ramp down, all samples were assessed for photochemical yield of Photosystem II (F_v/F_m). Following an 11 h hold at MMM, fragments were again photographed and snap-frozen in liquid nitrogen for subsequent laboratory processing. Artificial light was provided (500 µmol photons m^{-2} s^{-1}, no ramping, 12h:12h light:dark, 60% blue, 20% white, 10% green, and 10% red, 10 m, Lizard Island Light From 26 Feb 2012 | AIMS metadata | aims.gov.au) from beginning of each run until 7pm at night. Flow rates were set to 0.8 L min^{-1} (turn-over rate once per hour).

3.3.2 Species selection

Three coral species *Acropora tenuis, Pocillopora meandrina*, and *P. verrucosa* were chosen for this study. *A. tenuis* and *P. verrucosa* were chosen partly due to their wide-ranging distributions on the GBR (Lukoschek et al., 2016) and expected differences in thermal tolerance (Guest et al., 2012; Pratchett et al., 2013). *P. meandrina* was included to provide a within-genus comparison between two closely related species (Johnston et al., 2022) previously shown to possess different acute heat tolerances (Marzonie et al., 2022). Species-level identification of the *Pocillopora* species was performed by RFLP assays (Fig 3.1F-G, see section *3.3.4.1* below). Photosynthetic performance was assessed for all three species across the GBR and the resulting acute heat tolerance trait (ED50, see below) was used in the environmental co-variates analysis. To explore acute heat tolerance further, physiological

measurements (tissue colour change, catalase activity, protein, and chlorophyll-*a* content) and Symbiodiniaceae community composition were assessed for *P. meandrina* and *P. verrucosa* to ensure deeper characterisation of the acute heat stress response.

3.3.3 Physiological measurements

Maximum photochemical yield (F_v/F_m, dimensionless) was assessed for all species by chlorophyll-*a* fluorescence. Corals were dark acclimated for 30 min prior to measurement by Pulse Amplitude Modulated (PAM) Fluorometry using a Diving-PAM (Heinz Walz GmbH, Effeltrich, Germany, MI = 8, SI = 8, saturation width = 0.8, Gain = 3, Damp = 2). A clear piece of PVC tube was used to maintain a set distance (2 mm) from the coral fragment and the fibre-optic probe (6 mm Ø). *Acropora tenuis* measurements were taken at 1/3 distance from the fragment tip on opposite sides of the fragment to minimise overlap between replicate measurements. *Pocillopora* measurements were taken on flat tissue surfaces which were not shaded from the experimental lights by other parts of the fragment. Each fragment was measured 2-3 times, and the values averaged. As ED50 is relatively new in coral research outside ecotoxicology (see Voolstra et al., 2020), other physiological metrics of coral health (including chlorophyll-*a* and protein content, catalase enzyme activity, and tissue colour) were also assessed for responses to acute heat stress. Changes in coral tissue colour was assessed by photographs following Nielsen et al (2020, 2022). Photographs were taken of each fragment before and after treatment, including the CoralWatch Coral Health Chart as a colour standard (Siebeck et al., 2006) and all photographs were processed with ImageJ. All laboratory-based physiological assays were prepared using the air-tissue stripping technique and conducted as previously detailed in **Chapter 2** (Nielsen et al., 2022), and quantified with spectrophotometric-based protocols. Chlorophyll pigments were ethanol extracted (Ritchie, 2006) and total water-soluble protein content quantified with the Bio-Rad *DC* Protein Assay following the manufacturer's recommendations. Catalase enzyme activity was calculated over the linear part of the absorption curve as a change in H_2O_2 concentration over time (Krueger et al., 2015).

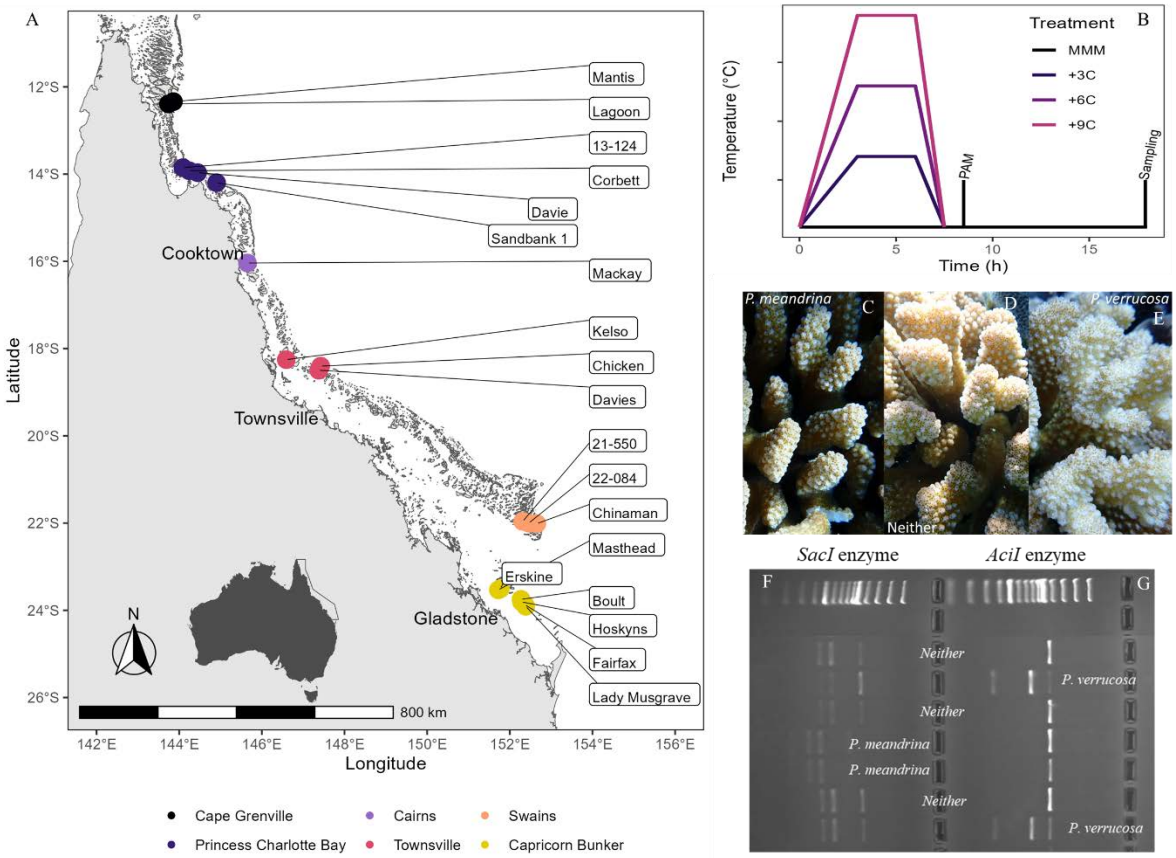

Figure 3.1 Collection details and experimental design. (A) Map of collection sites with reefs coloured by their respective GBR reef sectors. (B) Representative experimental heating profile indicating the four temperature treatments (MMM, +3ºC, +6ºC, +9ºC), time point of quantification of maximum photochemical yield (F_v/F_m) marked as PAM on the profile, and preservation (sampling) for laboratory assays. (C) Example colony confirmed by RFLP as *Pocillopora meandrina*. (D) Example colony that was not assigned as either *P. meandrina* or *P. verrucosa* by RFLP, and (E) Example colony confirmed as *Pocillopora verrucosa* by RFLP. (F) *SacI* enzyme RFLP to identify *P. meandrina* samples with the presence of two bands compared to three (not *P. meandrina*) and (G) *AciI* enzyme RFLP to identify *P. verrucosa* samples with the presence of three bands compared to one (not *P. verrucosa*).

3.3.4 Symbiodiniaceae composition

3.3.4.1 DNA extraction and *Pocillopora* identification

DNA was extracted from frozen coral samples following a modified Wayne's approach (Wilson et al., 2003). Tissue (~20 mg) was removed with a scalpel in a petri dish. The lysis buffer (250 µL; MilliQ 159.5 µL, Tris pH 9 27.5 µL, EDTA 55 µL, NaCl 5.5 µL, SDS 27.5 µL) was added to the petri dish and used to transfer the coral tissue to a microcentrifuge tube (1.5 mL). Scalpel and forceps were cleaned in bleach (10%) and MilliQ between samples. A new petri dish was used for each sample. Samples were vortexed (5 s) and incubated for 30

min (37ºC). Samples were transferred to ice and 7 µL of Proteinase K was added along with ~ 10 acid-washed glass beads (710-1,180 µm). The samples were bead-beaten (FastPrep FP24-5G, All-Metal QuickPrep, 30 s X 3 at 4 m s^{-1}) before being incubated for 1 hour (65ºC, 30 rpm). Then 62.5 µL of KOAc (5M) was added, samples vortexed and incubated on ice for 30 min. Samples were centrifuged (15 min, 14,680 rpm) and the resulting supernatant transferred to a clean tube (1.5 mL). RNA-ase (10 µL) was added and samples vortexed before incubation at 37ºC for 30 min. DNA was precipitated by the addition of 250 µL of isopropanol (100%), vortexing, and centrifuging (15 min, 13,000 rpm). The supernatant was discarded and ethanol added (250 µL, 70%). Tubes were gently flicked to resuspend the DNA before centrifuging again (5 min, 13,000 rpm). The pellets were air-dried until no droplets were visible (15-20 min) and 50 µL of UltraPure H_2O was added. Samples were left in the fridge (4ºC) for a minimum of 24 h to allow DNA to fully resuspend in the water. DNA concentrations were checked by Qubit High-Sensitivity assays where all samples were diluted 1:10 to avoid overloading the Qubit reader (max concentration 100 µg $µL^{-1}$).

DNA extracted from *Pocillopora* samples was normalised to a concentration of 10 ng $µL^{-1}$ with UltraPure H_2O. Species ID was confirmed for all extracted colonies using Restriction Fragment Length Polymorphism assays (RFLP) with the *AciI* restriction enzyme kit (Johnston et al., 2018; Magalon et al., 2007). The PCR mix consisted of 4 µL MyTaq Buffer (5x), 0.4 µL MyTaq Polymerase, 0.25 µL of the forward and reverse primers (ORF FatP6.1, Appendix B.2), 0.3 µL BSA, and 12.8 µL MilliQ per sample. 2 µL DNA (10 ng $µL^{-1}$) was added to each tube to make a total volume of 20 µL. PCR conditions were as follows; initial denaturation of 60 s at 94ºC followed by 40 cycles of elongation (30 s at 94ºC, 30 s at 53 ºC, 75 s at 72 ºC), and final incubation at 72 ºC for 5 min. After PCR, samples were digested with the *AciI* enzyme kit (0.1 µL enzyme, 1.0 µL 10x NE buffer, 8.9 µL PCR product) first at 37 ºC (1 h) followed by 20 min at 65 ºC. Digested samples were visualised on a gel (3 µL digested product, 2% agarose TAE, 90 min, 70 V) using a 100 bp ladder (GeneRuler) as a reference. Samples showing three bands (209, 338, 431 bp) were confirmed to be *P. verrucosa*. Samples where only two bands were visible were further investigated to test if they were *P. meandrina* which was confirmed by digestion with the *Sac*I enzyme (0.05 µL enzyme; 1 µL 10xNE buffer; 8.95 µL PCR product per sample). This was incubated for 1 h (37 ºC) and digestion halted by incubation at 65 ºC for 20 min. Gels were visualised similarly to the *verrucosa* RFLP gels and corals showing two bands (298, 682 bp) were designated as *P. meandrina*. Corals that could not be confirmed as

either *P. meandrina* or *P. verrucosa* were classed as "*unidentified*" although likely to be a cryptic species of either *P. meandrina* or *P. verrucosa* as per Johnston et al., (2022). These unidentified samples were excluded from analysis (Fig. 3.1 C-E).

3.3.4.2 ITS2 Sequencing

Symbiodiniaceae DNA was amplified by PCR targeting the ITS2 gene region using primers from Pochon et al., (2001). For each sample, the master mix contained the following: UltraPure water (16.5 µL), forward and reverse primer (Appendix B.2), 1 µL each, final primer concentration of 0.4 µM each), MyTaq buffer (5x, 5 µL), MyTaq DNA polymerase (2.5U, 0.5 µL), and 10 ng of DNA template in 1 µL buffer. The PCR heated to 95ºC for 3 min followed by 30 cycles consisting of a hold at 95ºC (30 s), 59ºC (30 s), and 72ºC (30 s). This was followed by a final hold at 72ºC for 7 min. PCR products were visualised on an agarose gel (2% agarose, 0.5x TBE, 90 V, 30 min, EtBr stain) on the Fusion FX® Imager (Vilber Lourmat, Collégien, France). PCR products were randomised across species within plates and submitted to Ramaciotti Centre for Genomics (UNSW, Sydney, Australia). Samples were sequenced on a single run of the Illumina Mi-Seq v3 platform using 2x300bp read lengths.

3.3.5 Thermal covariates of acute heat tolerance

To examine the extent to which thermal history characteristics underly differences in acute thermal tolerance between species, nineteen temperature variables were selected (Appendix B.3). Maximum monthly mean (MMM) temperatures were obtained from NOAA Coral Reef Watch Operational Daily Near-Real-Time Global 5-km Satellite Coral Bleaching Monitoring Products, accessed through ERDDAP - NOAA Coral Reef Watch Operational Daily Near-Real-Time Global 5-km Satellite Coral Bleaching Monitoring Products - Data Access Form (hawaii.edu) for each individual reef coordinate. These describe both long-term patterns in Sea Surface Temperatures (SST) as well as disturbance history characteristics (DHWs). Long-term SST and DHW variables were collected in weekly time-steps from 1985 until 1 week prior to reef-specific collection dates while recent variables covered only the five years immediately prior to collection.

3.3.6 Statistical methods

3.3.6.1 Acute heat tolerance and ED50

To enable comparisons of heat required to stress multiple populations and quantify acute heat tolerance, ED50 values were calculated from the maximum photochemical yield (F_v/F_m) data at 15 reefs. Four reefs had to be omitted due to insufficient declines in F_v/F_m to derive ED50s. The ED50 response curves (Evensen et al., 2021; Marzonie et al., 2022) were constructed in R (R Core Team, 2022), using the *medrm()* function (Package medrc, Gerhard & Ritz, 2018; Ritz et al., 2015) with a three parameter log logistic regression (LL.3) to account for slope. The higher the ED50 values, the greater the acute heat tolerance of the individual or species. Absolute acute heat tolerance (ED50) was modelled as the temperature required to reduce photosynthetic efficiency by 50% relative to MMM-treated corals while relative acute heat tolerance (ºC above MMM) was modelled as the temperature above local MMM required to reduce photosynthetic efficiency by 50% relative to MMM-treated corals. Significant differences in acute heat tolerance between species were assessed by *emmeans()* in the DHARMa R package (Hartig & Lohse, 2021).

3.3.6.2 Thermal history

Thermal history co-variates of acute heat tolerance were visualised by Principal Component Analysis (PCA) constructed in the R package vegan (Oksanen et al., 2020) to reduce dimensionality (Appendix B.4). Each variable was initially correlated (Pearson correlation) to acute heat tolerance (ED50) for each of the three coral host species (*A. tenuis, P. meandrina*, and *P. verrucosa*) which revealed two variables to be significantly correlated across all species; number of heating events where heat stress exceeded 3-DHW (DHW3) and maximum SST (max_SST). These variables were checked for low collinearity (variance inflation scores < 3) using the *vif()* function in the R package car (Fox & Weisberg, 2019). The effect of a species interaction with either thermal history variable was compared by AICc scores and found not to significantly improve the model. Therefore, the linear model was fit as ED50 ~ species + max_SST + DHW3. The goodness-of-fit of the model was assessed by the *check_model()* function in the R package performance (Appendix B.5, Lüdecke et al., 2021).

3.3.6.3 Symbiont community

Demultiplexed .fastq files (forward and reverse) were submitted to SymPortal (Hume et al., 2019). This framework first removes non-Symbiodiniaceae sequences and then groups remaining Symbiodiniaceae sequences by genera. SymPortal then defines 'Defining Intragenomic Variants' (DIVs) by identifying within-sample informative intragenomic sequences. ITS2 type profiles are predicted from repeated co-occurrence of DIVs with similar relative abundances within samples. This results in distinct taxonomic units below, at, or above the species level (Hume et al., 2019), the meaning of which is currently under debate (Davies et al., 2022). Only samples with more than 1,000 reads were used for analysis to generate DIV count tables and Generalised UniFrac distance (d = 0.5) was used to construct distance matrices. Using generalised UniFrac distances take into account the weight on abundant lineages, and so the resulting distance is not dominated by highly abundant lineages (Chen et al., 2012). Principal Coordinate Analysis (PCoA) was used to visualise community differences and plot DIVs and environmental factors associated with the data patterns. PCoAs were conducted with the *cmdscale()* function in the vegan R package (Oksanen et al., 2020). Environmental factors were fitted to the PCoA by the *envfit()* function. These patterns were formally analysed by PERMANOVAs conducted also in R, using the *adonis3()* function with 999 permutations (Chen et al., 2022).

3.3.6.4 Physiology

Differences in physiology between treatments were examined by fitting linear mixed effects models in R (R Core Team, 2022) using the *lme()* function in the nlme package (Pinheiro et al., 2017). All models were fitted by restricted maximum likelihood and specified with an interaction of species and treatment as fixed effects with colony ID fitted as a random effect. Model assumptions were checked for normality and homoscedasticity with qq plots in the car package. Significant differences were assessed by Wald's tests and estimated marginal means (*emmeans(),* Lenth, 2023). Correlations between physiological metrics and ED50s were performed using the Spearman rank-correlations.

3.3.6.5 Co-variates of acute heat tolerance (ED50)

To investigate how the multiple predictors discussed above influence acute heat tolerance together, a linear model (ED50 ~ species + max_SST + DHW3 + Chla + catalase + protein + PCo1 + PCo2) was fitted to all complete data cases in the nlme() R package. Variance inflation was examined using variance inflation scores (*vif()*) while model performance was calculated

using *check_model()* in the performance R package as above. The relative importance of each variable was extracted using the *calc.relimp()* function (relaimpo package). Due to the lack of symbiont community and physiology data for *A. tenuis*, this species was omitted from this analysis. Physiological data used was collected in the MMM treatment.

3.4 Results

3.4.1 Latitudinal collection gradient in Pocillopora

From a total sample set of 309 corals collected from the *Pocillopora* genus, 141 were confirmed as *P. verrucosa,* 96 as *P. meandrina*, and 72 as neither (Table 3.1). Both *P. verrucosa* and *P. meandrina* showed strong latitudinal trends in spatial distribution. The northern sectors of Cape Grenville, Princess Charlotte Bay, and Cairns accounted for 74% of the collected *P. verrucosa* samples while the southern sectors (Swains and Capricorn Bunker) accounted for just 5% of samples. In contrast, the northern sectors held 27% of collected *P. meandrina* and 30% unidentified *Pocillopora* samples while the southern sectors accounted for 66% and 59% of *P. meandrina* and unidentified *Pocillopora* samples, respectively. The 72 unidentified colonies were excluded from analyses as their species identification could not be confirmed.

Table 3.1 Latitudinal gradient in *Pocillopora* collections. Numbers indicate the number of colonies sampled per species within each reef sector. Total colony count per sector is given in the right column and total species counts are shown on the bottom row. Sectors are listed from north to south.

Sector	*A. tenuis*	*P. meandrina*	*P. verrucosa*	Unidentified *Pocillopora*	Total colony count
Cape Grenville	30	5	48	2	85
Princess Charlotte Bay	69	19	48	15	151
Cairns	15	2	8	5	30
Townsville	45	7	30	8	90
Swains	30	30	4	15	79
Capricorn Bunker	92	34	3	28	157
Species total colonies	281	97	141	73	**592**

3.4.2 Species-level differences in acute heat tolerance

All three coral species (*A. tenuis, P. meandrina*, and *P. verrucosa*) exhibited significant declines in maximum photosynthetic yield (F_v/F_m) with increasing treatment temperatures (Wald's test, species * treatment, df = 9, F = 9.23, $p < 0.0001$; Appendix B.6). Values of acute heat tolerance (ED50) derived from the temperature-driven declines of F_v/F_m differed between the coral species (Fig 3.2A). Absolute acute heat tolerance (ED50) values ranged by 0.99ºC between the three species with *P. verrucosa* showing the greatest acute heat tolerance (ED50) across the data set at 36.21 ± 0.131ºC (*meandrina – verrucosa*, t ratio = -3.712, p = 0.0007;

tenuis – verrucosa t ratio = -4.135, p = 0.0001, respectively). *P. meandrina* (35.22 ± 0.108ºC) and *A. tenuis* (35.31 ± 0.076ºC) did not differ in their absolute acute heat tolerances (ED50; t ratio = -0.113, p = 0.993, Appendix B.7). Although relative acute heat tolerance (ºC above MMM) showed a narrower range for the three species (0.22ºC) than absolute acute heat tolerance (ED50; 0.99ºC), there were no significant differences in relative heat tolerance between the three species (Appendix B.8). Therefore, relative acute heat tolerance (ºC above MMM) was not analysed further.

3.4.3 Thermal covariates of acute thermal tolerance

Coral acute heat tolerance (ED50) exhibited significant variation across the GBR for each of the three species (Fig 3.2B). At the level of reef sector, all three species exhibited similar trends whereby ED50 values were higher in the northern-most sector (36.31 ± 0.11 ºC) compared to the central (Townsville, 35.77 ± 0.05 ºC) and the most southern sector (Capricorn Bunker, 34.98 ± 0.05 ºC) (Fig 3.2B, Appendix B.9). However, there were significant differences between species within these reef sectors. In the Northern sector, *P. verrucosa* recorded significantly higher ED50 values (36.46 ± 0.13 ºC) than *P. meandrina* (35.97 ± 0.28 ºC, Post Hoc Tukey's t = -2.06, p = 0.026, Fig 3.2B) and *A. tenuis* (36.23 ± 0.19 ºC; t = -3.03m p = 0.0076, Appendix B.24). In the Townsville sector, only *A. tenuis* and *P. verrucosa* differed significantly in their respective ED50 values with *P. verrucosa* recording half a degree higher acute heat tolerance (36.08 ± 0.07 ºC) than *A. tenuis* (35.57 ± 0.06 ºC; t = -4.7, p < 0.001, Fig 3.2B). In the Capricorn Bunker sector, *P. verrucosa* again recorded the highest acute heat tolerance (35.89 ± 0.22 ºC) compared to both *A. tenuis* (34.97 ± 0.06 ºC; t = -2.375, p = 0.048) and *P. meandrina* (34.93 ± 0.09 ºC; t = 3.204, p = 0.004) which also differed significantly to *A. tenuis* (t = 2.48, p = 0.037, Fig 3.2B) in this sector. Finally, there was no difference in acute heat tolerance between the three species in the Swains sector (Fig 3.2B, Appendix B.24).

The reef sectors were also characterised by differences in thermal history (Table 3.2, Appendix B.4). The northern sectors recorded higher maximum and average SSTs compared to the southern sectors, with the highest average SST (26.8 ºC) recorded in the northern sector of Cape Grenville. Similarly, the highest heat stress (DHW) recorded during the time series (1985 - 1 month prior to collection) was in the Princess Charlotte Bay sector (11.9 DHW) compared to 5.9 – 6.3 DHW in the Swains and Capricorn Bunker, respectively. Except for

Cairns (n = 5), the northern sectors (n = 9.5 in Cape Grenville and n = 10 in Princess Charlotte Bay) recorded more frequent marine heat waves (DHW>2) than the southern sectors (n = 5 Swains; n = 5.8 in the Capricorn Bunker.). Finally, the occurrence of DHW > 3 was similar across the GBR sectors (3 – 5.7, Table 3.2).

Each species was characterised by a different relationship between acute heat tolerance (ED50) and the suite of 19 thermal history variables examined (Fig 3.2C, Appendix B.10). While ED50s of both *A. tenuis* and *P. meandrina* showed significant positive correlations with 11 thermal history variables, including maximum SST (cor = 0.47 and 0.6, respectively), ED50s of *P. verrucosa* were only positively associated with the maximum SST (cor = 0.33 p = 0.025, Fig 3.2C). All three species showed significant negative effects on ED50 by number of heating where heat stress exceeded 3 DHW (*P. meandrina* = -0.28, *A. tenuis* = -0.41, *P. verrucosa* = -0.51). Interestingly, the effect of mean heat stress during heating events (mean_DHW) differed between the two *Pocillopora* species. In *P. meandrina*, ED50 values were positively correlated with increasing mean_DHW (cor = 0.31, p = 0.023) while in *P. verrucosa* this correlation was negative (cor -0.31, p = 0.03, Fig 3.2C). As such, acute heat tolerance of *P. meandrina* and *P. verrucosa* exhibit different responses as heat stress event loading (DHW) increases. Further, the annual variability in SSTs (range_SST) was not correlated to ED50 in *P. verrucosa* (cor = 0.04) while this variable recorded strong negative correlations with ED50 values in both *P. meandrina* (cor = -0.51) and *A. tenuis* (cor = -0.65), leading to a decrease in acute heat tolerance (ED50) as annual temperature variability (range_SST) increased. Additionally, ED50 values in *P. verrucosa* were significantly negatively correlated with frequency of heatwaves (DHW2 p = 0.026, DHW3 p = 0, and DHW4 p = 0, Fig 3.2C), whereby acute heat tolerance (ED50) was reduced on reefs that recorded frequent heat stress events.

Differences in ED50 across the GBR owing to environmental history were predicted by a linear model incorporating species identity, maximum SST, and the number of mild heating events (DHW > 3, Fig 3.2D) fitted to all data. Together, this model accounted for 51% of the variability within the ED50 response (R^2 = 0.509) with max_SST contributing the most to the model (24.5%), followed by species identity (15.5%) and number of heating events where DHW > 3 (10.96%)

Table 3.2 Sector-wide averages of thermal variables from a sampling period of 1985 – 1 month prior to collection). MMM = maximum monthly mean climatology, SST = sea surface temperature, DHW = degree heating week. The highest heat stress loading (max_DHW) represents the highest value recorded within the sector. Sectors are listed from north to south.

Region	**Sector**	**MMM** (ºC)	**max_SST** (ºC)	**min_SST** (ºC)	**mean_SST** (ºC)	**DHW > 2**	**DHW > 3**	**DHW > 8**	**Max DHW**
North	Cape Grenville	28.5	30.2	22.7	26.8	9.5	3.5	1.0	9.99
North	Princess Charlotte Bay	28.6	30.5	22.4	26.6	10.0	4.5	1.3	11.9
North	Cairns	28.6	31.0	21.8	26.4	5.0	3.0	1.0	8.8
Central	Townsville	28.5	30.7	21.4	26.3	9.3	5.7	0.3	8.9
South	Swains	27.5	29.6	20.4	25.0	5.0	3.0	0.0	5.9
South	Capricorn Bunker	27.1	29.0	19.3	24.4	5.8	5.0	0.0	6.3

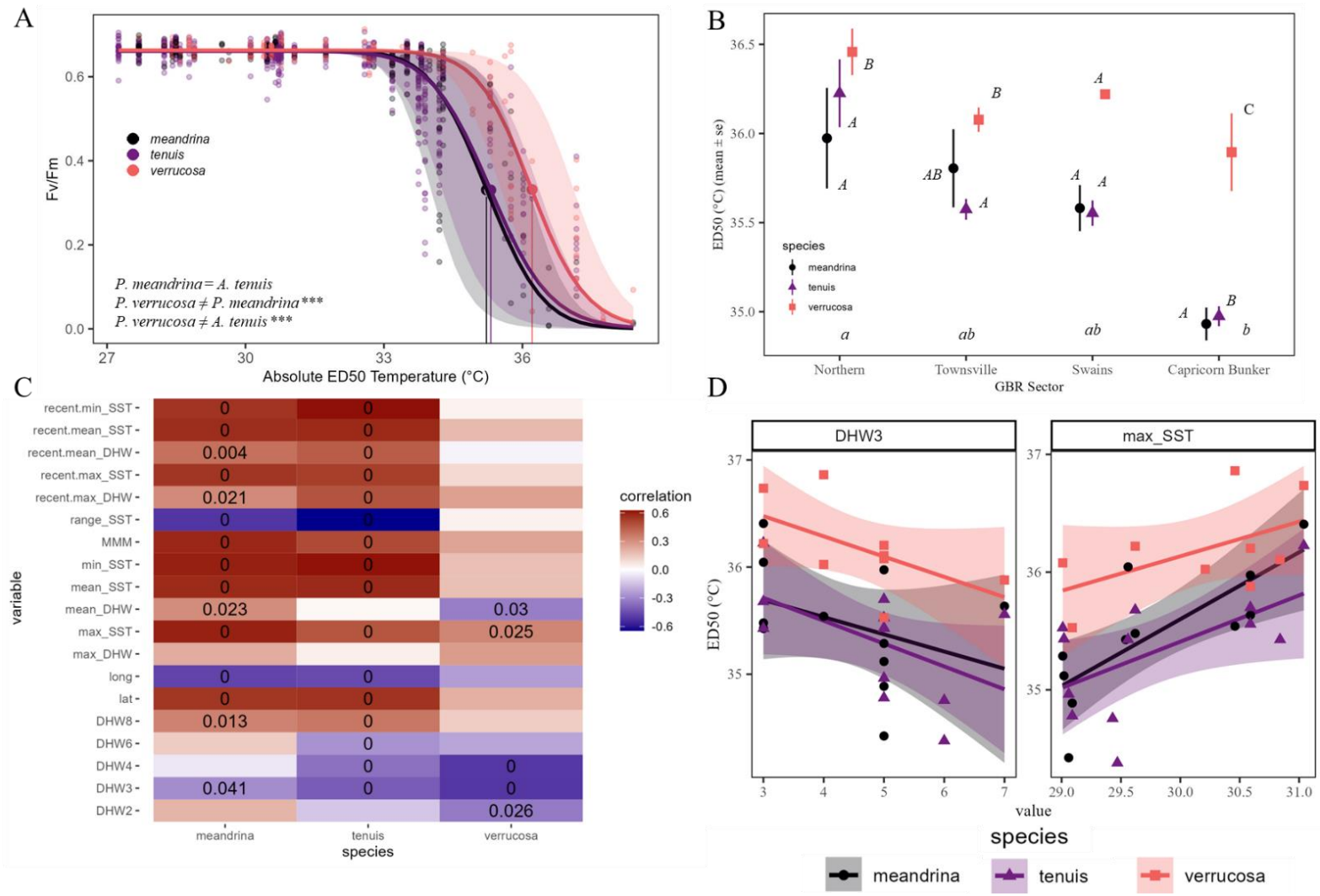

Figure 3.2 Acute heat tolerance patterns of three coral species across the GBR. (A) ED50 between *P. meandrina* (black), *A. tenuis* (purple), and *P. verrucosa* (orange) from log-logistic regressions. Bands indicate 95% CI of the ED50 estimate. Post-hoc comparisons show species contrasts and the asterisks indicate

the statistical significance level ($p < 0.05$ *, $p < 0.001$ **, $p < 0.0001$ ***) from Post Hoc Tukey's tests.. (B) Mean species ED50 values across four reef sectors (north to south). Points show the mean ED50 per species per sector (*P. meandrina* = black circle, *P. verrucosa* = orange square, and *A. tenuis* = purple triangle) and the whiskers indicate the standard error. Post-hoc comparisons show sector-level contrasts in small itallics while within-sector differences between species are shown in capital itallics. (C) Heatmap correlations (Pearson correlation, $p < 0.05$) between 19 thermal history variables and species ED50. Recent SST and DHW variables are grouped together, followed by long-term SST and DHW trends. Finally, heat wave variables are grouped together. Tile values show significance results from Pearson correlation tests. Non-significant p-values are not shown. (D) Linear regression of ED50 and two thermal variables significantly correlated with all species; this included the number of heating events where heat stress exceeded 3 DHW (DHW3) and the maximum SST (max_SST) recorded. Each point represents an individual reef.

3.4.4 Dominant Symbiodiniaceae association shows host-specificity and geographic stability

The number of ITS2-type profiles identified differed between *P. verrucosa* (n = 17) and *P. meandrina* (n = 11), and each profile was unique to their respective host species (Appendix B.12 and B.13). The dominant symbiont type profile differed between the two species but was remarkably stable within species between the six reef sectors (Fig 3.3). In *P. meandrina* the ITS2-type profile C1/C42.2/C42u-C1b-C42a-C115l-C1au-C1az-C115d was the most abundant except in the Capricorn Bunker (most abundant = C1/C42.2/C42g/C42a-C1b-C1au-C1az-C42h-C3), while in *P. verrucosa*, C1d/C1/C42.2/C3-C1b-C3cg-C45c-C115k-C1au-C41p was the most abundant type profile across the GBR, with the exception of the Capricorn Bunkersector (Fig 3.3, Appendix B.14). Presence (and abundance) of the C1d DIV in the *P. verrucosa* colonies along with the absence in *P. meandrina* suggests that *Cladocopium pacificum* (Johnston et al., 2022; Turnham et al., 2021) is most likely the dominant symbiont species harboured by *P. verrucosa* (Appendix B.14). Despite low absolute abundance, both the C42-a and C42-b DIVs, diagnostic of *C. latusorum* (Davies et al., 2022; Johnston et al., 2022; Turnham et al., 2021) were present in the *P. meandrina* samples and absent in *P. verrucosa* (Appendix B.15). Additionally, two out of the 141 *P. verrucosa* samples co-associated with symbionts of the genus *Durusdinium* (<10% relative abundance, ITS2-type profiles D1-D2d-D1aa-D1z-D1hy and D1/D2d-D1aa-D1z) with one sample from the Cairns and one from the Princess Charlotte Bay sector.

3.4.5 Symbiodiniaceae community composition varied across environmental gradients and acute heat tolerance

Symbiodiniaceae community composition (DIVs) varied significantly between *Pocillopora meandrina* and *P. verrucosa* (PERMANOVA; df = 1, p = 0.0001, R2 = 0.49, F = 230.27, Fig 3.4A). Community differences of symbionts between the two coral hosts were primarily associated with Principal Coordinate 1 (PCo1 33.3% of variation explained). *P. verrucosa* samples were differentiated along PCo2 (7.8% variation explained), which corresponded to clustering between the reef sectors for this species (Fig 3.4A); specifically, the two northern-most sectors (Cape Grenville and Princess Charlotte Bay) separating from the Cairns and Townsville sectors further south. Reef-level differences in intra-species symbiont community composition were evidenced by significant differences across environmental variables including latitude, coral cover, frequency of marine heatwaves (DHW > 3), and the maximum

SST recorded (Appendix B.16 and B.17). These results highlight variability in symbiont community composition of *P. verrucosa* and *P. meandrina* on the GBR at the scale of reef sector.

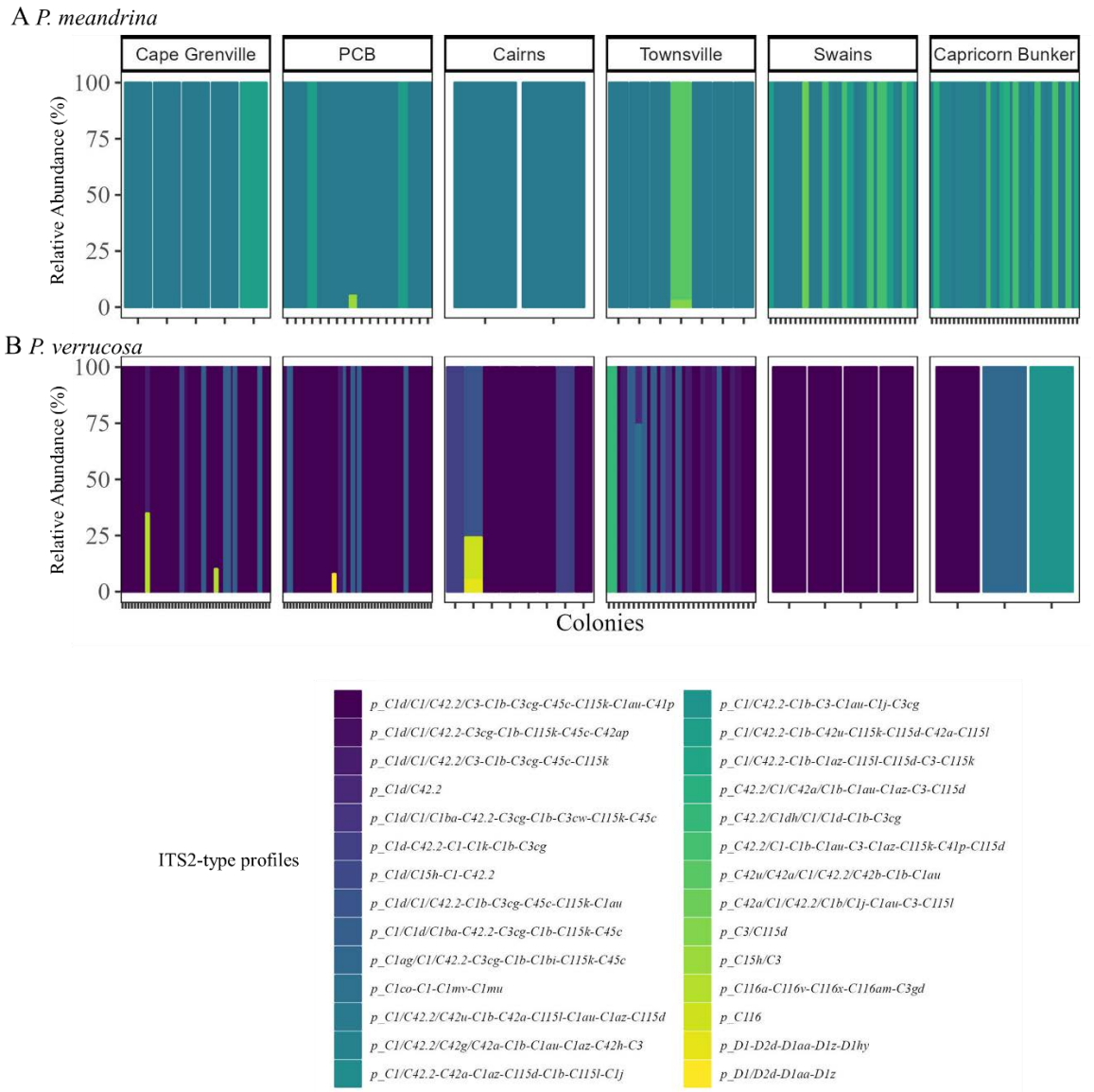

Figure 3.3 Relative abundance (%) of the 28 ITS2-type profiles recovered by the SymPortal analytical framework in *P. meandrina* (A) and *P. verrucosa* (B) across the six reef sectors of the GBR (listed from north to south). PCB = Princess Charlotte Bay. Each vertical bar corresponds to a sample.

Interestingly, symbiont community composition within *P. meandrina* was significantly correlated with acute heat tolerance (ED50, PEMANOVA df = 1, R^2 = 10.17, p = 0.001), whereby the greatest variation in ED50 separated primarily along PCo2 (23.3% variation explained, Fig 3.4B, Appendix B.18). Although no single DIV was associated with increased

heat tolerance, there was a trend towards corals with high ED50s having a greater abundance of the C42u, C42az, and C41p DIVs compared to those with low ED50 (Appendix B.19). The two *P. verrucosa* colonies that hosted *Durusdinium* also recorded 0.2ºC higher ED50s (37.36 – 37.38ºC) than the other colonies hosting *Cladocopium* (35.04 – 37.16ºC, Appendix B.20). Despite high community structure by environment, Symbiodiniaceae community composition did not account for colony-level differences in F_v/F_m -derived ED50 threshold temperatures in *P. verrucosa* (Appendix B.16).

3.4.6 Physiological condition in the absence of heat stress as a predictor of acute heat tolerance

Physiological condition (catalase activity, protein, and chlorophyll-*a* content) of corals were assessed in the MMM treatment for both *P. verrucosa* and *P meandrina* (n = 51 and n = 45, respectively) and compared to corresponding colony values of acute heat tolerance (ED50). In *P. verrucosa*, only chlorophyll-*a* content significantly correlated with ED50 (S = 7,800, cor = 0.49, p = 0.001, Fig 3.5A). In *P. meandrina* protein content negatively (S = 23,040, cor = -0.62, p < 0.0001) and catalase activity positively correlated (S = 9,626, cor = 0.32, p = 0.003) with ED50s (Fig 3.5A). In *P. meandrina*, protein content and catalase activity explained 39.4% and 3.3% of the variation in ED50s while in *P. verrucosa*, chlorophyll-*a* content accounted for 17% of ED50 variation. Additionally, both chlorophyll-*a* and protein content in the MMM treatment differed significantly between the two species (Post-Hoc Tukeys; chlorophyll t = -3.002, p = 0.009; protein t = 3.582, p = 0.0014, Fig 3.5B) while there was no species difference in catalase activities (Appendix B.21).

When all traits were combined, variability in acute heat tolerance (ED50) was most strongly predicted by the maximum SST (max_SST, 19.2%). Overall, the linear model accounted for 75% of the variation in ED50. Protein content was by far the strongest physiological co-variate examined, accounting for 16.8%, followed closely by coral species (15.5%). When modelled as principal coordinates, symbiont communities along PCo1 accounted for 12.2% of ED50 variation. This axis also corresponds to the main split between the two coral host species *P. verrucosa* and *P. meandrina*. In contrast, the axis associated with community differences within species (PCo2), accounted for only 1.6% of variation. Chlorophyll content (4.2%), catalase activity (2.9%) and number of marine heat waves where DHW > 3 (4.33%) all accounted for less than 5% of trait variation.

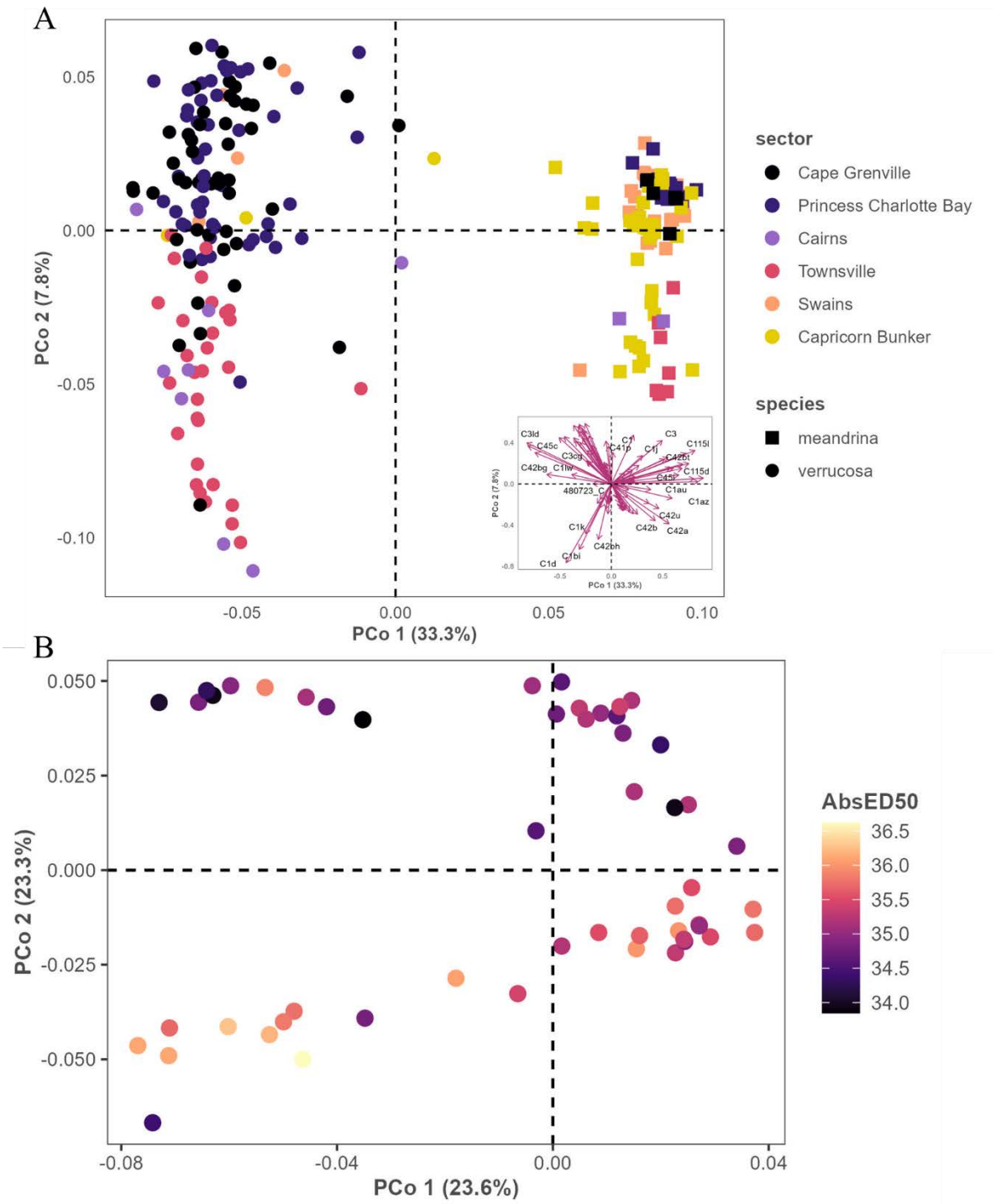

Figure 3.4 Symbiont communities differed between coral host species and environments based on generalised UniFrac distance matrices. (A) Principal Coordinate Analysis (PCoA) of the species-split in symbiont community composition between *P. meandrina* (squares) and *P. verrucosa* (circles). Insert shows how the individual DIVs are correlated to the ordinated space. Points are coloured by the six reef regions. Principal Coordinate 1 accounted for 33.3% of the variability in symbiont communities while PCo2 accounted for 7.8%. (B) Acute thermal tolerance (ED50) was significantly associated with symbiont community composition in *P. meandrina*. Points are coloured by colony-level ED50 (range = 33.85 – 36.62°C; PCo1 accounted for 23.6% of data variation while PCo2 accounted for 23.3%.

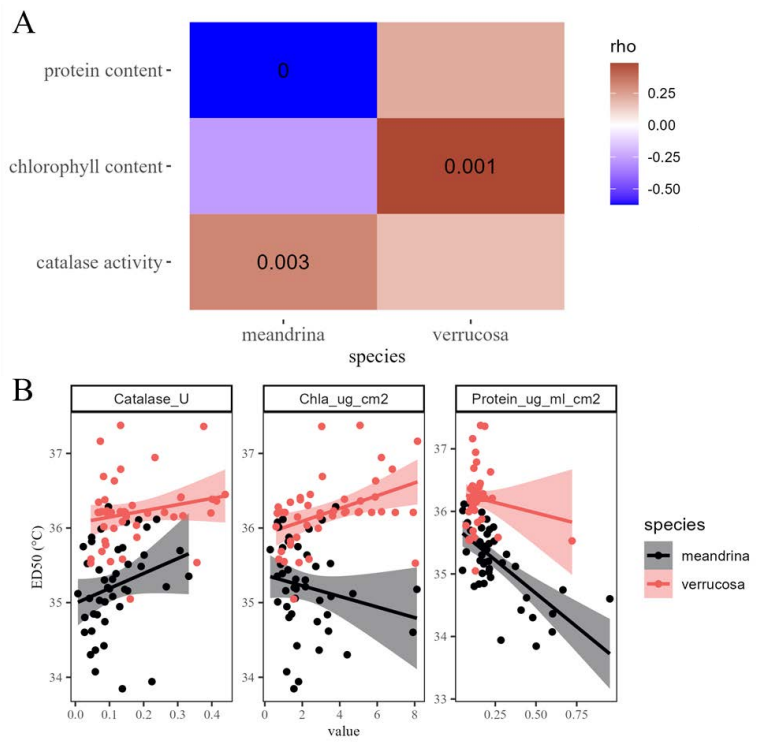

Figure 3.5 Physiological condition in relation to acute heat tolerance (ED50). (A) Correlation heatmap of three physiological traits (protein and chlorophyll-*a* content, and catalase activity) against colony ED50s. Tile colour corresponds to Spearman's rank correlation (rho) and the tile numbers indicate the statistical significance of the correlation. Non-significant values are not shown. (B) Linear regressions of three physiological traits against ED50 between the two species; *P. meandrina* (black) and *P. verrucosa* (orange). The bands show 95% confidence intervals.

3.5 Discussion

Documenting the sources of variation in coral thermal tolerance at scale is key to understanding the survival of coral reefs under continued warming. While multiple drivers of heat tolerance across biological scales and organisation have been extensively investigated (for example reviewed in Cziesielski et al., 2019; McClanahan, 2022; McLachlan et al., 2020; van Woesik et al., 2022), there has been little integration across large (> 1,000 km), reef-system wide geographic scales to date (but see Marzonie et al., 2022). After quantifying coral responses to acute heat stress across 11.5^{o} of latitude on the GBR, I found strong variation in heat tolerance among species and reef sectors. The differences in acute heat tolerance between species potentially reflect inherent species-level differences in thermal tolerance potential among the three species. Based on contrasting effects of symbiont communities and physiological condition on acute heat tolerance documented here, it is clear that multiple factors govern coral thermal tolerance across large spatial scales.

3.5.1 Species-level differences in acute thermal tolerance (ED50)

Coral thermal tolerance differs among genera (Loya et al., 2001; Marshall & Baird, 2000) with *Acropora* and *Stylophora* typically identified as among the least tolerant (Baker et al., 2008; Guest et al., 2012). This assertion is confounded by large variation among species within a genus. Using a standardised measure of acute heat tolerance (ED50), this study found that *P. verrucosa* recorded significantly higher acute heat tolerance than *P. meandrina* and *A. tenuis.* The high acute heat tolerance of *P. verrucosa* relative to *P. meandrina* could reflect distribution ranges defined by thermal history, whereby *P. verrucosa* with a high thermal optimum (29.5^{o}C, Álvarez-Noriega et al., 2023) favours a warmer environment than *P. meandrina.* Similar results have been reported in Hawaii where *P. meandrina* are predominantly found on cooler reefs (Johnston et al., 2018), suggesting that this species indeed has a lower temperature tolerance (Marzonie et al., 2022). This is further supported by a general pattern within reef sector whereby *P. verrucosa* recorded the highest and *P. meandrina* the lowest acute heat tolerances throughout. Further, acute heat tolerance was higher in the northern sectors in all three species examined here. A similar positive, linear relationship between local MMM and acute heat tolerance (ED50) was reported by Evensen et al., (2022) in the Red Sea.

While the ED50 obtained for *P. verrucosa* in this study (36.21ºC) was similar to that calculated from comparable experiments conducted in the Red Sea (35.15 - 36.73ºC; Evensen et al., 2022), *P. verrucosa* was found to be the least tolerant species examined out of *Stylophora pistillata*, *Porites lobata*, and *Acropora hemprichii* in that region. The reef regions (Red Sea vs GBR) vary in their MMM gradients. The Red Sea show a greater range of MMM (4.5ºC, Evensen et al., 2022) than the GBR (1.6 ºC in this study), and this greater long-term thermal gradient may account for the contrasting species tolerance rankings observed in the Red Sea and on the GBR. Further, the relative ED50s obtained here for *P. verrucosa* (7.73ºC) and *P. meandrina* (7.75ºC) also fall within the range of relative ED50s previously reported from the Coral Sea for these species (7.74 ºC and 7.42ºC, respectively; Marzonie et al., 2022). However, in contrast to Marzonie et al., (2022), the present study finds no difference in the relative heat tolerance between the two *Pocillopora* species, potentially due to the sample under-representation of *P. meandrina* in the north and of *P. verrucosa* in the south. The narrow range and lack of significant differences between species in the relative ED50s could indicate that GBR coral populations are at least somewhat adapted to their local environments, having matched their acute heat tolerance to long-term MMM trends.

3.5.2 Sector-specific thermal disturbance history is a strong driver of coral acute thermal tolerance.

Thermal history can impact coral thermal tolerance, generally leading to higher heat tolerance in individuals from highly variable environments (Barshis et al., 2018; Gilchrist, 1995; Mayfield et al., 2012). The thermal disturbance history of the GBR is highly sector dependent (Cheung et al., 2021; Mellin et al., 2019) and it was therefore not surprising that acute heat tolerance differed at this scale. Decreasing acute heat tolerance in *P. verrucosa* was primarily driven by the frequency of marine heatwaves over DHW >3 while responses in both *P. meandrina* and *A. tenuis* were better explained by long-term SST trends. The higher acute heat tolerance in northern sectors correspond both to the more severe thermal stress disturbance history of this region and to higher long-term temperatures. For example, the Princess Charlotte Bay sector recorded the highest heat stress loading relative to the southern sectors. Additionally, colonies from the northern sectors (Cape Grenville, Princess Charlotte Bay, Cairns), were the only populations tested here that experienced more than eight DHW over the time series. These severe heatwave events were coupled with higher frequency of heat stress

in the north, particularly in the Cape Grenville and Princess Charlotte Bay sectors. However, increased frequency of mild heatwaves (DHW > 3) on the GBR did not result in increased acute thermal tolerance (ED50) in any of the three species whereas acute heat tolerance increased with increasing maximum SST. Similarly, in *Porites lobata* from the Red Sea, recent, severe bleaching led to decreased ED50s (Evensen et al., 2022). The decline in acute heat tolerance with increasing frequency of mild heatwaves could indicate that regular heatwaves may be eroding thermal tolerance of the populations overall. These results are in contrast to Hughes et al., (2021), where the authors highlight that recurrent, frequent (every 1 - 3 year events) increase bleaching thresholds due to hardening, similar to results from the Coral Sea where the frequency of mild heatwaves (DHW > 4) resulted in an increase in acute heat tolerance (ED50, Marzonie et al., 2022). The Coral Sea recorded a higher frequency of mild marine heatwaves compared to the reefs examined here and is further characterised by large, spatially isolated reefs, highly limiting the possibility of gene flow between reefs, giving rise to populations likely to show high local adaptation (Benzie, 1994; Payet et al., 2022). In contrast, the GBR is characterised by high levels of gene flow between populations (Bay et al., 2006; Smith-Keune & van Oppen, 2006), potentially increasing the time required for local adaptation to occur and therefore showing a negative correlation between acute heat tolerance and the frequency of mild marine heat waves.

3.5.3 Symbiont communities are highly structured by host species and thermal environment

Symbiodiniaceae composition is an important component of coral holobiont thermal tolerance (Strader & Quigley, 2022). Both *Pocillopora* species examined here are known to transmit Symbiodiniaceae vertically (Apprill et al., 2009; Hirose et al., 2000), and have co-evolved with their symbionts (Johnston et al., 2022; Turnham et al., 2021). In the current study, host species showed clear differences in community composition both with regards to the dominant symbiont type and the make-up of communities between populations. The split in dominant type between the two *Pocillopora* species reflects the established and highly host-specific associations observed between *Cladocopium pacificum* (*P. verrucosa)* and *C. latusorum* (*P. meandrina*) in the Pacific (Johnston et al., 2022; Turnham et al., 2021). This is further supported by the presence of the diagnostic ITS2 sequences for *C. pacificum* (C1d) in *P. verrucosa* and *C. latusorum* (C42a and C42b) in *P. meandrina* in this study (Davies et al., 2022). These dominant, host-specific associations have been shown to be stable across

environmental gradients in *Pocillopora* in the Red Sea (Sawall et al., 2014) and the Pacific (Turnham et al., 2021) as was also the case in the present study. Further, the dominant ITS2-type profile reported here for *P. verrucosa* corresponds to the dominant profile reported by Grima et al., (2022) in the northern GBR. Interestingly, the wider community composition varied significantly across the spatial and thermal gradients examined here, particularly within *P. verrucosa*. High environmental structuring of symbiont communities were also reported for *A. tenuis* (Cooke et al., 2020; Matias et al., 2022) and this could therefore represent a reef-system characteristic of the GBR. As such, identifying structuring of symbiont communities by environment within coral host species is an important consideration and potential restraint for assisted management (Buerger et al., 2020; Quigley et al., 2018). Symbiont community make-up within *P. meandrina* contributed significantly to colony-level acute heat tolerance (ED50) where high heat tolerance was associated with changes in abundance of some ITS2 sequence variants. Similarly, Hoadley et al., (2021) documented significant effects of symbiont community within *Cladocopium C15* lineages on coral heat tolerance, supporting that fine-scale differences in community composition within Symbiodiniaceae can indeed affect holobiont heat tolerance. However, as dominant symbiont type was host-specific, it was not possible to determine if host species differences in ED50s were driven primarily by symbiont type or coral species.

3.5.4 Relationship between acute heat tolerance and physiology

Changes in photosynthetic performance and declines in physiological traits are common indicators of heat stress in corals (Gardner et al., 2017b; Grottoli et al., 2021; Nitschke et al., 2018). The F_v/F_m-derived trait ED50 used here has been proposed as a rapid proxy of heat tolerance for use in large-scale assessments (Cunning et al., 2021; Evensen et al., 2021; Nielsen et al., 2022). Yet, few studies have quantified the relationship between this trait and common physiological responses to heat stress. Here, colony-level ED50 only correlated to chlorophyll-*a* content in *P. verrucosa* but not in *P. meandrina*. This is surprising given that the trait (ED50) is derived from fluorescence measurements of chlorophyll-*a*, and it was therefore expected that ED50 should reflect chlorophyll-*a* concentrations. However, the relationship between chlorophyll content and photosynthetic efficiency is not always conserved (Magney et al., 2020). In corals, numerous factors can regulate fluorescence quenching (Nitschke et al., 2022), such as self-shading and within-tissue light gradients (Wangpraseurt et al., 2019), which can

disrupt the relationship between chlorophyll content and photosynthetic efficiency further. The lack of a relationship between ED50 and chlorophyll-*a* content in *P. meandrina* could potentially reflect photo-physiological differences between the dominant symbiont types harboured (Lohr et al., 2019; Suggett et al., 2022). Corals with higher catalase activity recorded higher acute heat tolerance, perhaps because these higher enzyme activities allow the coral to respond faster to thermal stress and the production of harmful reactive oxygen species (Teixeira et al., 2013). Protein content, and high energetic reserves more broadly, are typically recognised as key drivers of both bleaching resistance (Anthony et al., 2009; Gibbin et al., 2018) and recovery potential (Schoepf et al., 2015a). In keeping with this, protein content was the best of three physiological predictors of acute heat tolerance (ED50) although the relationship was surprisingly negative. The extent to which high protein content leads to higher thermal tolerance is likely to be both species- and population specific (Jung et al., 2021).

Coral thermal tolerance is a complex trait governed across multiple biological scales. This study documented significant differences in acute heat tolerance (ED50) between *P. meandrina*, *Acropora tenuis*, and *P. verrucosa* sampled across 11.5^{o} latitudes on the GBR. Warmer, northern reefs hosted more thermally-tolerant corals (Cornwell et al., 2021), and acute heat tolerance showed evidence of adaptation to local thermal environments (Jurriaans & Hoogenboom, 2019). When all co-variates were combined, maximum SST exerted the largest effect on coral acute heat tolerance followed closely by protein content and species identity while within-host species symbiont community differences had little overall effect. Having established the respective roles and impacts of thermal history and symbiont community on coral thermal tolerance, much variation remains unexplained. For example, host-specific genetic variation and transcriptional plasticity in response to heat stress were not examined here. Despite high levels of reef-connectivity on the GBR, it is unlikely that heat-adapted coral genotypes would spread beyond the northern sectors naturally within the short period of time needed given current warming rates (Quigley et al., 2019), necessitating genetic management interventions. Such interventions, like assisted gene flow, require foundational knowledge of thermally tolerant corals and where to find them. Based on the spatial scale and high-throughput experimental design of the present study, these acute heat stress assays lend themselves well to document not only the geographical locations of thermally tolerant populations but also to investigate the underlying mechanisms, whether environmental, symbionts, or host genetics.

Chapter 4 Does gene expression plasticity underpin acute heat tolerance in a population of reef-building coral?

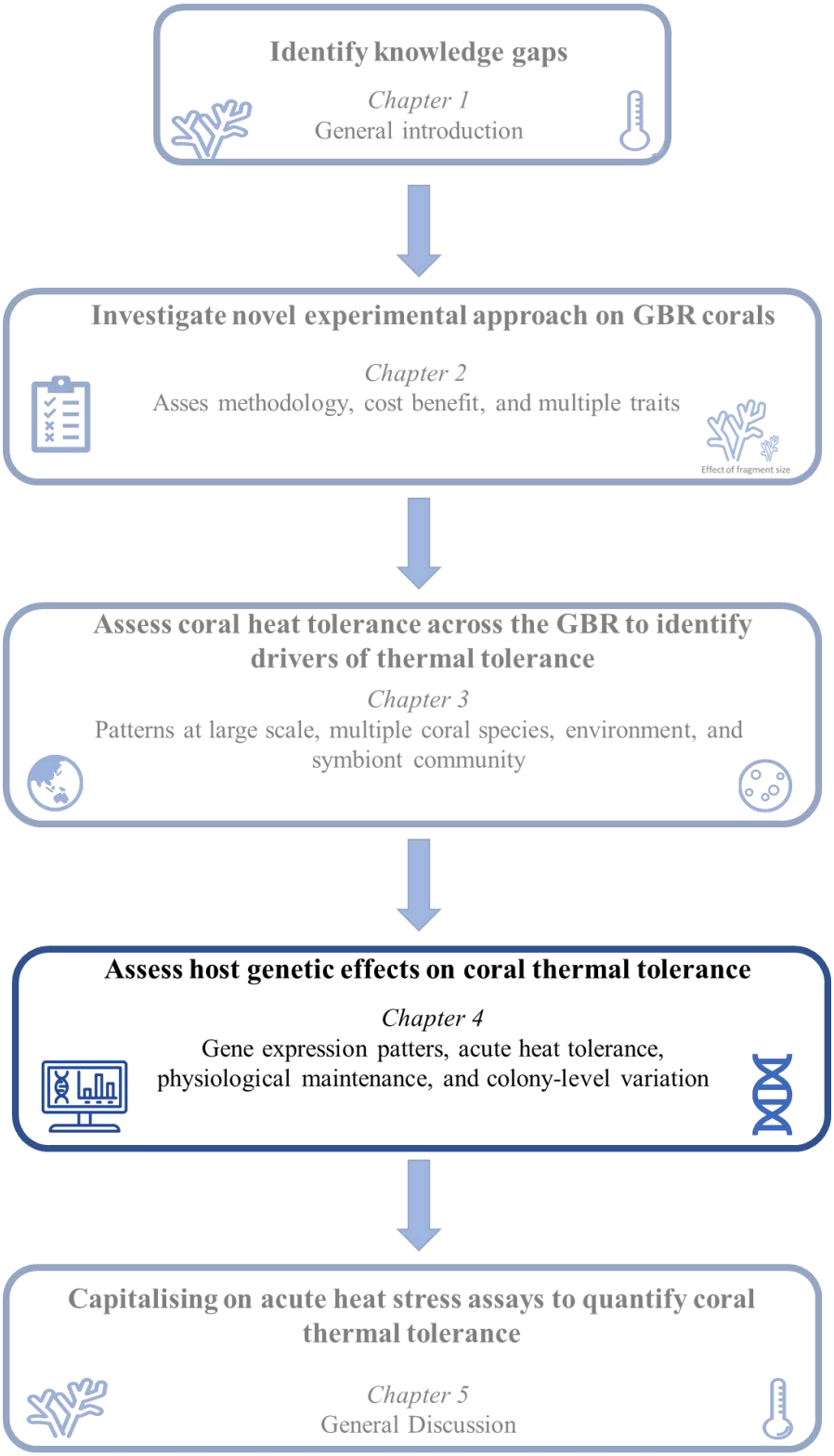

4.1 Abstract

Reef-building corals exhibit high variation in their thermal tolerance, which may contribute to critical differences in survival following mass bleaching events. Heat tolerance is, therefore, an important trait governing corals' survival under climate change, and there is an urgent need to understand its mechanistic drivers. Although the molecular responses of corals to heat stress are now well documented, fewer studies have linked transcriptomic responses directly to physiological outcomes related to heat tolerance. To examine the molecular basis of heat tolerance, here I combined RNA sequencing with physiological measurements of heat stress (F_q'/F_m', tissue colour, and mass changes) to identify tolerant individuals, and quantified gene expression profiles associated with high heat tolerance in corals following acute heat stress exposure at 34ºC relative to ambient (27.5ºC) conditions with multiple partial coral colonies (n = 30) of the species *Acropora tenuis* sourced from the central Great Barrier Reef (Davies) Numerous genes recognised to form part of a shared coral heat stress response were upregulated in response to acute heat stress following a recovery period, such as heat shock proteins, photoprotective genes encoding for ubiquitin-, green fluorescent protein-, and Ras-like proteins. A relatively smaller number of "frontloaded" genes were also identified in highly tolerant individuals. These included an ATP-dependent DNA helicase, sodium- and chloride-dependent GABA transporter 2, and Kelch-like protein 28. This study furthers our understanding of both biochemical and transcriptomic responses to thermal stress in a common reef-building coral species. It also identifies genes indicative of acute heat tolerance for further validation and gene expression biomarker development.

4.2 Introduction

Corals must respond to increasing warming, either through phenotypic plasticity or genetic adaptation, to ensure their persistence under continued climate change (Chevin & Hoffmann, 2017; Drury et al., 2022a). Severe thermal stress events leading to mortality may act as selective pressures on coral populations (Barshis et al., 2018) potentially increasing the proportion of better-suited genotypes over time through local adaptation. Although corals have demonstrated some ability to adapt to their local environment (Howells et al., 2016; Kirk et al., 2018; Thomas et al., 2018), the molecular mechanisms underpinning patterns of local adaptation are not well understood. On shorter time scales, individual corals can respond to environmental disturbances rapidly through changes in gene expression (Barshis et al., 2013; Traylor-Knowles et al., 2017; Whitehead & Crawford, 2006), the proximate mechanism linking coral genotypes to phenotypes (Kenkel & Matz, 2016). While the general transcriptomic environmental stress response of corals has been well-studied (Cziesielski et al., 2019; Dixon et al., 2020; Drury et al., 2017), heat tolerance is a complex trait for which the loci responsible remain poorly defined and associated genetic variation poorly mapped.

High-resolution transcriptomic analysis enables the identification of functional mechanisms underlying organism responses to perturbations (De Nadal et al., 2011; López-Maury et al., 2008). Gene expression analysis has been widely used to interrogate the underlying mechanisms of coral thermal stress and has identified a core, molecular heat stress response (Cziesielski et al., 2019). Many of these co-regulated genes are involved with regulating cell death, immune responses, heat shock proteins (HSPs), protein folding and degradation, as well as dealing with reactive oxygen species and growth regulation (Bellantuono et al., 2012; Cziesielski et al., 2018; Fitt et al., 2009; Granados-Cifuentes et al., 2013; Kenkel et al., 2014; Maor-Landaw & Levy, 2016; Seneca & Palumbi, 2015). Some heat response genes have been proposed as gene expression biomarkers (GEBs, reviewed in Louis et al., 2017) with the purpose of detecting early-onset coral heat stress, prior to the manifestation of visual and other physiological indicators (Morgan et al., 2001). Such markers provide a valuable heat stress screening tool which may be scaled rapidly (Kenkel et al., 2013). Further, heat tolerance and thermal resilience of an individual may be predictable from gene expression profiles (Avila-Magaña et al., 2021; Bay & Palumbi, 2017; Kenkel et al., 2014), for example through quantification of frontloaded gene expression levels (Barshis et al., 2013). Frontloading of genes (i.e. higher expression levels in resilient individuals compared to sensitive ones in the

absence of stressors), was recently shown to increase resilience to environmental disturbances in juvenile corals (Vidal-Dupiol et al., 2022). Combining transcriptomic analyses with physiological measures of coral heat tolerance may increase our ability to detect GEBs and increase our understanding of the functional molecular mechanisms underlying heat tolerance in corals.

Thermal tolerance of the coral holobiont is partially dictated by the symbiont community (Berkelmans & van Oppen, 2006; Howells et al., 2011; Ziegler et al., 2017). The holobiont heat stress response involves breakdown of symbiosis leading to bleaching (Rowan, 2004; Suggett & Smith, 2011), combined with independent physiological and transcriptional responses to stress in the host (Bay et al., 2013; Bellantuono et al., 2012; Kirk et al., 2018) and associated symbionts (Cunning & Baker, 2020; and reviewed in Jiang et al., 2021). The variability in light harvesting and utilisation strategies between different symbiont types (Lohr et al., 2019) may indicate different adaptive strategies for optimising photosynthetic output and minimising photosynthetic stress during heating (Nitschke et al., 2022; Suggett et al., 2015). Rapid light curves (RLCs) allow estimation of multiple photochemical parameters including how the photosynthetic apparatus handles excess light through quantification of photochemical and non-photochemical quenching (Appendix C.1, Nitschke et al., 2018; Ralph & Gademann, 2005; White & Critchley, 1999), providing high-resolution data on photo-physiological responses to heat stress. Holobiont-level physiological measures of heat tolerance should also be considered when quantifying coral heat tolerance (Grottoli et al., 2021; Nielsen et al., 2022). Coral tissue colour is a quick and cost-effective proxy of bleaching (Chow et al., 2016; Siebeck et al., 2006) which can be readily quantified following acute heat stress assays (Nielsen et al., 2022). Capturing multiple physiological measures of heat tolerance is required to understand thermal stress responses (Gardner et al., 2017a).

Studies that pair gene expression measurements (RNA-Seq) with quantified heat tolerance of corals are now required to examine physiological and transcriptomic drivers of heat stress responses as they are being mounted by the coral animal and associated symbionts. Recently, ED50 (Effective-Dose 50, Dimmitt et al., 2017) has been proposed to rapidly quantify coral heat tolerance in large sample sizes (**Chapter 3**; Cunning et al., 2021; Evensen et al., 2022; Marzonie et al., 2022). The trait, derived from photochemical efficiency measurements (F_v/F_m), documents the temperature required to reduce photosynthetic performance by 50% relative to controls and has confirmed differential acute heat tolerance

between coral species and populations, across both large (Evensen et al., 2022; Marzonie et al., 2022) and small spatial scales (Evensen et al., 2021). Finally, organism thermal resilience can also be quantified in terms of their ability to maintain homeostasis under stress (Kenkel & Matz, 2016; López-Maury et al., 2008; Ruiz-Jones & Palumbi, 2017). Examining coral heat stress responses using multi-trait analyses incorporating physiology and gene expression is necessary to begin to disentangle these complex factors (Cziesielski et al., 2018; Gardner et al., 2017a).

Here, I examine the mechanistic drivers of acute heat tolerance in the model coral species, *Acropora tenuis,* by comparing transcriptomic responses to physiological measures of thermal tolerance. I describe significant gene expression differences in response to acute heating in the host and find a much smaller set of differentially expressed genes in the dominant symbiont partner of the coral animal. Gene expression patterns were further differentiated between highly tolerant and sensitive individuals by comparing 25 differentially expressed genes in the heated treatment and nine frontloaded genes significantly upregulated in the ambient treatment. Finally, in recognising that thermal tolerance is a multi-variable trait, colony-level physiological maintenance was derived from multiple traits (photosynthetic efficiency, tissue colour change, and mass changes) and these were used to construct a gene co-expression network to identify gene modules associated with physiological maintenance following heat stress. This was used as a proxy of resilience. Together, the results of this study highlight the utility of combining transcriptomic analyses with physiological responses to heat stress to increase understanding of mechanistic drivers and molecular predictors of heat tolerance in corals.

4.3 Materials and methods

4.3.1 Coral collection and husbandry

Partial colonies (n = 30) of *Acropora tenuis* were collected from Davies Reef (18°49.620'S, 147°37.608'E) on the Great Barrier Reef (GBR) between March 10th-12th 2019 (GBRMPA permit # G12/35236.1). Corals were held in outdoor, partially shaded aquaria and maintained at ambient temperature (27.5°C) at the National Sea Simulator Facility at the Australian Institute of Marine Science. Corals were fragmented into ~40 fragments per colony and transferred into indoor aquaria (280 L) on March 22nd – 24th to acclimate to indoor conditions. During this time, corals were fed *Artemia* daily (5 mL^{-1}) before being transferred to experimental tanks on May 25-27th 2019 after 64 days of acclimation (55 L, flow rate = 55 L h^{-1}, Fig 1B). Each tank was fitted with a circulation pump (Turbelle® nanostream® 6055, Tunze, Penzburg, Germany), and a Hydra light suspended above the tank (AquaIllumination®, 400-700 nm, C2 Development, Ames, Iowa, USA; 350 µmol m^{-1} s^{-1}, 3 h ramping, 12:12 h light:dark).

4.3.2 Experimental conditions and design

For each of the 30 coral colonies, coral nubbins (n = 40 total) were split into five groups (n = 8 nubbins per group). For each individual colony, these eight nubbins per treatment were randomly assigned to tanks and separately exposed to five different temperature treatments; ambient (27.5°C), 30, 32, 34, and 35.5°C (Appendix C.2). Each temperature treatment had four replicate tanks and temperature ramping commenced on separate days for each treatment (30°C on May 30th, ambient on June 1st, 32°C on June 3rd, 35.5°C on June 5th, and 34°C on June 7th), and were staggered due to logistical constraints associated with water delivery at required temperatures and sampling time to complete photographing and PAM fluorometry. All sampling time points were relative to the starting time of each treatment. Temperature ramped from ambient to treatment temperature over 3 h and was maintained for 3 h at treatment temperature (Fig 4.1A), before rapidly (1 h) ramping down to ambient. Destructive sampling by preservation in liquid nitrogen occurred at 6 h, 24, h, 10 d, and 5 wks after the end of heat stress (Fig 4.1A, Table 4.1). At each sampling time-point, two replicate fragments per colony per treatment were preserved. Samples preserved at the 24 h sampling point in the ambient and

34°C treatments were used for the gene expression analysis by RNA-Seq. Corals were maintained in aquaria for five weeks post heat stress to assess the impacts of acute heating on recovery and survival.

Table 4.1 Sampling overview.

Sampling time point	Fragments in system prior to sampling	Sampling activity undertaken
T0	1200	Prior photographs Prior weighing
6 h	1200	Photographs RLC Destructive sampling
24 h	900	Photographs RLC Destructive sampling
10 d	600	Photographs Weighing RLC Destructive sampling
5 wks	300	Photographs Weighing RLC Destructive sampling

4.3.3 Physiological traits

All fragments were photographed (Nikon® D18, four Ikelite strobes) prior to treatment and again at each sampling time point following Nielsen et al., (2020). All fragments assigned to the 10 days and five weeks sampling time point were weighed (Davies, 1989) prior to treatment and again before sampling, and mass change was reported as mass change in g d^{-1} g^{-1} . Photosynthetic efficiency was assessed at each sampling time point by Rapid Light Curves (RLCs, 1 h low light incubation <75 PAR, eight actinic light steps (Appendix C.1b), 20 s, Diving-PAM, Heinz Walz GmbH, Effeltrich, Germany; MI = 4, Gain = 4, SI = 8, SW = 0.8s, Damp = 2, LC-width = 20s, LC-int = 3, probe = 6 mm). RLCs are comprised of multiple, short light steps increasing in intensity (Ralph & Gademann, 2005). While these curves are generally too short to ensure maximum induction of photoprotective mechanisms (González-Guerrero et al., 2021), they are useful for corals due to their speed of assessments. Multiple photosynthesis parameters were used to calculate the maximum (F_v/F_m) and effective ($F_q`/F_m`$) photochemical efficiency. For full definitions of the photosynthesis parameters, please see Appendix C.1. A response curve was fitted using least squares non-linear regression (Hennige et al., 2010;

Nitschke et al., 2018) which produced an estimate of the minimum saturating light irradiance required to saturate photosystem II (E_k).

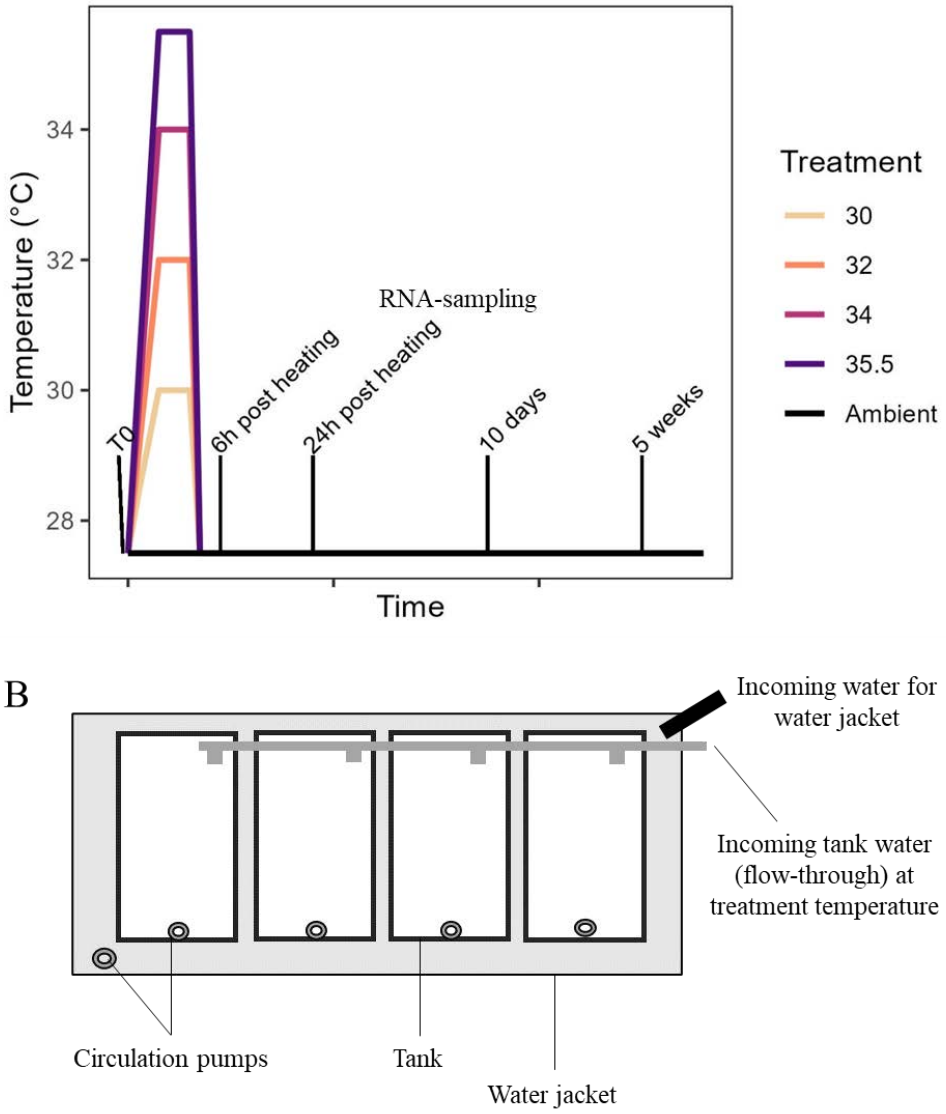

Figure 4.1 Experimental design and tank set-up. (A) Temperature treatment profiles and sampling design through time. Time series on x-axis not to scale. (B) Schematic of treatment tank setup with one system per treatment.

4.3.4 Physiological maintenance (PM)

Composite metrics of multiple physiological traits have been used to quantify coral thermal tolerance (Humanes et al., 2022). To rank individual colonies based on their ability to maintain physiological homeostasis during heat stress, I calculated mean colony performance across

physiological traits (colour change, weight change, and photosynthesis performance) in the 34 °C treatment. For each trait, mean colony changes were calculated for each treatment (see Appendix C.4 for trait-specific sample sizes and trait ranges). For colour and weight changes, colonies were given a rank score from 1 – 30, with 1 being the least tolerant colony and 30 being the most tolerant. For E_k and F_q'/F_m', colonies were scored from 1 – 23 due to missing data for seven colonies. For colour change, low maintenance was defined as the greatest decrease in tissue colour in the 34°C treatment where highly tolerant colonies showed little to no colour change. For weight changes, the least tolerant colonies were those which recorded the greatest weight loss ($-7.04 * 10^{-4}$ g d^{-1} g^{-1}) while tolerant corals recorded little to no weight loss and even recorded a slight weight gain in some cases (greatest weight gain = $1.79 * 10^{-4}$ g d^{-1} g^{-1}). For photosynthetic performance, scores were derived from both minimum saturating irradiance (E_k) where tolerant colonies had a high minimum saturating irradiance (E_k) value and F_q'/F_m' where tolerant individuals recorded high values. Each raw ranking score was then normalised (score / n genotypes) to produce normalised ranks between 0 - 1 and account for the different number of genotypes included in the four traits. The average of normalised ranks was then calculated to produce a composite score of physiological maintenance (PM, Appendix C.4-5). The 20% of genotypes with the lowest PM were classed as "low" performers while the 20% of genotypes which recorded the highest average PM scores were classed as "high" performers. As one of the six high-performing genotypes did not have photosynthesis data, an extra genotype was included here.

4.3.5 RNA extraction and sequencing

To quantify gene expression in response to acute heat stress, samples from the 34°C treatment were compared to those from the ambient treatment at the 24 h time point. The most extreme treatment was not included due to severe tissue sloughing which impacts down-stream analyses (Voolstra et al., 2021b). Working with preserved samples, a small piece (<5 mm) was cut by scissors from below the apical corallite and placed in a 1.5 mL microcentrifuge tube where ~100 µL of acid-washed glass beads (710-1,189 µm) were added along with 600 µL of Buffer RLT (supplied with the Qiagen RNeasy Mini Kit), and 6 µL of BME (β-mercaptoethanol). The samples were stored on ice and all tools were cleaned between samples with 70% ethanol followed by RNAZap (Invitrogen, MA, USA). The samples were vortexed in pairs at maximum speed for 30 sec and rested on ice. This was repeated five times so all samples were vortexed

for a total of 2 min 30 sec. If tissue was still visible on the fragment, samples were vortexed for another 30 sec and checked again. The liquid was transferred into a clean microcentrifuge tube (1.5 mL) and centrifuged (3 min, 10k rpm, 4ºC). Without disturbing any of the resulting skeletal debris and bead pellet, the liquid was withdrawn and placed into a new clean microcentrifuge tube (1.5 mL) and total RNA was extracted using the Qiagen RNeasy Mini Kit following manufacturer's protocol. In brief, 600 µL of ethanol (70%) was added to the buffer and mixed by pipetting. Ethanol, buffer, and precipitate (700 µL) was transferred to a spin column placed in a collection tube and centrifuged at 10k rpm for 30 sec at 4ºC. Flow-through was discarded. This was repeated until all of the sample had passed through the spin column. Buffer RW1 (350 µL) was added to each sample, incubated on the benchtop at room temperature for 5 min, centrifuged (30 sec, 10k rpm, 4ºC) and the flow through was discarded. Working at room temperature, 80 µL of DNase solution was added directly to the column membrane and left to incubate for 15 min. Buffer RW1 (350 µL) was then added to each sample and centrifuged at 10k rpm (30 sec, 4ºC). Then 500 µL of Buffer RPE was added and the spin columns centrifuged (30 sec, 10k rpm, 4ºC) following a 1 min incubation at room temperature. The flow through was discarded. This was repeated a second time (500 µL, 2 min, 10k rpm, 4ºC) after which the spin column was placed into a clean collection tube and spun dry (10k rpm, 1 min, 4ºC). To elute RNA, 60 µL of RNase-free water was added directly to the spin-column membrane. Samples were incubated at room temperature for 5 min before being centrifuged (1 min, 10k rpm, room temperature) to elute RNA. The RNA elution was repeated using the same 60 µL followed by a 5 min incubation at room temperature.

The quantity of total RNA extracted was obtained using the Qubit HS RNA quantification kit on a Qubit 3.0 Fluorometer (Thermo Fisher Scientific). RNA purity was assessed by absorbance ratios on the Nanodrop 2000 (Thermo Fisher Scientific). All samples were analysed on the Bioanalyzer 2100 (Agilent, Santa Clara, CA, USA) to obtain the RNA integrity number (RIN, Schroeder et al., 2006). Extracted samples were shipped on dry ice to a commercial sequencing provider (Novogene, Hong Kong) for library preparation and sequencing. Upon sample receipt at the sequencing facility, mRNA was purified from the total extracted RNA samples by poly-T oligo-attached magnetic beads. The first strand of cDNA was then synthesised by random hexamer primers while the second cDNA strand was synthesised by dUTP rather than dTTP and directional libraries were generated. Quantified and

quality-controlled libraries were pooled and sequenced on the NovaSeq 6000 Illumina platform on a single S4 lane, returning paired-end 150bp reads.

4.3.6 Coral and Symbiodiniaceae gene expression

Raw RNA-seq reads were assessed using the moqc (github.com/marine-omics/moqc) Nextflow (Ewels et al., 2020) pipeline to confirm that read quality was high and that bacterial or unexpected eukaryotic taxa did not account for a significant fraction of reads (e.g. > 10%). Taxonomic profiling by moqc was based on classifying a subset of 1 million reads per sample by KrakenUniq (Breitwieser et al., 2018; Wood & Salz, 2014) using a custom database designed for corals and their symbionts (github.com/marine-omics/moqc). Results from this KrakenUniq step were visualised with Krona interactive plots (Ondov et al., 2011) and used to identify the dominant Symbiodiniaceae genus in each sample. Quality of reads were assessed by fastp (Chen et al., 2018) and a report for all samples was generated using MultiQC (version 1.11, Ewels et al., 2016).

After passing initial quality checks, all samples were processed using a second custom Nextflow pipeline (github.com/marine-omics/morp) designed for dual organism alignment (e.g. coral and symbiont). In this pipeline, the reference transcriptomes of *Acropora tenuis* (Cooke et al., 2020; Liew et al., 2016; ReFuGe 2020 Consortium, 2015) and *Cladocopium goreaui* (Chen et al., 2022) were concatenated to create a combined reference and this was then indexed using bowtie2 (Langmead & Salzberg, 2012). Adapter and quality trimmed reads (via fastp) were then mapped to this combined reference using bowtie2 and quantified at the transcript level using RSEM (Li & Dewey, 2011). Transcript counts generated by RSEM were then imported into R statistical software (R Core Team, 2022) using *tximport()* (Soneson et al., 2015). Four unpaired genotypes (i.e. where one treatment was not sequenced) were excluded from analysis to result in an equal (balanced) sample design. Further, sample-to-sample distances were visualised on a heatmap which further identified a separate sample cluster, comprised of six samples which were also removed given potential species misidentification (Appendix C.6). A total of 34 paired (ambient and heated) samples were included in the analysis, representing 17 genotypes. Low abundance genes were defined as those with read counts < 20 in more than half the samples and 42,086 such genes were excluded. Normalisation, statistical modelling and differential gene expression was performed with the *DESeq2* package (Love et al., 2014), which modelled errors using a negative binomial

distribution and Wald's tests were used to determine statistical significance between gene expression across treatment groups. All genes across both organisms (coral host and symbiont) were analysed simultaneously with a False Discovery Rate (FDR) adjustment of 0.05 to account for statistical inflation due to multiple testing. Differentially expressed genes (DEGs) were then separated based on organism of origin prior to gene enrichment analyses.

Rank-based gene ontology analysis with adaptive clustering was used to identify enriched clusters in response to heat stress (Wright et al., 2015) using the GO_MWU procedure with Uniprot accession IDs used for each gene identified from the coral host. This method does not rely on previously identifying genes as significantly differentially expressed but rather examines all genes present and uses a continuous measure (logFold2Change) to determine enrichment.

4.3.7 Identification of co-expression gene modules associated with physiological maintenance under acute heat stress.

Weighted gene co-expression network analysis (WGCNA) was undertaken to identify sets of genes (modules) with similar expression profiles that were also significantly associated with physiological maintenance (PM) in recognition of the multifaceted physiological and transcriptomic responses to heat stress in corals. Host gene count tables from all samples were analysed with the WGCNA R package (Langfelder & Horvath, 2008, 2023; Zhang & Horvath, 2005). Outlying genes were identified with the in-built package function *goodSamplesGenes()*, and outliers were visualised on a hierarchical cluster dendrogram (*hclust()*) and also on a PCA before being filtered out. All samples (n = 18) passed this quality control step, but 5,027 outlying genes were removed (Appendix C.7). A *DESeq2* object was created (Love et al., 2014) and genes which did not have at least 15 counts in more than 75% of all samples were filtered out before a variance-stabilising transformation was applied with the package function *vst()*. After removal of low count genes, a total of 11,644 genes were analysed. The soft power threshold was selected by examination of the *pickSoftThreshold()* outputs accounting for a scale free topology model fit of $R^2 > 0.8$ with minimal mean connectivity. Here, a power of 12 was used (Appendix C.7.3). The network was constructed with the *blockwiseModules()* function with a mergeCutHeight of 0.25, and a minimal module size of 30 genes. Treatment (ambient vs 34ºC) and physiological maintenance (PM) category (low vs high) were coded as

binary variables prior to calculation of correlation coefficients of module eigengenes and significant associations were visualised on a heatmap.

4.3.8 Statistical methods

4.3.8.1 Physiological responses to acute heat stress

To document declines in physiological traits (colour change, buoyant weights, and F_q'/F_m') across treatments, generalised linear mixed effect models were fitted with the R function *glmmTMB()* from that package with restricted maximum likelihood (Brooks et al., 2017). Treatment and genotype ID were modelled as fixed effects, assuming a Gaussian distribution of all dependent variables and model assumptions of normality and homoscedasticity of plotted residuals were checked with the DHARMa package (Hartig & Lohse, 2021). Adjusted *p*-values for the Post-Hoc Tukey's HSD tests were obtained using the single-step method. To specifically test for differences between genotypes within the 34ºC treatment, linear mixed effect models were fitted, also with restricted maximum likelihoods with the *lme()* function in the nlme package (Pinheiro et al., 2017). Here, genotype was modelled as the single fixed effect while tank was included as a random effect. Assumptions of normality and homoscedasticity were checked by *qqPlot()* in the car package (Fox & Weisberg, 2019) and Wald's tests conducted. Adjusted p-values for Post-Hoc Tukey's HSD tests were calculated with the Bonferroni adjustment (Whitlock & Schluter, 2009). All analyses were performed in R (version 4.2.1; R Core Team, 2022).

4.3.8.2 ED50

As the development of a rapid proxy of coral thermal tolerance is central to the overall thesis, acute heat tolerance (ED50) was quantified at the 24 h sampling point, where the maximum PSII photochemical efficiency (F_v/F_m) was calculated from the rapid light curve data for each genotype. Seven genotypes with missing data in the 35.5ºC treatment were excluded from the analysis. The average F_v/F_m was calculated for each genotype (n = 23) across two replicate samples and modelled using a three parameter logistic regression model with the *drm()* function in the drc R package (Ritz et al., 2015).

To correlate gene expression profiles to acute thermal tolerance (ED50), differential gene expression was recalculated with the DESeq() function (Love et al., 2014). ED50 category was used as the grouping factor of interest and reflected the top eight performing genotypes (highest

ED50), middle eight genotypes and bottom seven genotypes (lowest ED50s). Samples identified previously as outliers and those where ED50s could not be calculated due to insufficient declines in photosynthetic output were excluded from analysis, and each treatment was analysed separately, with 19 samples in the ambient treatment and 14 in the heat treatment. Given the overall thesis aim of understanding how rapid proxies of heat tolerance (here ED50) relate to coral physiology it was important to investigate gene expression patterns solely based on ED50 performance.

4.4 Results

4.4.1 Colony-level variation in physiological responses to acute heat stress

Over time, all coral individuals exhibited decreases in photosynthetic performance, loss of tissue colour, and reduced growth as acute thermal stress increased (Appendix C.8, C9, C.11, C.13). At 34°C, corals exhibited significant variability in physiological responses to acute heat stress between individual colonies. While tissue colour change decreased significantly across treatments (Wald's test, df = 4, F = 544.15, $p < 0.0001$, Appendix C.9), there were also significant differences in colour loss between individuals at 34°C (Wald's test, df = 29, F = 37.56, $p < 0.0001$, Fig 4.2A, Appendix C.10). Colour change ranged from a decrease in colour (-3.65, genotype ID 16) to an increase and darkening in colour (0.13, genotype ID 27). In total, 11 statistically significant groupings were identified using the Tukey's HSD test (Fig 4.2A, Appendix C.10). Effective photochemical efficiency (F_q'/F_m') also showed differences between individual colonies (Wald's test, df = 22, F = 6.96, $p < 0.0001$, Fig 4.2B). Significant differences were influenced primarily by the low performance of genotype ID 20 (0.549 ± 0.0125, Fig 4.2B, Appendix C.12) compared to the other 21 genotypes (range 0.615 – 0.704). Weight changes showed significant treatment effects 10 days after the end of heating (Wald's test, df = 3, F = 13.61, $p < 0.0001$, Appendix C.13) with genotype differences within the 34°C treatment (Wald's test, df = 29, F = 2.21, p = 0.0206, Fig 4.2C, Appendix C.14). Finally, acute thermal tolerance (ED50) also showed significant differences between genotypes and ranged by 0.94°C (mean= 35.27°C) between the lowest (34.8°C genotype ID 24) and highest (35.74°C genotype ID 30) ED50 (Fig 4.2C, Appendix C.15, Appendix C.29).

Overall, physiological responses differed by genotype across these traits whereby some individuals were able to maintain physiological homeostasis at high temperature. For example, genotype ID 8 showed high physiological maintenance across all traits (colour change, F_q'/F_m', weight change, and ED50), consistently ranking amongst the top five genotypes (Fig 4.2). Genotype ID 30 similarly showed a high capacity for physiological maintenance. However, most colonies showed contrasting physiology between traits. For example, genotype ID 16 recorded a relatively high ED50 (35.49°C) but high weight loss ($-1.58 * 10^{-4}$ g d^{-1} g^{-1}) while genotype ID 25 showed low photochemical efficiency (F_q'/F_m', 0.62) but remarkably little change in tissue colour (0.13). When a composite measure of physiological maintenance across four traits (colour change, weight change, F_q'/F_m', and E_k) was calculated, four genotypes were categorised as "high" scorers and five genotypes as "low" scorers (Fig 4.3, Appendix C.16 and

C.17). Correlations between the different physiological traits across genotypes revealed a significant correlation between tissue colour change and F_q'/F_m' (cor = 0.597, $p < 0.01$), with no other significant correlations detected (Appendix C.17b. and C.28).

4.4.2 Photosynthetic performance

The photo-physiological characteristics responded strongly in both treatments. The minimum saturating intensity (E_k) differed significantly between treatments (ANOVA, df = 4, F = 84.82, p = <0.0001, Fig 4.4A). The ambient treatment (27.5°C) and the 30°C treatments recorded similar high E_k means (187.1 and 174.3, respectively, Tukey's; t ratio = 1.64, p = 0.47). E_k means also did not differ significantly between the 32°C and 34°C treatments (126.2 and 132.6, respectively, Tukey's t ratio = -0.768, p = 0.94, Fig 4.4A). The 35.5°C treatment recorded the lowest E_k values (45.5). F_qF_{mMax} was relatively stable across all treatments but experienced significant declines in the 35.5°C treatment (ANOVA, df = 4, F = 485.8, $p < 0.0001$, Fig 4.4B, Appendix C.27). Additionally, corals in the 34°C treatment recorded significantly lower F_qF_{mMax} values than those in the 30°C treatment (Tukey's, t ratio = 3.36, p = 0.008). Only the hottest treatment (35.5°C) resulted in a shift of preferential photochemical (1-C: Fig 4.4D) vs non-photochemical (1-Q: Fig 4.4C) energy dissipation and resulted insignificant reductions in rETR relative to all other treatments (Fig 4.4E).

4.4.3 RNA-Seq yields and taxonomic classification

The average number of sequenced reads per sample was 47.27 million ± 1.107 million (mean ± SE, ~23.63 read pairs, range; 40 – 67 million reads). Most classified reads (64 ± 1.4 % per sample) belonged to *Acropora. Cladocopium* was identified as the primary symbiont genus (18.23 ± 0.7 % per sample, Fig 4.5A) in these samples. Symbionts from the genus *Durusdinium* symbionts were also present in all samples but at very low abundance (<0.56 ± 0.02 %, Appendix C.18). While most classified reads were identified as originating from the coral or its dominant symbiont via KrakenUniq, the mean mapping rate to the combined reference transcriptome was low ~38.51 ± 0.59 % (mean ± SE; range 26 – 46.3%). Coral host-derived reads mapped to 30,327 reference genes while symbiont-derived reads mapped to 45,322 genes (Appendix C.18).

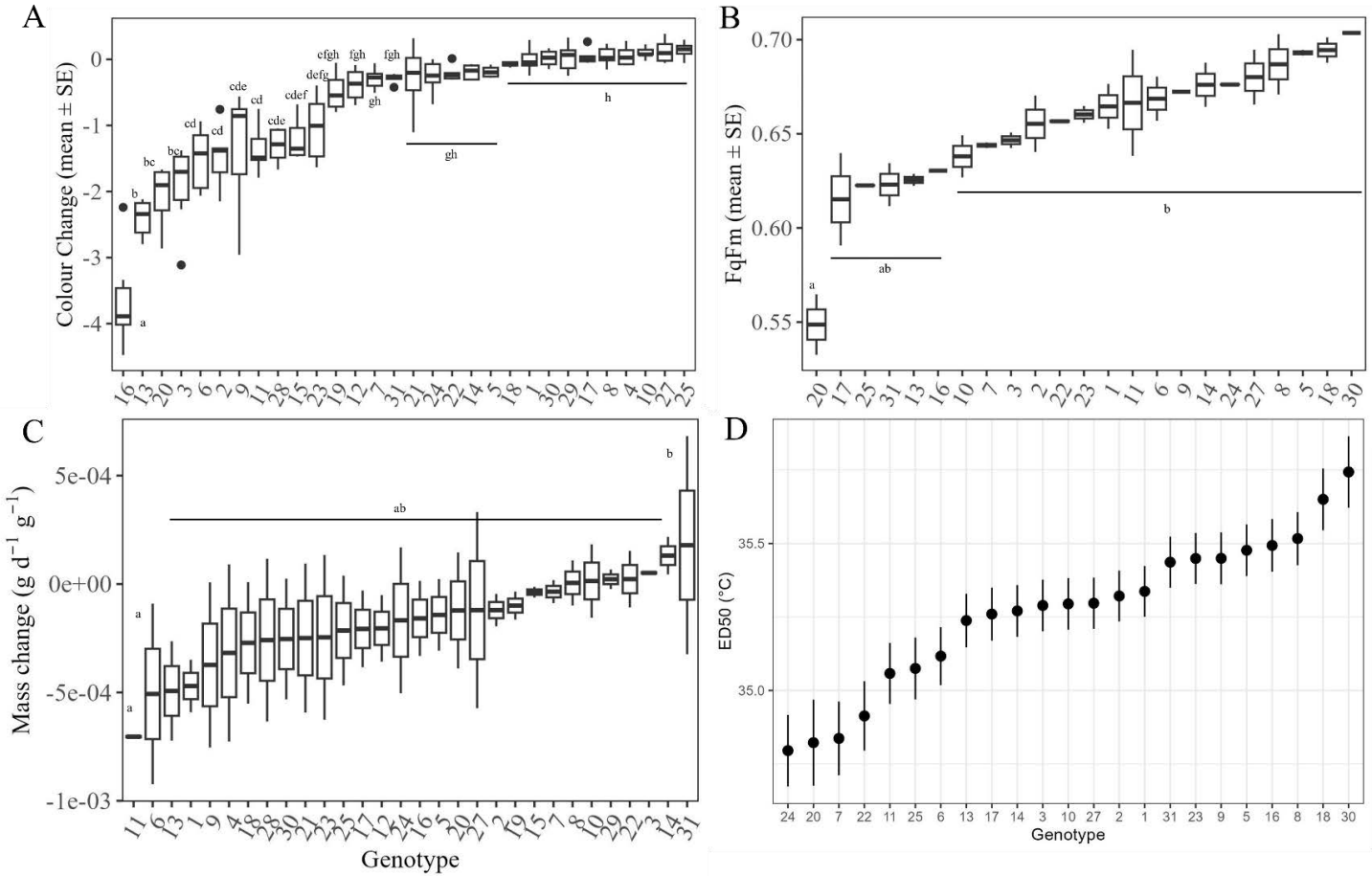

Figure 4.2 Colony-level variation in physiological responses to acute heat stress after heating. (A) Tissue colour change (final – initial colour score); (B) effective photochemical efficiency (F_q'/F_m'); (C) weight changes 10 days after heating expressed as grams per day per gram initial weight; (D) Colony-level ED50 used to define acute heat tolerance as low, mid, high. ED50 temperature is shown on the x-axis, the black circle indicates the mean ED50 per genotype and the whiskers show the 95% confidence intervals. Small lettering indicates Tukey's HSD post-hoc groupings with a Bonferroni correction. Genotype ID is listed from poorest to best performance (left – right). Tissue colour change (A), F_q'/F_m' (B), and ED50 (D) quantified 24 h after heating while weight changes (C) were quantified 10 days after heating. Finally, A – C was quantified in the 34ºC treatment, while ED50 (D) was derived from photosynthetic performance across all treatments.

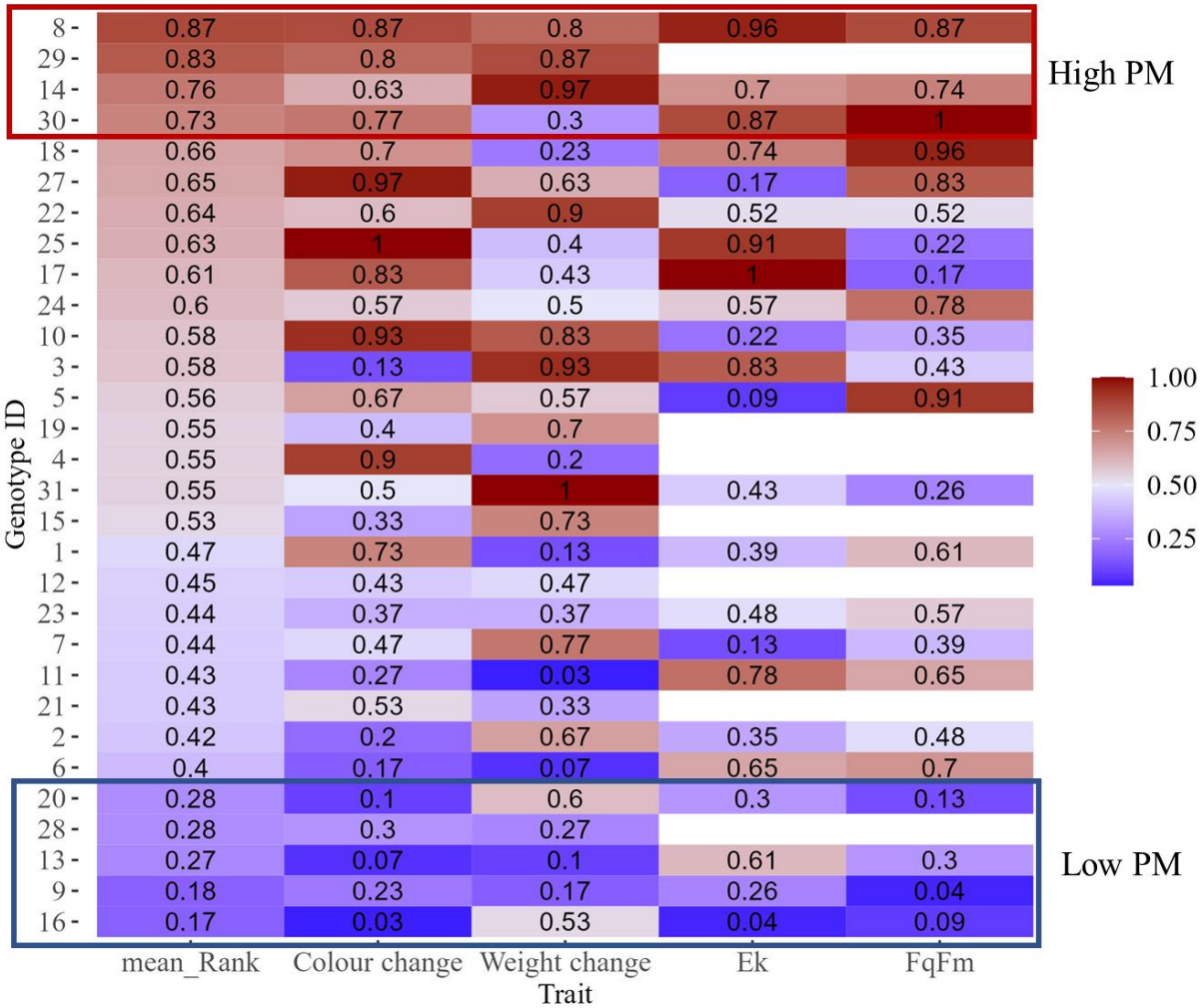

Figure 4.3 Physiological maintenance score (PM) across four traits. The tile colours and values indicate the normalised rankings (0-1). The boxes show the physiological maintenance score category (red = high PM, blue = low PM), where low scores < 0.28 and high scores > 0.70.

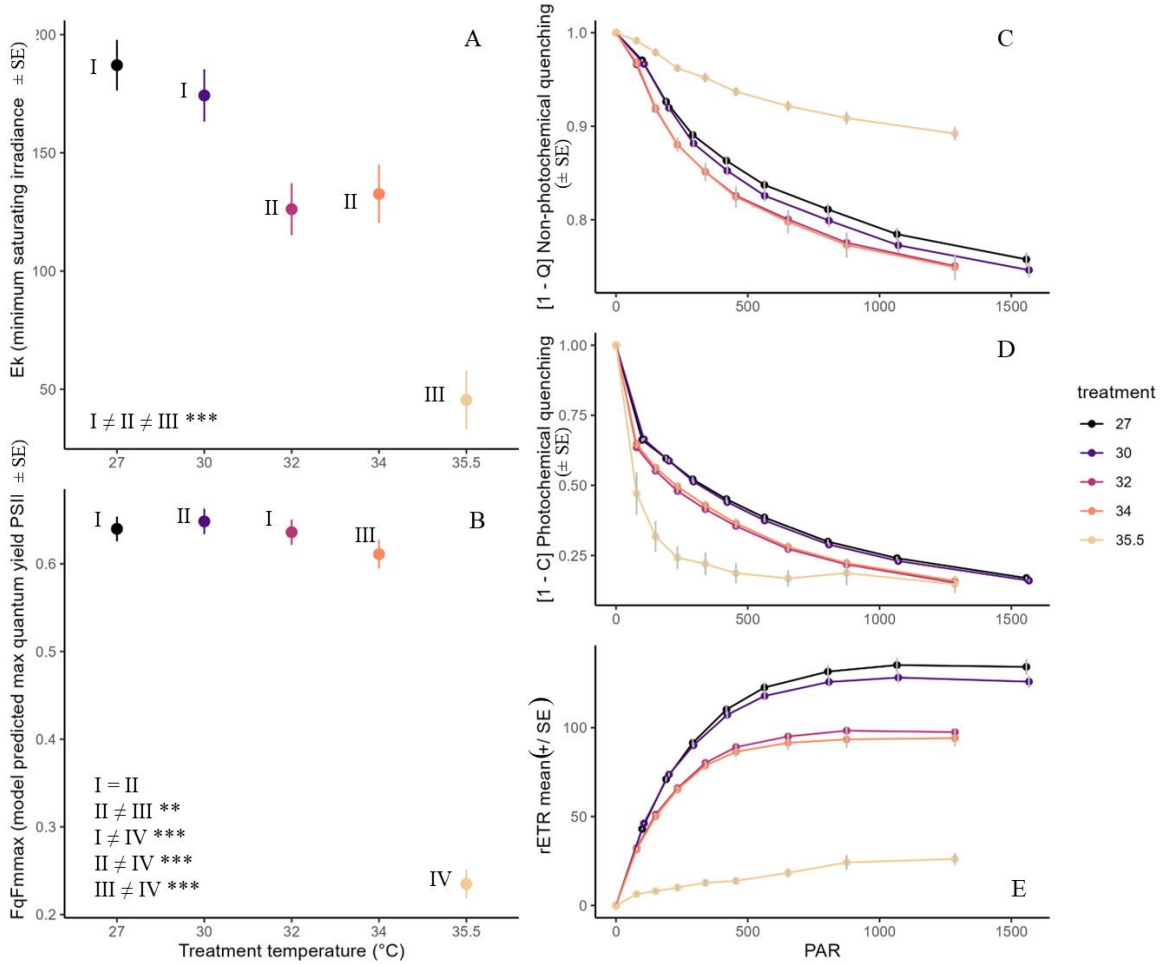

Figure 4.4 Photo-physiological performance derived from Rapid Light Curves24h after heat exposure across all five treatments. (A) Mean saturating intensity (E_k) by treatment. (B) Mean F_qF_{mMax} by treatment. (C) Light levels where non-photochemical quenching occurs (1-Q). (D) Photochemical quenching (1-C). (E) Relative Electron Transfer Each curve is coloured by treatment and presents the mean of that treatment at the respective PAR level. The bars on each curve indicate the standard errors.

4.4.4 Gene expression response to acute heat stress

After filtering low abundance genes, 13,293 were retained from the host reference and 20,270 from the symbiont reference. Of the host genes, 569 were significantly up-regulated (higher expression in heated treatment) and 266 downregulated 24 h after heat stress. In the symbiont reads retrieved, 17 genes were upregulated and seven downregulated (Appendix C.19). When visualised on a Principal Component plot, treatment was a much stronger driver of expression profiles in the host (Fig 4.5B) than it was in the symbionts (Fig 4.5D). In the host, treatments separated along PC2 (26.1% variation explained). Genotype appeared to be the main driver of separation along PC1 (48.5% variation explained), with one colony (ID 20) showing divergent

expression from all others (Fig 4.5C and E). Classic coral heat stress response genes such as heat shock proteins (hsp68 and hsp16.41), Ubiquitin-like proteins, and green-fluorescent-protein (GFP)-like fluorescent chromoproteins were significantly upregulated in response to treatment (Appendix C.20). Additionally, photoprotective genes such as Ubiquitin-protein ligases and Ras-related protein (Rab-30) were also significantly upregulated in response to heating (Appendix C.20).

In the coral host, 84.8 % of differentially expressed genes had gene ontology annotations (n = 11,269) and from these, a total of 28 GO terms were significantly ($P_{adj} < 0.05$) enriched among genes that changed expression in response to acute heating (Appendix C.21, Fig 4.6). Broadly, a suite of GO terms related to cytoskeleton activity (microtubule, microfilament, cytoskeletal protein binding, motor activity) were significantly up-regulated in response to heating. In contrast, DNA and RNA processing GO terms were down-regulated in response to heating (terms including structural constituent of ribosome, ncRNA, rRNA metabolic process, RNA processing, DNA replication checkpoint, and DNA metabolic process; Fig 4.6).

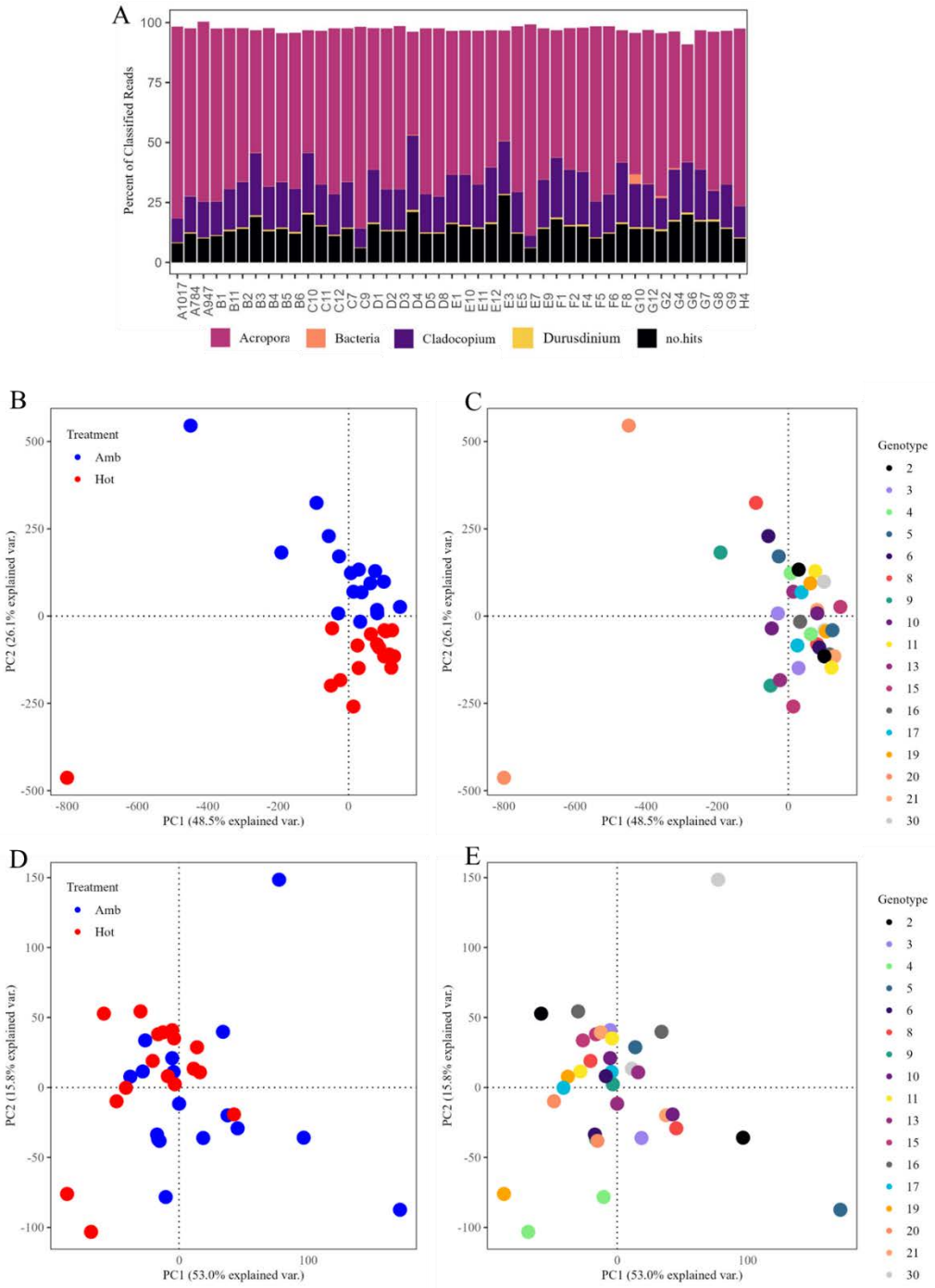

Figure 4.5 Gene expression differences in coral host and symbionts in response to acute heat stress. (A) Taxonomic classification of reads from KrakenUniq with each bar representing a sample. The dark pink bars show the proportion of reads classified as *Acropora*, the purple bars show reads from *Cladocopium*, orange reads originate from bacteria while the yellow reads show the proportion of reads from *Durusdinium*. The black bar shows the proportion of reads which could not be classified. Bars do not sum to 100% due to exclusion of some taxa such as background Symbiodiniaceae genera (*Breviolum* and *Fugacium*) . Gene expression patterns in *Acropora tenuis* in response to treatment (B) and genotype (C) visualised on a Principal Component (PCA) plot. PCA of gene expression patterns in *Cladocopium* spp in response to treatment (D) and coral host genotype (E). For B and D, dots are coloured by treatment (blue = ambient samples, red = heated 34ºC samples). For B-E, the proportion of data variability explained by each principal component is given in the axis title.

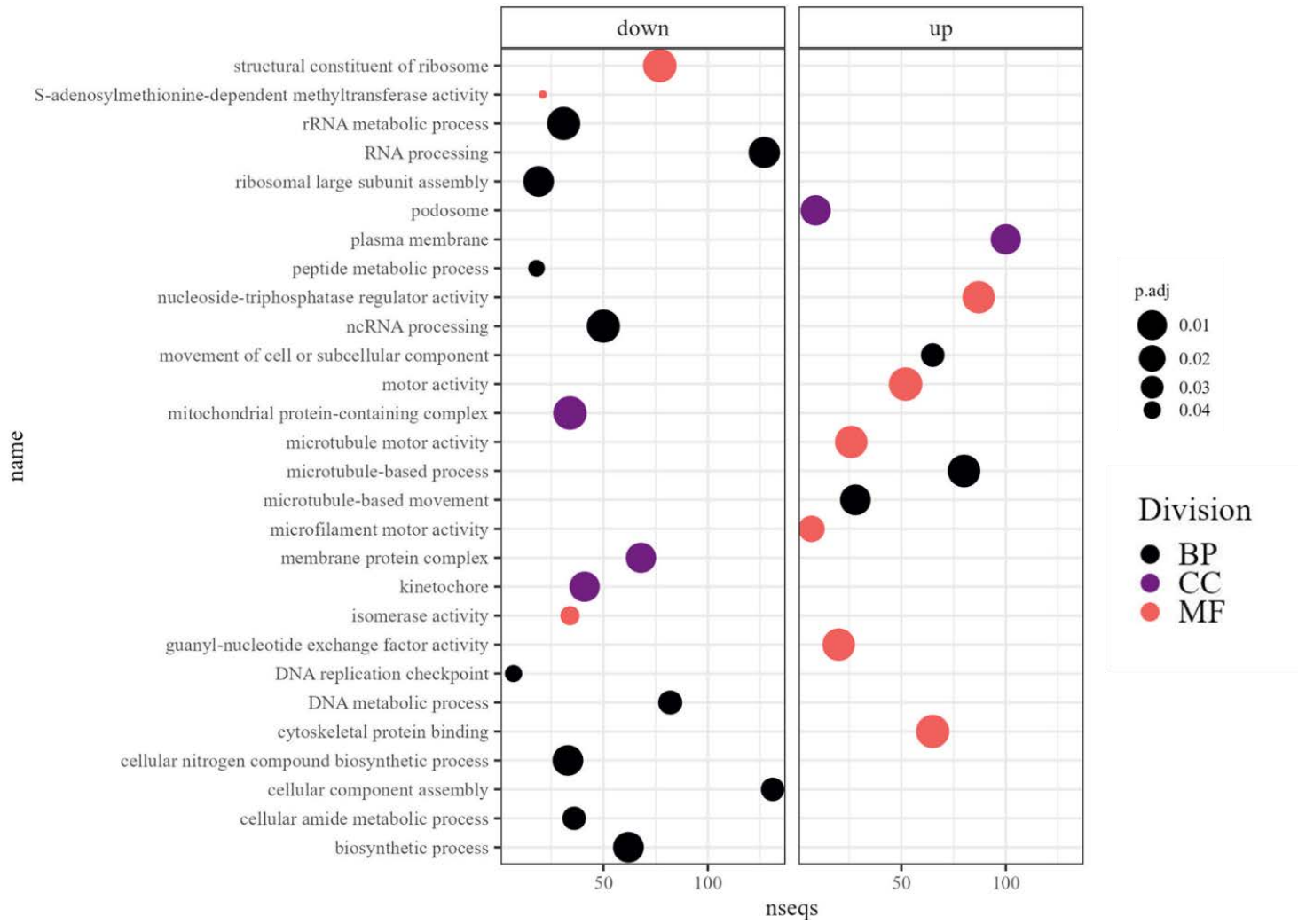

Figure 4.6 Gene ontology (GO) terms significantly enriched in response to acute heating.Points are coloured by ontology (Biological Process (BP) = black, Cellular Component (CC) = purple, Molecular function (MF) = orange) and the size corresponds to the adjusted p-value (P_{adj}). The number of genes identified within each term is shown on the x-axis and GO terms are given by name on the y axis. The terms are separated by direction of enrichment (down vs up).

4.4.5 Differential gene expression in tolerant vs intolerant individuals

In the heated treatment, eight host genes were significantly downregulated in heat tolerant vs sensitive individuals while 17 were upregulated (Fig 4.7A). Of these genes, annotations only existed for 16 (five down- and 11 upregulated, Appendix C.23). Tolerant individuals recorded significant downregulation of two Ubiquitin-protein ligases, and upregulation of a dual serine/threonine and tyrosine protein kinase, all of which are homologous to genes typically noted as part of the classic stress response proteins (Appendix C.23). The number of DEGs was similar in the ambient treatment with four down-regulated and nine up-regulated genes (Fig 4.7B) in the tolerant individuals. Here, three down- and six up-regulated genes had annotations. Interestingly, two genes were significantly upregulated in tolerant genotypes in both the ambient and heated treatment (ATP-dependent DNA helicase and sodium- and chloride-dependent GABA transporter, Appendix C.24). Further, GFP-like non-fluorescent chromoprotein was significantly down-regulated in tolerant individuals under ambient conditions. The symbiont profiles (Fig 4.7C and D) recorded a more muted response in the number of DEGs relative to the host, with only seven down-regulated genes reported in the heated treatment (Fig 4.7C). Finally, when visualised on a Principal Component plot, there was little separation between the three ED50 categories (low, mid, high) in either treatment (Fig 4.7E and F).

To investigate the relationship between gene expression patterns and genotype capacity for physiological maintenance (PM, section 4.4.1, Fig 4.3), I conducted a weighted gene co-expression network analysis (WGCNA). The 11,644 host genes were assigned to 12 gene modules (Fig 4.8A, Appendix C.25) of which three modules (grey, blue, brown) were significantly associated with differences in physiological maintenance (high vs low PM, Fig 4.8B). The blue module (n = 1,953 genes) was downregulated in individuals with high physiological maintenance capacities (high PM, cor = -0.57, Fig 4.8B) and significantly enriched for three ontologies, all pertaining to extracellular functions: extracellular space (GO:0005615), plasma membrane (GO:0005886), and the extracellular region (GO:0005576). Although both the brown (n = 981 genes) and grey (n = 2,939 genes) modules were significantly upregulated (grey cor = 0.5; brown cor = 0.65) in tolerant individuals, no terms were significantly enriched at the GO level .

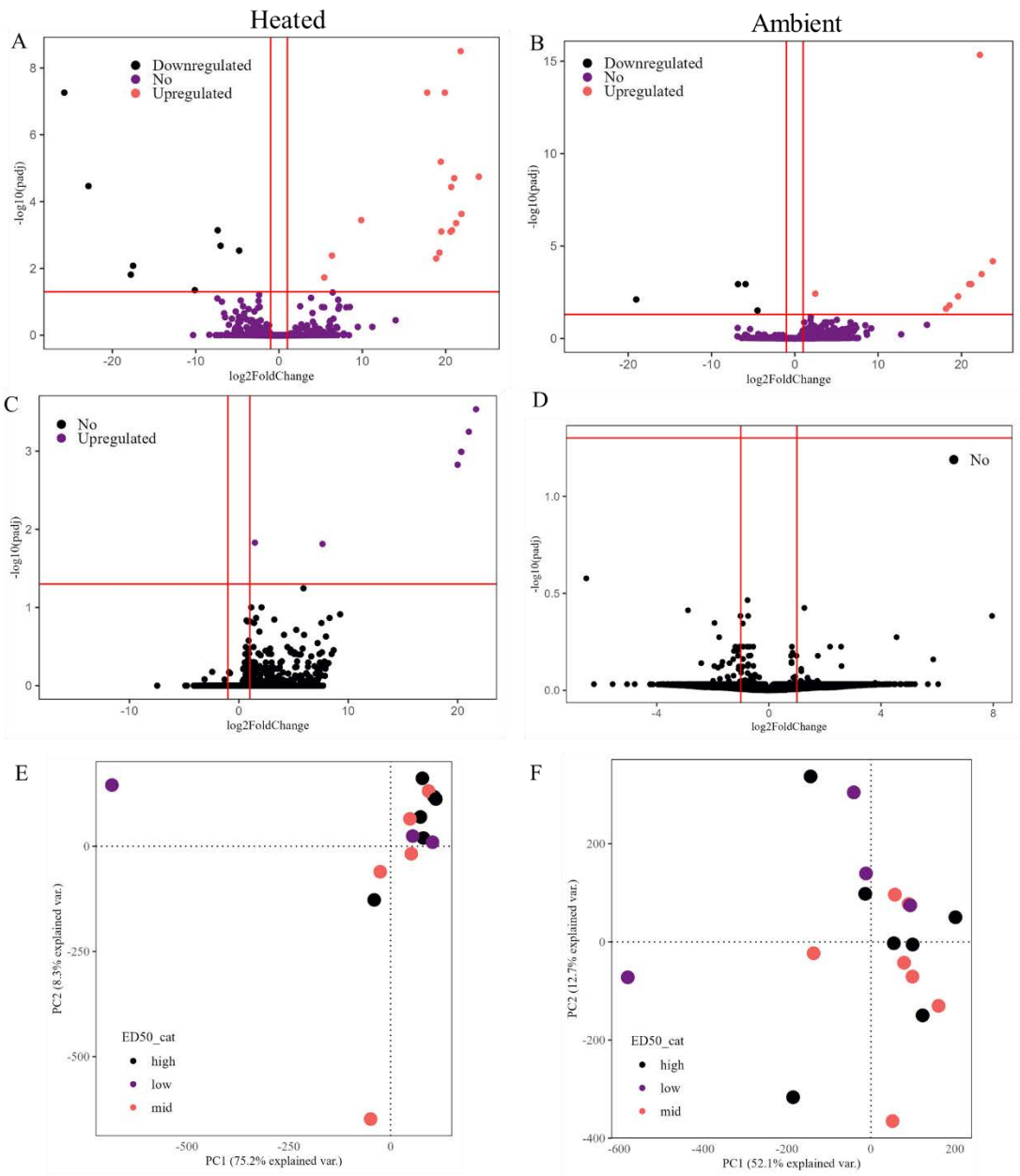

Figure 4.7 Differential gene expression between treatments with respect to acute heat tolerance. (A-D); volcano plots showing the direction of DEGs in the heated (left) and the ambient treatment (right). The red lines indicate the significance cut-offs applied (log2foldchange > 1, and $P_{adj} < 0.05$). Host DEGs (A and B). Symbiont DEGs (C and D). Principal Component ordination plot of host gene expression coloured by ED50 category in the heated (E) and the ambient (F) treatments.

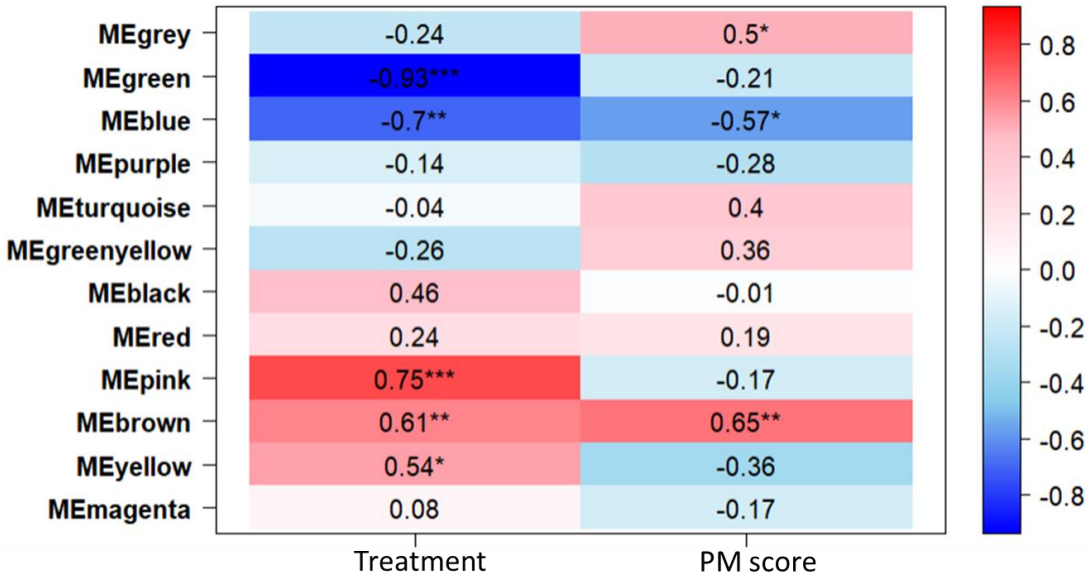

Figure 4.8 Modules identified by WGCNA and their association with Treatment and PM category. Gene clusters associated with treatment and physiological maintenance score (PM), respectively. Co-expression modules are named by their assigned colours. The heatmap colours correspond to the correlation coefficient between the module eigengenes and the trait (treatment and PM score). The numbers show this correlation coefficient and the asterisk indicate the significance level of the correlation where * $p < 0.05$, ** $p < 0.01$, *** $p < 0.001$.

4.5 Discussion

Gene expression is a key mechanism of coral thermal tolerance. As a fitness-related trait (Kenkel & Matz, 2016), it has important implications for continued reef survival and thus conservation efforts. Coupling high-throughput acute heat stress assays with transcriptomic responses enable the potential for rapid, large-scale assessment of underlying molecular drivers of heat tolerance in corals across species and populations. It does this by documenting the hundreds to thousands of loci involved in the coral heat stress response, critical for acute tolerance. This study also shows genotypic differences in physiology across multiple photosynthetic measures and tissue colour change in response to acute heating at 34ºC. It then correlates these physiological differences to significant differential gene expression patterns in 17 colonies of *Acropora tenuis* 24 h after the end of acute heat stress. Interestingly, I find a small number of frontloaded genes in highly tolerant genotypes (high ED50) to be significantly upregulated in the ambient treatment. Further, weighted gene co-expression network analysis revealed two gene modules that significantly associate with physiological maintenance (PM scores) and one module was also significantly enriched for three gene ontology terms, all related to extracellular proteins. Finally, the significant declines observed in multiple photosynthetic metrics indicate that corals suffered progressively deleterious heat stress across treatments with near photosynthetic inhibition at the most extreme temperature treatment (35.5ºC). Taken together, these results highlight that acute heat exposure impacts coral gene expression 24 h after exposure and identifies a small number of genes as potential gene expression markers of high acute heat tolerance.

4.5.1 Genes significantly associated with high acute heat tolerance as potential markers of tolerance

Coupling transcription responses to measures of holobiont thermal tolerance enables the detection of genes (or gene clusters) that are involved with thermal tolerance and may have important implications for the detection of genetic markers of thermal tolerance within a population (Bay & Palumbi, 2017b; Louis et al., 2017). A small number of genes (9) were significantly upregulated in the absence of thermal stress in highly tolerant individuals (high ED50). Some of these genes are involved in pathways typically activated under thermal stress. For example, one gene plays a critical role in DNA repair and recombination (Uniprot O50224,

Castillo-Tandazo et al., 2019), a key cellular process known to occur under plant (Dorn & Puchta, 2020) and coral heat stress (Maor-Landaw & Levy, 2016) while another functions as a transport mediator to maintain cellular communication functions (Uniprot P31646, Ikeda et al., 2012). Interestingly, the potentially photoprotective gene coding for Ubiquitin-protein ligase (Gabilly et al., 2019) was down-regulated in heat-tolerant individuals following acute heat exposure. The rapid acute heat tolerance trait (ED50) used in this study is a symbiont-derived response and the connection between ED50 and coral transcriptomic responses requires further investigation. Maintaining optimal conditions for symbiosis is a process that requires precise regulation of the environment within the coral and it was therefore surprising to document little transcriptomic differences between genotypes with high versus low ED50s. This is further supported by the small number of DEGs observed with respect to heat tolerance category (ED50 high vs low) compared to the number of DEGs observed with respect to treatment. Therefore, weighted gene co-expression network analysis was conducted on individual corals' ability to maintain physiological performance following heat stress (PM scores). This trait incorporated both holobiont- (colour change and weight changes) and symbiont-specific traits (E_k and F_q'/F_m'). One module which was significantly associated with PM scores was enriched for three gene ontologies (extracellular space, plasma membrane, and extracellular region). Plasma membrane ontologies have also been reported in comparisons of heat-stressed vs ambient coral larvae (Strader & Quigley, 2022), while genes associated with the extracellular space/region potentially result in growth advantage in blue coral under warmer temperatures (Guzman et al., 2019). Further, it is possible that corals which were able to maintain physiological homeostasis (high PM scores) lost less symbiont cells than their thermally sensitive counterparts (low PM scores), and therefore these corals were less active in the extracellular and plasma membrane regions. However, monitoring symbiont density changes was beyond the scope of the current study. The distinction between acute heat tolerance (ED50) and physiological maintenance (PM) was incorporated to acknowledge that thermal tolerance is a complex trait, as highlighted here by the complex patterns of responses observed between genotypes and traits (Appendix C.28). Genes with differential baseline expression levels could serve as indicators of heat tolerance but asserting this requires functional assays to confirm their biological function in coral under thermal stress.

4.5.2 Highly variable gene expression following acute heat stress

Since both physiological and molecular responses to heat stress depend on the duration and severity of the stressor (Bellantuono et al., 2012; Cleves et al., 2020a), it was of interest to investigate patterns of gene expression following an acute heat stress procedure and subsequent recovery period. In this study, I found that gene expression profiles were still significantly different between heated and ambient samples 24 hours after the end of the acute thermal challenge. I also found a large number of differentially expressed host genes in response to treatment (569 up and 266 down regulated), which is common for coral heat stress studies which normally report hundreds to thousands of DEGs (Dixon et al., 2020). Interestingly, the 34ºC temperature treatment resulted in more subtle difference in expression profiles within the symbionts where only 24 DEGs were detected, potentially due to the lower number of reads retrieved from the non-target symbionts fraction. Further characterisation of these genes would be of interest but was outside the scope of this study. This muted DEG response in the symbionts could lead to the interpretation that the symbiont community was resilient to the acute heat stress applied but likely reflects the reduced statistical power as fewer reads were obtained from symbionts compared with the coral host. Finally, it is possible that symbiont gene expression works on a timescale not captured in this study. Other studies have reported highly divergent numbers of symbiont DEGs in response to heat stress, spanning a couple of hundred (Avila-Magaña et al., 2021) to a few thousand genes (Gierz et al., 2017). Declines in coral tissue colour and symbiont photosynthetic performance strongly indicate that the symbionts experienced thermal stress at 34ºC. While the number of symbiont DEGs was low, colour change could have result from a loss of Symbiodiniaceae cells within the host tissues.

The signature of DEG changes 24 hrs after the cessation of heat stress was also noted by Savary et al., (2021) in response to their most extreme acute heat exposure (34.5ºC). The authors suggest that this temperature for *Stylophora pistillata* in the Red Sea therefore represents a thermal threshold and that corals experienced mortality at this temperature (Savary et al., 2021). In the present study, while the 34ºC treatment may have resulted in a thermal threshold for some individuals as shown by severe declines in tissue colour and photosynthetic efficiency, others were able to maintain photosynthetic efficiency or only recorded a slight decline relative to ambient-treated corals. Phenotypic plasticity in stress responses at the population level is an important consideration of coral acclimation potential as there are genetic differences underlying these responses as shown through significant heritability estimates

(Kenkel & Matz, 2016). As such, it was encouraging that the 30 colonies of *A. tenuis* tested here showed very different physiological responses to acute heat stress. It was therefore not unexpected that gene expression profiles would also record high variation between individuals (Cunning & Baker, 2020; Granados-Cifuentes et al., 2013). Here, acute heat tolerance (ED50) and gene expression patterns were assessed in 17 colonies, which is assumed to provide a high level of genetic coverage (Baums et al., 2019). Further analysis of the data generated here would be of interest to investigate associations between gene expression and certain alleles.

4.5.3 Gene expression profiles 24 hours post stress contain only some common indicators of coral thermal stress

Transcriptional responses to heat stress are well-described in cnidaria (Cleves et al., 2020b; Dixon et al., 2020; Maor-Landaw & Levy, 2016). Heat stress is often associated with increased expression of heat shock proteins, and proteins involved in DNA repair (Barshis et al., 2013; Juárez et al., 2018). In this study, some common heat stress-response genes were significantly up and down-regulated following the acute heat challenge. For example, two heat shock proteins and a GFP-like protein were significantly upregulated in response to heating. The upregulation of heat shock proteins is well-documented in the cnidarian heat stress response (Barshis et al., 2013; Eghtesadi-Araghi et al., 2010; Haguenauer et al., 2013) while GFP-like proteins have previously been down-regulated under thermal stress (Hume et al., 2013). However, GFP-like proteins have potential photoprotective abilities (Krasowska et al., 2021; Smith et al., 2013), and as such, its upregulation here is likely to represent a photo-protective response mounted alongside other common photo-protective genes upregulated in this study, including Ubiquitin-like proteins (Barshis et al., 2010; Gabilly et al., 2019) and Ras-related proteins (Starcevic et al., 2010). Despite documenting differential expression of such "core" stress-response genes (Cleves et al., 2020b; Dixon et al., 2020), these were not significantly enriched at the ontology level, and it is likely that the recovery period following the exposure to acute heat stress results in a more muted core heat stress response. Further, genes involved with nitrogen cycling, peptide processing, and biosynthetic processes were downregulated in response to heating. Changes to the nutrient cycling between coral host and symbionts contributes to the breakdown of the symbiosis (Morris et al., 2019; Rädecker et al., 2021), and downregulation of these genes therefore indicates that corals were indeed experiencing stress.

Coral thermal tolerance and the role of genetic variation is becoming an increasingly important trait to understand under continued climate change. As transcriptomic changes respond rapidly to environmental perturbations, these approaches further our understanding of coral acclimatory responses to acute thermal stress. Here, acute heat stress significantly impacted gene expression patterns in the host 24 h after exposure concurrent with substantial declines in symbiont-associated physiological traits. Further, by combining transcriptomic analyses with physiological measures of tolerance, this study found a small number of frontloaded host genes in resilient individuals that could be potential gene expression markers of high acute heat tolerance and found multiple genes to be associated with physiological maintenance following acute heat stress. These results add to our existing knowledge of the molecular thermal stress response in corals from an acute perspective. Taken together, the colony variability in gene expression, acute heat tolerance, and physiological responses to acute heat stress observed within this single coral population highlight the need to carefully consider the role of the coral host when managing coral populations and provides evidence of genetic variation in acute heat tolerance already present within a single population, a necessity for potential acclimation and adaptation.

Chapter 5 General Discussion

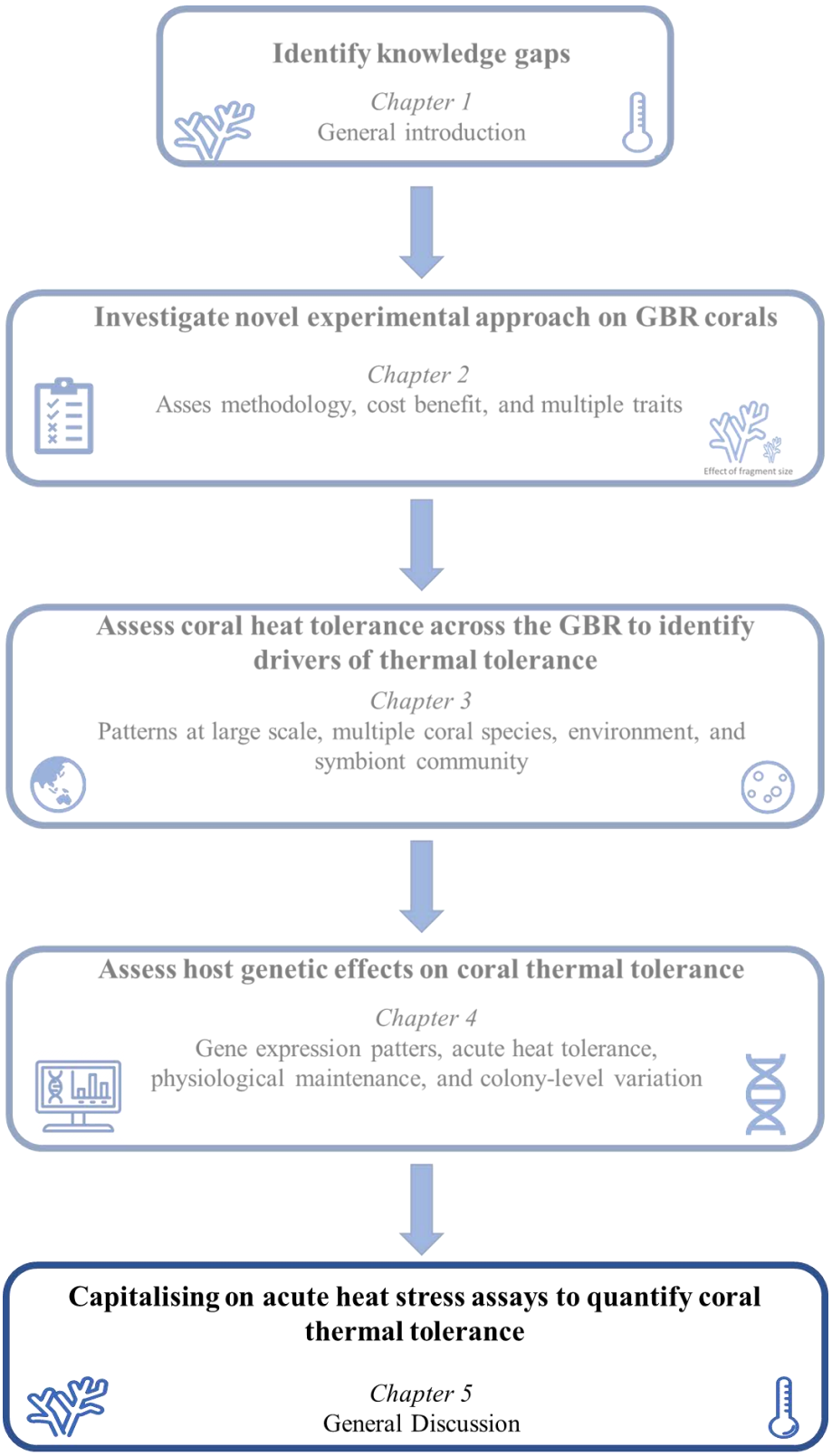

5.1 Thesis summary

This thesis employed a recently developed high-throughput experimental approach to quantify the heat tolerance of three key reef-building coral species across the latitudinal extent of the Great Barrier Reef (GBR). Acute heat stress assays have been suggested as an avenue for rapidly scaling efforts to investigate temperature tolerance across multiple species and populations (Quigley et al., 2022a; Voolstra et al., 2023; Voolstra et al., 2021a). My thesis particularly focussed on the fundamental technical aspects of acute heat stress assays during large-scale field applications to examine the upper heat tolerance limits of several coral species. I describe how multiple factors influence the acute heat tolerance of coral, including symbiont community composition, host gene expression plasticity, and thermal disturbance histories. My research therefore highlights the complexity of studying coral thermal tolerance at scale and provides recommendations for improvements to the method, and in turn provide a framework to evolve more effective application of heat stress assays in the future.

In **Chapter 2**, I examined key experimental and methodological considerations for the application of acute heat stress assays to quantify coral thermal tolerance in a field-setting. I described how photosynthetic performance – a well-used diagnostic of coral heat sensitivity (e.g. Leggat et al., 2022; Nitschke et al., 2018) – may serve as the best-candidate rapid proxy of acute heat tolerance. The chapter also highlighted the need to consider multiple physiological traits when assessing corals' responses to heat stress. Further, using photosynthetic performance as a rapid proxy for acute heat tolerance, in **Chapter 3** I applied acute heat stress assays to examine > 500 coral colonies from three species across 11.5° latitude along the GBR. I documented higher heat tolerance in *Pocillopora verrucosa* compared to both *Pocillopora meandrina* and *Acropora tenuis* and demonstrate reef-sector differences in tolerance, explained primarily by recent thermal disturbance histories as well as long-term trends in SST. I found that dominant symbiont taxa differed between the two *Pocillopora* species and document how differences in the background symbiont community partially explain colony-level variation in acute heat tolerance (ED50) in P. *meandrina*, before describing the relationship between common physiological indicators of coral heat stress (catalase activity, protein and chlorophyll content) and F_v/F_m-derived ED50s. While these results document physiological changes in response to acute heat stress, little remains known about the underlying genetic mechanisms regulating responses to such rapid temperature stress.

Therefore, in **Chapter 4**, I examined transcriptome-wide patterns of gene expression within a single population of *A. tenuis* in response to severe, acute heating. Expression patterns were affected 24 h after the end of the thermal challenge with strong evidence of genotypic variation in physiological responses to heat stress. I document a small number of significantly upregulated genes associated with high acute heat tolerance in the ambient treatment which could therefore be predictive of high acute heat tolerance. Overall, this thesis demonstrates the possibility of undertaking large-scale assessments of coral heat tolerance utilising a field-deployable system, opening opportunities to rapidly map tolerant populations for reef management purposes, both across and within populations In the following, I will explore the broader context of the main findings to, in turn, provide recommendations for further optimising and ground-truthing of the methodology. I conclude with an overview of the potential of these assays to elucidate the drivers and mechanisms of coral thermal tolerance at scale.

5.2 The need for standardised approaches to study coral thermal tolerance

Twenty-first century management has an urgent need to better understand the drivers of coral thermal tolerance at scale given the unprecedented rates of global warming (Donner et al., 2005; Matz et al., 2020; van Woesik et al., 2022). Approaches such as genome-wide association studies (GWAS) and seascape genomics to predict heat tolerance require large sample sizes, as well as evidence from multiple levels of biological organisation (Fuller et al., 2020; Liggins et al., 2019; Thomas et al., 2022). Traditional quantification of coral heat tolerance has relied on long-term (8 - 40 days) ramp-and-hold aquarium-based experiments (Gibbin et al., 2015; Glynn & D'Croz, 1990; Jokiel & Coles, 1977; McLachlan et al., 2020). Such approaches are therefore still impractical when considered at reef-system spatial scales, such as the latitudinal extent of the GBR. In contrast, acute heat stress assays provide a potential experimental framework for analysing coral tolerance with the assays taking < 1 day to complete. Acute heat stress assays were developed to test differential heat tolerance of corals experiencing severe, daily thermal fluctuations in distinct, but spatially close, reef areas in American Samoa (Palumbi et al., 2014). Such assays have since been deployed in multiple reef systems and have successfully resolved differential thermal tolerance within and between diverse reef environments (Cornwell et al., 2021; Cunning et al., 2021; Marzonie et al., 2022; Voolstra et al., 2020).

Physiological responses to acute heat stress assayed in this thesis were indeed quantifiable in GBR corals and resembled those documented as responses to long-term thermal stress. Previous studies of acute heat tolerance have primarily quantified declines in chlorophyll content and photosynthetic performance (Cunning et al., 2021; Evensen et al., 2021; Voolstra et al., 2020), while relatively little is known about other physiological responses to acute heating in corals. In addition to the aforementioned declines in photosynthetic efficiency (F_v/F_m), in **Chapters 2** and **3** I also documented significant declines in multiple physiological traits commonly associated with the coral heat stress response, including chlorophyll-*a* and protein content (Oliver & Palumbi, 2011; Voolstra et al., 2020). While previous studies have demonstrated that protein expression levels can respond to heating within 90 min (Traylor-Knowles et al., 2017), it is likely that marked declines in protein content reported here were associated with tissue loss rather than rapid catabolism (DeMerlis et al., 2022). Overall, I found that physiological trait responses declined through time during the recovery period, further complicating comparisons between long- and short-term studies. However, these temporal declines were only investigated in one coral species (*A. tenuis*) and hence caution should be exerted if extrapolating either across species or rates of decline to enable comparisons. Further, temperature-induced stress responses should be considered relative to the amount of experimental heat stress applied (Leggat et al., 2022) and therefore, studies utilising acute heat stress assays would benefit from reporting temperature treatments relative to site-specific Maximum Monthly Mean climatology temperatures (Skirving et al., 2020). Finally, the outcomes of heat stress studies, and more recently, of acute heat stress assays, remain complicated to resolve because of variance in factors within experimental designs (including fragment size, acclimation, exposure time and severity, and sampling time points) and quantified traits. Here, I document acute heat stress responses from the transcriptomic and level through to physiology and higher-order proxy traits (tissue colour change and ED50) and find the acute heat stress response to be highly trait dependent. This underpins that trait selection must be a specific consideration of the research question (**Chapter 2**) and consideration of multiple co-variates is required (**Chapter 3**) to fully elucidate the acute heat stress response in corals. As such, this thesis highlights not only the need for experimental standardisation but also the benefit of ensuring that this information is widely available and feasible to implement.

5.3 Identified drivers of coral heat tolerance

5.3.1 *Transcriptional responses as indicators of acute heat tolerance*

Transcriptional studies have provided a wealth of information about the processes and regulation involved in mounting coral responses to stress (Cziesielski et al., 2019; Bellantuono et al. 2012; Seneca and Palumbi 2015). Responses can be mounted rapidly (hours), for example to increase reactive oxygen scavenging capacity and heat shock protein content (Alderdice et al., 2021; Bay et al., 2009; Traylor-Knowles et al., 2017). Few studies have examined gene expression profiles following acute heat stress assays (e.g. Dixon et al., 2015; Savary et al., 2021; Voolstra et al., 2021b) while responses to chronic heat exposure (> 2 days) have received the majority of attention (for example reveiwed in Cziesielski et al., 2019; Dixon et al., 2020; Drury, 2020). The transcriptional and physiological results documented here (**Chapter 4**) together with previous work (Savary et al., 2021; Thomas et al., 2022; Voolstra et al., 2021b) highlights that heat challenge employed by acute heat stress assays is sufficiently stressful to elicit detectable changes in gene expression. However, the magnitude of differentially expressed genes detected was lower than for many long-term heat stress experiments. Savary et al., (2021) suggested that sampling 12 hours after acute heat exposure may have failed to detect some differentially expressed genes, either due to a delay in mounting the response or due to a return to baseline expression, both of which require sampling through time to resolve. The time required for genes to return to baseline expression levels can provide information on the recovery potential of individuals following episodes of heat stress (Walker et al., 2022) but the temporal characteristics of the molecular acute heat stress response are poorly defined. Further, only one study has directly compared gene expression patterns between acute heat stress assays and chronic heat exposure experiments (Savary et al., 2021). Therefore, it is currently unknown whether the acute and chronic molecular heat stress responses involve similar pathways. Finally, it is important to contextualise transcriptional studies which typically rely on correlational results, with respect to physiology and heat resilient phenotypes (Cziesielski et al., 2019; Kirk et al., 2018; Latimer et al., 2015).

Expression markers that allow for rapid screening of thermal tolerance have been used widely in crop evolution (Rustamova et al., 2019), and similar principles have been applied to corals (Lundgren et al., 2013; Weis, 2010). This relies on the principle that expression levels of certain genes implicated in thermal tolerance can reliably predict holobiont tolerance (Bay & Palumbi, 2017; Strader & Quigley, 2022). In **Chapter 4**, I identified significantly

upregulated genes associated with high acute heat tolerance (ED50). The higher expression levels in the baseline condition is referred to as frontloading (Barshis et al., 2013), a potential anticipatory protective genetic mechanism (Teixeira et al., 2013), promoting higher heat tolerance in these corals (Fifer et al., 2021). Front-loading has been proposed as a genetic mechanism enhancing coral heat tolerance (Barshis et al., 2013). However, few of these potential gene expression markers of heat tolerance (Louis et al., 2017) have been experimentally validated to increase thermal tolerance (Parkinson et al., 2020). Finally, incorporating molecular-based insights into phenotyping of heat tolerance more effectively, is a logical direction for these high-throughput assays given the reduced time and cost requirements over traditional long-term ramp-and-hold experiments.

5.3.2 Coral heat tolerance influenced by local thermal history

Corals show evidence of adaptation to local thermal regimes at a variety of scales including within-reef habitats (e.g. Marhoefer et al., 2021; Thomas et al., 2022) and across latitudes (e.g. Dixon et al., 2015; Howells et al., 2013; Johnston et al., 2018). Locally variable environments can result in higher heat tolerance (DeMerlis et al., 2022; Oliver & Palumbi, 2011) although few studies have examined environmental covariates of increased heat tolerance across entire reef systems (but see Baumann et al., 2016; Dalton & Carroll, 2011; Osman et al., 2018). In **Chapter 3**, I show that absolute acute heat tolerance (ED50) across three coral species varied significantly between reef sectors and was predicted by site-specific maximum SSTs and the number of marine heating events where heat stress exceeded 3ºC - heating weeks (DHW). The presence of higher acute heat tolerance at reefs with higher maximum SSTs in this thesis indicates local adaptation at a latitudinal scale (Evensen et al., 2022; Fuller et al., 2020; Howells et al., 2013) as has also been evidenced recently through the application of seascape genomics (Liggins et al., 2019; Selmoni et al., 2020). This is further supported by the lack of difference in relative heat tolerance (ºC above local MMM), suggesting that corals across the GBR have matched thermal tolerance to their local MMM, unlike Coral Sea corals (Marzonie et al., 2022). Similarly, sites characterised by high maximum SSTs hosted stress-tolerant coral species in Belize (Baumann et al., 2016). However, global patterns of high SST as a driver of heat tolerance have been debated (Sully et al., 2019). It is possible that heatwave disturbance histories work in synergy with high maximum SSTs (Quigley & van Oppen, 2022) and that these patterns are therefore dependent on multiple thermal co-variates. For example, acute heat

tolerance was negatively impacted by the frequency of mild marine heatwaves in this thesis while previous research on similar species in the Coral Sea identified a positive correlation of marine heatwave frequency on acute heat tolerance (Marzonie et al., 2022). As such, patterns of thermal co-variates of acute heat tolerance likely require further investigation to ascertain whether species- and reef-system specific.

5.3.3 Species-specific influence of Symbiodiniaceae communities on acute heat tolerance

Endosymbiotic Symbiodiniaceae are important determinants of coral holobiont thermal tolerance (Berkelmans & van Oppen, 2006; Howells et al., 2011) and physiology (Wall et al., 2020; Yuyama & Higuchi, 2014). These symbionts differ in their photo-physiological characteristics (Chang et al., 1983; Cooper et al., 2011; Hoadley et al., 2021; Nitschke et al., 2022). Therefore, when examining patterns of heat tolerance at scale, it is important to consider the diversity of these symbiont communities. In **Chapter 3**, I found that acute heat tolerance was only significantly associated with the symbiont communities of *P. meandrina* and not *P. verrucosa*. Contrary to Grima et al., (2022), *P. verrucosa* examined here showed greater community variability than *P. meandrina*. This highlights that small spatial scale studies of symbiont communities are likely to under-representing community variability evident at larger spatial scales. While *Pocillopora* corals generally have highly conserved symbiont partners (Johnston et al., 2022; Turnham et al., 2021) due to their vertical transmission mode (Baird et al., 2009). Latitudinal differentiation in *P. verrucosa* symbiont communities were observed here, similarly to recent results from the South China Sea (Chen et al., 2021), potentially due to rapid diversification of these symbionts (D'Angelo et al., 2015; Howells et al., 2016).

Interestingly, the two *P. verrucosa* colonies which contained *Durusdinium*-type symbionts recorded greater acute heat tolerance (ED50) than colonies which only associated purely with *Cladocopium*-type symbionts. While *Pocillopora spp* generally associate with *Cladocopium*-type symbionts, these data support that associations with *Durusdinium* are possible (Ros et al., 2021; Torres et al., 2021) and recent evidence from the eastern Pacific suggests that the *Pocillopora-Durusdinium* association may become more abundant following episodes of heating (Palacio-Castro et al., 2022). Encouragingly for conservation efforts, Haydon et al., (2023) found the *Pocillopora-Durusdinium* association to be maintained following transplantation and symbiont shuffling may remain an important resilience feature for some species (Quigley et al., 2022b). However, the rarity of this association in natural reef systems (observed here in 1.4% of *P. verrucosa* samples) highlights the potential benefits of

assisted evolution approaches applied at scale (van Oppen et al., 2015). This necessitates detailed study of the cost and benefits of these associations (Buerger et al., 2020; Scharfenstein et al., 2022).

5.4 Utility of ED50 derived from photosynthetic performance as proxy of acute thermal tolerance

A high through-put proxy of acute thermal tolerance was needed to fully capitalise on the rapid heat stress experimental profile, both from a standardisation perspective but also due to the high throughput possible (for example, n = 3,409 unique samples presented in this thesis). Previous studies used the effective dose ED50 of photosynthetic performance (Cunning et al., 2021; Evensen et al., 2022; Marzonie et al., 2022) as a measure of acute heat tolerance. Photosynthesis is particularly sensitive to heat stress (Sharkey, 2005) and photosynthetic declines have long been used as an early indicator of potential heat stress in corals due to the direct link between photosynthetic output and energy transfer to the host (Roth & Deheyn, 2013; Saxby et al., 2003; Suggett & Smith, 2020). In **Chapter 2**, I describe how photosynthetic performance could serve as a potential rapid proxy trait of acute thermal tolerance based on temporal stability, the lack of interactions with fragment size, as well as the low time investment required to process large sample sizes before quantifying ED50 across the GBR in three species in **Chapter 3**. ED50 was only significantly impacted by symbiont community composition of one coral species and the relationship between physiological traits (protein and chlorophyll content, and catalase activity) and ED50 differed between the two *Pocillopora* species. This was surprising, given that ED50 was derived from measurements of photosynthetic efficiency. This potentially reflects differences in photo-physiological mechanisms employed by different symbionts harboured under heat stress (Hoadley et al., 2021; Lohr et al., 2019). However, it also highlights a potential over-simplification of coral heat tolerance, representing a holobiont trait by quantification of a purely symbiont-derived measure. Therefore, it is likely that not all measures of bleaching tolerance will show high congruence with ED50.

The GBR-wide absolute ED50 for *P. verrucosa* (36.21ºC) is similar to those reported for the same species in the Red Sea and the Coral Sea respectively (36.0ºC and 36.1 ºC, Evensen et al., 2022; Marzonie et al., 2022). This is despite the lower MMMs of GBR reefs used in this

thesis and a much narrower range of reef-specific MMMs compared to the Red Sea (1.6 ºC vs 4.55 ºC). Taken together, these results imply that ~36ºC may be a shared acute thermal tolerance threshold of *P. verrucosa* across ocean basins, potentially indicating that this species have similar long-term bleaching thresholds or thermal optima dynamics (Álvarez-Noriega et al., 2023) which could be the focus of further study. This thesis further investigates the variation and utility of the ED50 metric at two distinct organisational levels, both within and between populations. The variation in ED50 documented within a single population (Davies reef, 35.27 ± 0.054ºC, **Chapter 4**) closely matches the overall variation found across the GBR (35.31 ± 0.076ºC, **Chapter 3**). This finding potentially indicates that the ED50 trait is not governed by underlying spatial and environmental history but potentially highly genetically controlled by either host or symbiont (Cunning et al., 2022; Cornwell et al., 2021) Finally, the link between ED50 values, acute heat tolerance, and coral resilience to bleaching during natural marine heatwave events must be further investigated either through classic ramp-hold experiments relying on common indicators of heat stress (such as physiology) or in-field survival observations.

5.5 Limitations and future opportunities for acute heat stress assays

The relationship between experimentally derived acute heat tolerance and ecologically observed *in situ* bleaching resistance remains poorly understood. Further ground-truthing of this method is required to understand how acute heat tolerance relates to measures of long-term thermal tolerance including thermal breadth and thermal optimums (Abrego et al., 2022; Klepac & Barshis, 2022; Sinclair et al., 2016). As a priority, studies should aim to correlate acute heat tolerance to long-term heat resilience under laboratory-based experiments. Currently, only three studies have attempted this, all utilising *Stylophora pistillata* from the Red Sea (Evensen et al., 2021; Savary et al., 2021; Voolstra et al., 2020) with mixed results across physiology and gene expression patterns. The correlation between physiological and transcriptomic responses to both acute and long-term heat stress needs to be further extended to other species and regions. For example, recent work on the central GBR elucidated thermal performance curves of multiple coral species and identified the highest thermal optimum (T_{opt} Angilletta, 2006) in *P. verrucosa* (29.5ºC) while *A. tenuis* recorded a lower T_{opt} (28.2 ºC' Álvarez-Noriega et al., 2023). Promisingly, this supports the acute thermal tolerance species rankings presented in this thesis, supporting the acute assay experimental framework. The

temporal stability of acute heat stress responses also needs to be investigated. Cunning et al., (2021) demonstrated that although the absolute value of ED50 showed seasonality, the overall rankings of thermally tolerant colonies did not. Encouragingly, Morikawa & Palumbi, (2019) showed higher bleaching resistance during a natural bleaching event in coral fragments that originated from colonies with high acute heat tolerance. It is imperative to understand how these acute *ex-situ* experiments compare with long-term bleaching and mortality resilience under natural marine heat wave conditions to leverage the spatial flexibility and high-throughput potential offered by acute heat stress assays.

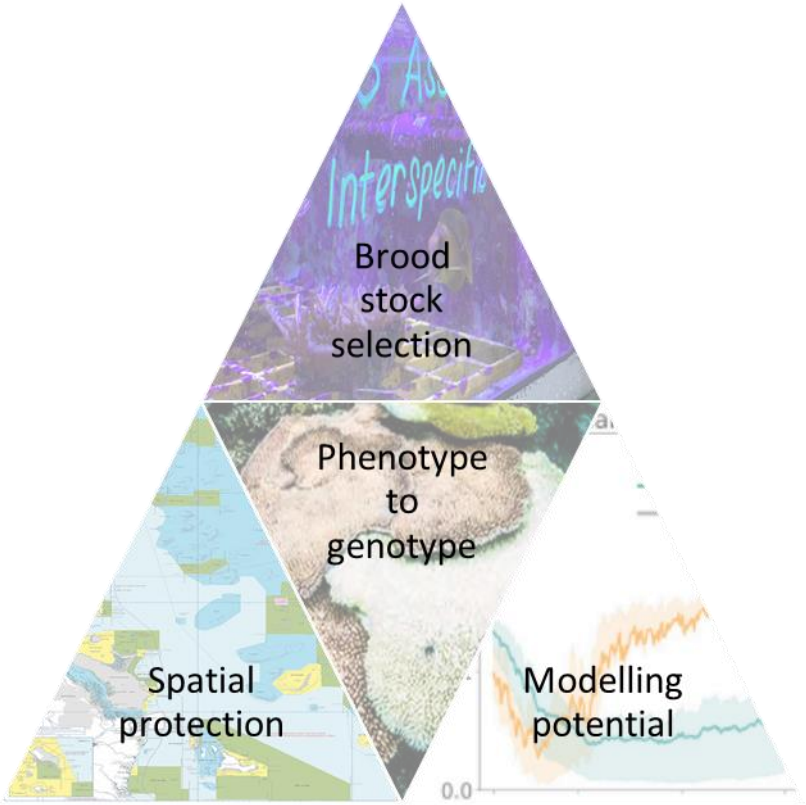

Figure 5.1 Contributions of acute heat stress assays to coral conservation. Image credits; bottom left to right; GBRMPA, Peter Mumby, McManus et al., 2021; top AIMS SeaSim

Continued global warming is likely to outpace phenotypic and adaptive capacities of many organisms (Radchuk et al., 2019), including corals (Matz et al., 2018), necessitating novel or improved conservation management solutions (Beever et al., 2016). Large-scale active management approaches require large volumes of data where acute heat stress assays can contribute to multiple aspects. Specifically, I considered how acute heat stress assays could support the following dimensions of knowledge and capacity building in conversation management: spatial protection, modelling potential, linking phenotypes-genotypes, and brood stock selection for active management interventions to seed enhanced corals onto reefs (Fig 5.1). Spatial protection, for example through the implementation of "Marine Protected Areas" (MPAs) and "no-take" zones, were particularly developed to support fisheries (Cicin-Sain & Belfiore, 2005) but are now commonly used for coral reef management (Kleypas et al., 2021; McClanahan et al., 2012; Mellin et al., 2019). The spatial footprint of acute heat stress assays allow for the identification of coral populations exhibiting high heat tolerance (Darling & Côté, 2018; Decarlo & Harrison, 2019; Quigley & van Oppen, 2022) across spatial scales and could therefore underpin better informed spatial protection for heat-resilient corals (Kalmus et al., 2022; Voolstra et al., 2023, Fig 5.1 "spatial protection"). However, MPAs are not sufficient to address the threats posed by climate change (Boersma & Parrish, 1999; Kearney et al., 2012) and we need to further our collective understanding of coral heat tolerance. High-resolution physiological data from acute heat stress assays can parameterise predictive models of coral persistence under climate change (Fig 5.1 "modelling potential") and may dramatically improve model prediction accuracy (Baskett, 2012; Mason et al., 2020), as shown for coral reef-associated fish (Illing & Rummer, 2017). Despite this, knowledge of thermal tolerance is often omitted in present models (Evans et al., 2015; Thompson et al., 2013). By combining standard protocols of phenotyping corals (Voolstra et al., 2021a) with multi-trait analyses including -omics approaches, acute heat stress assays can directly enhance our mechanistic understanding of coral responses to heat stress (Cziesielski et al., 2018, Fig 5.1 "phenotype to genotype"). Through genetic analyses these assays may enable estimation of adaptive genetic variation present within a population in key fitness traits (Kleypas et al., 2021). For example, incorporating adaptive responses into modelling projections of coral cover significantly increased the accuracy of bleaching frequency predictions (Logan et al., 2014). New management actions that involve the active genetic management of populations via a range of methods such as intraspecific hybridisation (also called assisted gene flow) and selective breeding (*A Research Review of Interventions to Increase the Persistence and Resilience of Coral Reefs*, 2019; Bay et al., 2019) are currently being examined on reefs and in laboratories

around the world (McLeod et al., 2022). These intervention methods require foundational knowledge of both the distribution of heat resilient coral populations and the drivers of differential heat tolerance (Caruso et al., 2021). Acute heat stress assays have been successful in selecting thermally-tolerant donor colonies for construction of resilient coral nurseries (Morikawa & Palumbi, 2019) and could be applied to identify stock populations ideal for selective breeding interventions (Matz et al., 2020, Fig 5.1 "broodstock selection"). As such, once outstanding questions about the connection between acute and long-term heat tolerance and temporal stability of the acute heat stress response have been addressed, these assays can provide a powerful tool to increase knowledge of large- and small-scale drivers of heat tolerance in corals.

Table 5.1 Recommendations to improve the use of the ED50 trait to quantify acute heat tolerance in corals.

	Recommendation	**Actions**
1	Determine link between ED50 and natural bleaching resilience	Compare ED50s to bleaching susceptibility, survival and recovery in the field during a natural bleaching event.
		Compare ED50s to long-term thermal challenges in aquaria
2	Understand genetic and transcriptomic drivers of heat tolerance	Compare transcriptomic responses to acute and long-term heat stress to develop markers of tolerance.
3	Development and wide implementation of standardised approaches and thermal stress indicators	Continued collaboration and communication globally with sharing of detailed methods and schematics of experimental systems.
		Selection of key indicators of thermal stress and bleaching resilience

5.6 Concluding remarks

Climate change has driven irreversible damage to ecosystems globally (Lee et al., 2023), including on coral reefs. The heat and bleaching tolerance of corals is an important factor in coral reef persistence, and we must further our understanding of drivers of high temperature tolerance in these key habitat-forming species. This thesis demonstrates the applicability of quantifying thermal tolerance of corals with an acute heat stress assay, providing the largest spatial scale assessment of heat tolerance to date. I showed that heat tolerance was driven by complex interactions of thermal history, symbiont communities, physiology, and coral host genetics. The data generated from studies that combine large-scale assessments of coral heat

tolerance with fine-scale quantification of thermal stress responses will provide baseline information that support multiple modelling and management objectives, making such projects highly impactful in coral reef conservation and management under climate change.

References

A Research Review of Interventions to Increase the Persistence and Resilience of Coral Reefs. (2019). https://doi.org/https://doi.org/10.17226/25279

Abrego, D., Baird, A. H., Howells, E. J., & Smith, S. D. . (2022). Pools of resilience. *Bulletin of Marine Science*, *98*(1), 51–52. https://doi.org/https://doi.org/10.5343/bms.2021.0019

Abrego, David, Ulstrup, K. E., Willis, B. L., & van Oppen, M. J. H. (2008). Species-specific interactions between algal endosymbionts and coral hosts define their bleaching response to heat and light stress. *Proceedings. Biological Sciences / The Royal Society*, *275*(1648), 2273–2282. https://doi.org/10.1098/rspb.2008.0180

AIMS. (2022). *Continued coral recovery leads to 36-year highs across two-thirds of the Great Barrier Reef; Annual Summary Report Of Coral Reef Condition*. https://www.aims.gov.au/sites/default/files/2022-08/AIMS_LTMP_Report_on GBR_coral_status_2021_2022_040822F3.pdf

Aitken, S. N., & Bemmels, J. B. (2016). Time to get moving: Assisted gene flow of forest trees. *Evolutionary Applications*, *9*(1), 271–290. https://doi.org/10.1111/eva.12293

Aitken, S. N., & Whitlock, M. C. (2013). Assisted Gene Flow to Facilitate Local Adaptation to Climate Change. *Annual Review of Ecology, Evolution, and Systematics*, *44*(1), 367–388. https://doi.org/10.1146/annurev-ecolsys-110512-135747

Al-Moghrabi, S., Allemand, D., Couret, J. M., & Jaubert, J. (1995). Fatty acids of the scleractinian coral *Galaxea fascicularis*: effect of light and feeding. *Journal of Comparative Physiology B*, *165*(3), 183–192. https://doi.org/10.1007/BF00260809

Alderdice, R., Suggett, D. J., Cárdenas, A., Hughes, D. J., Kühl, M., Pernice, M., & Voolstra, C. R. (2021). Divergent expression of hypoxia response systems under deoxygenation in reef-forming corals aligns with bleaching susceptibility. *Global Change Biology*, *27*(2), 312–326. https://doi.org/10.1111/gcb.15436

Álvarez-Noriega, M., Marrable, I., Noonan, S. H. C., Barneche, D. R., & Ortiz, J. C. (2023). Highly conserved thermal performance strategies may limit adaptive potential in corals. *Proceedings of the Royal Society B: Biological Sciences*, *290*(1990). https://doi.org/10.1098/rspb.2022.1703

Angilletta, M. J. (2006). Estimating and comparing thermal performance curves. *Journal of Thermal Biology*, *31*(7), 541–545. https://doi.org/10.1016/j.jtherbio.2006.06.002

Angilletta, M. J. J. (2009). *Thermal adaptation*. Oxford University Press. https://doi.org/10.1093/acprof.oso/9780198570875.001.1

Angilletta, M. J., Wilson, R. S., Navas, C. A., & James, R. S. (2003). Tradeoffs and the evolution of thermal reaction norms. *Trends in Ecology and Evolution*, *18*(5), 234–240. https://doi.org/10.1016/S0169-5347(03)00087-9

Anthony, K. R N., & Hoegh-Guldberg, O. (2003). Kinetics of Photoacclimation in Corals. *Oecologia*, *134*, 23–31.

Anthony, Kenneth R.N., Helmstedt, K. J., Bay, L. K., Fidelman, P., Hussey, K. E., Lundgren, P., Mead, D., McLeod, I. M., Mumby, P. J., Newlands, M., Schaffelke, B., Wilson, K. A., & Hardisty, P. E. (2020). Interventions to help coral reefs under global change—A complex decision challenge. *PLoS ONE*, *15*(8 August), 1–14. https://doi.org/10.1371/journal.pone.0236399

Anthony, Kenneth R.N., Hoogenboom, M. O., Maynard, J. A., Grottoli, A. G., & Middlebrook, R. (2009). Energetics approach to predicting mortality risk from environmental stress: A case study of coral bleaching. *Functional Ecology*, *23*(3), 539–550. https://doi.org/10.1111/j.1365-2435.2008.01531.x

Apprill, A., Marlow, H. Q., Martindale, M. Q., & Rappé, M. S. (2009). The onset of microbial associations in the coral Pocillopora meandrina. *ISME Journal*, *3*(6), 685–699. https://doi.org/10.1038/ismej.2009.3

Ashcroft, M. B. (2010). Identifying refugia from climate change. *Journal of Biogeography*, *37*(8), 1407–1413. https://doi.org/10.1111/j.1365-2699.2010.02300.x

Avila-Magaña, V., Kamel, B., DeSalvo, M., Gómez-Campo, K., Enríquez, S., Kitano, H., Rohlfs, R. V., Iglesias-Prieto, R., & Medina, M. (2021). Elucidating gene expression adaptation of phylogenetically divergent coral holobionts under heat stress. *Nature Communications*, *12*(1), 1–16. https://doi.org/10.1038/s41467-021-25950-4

Bainbridge, S. J. (2017). Temperature and light patterns at four reefs along the Great Barrier Reef during the 2015–2016 austral summer: understanding patterns of observed coral bleaching. *Journal of Operational Oceanography*, *10*(1), 16–29. https://doi.org/10.1080/1755876X.2017.1290863

Baird, A. H., Bhagooli, R., Ralph, P. J., & Takahashi, S. (2009). Coral bleaching: the role of the host. *Trends in Ecology and Evolution*, *24*(1), 16–20. https://doi.org/10.1016/j.tree.2008.09.005

Baird, A. H., Guest, J. R., Edwards, A. J., Bauman, A. G., Bouwmeester, J., Mera, H., Abrego, D., Alvarez-Noriega, M., Babcock, R. C., Barbosa, M. B., Bonito, V., Burt, J., Cabaitan, P. C., Chang, C. F., Chavanich, S., Chen, C. A., Chen, C. J., Chen, W. J., Chung, F. C., … Yusuf, S. (2021). An Indo-Pacific coral spawning database. *Scientific Data*, *8*(1), 1–9. https://doi.org/10.1038/s41597-020-00793-8

Bairos-Novak, K. R., Hoogenboom, M. O., van Oppen, M. J. H., & Connolly, S. R. (2021). Coral adaptation to climate change: Meta-analysis reveals high heritability across multiple traits. *Global Change Biology*, *27*(22), 5694–5710. https://doi.org/10.1111/gcb.15829

Baker, A. C. (2001). Reef corals bleach to survive change. *Nature*, *411*(6839), 765–766. https://doi.org/10.1038/35081151

Baker, A. C., Glynn, P. W., & Riegl, B. (2008). Climate change and coral reef bleaching: An ecological assessment of long-term impacts, recovery trends and future outlook. *Estuarine, Coastal and Shelf Science*, *80*(4), 435–471. https://doi.org/10.1016/j.ecss.2008.09.003

Baker, A. C., Starger, C. J., McClanahan, T. J., & Glynn, P. W. (2004). Corals' adaptive response to climate change. *Nature*, *430*(August), 741.

Barott, K. L., Huffmyer, A. S., Davidson, J. M., Lenzb, E. A., Matsuda, S. B., Hancock, J. R., Innis, T., Drury, C., Putnam, H. M., & Gates, R. D. (2021). Coral bleaching response is unaltered following acclimatization to reefs with distinct environmental conditions. *Proceedings of the National Academy of Sciences of the United States of America*, *118*(22). https://doi.org/10.1073/pnas.2025435118

Barshis, D.J., Stillman, J. H., Gates, R. D., Toonen, R. J., Smith, L. W., & Birkelands, C. (2010). Protein expression and genetic structure of the coral Porites lobata in an environmentally extreme Samoan back reef : does host genotype limit phenotypic plasticity ? *Molecular Ecology*, *19*, 1705–1720. https://doi.org/10.1111/j.1365-294X.2010.04574.x

Barshis, Daniel J., Birkeland, C., Toonen, R. J., Gates, R. D., & Stillman, J. H. (2018). High-frequency temperature variability mirrors fixed differences in thermal limits of the massive coral Porites lobata. *Journal of Experimental Biology*, *221*(24). https://doi.org/10.1242/jeb.188581

Barshis, Daniel J, Ladner, J. T., Oliver, T. A., Seneca, F. O., Traylor-Knowles, N., & Palumbi, S. R. (2013). Genomic basis for coral resilience to climate change. *Proceedings of the National Academy of Sciences of the United States of America*, *110*(4), 1387–1392. https://doi.org/10.1073/pnas.1210224110

Baskett, M. L. (2012). Integrating mechanistic organism-environment interactions into the basic theory of community and evolutionary ecology. *Journal of Experimental Biology*, *215*(6), 948–961. https://doi.org/10.1242/jeb.059022

Baumann, J. H., Townsend, J. E., Courtney, T. A., Aichelman, H. E., Davies, S. W., Lima, F. P., & Castillo, K. D. (2016). Temperature regimes impact coral assemblages along environmental gradients on lagoonal reefs in Belize. *PLoS ONE*, *11*(9), 1–19. https://doi.org/10.1371/journal.pone.0162098

Baums, I.B., Chamberland, V. F., Locatelli, N. S., & Conn, T. (2022). Maximizing Genetic Diversity in Coral Restoration Projects. In M.J.H van Oppen & M. Aranda Lastra (Eds.), *Coral Reef Conservation and Restoration in the Omics Age*. Spinger. https://doi.org/https://doi.org/10.1007/978-3-031-07055-6_3

Baums, Iliana B., Baker, A. C., Davies, S. W., Grottoli, A. G., Kenkel, C. D., Kitchen, S. A., Kuffner, I. B., LaJeunesse, T. C., Matz, M. V., Miller, M. W., Parkinson, J. E., & Shantz, A. A. (2019). Considerations for maximizing the adaptive potential of restored coral populations in the western Atlantic. *Ecological Applications*, *29*(8). https://doi.org/10.1002/eap.1978

Bay, L. K., Crozier, R. H., & Caley, M. J. (2006). The relationship between population genetic structure and pelagic larval duration in coral reef fishes on the Great Barrier Reef. *Marine Biology*, *149*(5), 1247–1256. https://doi.org/10.1007/s00227-006-0276-6

Bay, L. K., Rocker, M., Boström-Einarsson, L., Babcock, R., Burger, P., Cleves, P. A., Harrison, D., Negri, A. P., Quigley, K. M., Randall, C. J., van Oppen, M. J. H., & Webster, N. S. (2019). *Reef Restoration and Adaptation Program: Intervention Technical Summary*. https://researchers.mq.edu.au/en/publications/reef-restoration-and-adaptation-program-intervention-technical-su

Bay, L.K., Guerecheau, A., Andreakis, N., Ulstrup, K. E., & Matz, M. V. (2013). Gene Expression Signatures of Energetic Acclimatisation in the Reef Building Coral Acropora millepora. *PLoS ONE*, *8*(5), 1–10. https://doi.org/10.1371/journal.pone.0061736

Bay, Line K., Ulstrup, K. E., Nielsen, H. B., Jarmer, H., Goffard, N., Willis, B. L., Miller, D. J., & van Oppen, M. J. H. (2009). Microarray analysis reveals transcriptional plasticity in the reef building coral acropora millepora. *Molecular Ecology*, *18*(14), 3062–3075. https://doi.org/10.1111/j.1365-294X.2009.04257.x

Bay, R. A., & Palumbi, S. R. (2015). Rapid acclimation ability mediated by transcriptome changes in reef-building corals. *Genome Biology and Evolution*, *7*(6), 1602–1612. https://doi.org/10.1093/gbe/evv085

Bay, R. A., & Palumbi, S. R. (2017). Transcriptome predictors of coral survival and growth in a highly variable environment. *Ecology and Evolution*, *7*(13), 4794–4803. https://doi.org/10.1002/ece3.2685

Bay, R. A., Rose, N. H., Logan, C. A., & Palumbi, S. R. (2017). Genomic models predict successful coral adaptation if future ocean warming rates are reduced. *Science Advances*, *3*(11), 1–10. https://doi.org/10.1126/sciadv.1701413

Beever, E. A., O'Leary, J., Mengelt, C., West, J. M., Julius, S., Green, N., Magness, D., Petes, L., Stein, B., Nicotra, A. B., Hellmann, J. J., Robertson, A. L., Staudinger, M. D., Rosenberg, A. A., Babij, E., Brennan, J., Schuurman, G. W., & Hofmann, G. E. (2016). Improving Conservation

Outcomes with a New Paradigm for Understanding Species' Fundamental and Realized Adaptive Capacity. *Conservation Letters*, *9*(2), 131–137. https://doi.org/10.1111/conl.12190

Bellantuono, A. J., Granados-Cifuentes, C., Miller, D. J., Hoegh-Guldberg, O., & Rodriguez-Lanetty, M. (2012). Coral Thermal Tolerance: Tuning Gene Expression to Resist Thermal Stress. *PLoS ONE*, *7*(11), 1–14. https://doi.org/10.1371/journal.pone.0050685

Benzie, J. (1994). Patterns of gene flow in the Great Barrier Reef and Coral Sea. In A. Beaumont (Ed.), *Genetics and Evolution of Aquatic Organisms* (First). Chapman & Hall.

Béraud, E., Gevaert, F., Rottier, C., & Ferrier-Pagès, C. (2013). The response of the scleractinian coral Turbinaria reniformis to thermal stress depends on the nitrogen status of the coral holobiont. *Journal of Experimental Biology*, *216*(14), 2665–2674. https://doi.org/10.1242/jeb.085183

Berkelmans, R., & Willis, B. L. (1999). Seasonal and local spatial patterns in the upper thermal limits of corals on the inshore Central Great Barrier Reef. *Coral Reefs*, *18*(3), 219–228. https://doi.org/10.1007/s003380050186

Berkelmans, Ray, & van Oppen, M. J. H. (2006). The role of zooxanthellae in the thermal tolerance of corals: a "nugget of hope" for coral reefs in an era of climate change. *Proc. R. Soc. B*, *273*(1599), 2305–2312. https://doi.org/10.1098/rspb.2006.3567

Boersma, P. D., & Parrish, J. K. (1999). Limiting abuse: Marine protected areas, a limited solution. *Ecological Economics*, *31*(2), 287–304. https://doi.org/10.1016/S0921-8009(99)00085-3

Borowitzka, M. A. (2018). The 'stress' concept in microalgal biology—homeostasis, acclimation and adaptation. *Journal of Applied Phycology*, *30*(5), 2815–2825. https://doi.org/10.1007/s10811-018-1399-0

Boström-Einarsson, L., Babcock, R. C., Bayraktarov, E., Ceccarelli, D., Cook, N., Ferse, S. C. A., Hancock, B., Harrison, P., Hein, M., Shaver, E., Smith, A., Suggett, D., Stewart-Sinclair, P. J., Vardi, T., & McLeod, I. M. (2020). Coral restoration – A systematic review of current methods, successes, failures and future directions. *PLoS ONE*, *15*(1), 1–25. https://doi.org/10.1371/journal.pone.0226631

Breitwieser, F., Baker, D., & Salzberg, S. L. (2018). KrakenUniq: confident and fast metagenomics classification using unique k-mer counts. *Genome Biology*, *19*(198).

Brooks, M, E., Kristensen, K., van Benthem, K. J., Magnusson, A., Berg, C. W., Nielsen, A., Skaug, H. J., Maechler, M., & Bolker, B. M. (2017). *glmmTMB Balances Speed and Flexibility Among Packaages for Zero-inflated Generalized Linear Mixed Modelling* (pp. 378–400). The R Journal. https://journal.r-project.org/archive/2017/RJ-2017-066/index.html.

Brown, B. E., Dunne, R. P., Scoffin, T. P., & Le Tissier, M. D. A. (1994). Solar damage in intertidal corals. *Mar. Ecol. Prog. Ser.*, *105*, 219–230.

Bruno, J. F. (1998). Fragmentation in Madracis mirabilis (Duchassaing and Michelotti): How common is size-specific fragment survivorship in corals? *Journal of Experimental Marine Biology and Ecology*, *230*(2), 169–181. https://doi.org/10.1016/S0022-0981(98)00080-X

Buerger, P., Alvarez-Roa, C., Coppin, C. W., Pearce, S. L., Chakravarti, L. J., Oakeshott, J. G., Edwards, O. R., & van Oppen, M. J. H. (2020). Heat-evolved microalgal symbionts increase coral bleaching tolerance. *Science Advances*, *6*(20), 1–9. https://doi.org/10.1126/sciadv.aba2489

Cantin, N. E., van Oppen, M. J. H., Willis, B. L., Mieog, J. C., & Negri, A. P. (2009). Juvenile corals can acquire more carbon from high-performance algal symbionts. *Coral Reefs*, *28*(2), 405–414. https://doi.org/10.1007/s00338-009-0478-8

Carilli, J., Donner, S. D., & Hartmann, A. C. (2012). Historical temperature variability affects coral

response to heat stress. *PLoS ONE*, *7*(3), 1–9. https://doi.org/10.1371/journal.pone.0034418

Carturan, B. S., Parrott, L., & Pither, J. (2018). A modified trait-based framework for assessing the resilience of ecosystem services provided by coral reef communities. *Ecosphere*, *9*(5). https://doi.org/10.1002/ecs2.2214

Caruso, C., Hughes, K., & Drury, C. (2021). Selecting Heat-Tolerant Corals for Proactive Reef Restoration. *Frontiers in Marine Science*, *8*(May 2021). https://doi.org/10.3389/fmars.2021.632027

Castillo-Tandazo, W., Smeets, M. F., Murphy, V., Liu, R., Hodson, C., Heierhorst, J., Deans, A. J., & Walkley, C. R. (2019). ATP-dependent helicase activity is dispensable for the physiological functions of Recql4. *PLoS Genetics*, *15*(7), 1–19. https://doi.org/10.1371/journal.pgen.1008266

Chang, S. S., Prezelin, B. B., & Trench, R. K. (1983). Mechanisms of photoadaptation in three strains of the symbiotic dinoflagellate Symbiodinium microadriaticum. *Marine Biology*, *76*, 219–229.

Chen, B., Yu, K., Liao, Z., Yu, X., Qin, Z., Lianf, J., Wang, G., Wu, Q., & Jiang, L. (2021). Microbiome community and complexity indicate environmental gradient acclimatisation and potential microbial interaction of endemic coral holobionts in the South China Sea. *Science of The Total Environment*, *765*, 142690. https://doi.org/https://doi.org/10.1016/j.scitotenv.2020.142690

Chen, J., Zhang, X., & Yang, L. (2022). *GUniFrac: Generalized UniFrac Distances, Distance-Based Multivariate Methods and Feature-Based Univariate Methods for Microbiome Data Analysis* (1.7). https://cran.r-project.org/package=GUniFrac

Chen, Jun, Bittinger, K., Charlson, E. S., Hoffmann, C., Lewis, J., Wu, G. D., Collman, R. G., Bushman, F. D., & Li, H. (2012). Associating microbiome composition with environmental covariates using generalized UniFrac distances. *Bioinformatics*, *28*(16), 2106–2113. https://doi.org/10.1093/bioinformatics/bts342

Chen, S., Zhou, Y., Chen, Y., & Gu, J. (2018). fastp: an ultra-fast all-in-one FASTQ preprocessor. *Bioinformatics*, *34*(17), i884–i890. https://doi.org/10.1093/bioinformatics/bty560

Chen, Y., Shah, S., Dougan, K. E., van Oppen, M. J. H., Bhattacharya, D., & Chan, C. X. (2022). Improved Cladocopium goreaui Genome Assembly Reveals Features of a Facultative Coral Symbiont and the Complex Evolutionary History of Dinoflagellate Genes. *Microorganisms*, *10*(8). https://doi.org/10.3390/microorganisms10081662

Cheung, M. W. M., Hock, K., Skirving, W., & Mumby, P. J. (2021). Cumulative bleaching undermines systemic resilience of the Great Barrier Reef. *Current Biology*, *31*(23), 5385-5392.e4. https://doi.org/10.1016/j.cub.2021.09.078

Chevin, L. M., & Hoffmann, A. A. (2017). Evolution of phenotypic plasticity in extreme environments. *Philosophical Transactions of the Royal Society B: Biological Sciences*, *372*(1723). https://doi.org/10.1098/rstb.2016.0138

Chow, M. H., Tsang, R. H. L., Lam, E. K. Y., & Ang, P. (2016). Quantifying the degree of coral bleaching using digital photographic technique. *Journal of Experimental Marine Biology and Ecology*, *479*, 60–68. https://doi.org/10.1016/j.jembe.2016.03.003

Cicin-Sain, B., & Belfiore, S. (2005). Linking marine protected areas to integrated coastal and ocean management: A review of theory and practice. *Ocean and Coastal Management*, *48*(11–12), 847–868. https://doi.org/10.1016/j.ocecoaman.2006.01.001

Claar, D. C., Szostek, L., McDevitt-Irwin, J. M., Schanze, J. J., & Baum, J. K. (2018). Global patterns and impacts of El Niño events on coral reefs: A meta-analysis. *PLoS ONE*, *13*(2), 1–22. https://doi.org/10.1371/journal.pone.0190957

Cleves, P. A., Krediet, C. J., Lehnert, E. M., Onishi, M., & Pringle, J. R. (2020). Insights into coral bleaching under heat stress from analysis of gene expression in a sea anemone model system. *Proceedings of the National Academy of Sciences of the United States of America*, *117*(46), 28906–28917. https://doi.org/10.1073/pnas.2015737117

Cleves, P. A., Shumaker, A., Lee, J. M., Putnam, H. M., & Bhattacharya, D. (2020). Unknown to Known: Advancing Knowledge of Coral Gene Function. *Trends in Genetics*, *36*(2), 93–104. https://doi.org/10.1016/j.tig.2019.11.001

Cleves, P. A., Tinoco, A. I., Bradford, J., Perrin, D., Bay, L. K., & Pringle, J. R. (2020). Reduced thermal tolerance in a coral carrying CRISPR-induced mutations in the gene for a heat-shock transcription factor. *Proceedings of the National Academy of Sciences of the United States of America*, *117*(46), 28899–28905. https://doi.org/10.1073/pnas.1920779117

Cocciardi, J. M., Hoskin, C. J., Morris, W., Warburton, R., Edwards, L., & Higgie, M. (2019). Adjustable temperature array for characterizing ecological and evolutionary effects on thermal physiology. *Methods in Ecology and Evolution*, *2019*(March), 1339–1346. https://doi.org/10.1111/2041-210X.13236

Coles, S., & Jokiel, P. (1977). Effects of temperature on photosynthesis and respiration in hermtypic corals. *Marine Biology*, *43*(3), 209–216. https://doi.org/10.1007/bf00402313

Coles, S. L., & Brown, B. E. (2003). Coral bleaching - Capacity for acclimatization and adaptation. *Advances in Marine Biology*, *46*, 183–223. https://doi.org/10.1016/S0065-2881(03)46004-5

Conlan, J. A., Jones, P. L., Turchini, G. M., Hall, M. R., & Francis, D. S. (2014). Changes in the nutritional composition of captive early-mid stage Panulirus ornatus phyllosoma over ecdysis and larval development. *Aquaculture*, *434*, 159–170. https://doi.org/10.1016/j.aquaculture.2014.07.030

Cooke, I., Ying, H., Forêt, S., Bongaerts, P., Strugnell, J. M., Simakov, O., Zhang, J., Field, M. A., Rodriguez-Lanetty, M., Bell, S. C., Bourne, D. G., van Oppen, M. J. H., Ragan, M. A., & Miller, D. J. (2020). Genomic signatures in the coral holobiont reveal host adaptations driven by Holocene climate change and reef specific symbionts. *Science Advances*, *6*(48). https://doi.org/10.1126/sciadv.abc6318

Cooper, T. F., Ulstrup, K. E., Dandan, S. S., Heyward, A. J., Kühl, M., Muirhead, A., O'Leary, R. A., Ziersen, B. E. F., & van Oppen, M. J. H. (2011). Niche specialization of reef-building corals in the mesophotic zone: Metabolic trade-offs between divergent Symbiodinium types. *Proceedings of the Royal Society B: Biological Sciences*, *278*(1713), 1840–1850. https://doi.org/10.1098/rspb.2010.2321

Cornwell, B., Armstrong, K., Walker, N., Lippert, M., Nestor, V., Golbuu, Y., & Palumbi, S. R. (2021). Widespread variation in heat tolerance and symbiont load are associated with growth tradeoffs in the coral acropora hyacinthus in palau. *ELife*, *10*, 1–15. https://doi.org/10.7554/eLife.64790

Costanza, R., de Groot, R., Sutton, P., van der Ploeg, S., Anderson, S. J., Kubiszewski, I., Farber, S., & Turner, R. K. (2014). Changes in the global value of ecosystem services. *Global Environmental Change*, *26*(1), 152–158. https://doi.org/10.1016/j.gloenvcha.2014.04.002

Cox, J., Schubert, A. M., Travisano, M., & Putonti, C. (2010). Adaptive evolution and inherent tolerance to extreme thermal environments. *BMC Evolutionary Biology*, *10*(1). https://doi.org/10.1186/1471-2148-10-75

Crabbe, M. (2012). Environmental effects on coral growth and recruitment in the Caribbean. *Journal of the Marine Biological Association of the United Kingdom*, *92*(04), 747–752. https://doi.org/10.1017/S0025315411001913

Cunning, R, Gillette, P., Capo, T., Galvez, K., & Baker, A. C. (2015). Growth tradeoffs associated with thermotolerant symbionts in the coral Pocillopora damicornis are lost in warmer oceans. *Coral Reefs*, *34*(1), 155–160. https://doi.org/10.1007/s00338-014-1216-4

Cunning, R, Parker, K. E., Johnson-Sapp, K., Karp, R. F., Wen, A. D., Williamson, O. M., Bartels, E., D'Alessandro, M., Gilliam, D. S., Hanson, G., Levy, J., Lirman, D., Maxwell, K., Million, W. C., Moulding, A. L., Moura, A., Muller, E. M., Nedimyer, K., Reckenbeil, B., … Baker, A. C. (2021). Census of heat tolerance among Florida's threatened staghorn corals finds resilient individuals throughout existing nursery populations. *Proceedings of the Royal Society B: Biological Sciences*, *288*(1961). https://doi.org/10.1098/rspb.2021.1613

Cunning, Ross, & Baker, A. C. (2020). Thermotolerant coral symbionts modulate heat stress-responsive genes in their hosts. *Molecular Ecology*, *29*(15), 2940–2950. https://doi.org/10.1111/mec.15526

Cunning, Ross, Yost, D. M., Guarinello, M. L., Putnam, H. M., & Gates, R. D. (2015). Variability of Symbiodinium communities in waters, sediments, and corals of thermally distinct reef pools in American Samoa. *PLoS ONE*, *10*(12), 1–17. https://doi.org/10.1371/journal.pone.0145099

Cziesielski, M. J., Liew, Y. J., Cui, G., Schmidt-Roach, S., Campana, S., Marondedze, C., & Aranda, M. (2018). Multi-omics analysis of thermal stress response in a zooxanthellate cnidarian reveals the importance of associating with thermotolerant symbionts. *Proceedings of the Royal Society B: Biological Sciences*, *285*(1877). https://doi.org/10.1098/rspb.2017.2654

Cziesielski, M. J., Schmidt-Roach, S., & Aranda, M. (2019). The past, present, and future of coral heat stress studies. *Ecology and Evolution*, *9*(17), 10055–10066. https://doi.org/10.1002/ece3.5576

D'Angelo, C., Hume, B. C. C., Burt, J., Smith, E. G., Achterberg, E. P., & Wiedenmann, J. (2015). Local adaptation constrains the distribution potential of heat-tolerant Symbiodinium from the Persian/Arabian Gulf. *ISME Journal*, *9*(12), 2551–2560. https://doi.org/10.1038/ismej.2015.80

D'Angelo, C., & Wiedenmann, J. (2012). An experimental mesocosm for long-term studies of reef corals. *Journal of the Marine Biological Association of the United Kingdom*, *92*(4), 769–775. https://doi.org/10.1017/S0025315411001883

Dalton, S. J., & Carroll, A. G. (2011). Monitoring coral health to determine coral bleaching response at high latitude eastern Australian Reefs: An applied model for a changing climate. *Diversity*, *3*(4), 592–610. https://doi.org/10.3390/d3040592

Darling, E. S., & Côté, I. M. (2018). Seeking resilience in marine ecosystems. *Science*, *359*, 986–987. https://doi.org/10.1126/science.aas9852

Davies, P. S. (1989). Short-tern growth measurements of corals using an accurate buoyant weighing technique. *Marine Biology*, *101*, 389–395.

Davies, S., Gamache, M. H., Howe-Kerr, L. I., Kriefall, N. G., Baker, A. C., Banaszak, A. T., Bay, L. K., Bellantuono, A. J., Bhattacharya, D., Chan, C. X., Claar, D. C., Coffroth, M. A., Cunning, R., Davy, S. K., del Campo, J., Diaz-Almeyda, E. M., Frommlet, J. C., Fuess, L. E., Gonzalez-Pech, R. A., … Parkinson, J. E. (2022). Building Consensus around the Assessment and Interpretation of Symbiodiniaceae Diversity. *LaJeunesse TC*, *16*(June), 1–66. https://doi.org/10.20944/preprints202206.0284.v1

Davies, S. W., Ries, J. B., Marchetti, A., & Castillo, K. D. (2018). Symbiodinium functional diversity in the Coral Siderastrea siderea Is influenced by thermal stress and reef environment, but not ocean acidification. *Frontiers in Marine Science*, *5*(APR), 1–14. https://doi.org/10.3389/fmars.2018.00150

Day, T., Nagel, L., Van Oppen, M. J. H., & Caley, M. J. (2008). Factors Affecting the Evolution of Bleaching Resistance in Corals. *Source: The American Naturalist*, *171*(2), 72–88. https://doi.org/10.1086/524956

De Nadal, E., Ammerer, G., & Posas, F. (2011). Controlling gene expression in response to stress. *Nature Reviews Genetics*, *12*(12), 833–845. https://doi.org/10.1038/nrg3055

De Souza, M. R., Caruso, C., Ruiz-Jones, L., Drury, C., Gates, R., & Toonen, R. J. (2022). Community composition of coral-associated Symbiodiniaceae differs across fine-scale environmental gradients in Kāne'ohe Bay. *Royal Society Open Science*, *9*(9). https://doi.org/10.1098/rsos.212042

Decarlo, T. M., & Harrison, H. B. (2019). An enigmatic decoupling between heat stress and coral bleaching on the Great Barrier Reef. *PeerJ*, *7*, e7473. https://doi.org/https://doi.org/10.7717/peerj.7473

Delbeek, J, C. (2001). Coral farming: past, present and future trends. *Aquarium Sciences and Conservation*, *3*, 171–181.

Deloitte Access Economics. (2017). At what price? The economic, social and icon value of the Great Barrier Reef. *Deloitte Access Economics*, 92.

DeMerlis, A., Kirkland, A., Kaufman, M., Mayfield, A., Formel, N., Kolodziej, G., Manzello, D., Lirman, D., Traylor-Knowles, N., & Enochs, I. (2022). Pre-exposure to a variable temperature treatment improves the response of Acropora cervicornis to acute thermal stress. *Coral Reefs*, *41*, 435–445. https://doi.org/https://doi.org/10.1007/s00338-022-02232-z

Deschaseaux, E. S. M., Deseo, M. A., Shepherd, K. M., Jones, G. B., & Harrison, P. L. (2013). Air blasting as the optimal approach for the extraction of antioxidants in coral tissue. *Journal of Experimental Marine Biology and Ecology*, *448*, 146–148. https://doi.org/10.1016/j.jembe.2013.07.002

Dimmitt, S., Stampfer, H., & Martin, J. H. (2017). When less is more – efficacy with less toxicity at the ED50. *British Journal of Clinical Pharmacology*, *83*(7), 1365–1368. https://doi.org/10.1111/bcp.13281

Dixon, A., Forster, P. M., Heron, S. F., Stoner, A. M. K., & Beger, M. (2022). Future loss of local-scale thermal refugia in coral reef ecosystems. *PLOS Climate*, *1*(2), e0000004. https://doi.org/10.1371/journal.pclm.0000004

Dixon, G., Abbott, E., & Matz, M. (2020). Meta-analysis of the coral environmental stress response: Acropora corals show opposing responses depending on stress intensity. *Molecular Ecology*, *29*(15), 2855–2870. https://doi.org/10.1111/mec.15535

Dixon, G. B., Davies, S. W., Aglyamova, G. V., Meyer, E., Bay, L. K., & Matz, M. V. (2015). Genomic determinants of coral heat tolerance across latitudes. *Science*, *348*(6242), 1460–1462.

Donner, S. D., Skirving, W. J., Little, C. M., Oppenheimer, M., & Hoegh-Gulberg, O. (2005). Global assessment of coral bleaching and required rates of adaptation under climate change. *Global Change Biology*, *11*(12), 2251–2265. https://doi.org/10.1111/j.1365-2486.2005.01073.x

Dorn, A., & Puchta, H. (2020). DNA repair meets climate change. *Nature Plants*, *6*(12), 1398–1399. https://doi.org/10.1038/s41477-020-00804-x

Dove, S., Ortiz, J. C., Enríquez, S., Fine, M., Fisher, P., Iglesias-Prieto, R., Thornhill, D., & Hoegh-Guldberg, O. (2006). Response of holosymbiont pigments from the scleractinian coral Montipora monasteriata to short-term heat stress. *Limnology and Oceanography*, *51*(2), 1149–1158. https://doi.org/10.4319/lo.2006.51.2.1149

Drury, C., Dale, K. E., Panlilio, J. M., Miller, S. V., Lirman, D., Larson, E. A., Bartels, E., Crawford,

D. L., & Oleksiak, M. F. (2016). Genomic variation among populations of threatened coral: Acropora cervicornis. *BMC Genomics*, *286*(17). https://doi.org/10.1183/s12864-016-2583-8

Drury, Crawford. (2020). Resilience in reef-building corals: The ecological and evolutionary importance of the host response to thermal stress. *Molecular Ecology*, *29*(3), 448–465. https://doi.org/10.1111/mec.15337

Drury, Crawford, Dilworth, J., Majerová, E., Caruso, C., & Greer, J. B. (2022). Expression plasticity regulates intraspecific variation in the acclimatization potential of a reef-building coral. *Nature Communications*, *13*(1), 1–9. https://doi.org/10.1038/s41467-022-32452-4

Drury, Crawford, Manzello, D., & Lirman, D. (2017). Genotype and local environment dynamically influence growth, disturbance response and survivorship in the threatened coral, Acropora cervicornis. *PLoS ONE*, *12*(3), 1–21. https://doi.org/10.1371/journal.pone.0174000

Drury, Crawford, Martin, R. E., Knapp, D. E., Heckler, J., Levy, J., Gates, R. D., & Asner, G. P. (2022). Ecosystem-scale mapping of coral species and thermal tolerance. *Frontiers in Ecology and the Environment*, *20*(5), 285–291. https://doi.org/10.1002/fee.2483

Eakin, C. M., Lough, J. M., & Heron, S. F. (2009). Climate variability and change: Monitoring data and evidence for increased coral bleaching stress. In M. J. H. van Oppen & J. M. Lough (Eds.), *Coral Bleaching. Patterns, Processes, Causes and Consequences* (pp. 41–67). Springer. https://doi.org/10.1007/978-3-540-69775-6_4

Edmunds, P. J., & Burgess, S. C. (2018). Correction: Size-dependent physiological responses of the branching coral Pocillopora verrucosa to elevated temperature and PCO2(J. Exp. Biol. (2016) 219 (3896-3906) Doi: 10.1242/jeb.146381). *Journal of Experimental Biology*, *221*(23), 3896–3906. https://doi.org/10.1242/jeb.194753

Edmunds, P. J., & Putnam, H. M. (2020). Science-based approach to using growth rate to assess coral performance and restoration outcomes: Coral growth and future success. *Biology Letters*, *16*(7). https://doi.org/10.1098/rsbl.2020.0227rsbl20200227

Edmunds, P. J., Putnam, H. M., & Gates, R. D. (2012). Photophysiological Consequences of Vertical Stratification of Symbiodinium in Tissue of the Coral Porites lutea. *Biol. Bull*, *223*(2), 226–235.

Eghtesadi-Araghi, P., Darvish Bastami, K., & Nozhat, F. (2010). Seventy-kilodalton protein density in Porites spp.: Possible useful proxy for cold stress in coral reefs. *Comparative Clinical Pathology*, *21*(5), 693–697. https://doi.org/10.1007/s00580-010-1159-2

Evans, T. G., Diamond, S. E., & Kelly, M. W. (2015). Mechanistic species distribution modelling as a link between physiology and conservation. *Conservation Physiology*, *3*(1), 1–16. https://doi.org/10.1093/conphys/cov056

Evensen, N. R., Fine, M., Perna, G., Voolstra, C. R., & Barshis, D. J. (2021). Remarkably high and consistent tolerance of a Red Sea coral to acute and chronic thermal stress exposures. *Limnology and Oceanography*, 4–45. https://doi.org/10.1002/lno.11715

Evensen, N., Voolstra, C., Fine, M., Perna, G., Buitrago-López, C., Cárdenas, A., Banc-Prandi, G., Rowe, K., & Barshis, D. (2022). Empirically derived thermal thresholds of four coral species along the Red Sea using a portable and standardized experimental approach. *Coral Reefs*, *accepted*. https://doi.org/10.1007/s00338-022-02233-y

Ewels, P., Magnusson, M., Lundin, S., & Käller, M. (2016). MultiQC: summarise analysis results from multiple tools and samples in a single report. *Bioinformatics*, *1:32*(19), 3047–3048. https://doi.org/10.1093/bioinformatics/btw354.

Ewels, P., Peltzer, A., Fillinger, S., Patel, H., Alneberg, J., Wilm, A., Carcia, M., Tommaso, P., & Nahsen, S. (2020). The nf-core framework for community-curated bioinformatics pipelines. *Nat*

Biotechnol. https://doi.org/10.1038/s41587-020-0439-x.

Fifer, J., Bentlage, B., Lemer, S., Fujimura, A. G., Sweet, M., & Raymundo, L. J. (2021). Going with the flow: How corals in high-flow environments can beat the heat. *Molecular Ecology*, *30*(9), 2009–2024. https://doi.org/10.1111/mec.15869

Fitt, W. K., Gates, R. D., Hoegh-Guldberg, O., Bythell, J. C., Jatkar, A., Grottoli, A. G., Gomez, M., Fisher, P., Lajuenesse, T. C., Pantos, O., Iglesias-Prieto, R., Franklin, D. J., Rodrigues, L. J., Torregiani, J. M., van Woesik, R., & Lesser, M. P. (2009). Response of two species of Indo-Pacific corals, Porites cylindrica and Stylophora pistillata, to short-term thermal stress: The host does matter in determining the tolerance of corals to bleaching. *Journal of Experimental Marine Biology and Ecology*, *373*(2), 102–110. https://doi.org/10.1016/j.jembe.2009.03.011

Fitt, William K., Brown, B. E., Warner, M. E., & Dunne, R. P. (2001). Coral bleaching: Interpretation of thermal tolerance limits and thermal thresholds in tropical corals. *Coral Reefs*, *20*(1), 51–65. https://doi.org/10.1007/s003380100146

Fox, J., & Weisberg, S. (2019). *An {R} Companian to Applied Regression* (No. 3). https://socialsciences.mcmaster.ca/jfox/Books/Companion/

Fuller, Z. L., Mocellin, V. J. L., Morris, L. A., Cantin, N., Shepherd, J., Sarre, L., Peng, J., Liao, Y., Pickrell, J., Andolfatto, P., Matz, M., Bay, L. K., & Przeworski, M. (2020). Population genetics of the coroal Acropora millepora: Toward genomic prediction of bleaching. *Science*, *369*(6501). https://doi.org/10.1126/science.aba4674

Gabilly, S. T., Baker, C. R., Wakao, S., Crisanto, T., Guan, K., Bi, K., Guiet, E., Guadagno, C. R., & Niyogi, K. K. (2019). Regulation of photoprotection gene expression in Chlamydomonas by a putative E3 ubiquitin ligase complex and a homolog of CONSTANS. *Proceedings of the National Academy of Sciences of the United States of America*, *116*(35), 17556–17562. https://doi.org/10.1073/pnas.1821689116

Gardner, S. G., Raina, J. B., Nitschke, M. R., Nielsen, D. A., Stat, M., Motti, C. A., Ralph, P. J., & Petrou, K. (2017). A multi-trait systems approach reveals a response cascade to bleaching in corals. *BMC Biology*, *15*(1), 117. https://doi.org/10.1186/s12915-017-0459-2

Gardner, S. G., Raina, J. B., Ralph, P. J., & Petrou, K. (2017). Reactive oxygen species (ROS) and dimethylated sulphur compounds in coral explants under acute thermal stress. *Journal of Experimental Biology*, *220*(10), 1787–1791. https://doi.org/10.1242/jeb.153049

Gates, R. D., Baghdasarian, G., & Muscatine, L. (1992). Temperature stress causes host-cell detachment in symbiotic Cnidarians: implications for coral bleaching. *Biological Bulletin*, *182*(3), 324–332. https://doi.org/Doi 10.2307/1542252

Genevier, L. G. C., Jamil, T., Raitsos, D. E., Krokos, G., & Hoteit, I. (2019). Marine heatwaves reveal coral reef zones susceptible to bleaching in the Red Sea. *Global Change Biology*, *25*(7), 2338–2351. https://doi.org/10.1111/gcb.14652

Gerhard, D., & Ritz, C. (2018). *medrc: Mixed effect dose-response curves* (1.1-0). https://rdrr.io/github/DoseResponse/medrc/

Gianrossi, R., Detrano, R., Mulvihill, D., Lehmann, K., Dubach, P., Colombo, A., McArthur, D., & Froelicher, V. (1989). Exercise-induced ST depression in the diagnosis of coronary artery disease. A meta-analysis. *Circulation*, *80*(1), 87–98. https://doi.org/10.1161/01.CIR.80.1.87

Gibbin, E. M., Krueger, T., Putnam, H. M., Barott, K. L., Bodin, J., Gates, R. D., & Meibom, A. (2018). Short-term thermal acclimation modifies the metabolic condition of the coral holobiont. *Frontiers in Marine Science*, *5*(FEB), 1–11. https://doi.org/10.3389/fmars.2018.00010

Gibbin, E. M., Putnam, H. M., Gates, R. D., Nitschke, M. R., & Davy, S. K. (2015). Species-specific differences in thermal tolerance may define susceptibility to intracellular acidosis in reef corals.

Marine Biology, *162*(3), 717–723. https://doi.org/10.1007/s00227-015-2617-9

Gierz, S. L., Forêt, S., & Leggat, W. (2017). Transcriptomic analysis of thermally stressed Symbiodinium reveals differential expression of stress and metabolism genes. *Frontiers in Plant Science*, *8*(February), 1–20. https://doi.org/10.3389/fpls.2017.00271

Gilchrist, G. W. (1995). Specialists and Generalists in Changing Environments . I . Fitness Landscapes of Thermal Sensitivity. *The American Naturalist*, *146*(2), 252–270.

Glynn, P. W., & D'Croz, L. (1990). Experimental evidence for high temperature stress as the cause of El Niño-coincident coral mortality. *Coral Reefs*, *8*(4), 181–191. https://doi.org/10.1007/BF00265009

González-Guerrero, L. A., Vásquez-Elizondo, R. M., López-Londoño, T., Hernán, G., Iglesias-Prieto, R., & Enríquez, S. (2021). Validation of parameters and protocols derived from chlorophyll a fluorescence commonly utilised in marine ecophysiological studies. *Functional Plant Biology*. https://doi.org/10.1071/FP21101

Granados-Cifuentes, C., Bellantuono, A. J., Ridgway, T., Hoegh-Guldberg, O., & Rodriguez-Lanetty, M. (2013). High natural gene expression variation in the reef-building coral Acropora millepora: potential for acclimative and adaptive plasticity. *BMC Genomics*, *14*(1), 228. https://doi.org/10.1186/1471-2164-14-228

Grima, A. J., Clases, D., Gonzalez de Vega, R., Nitschke, M. R., Goyen, S., Suggett, D. J., & Camp, E. F. (2022). Species-specific elementomes for scleractinian coral hosts and their associated Symbiodiniaceae. *Coral Reefs*, *41*(4), 1115–1130. https://doi.org/10.1007/s00338-022-02259-2

Grottoli, A. G., Toonen, R. J., van Woesik, R., Vega Thurber, R., Warner, M. E., McLachlan, R. H., Price, J. T., Bahr, K. D., Baums, I. B., Castillo, K. D., Coffroth, M. A., Cunning, R., Dobson, K. L., Donahue, M. J., Hench, J. L., Iglesias-Prieto, R., Kemp, D. W., Kenkel, C. D., Kline, D. I., … Wu, H. C. (2021). Increasing comparability among coral bleaching experiments. *Ecological Applications*, *31*(4), 1–17. https://doi.org/10.1002/eap.2262

Grottoli, Andrea G, Wilkins, M. J., Johnston, M. D., Levas, S., Schoepf, V., Dalcin, M. P., Wilkins, M. J., Warner, M. E., Cai, W.-J., Hoadley, K. D., Pettay, D. T., & Melman, T. F. (2018). Coral physiology and microbiome dynamics under combined warming and ocean acidification. *PloS One*, *13*(1), e0191156.

Guest, J. R., Baird, A. H., Maynard, J. A., Muttaqin, E., Edwards, A. J., Campbell, S. J., Yewdall, K., Affendi, Y. A., & Chou, L. M. (2012). Contrasting patterns of coral bleaching susceptibility in 2010 suggest an adaptive response to thermal stress. *PLoS ONE*, *7*(3), 1–8. https://doi.org/10.1371/journal.pone.0033353

Guzman, C., Atrigenio, M., Shinzato, C., Aliño, P., & Conaco, C. (2019). Warm seawater temperature promotes substrate colonization by the blue coral, Heliopora coerulea. *PeerJ*, *7*, e7785. https://doi.org/https://doi.org/10.7717/peerj.7785

Haguenauer, A., Zuberer, F., Ledoux, J. B., & Aurelle, D. (2013). Adaptive abilities of the Mediterranean red coral Corallium rubrum in a heterogeneous and changing environment: From population to functional genetics. *Journal of Experimental Marine Biology and Ecology*, *449*, 349–357. https://doi.org/10.1016/j.jembe.2013.10.010

Harriott, V. J. (1998). Growth of the staghorn coral Acropora formosa at Houtman Abrolhos, Western Australia. *Marine Biology*, *132*(2), 319–325. https://doi.org/10.1007/s002270050397

Harrison, X. A., Donaldson, L., Correa-Cano, M. E., Evans, J., Fisher, D. N., Goodwin, C. E. D., Robinson, B. S., Hodgson, D. J., & Inger, R. (2018). A brief introduction to mixed effects modelling and multi-model inference in ecology. *PeerJ*, *2018*(5), 1–32.

https://doi.org/10.7717/peerj.4794

Hartig, F., & Lohse, L. (2021). *Package "DHARMa" Residual Diangonstics for Hierarchical (Multi-Level/Mixed) Regression Models* (0.4.4). CRAN. https://cran.rstudio.com/web/packages/DHARMa/DHARMa.pdf

Haydon, T. D., Matthews, J. L., Seymour, J. R., Raina, J.-B., Seymour, J. E., Chartrand, K., Camp, E. F., & Suggett, D. J. (2023). Metabolomic signatures of corals thriving across extreme reef habitats reveal strategies of heat stress tolerance. *Proc. R. Soc. B*, *290*, 20221877. https://doi.org/http://doi.org/10.1098/rspb.2022.1877

Hazraty-Kari, S., Tavakoli-Kolour, P., Kitanobo, S., Nakamura, T., & Morita, M. (2022). Adaptations by the coral Acropora tenuis confer resilience to future thermal stress. *Communications Biology*, *5*(1), 1–10. https://doi.org/10.1038/s42003-022-04309-5

Hennige, S. J., Smith, D. J., Walsh, S. J., McGinley, M. P., Warner, M. E., & Suggett, D. J. (2010). Acclimation and adaptation of scleractinian coral communities along environmental gradients within an Indonesian reef system. *Journal of Experimental Marine Biology and Ecology*, *391*(1–2), 143–152. https://doi.org/10.1016/j.jembe.2010.06.019

Hirose, M., Kinzie 3rd, R. A., & Hikada, M. (2000). Early development of zooxanthella-containing eggs of the corals Pocillopora verrucosa and P. eydouxi with special reference to the distribution of zooxanthellae. *The Biological Bulletin*, *199*(1), 68–75. https://doi.org/https://doi.org/10.2307/1542708

Hoadley, K. D., Pettay, D. T., Lewis, A., Wham, D., Grasso, C., Smith, R., Kemp, D. W., LaJeunesse, T., & Warner, M. E. (2021). Different functional traits among closely related algal symbionts dictate stress endurance for vital Indo-Pacific reef-building corals. *Global Change Biology*, *27*(20), 5295–5309. https://doi.org/10.1111/gcb.15799

Hoegh-Guldberg, O., Jacob, D., Taylor, M., Guillén Bolaños, T., Bindi, M., Brown, S., Camilloni, I. A., Diedhiou, A., Djalante, R., Ebi, K., Engelbrecht, F., Guiot, J., Hijioka, Y., Mehrotra, S., Hope, C. W., Payne, A. J., Pörtner, H.-O., Seneviratne, S. I., Thomas, A., … Zhou, G. (2019). The human imperative of stabilizing global climate change at 1.5°C. *Science*, *365*(6459), eaaw6974. https://doi.org/10.1126/science.aaw6974

Hoegh-Guldberg, Ove. (1999). Climate change, coral bleaching and the future of the world's coral reefs. *Marine and Freshwater Research*, *50*(8), 839–866. https://doi.org/10.1071/MF99078

Hoey, A., Howells, E., Johansen, J., Hobbs, J.-P., Messmer, V., McCowan, D., Wilson, S., & Pratchett, M. (2016). Recent Advances in Understanding the Effects of Climate Change on Coral Reefs. *Diversity*, *8*(2), 12. https://doi.org/10.3390/d8020012

Holmes, G., Ortiz, J., Kaniewska, P., & Johnstone, R. (2008). Using three-dimensional surface area to compare the growth of two Pocilloporid coral species. *Marine Biology*, *155*(4), 421–427. https://doi.org/10.1007/s00227-008-1040-x

Howells, E.J, Beltran, V. H., Larsen, N. W., Bay, L. K., Willis, B. L., & van Oppen, M. J. H. (2011). Coral thermal tolerance shaped by local adaptation of photosymbionts. *Nat. Clim. Chang.*, *2*(February), 116–120. https://doi.org/10.1038/nclimate1330

Howells, Emily J., Abrego, D., Meyer, E., Kirk, N. L., & Burt, J. A. (2016). Host adaptation and unexpected symbiont partners enable reef-building corals to tolerate extreme temperatures. *Global Change Biology*, *22*(8), 2702–2714. https://doi.org/10.1111/gcb.13250

Howells, Emily J., Bay, L. K., & Bay, R. A. (2022). *Identifying, Monitoring, and Managing Adaptive Genetic Variation in Reef-Building Corals under Rapid Climate Warming*. *September*, 55–70. https://doi.org/10.1007/978-3-031-07055-6_4

Howells, Emily J., Berkelmans, R., van Oppen, M. J. H., Willis, B. L., & Bay, L. K. (2013). Historical

thermal regimes define limits to coral acclimatization. *Ecology*, *94*(5), 1078–1088. https://doi.org/10.1890/12-1257.1

Howlett, L., Camp, E. F., Edmondson, J., Henderson, N., & Suggett, D. J. (2021). Coral growth, survivorship and return-on-effort within nurseries at high-value sites on the Great Barrier Reef. *PLoS ONE*, *16*(1 January), 1–15. https://doi.org/10.1371/journal.pone.0244961

Hughes, T.P., Kerry, J., Álvarez-Noriega, M., Álvarez-Romero, J., Anderson, K., Baird, A., Babcock, R., Beger, M., Bellwood, D., Berkelmans, R., Bridge, T., Butler, I., Byrne, M., Cantin, N., Comeau, S., Connolly, S., Cumming, G., Dalton, S., Diaz-Pulido, G., … Wilson, S. (2017). Global warming and recurrent mass bleaching of corals. *Nature*, *543*, 373–377. https://doi.org/10.1038/nature21707

Hughes, Terry P., Anderson, K. D., Connolly, S. R., Heron, S. F., Kerry, J. T., Lough, J. M., Baird, A. H., Baum, J. K., Berumen, M. L., Bridge, T. C., Claar, D. C., Eakin, C. M., Gilmour, J. P., Graham, N. A. J., Harrison, H., Hobbs, J. P. A., Hoey, A. S., Hoogenboom, M., Lowe, R. J., … Wilson, S. K. (2018). Spatial and temporal patterns of mass bleaching of corals in the Anthropocene. *Science*, *359*(6371), 80–83. https://doi.org/10.1126/science.aan8048

Hughes, Terry P., Kerry, J. T., Connolly, S. R., Álvarez-Romero, J. G., Eakin, C. M., Heron, S. F., Gonzalez, M. A., & Moneghetti, J. (2021). Emergent properties in the responses of tropical corals to recurrent climate extremes. *Current Biology*, *31*(23), 5393-5399.e3. https://doi.org/10.1016/j.cub.2021.10.046

Humanes, A., Lachs, L., Beauchamp, E. A., Bythell, C., Edwards, A. J., Golbuu, Y., Martinez, H. M., Palmowski, P., Treumann, A., Steeg, E. Van Der, Hooidonk, R. Van, & Guest, J. R. (2022). *Within-population variability in coral heat tolerance indicates climate adaptation potential*.

Hume, B. C. C., Smith, E. G., Ziegler, M., Warrington, H. J. M., Burt, J. A., LaJeunesse, T. C., Wiedenmann, J., & Voolstra, C. R. (2019). SymPortal: A novel analytical framework and platform for coral algal symbiont next-generation sequencing ITS2 profiling. *Molecular Ecology Resources*, *19*(4), 1063–1080. https://doi.org/10.1111/1755-0998.13004

Hume, B., D'Angelo, C., Burt, J., Baker, A. C., Riegl, B., & Wiedenmann, J. (2013). Corals from the Persian/Arabian Gulf as models for thermotolerant reef-builders: Prevalence of clade C3 Symbiodinium, host fluorescence and ex situ temperature tolerance. *Marine Pollution Bulletin*, *72*(2), 313–322. https://doi.org/10.1016/j.marpolbul.2012.11.032

Ikeda, S., Tachikawa, M., Akanuma, S. I., Fujinawa, J., & Hosoya, K. I. (2012). Involvement of γ-aminobutyric acid transporter 2 in the hepatic uptake of taurine in rats. *American Journal of Physiology - Gastrointestinal and Liver Physiology*, *303*(3), 291–297. https://doi.org/10.1152/ajpgi.00388.2011

Illing, B., & Rummer, J. L. (2017). Physiology can contribute to better understanding, management, and conservation of coral reef fishes. *Conservation Physiology*, *5*(1), 1–11. https://doi.org/10.1093/conphys/cox005

Iwabuchi, B. L., & Gosselin, L. A. (2020). Implications of acute temperature and salinity tolerance thresholds for the persistence of intertidal invertebrate populations experiencing climate change. *Ecology and Evolution*, *10*(14), 7739–7754. https://doi.org/10.1002/ece3.6498

Jiang, J., Wang, A., Deng, X., Zhou, W., Gan, Q., & Lu, Y. (2021). How Symbiodiniaceae meets the challenges of life during coral bleaching. *Coral Reefs*, *40*(4), 1339–1353. https://doi.org/10.1007/s00338-021-02115-9

Johnston, E. C., Cunning, R., & Burgess, S. C. (2022). *Cophylogeny and specificity between cryptic coral species (Pocillopora spp .) at Mo ' orea and their symbionts (Symbiodiniaceae)*.

Johnston, E. C., Forsman, Z. H., & Toonen, R. J. (2018). A simple molecular technique for distinguishing species reveals frequent misidentification of Hawaiian corals in the genus Pocillopora. *PeerJ*, *2018*(2), 1–14. https://doi.org/10.7717/peerj.4355

Jokiel, P. L., & Coles, S. L. (1977). Effects of Temperature on the Mortality and Growth of Hawaiian Reef Corals. *Marine Biology*, *43*(3), 201–208.

Jones, A., & Berkelmans, R. (2010). Potential costs of acclimatization to a warmer climate: Growth of a reef coral with heat tolerant vs. sensitive symbiont types. *PLoS ONE*, *5*(5). https://doi.org/10.1371/journal.pone.0010437

Jones, A., & Berkelmans, R. (2012). The photokinetics of thermo-tolerance in Symbiodinium. *Marine Ecology*, *33*(4), 490–498. https://doi.org/10.1111/j.1439-0485.2012.00514.x

Jones, A. M., & Berkelmans, R. (2011). Tradeoffs to Thermal Acclimation: Energetics and Reproduction of a Reef Coral with Heat Tolerant Symbiodinium Type-D. *Journal of Marine Biology*, *2011*, 1–12. https://doi.org/10.1155/2011/185890

Juárez, O. E., Lafarga-De la Cruz, F., Leyva-Valencia, I., López-Landavery, E., García-Esquivel, Z., Díaz, F., Re-Araujo, D., Vadopalas, B., & Galindo-Sánchez, C. E. (2018). Transcriptomic and metabolic response to chronic and acute thermal exposure of juvenile geoduck clams Panopea globosa. *Marine Genomics*, *42*(October), 1–13. https://doi.org/10.1016/j.margen.2018.09.003

Jung, E. M. U., Stat, M., Thomas, L., Koziol, A., & Schoepf, V. (2021). Coral host physiology and symbiont dynamics associated with differential recovery from mass bleaching in an extreme, macro-tidal reef environment in northwest Australia. *Coral Reefs*, *40*(3), 893–905. https://doi.org/10.1007/s00338-021-02094-x

Jurriaans, S., & Hoogenboom, M. O. (2019). Thermal performance of scleractinian corals along a latitudinal gradient on the Great Barrier Reef. *Philosophical Transactions of the Royal Society B: Biological Sciences*, *374*(1778). https://doi.org/10.1098/rstb.2018.0546

Kalmus, P., Ekanayaka, A., Kang, E., Baird, M., & Gierach, M. (2022). Past the Precipice? Projected Coral Habitability Under Global Heating. *Earth's Future*, *10*(5), 1–14. https://doi.org/10.1029/2021EF002608

Kearney, R., Buxton, C. D., & Farebrother, G. (2012). Australia's no-take marine protected areas: Appropriate conservation or inappropriate management of fishing? *Marine Policy*, *36*(5), 1064–1071. https://doi.org/10.1016/j.marpol.2012.02.024

Kellermann, V., Chown, S. L., Schou, M. F., Aitkenhead, I., Janion-Scheepers, C., Clemson, A., Scott, M. T., & Sgrò, C. M. (2019). Comparing thermal performance curves across traits: How consistent are they? *Journal of Experimental Biology*, *222*(11). https://doi.org/10.1242/jeb.193433

Kenkel, C. D., Meyer, E., & Matz, M. V. (2013). Gene expression under chronic heat stress in populations of the mustard hill coral (Porites astreoides) from different thermal environments. *Molecular Ecology*, *22*(16), 4322–4334. https://doi.org/10.1111/mec.12390

Kenkel, C. D., Setta, S. P., & Matz, M. V. (2015). Heritable differences in fitness-related traits among populations of the mustard hill coral, Porites astreoides. *Heredity*, *115*(6), 509–516. https://doi.org/10.1038/hdy.2015.52

Kenkel, C. D., Sheridan, C., Leal, M. C., Bhagooli, R., Castillo, K. D., Kurata, N., Mcginty, E., Goulet, T. L., & Matz, M. V. (2014). Diagnostic gene expression biomarkers of coral thermal stress. *Molecular Ecology Resources*, *14*(4), 667–678. https://doi.org/10.1111/1755-0998.12218

Kenkel, C.D., & Matz, M. V. (2016). Gene expression plasticity as a mechanism of coral adaptation to a variable environment. *Nature Ecology & Evolution*, *1*. https://doi.org/10.1038/s41559-016-0014

Kenkel, Carly D., Sheridan, C., Leal, M. C., Bhagooli, R., Castillo, K. D., Kurata, N., Mcginty, E., Goulet, T. L., & Matz, M. V. (2013). Diagnostic gene expression biomarkers of coral thermal stress. *Molecular Ecology Resources*, *14*(4), 667–678. https://doi.org/https://doi.org/10.1111/1755-0998.12218

Kenny, B., Preuss, C., & McPhee, A. (2022). ED50. In *StatPearls*. https://www.ncbi.nlm.nih.gov/books/NBK538269/

Kim, K. S., Chou, H., Funk, D. H., Jackson, J. K., Sweeney, B. W., & Buchwalter, D. B. (2017). Physiological responses to short-term thermal stress in mayfly (Neocloeon triangulifer) larvae in relation to upper thermal limits. *Journal of Experimental Biology*, *220*(14), 2598–2605. https://doi.org/10.1242/jeb.156919

Kingsolver, J. G., Diamond, S. E., & Buckley, L. B. (2013). Heat stress and the fitness consequences of climate change for terrestrial ectotherms. *Functional Ecology*, *27*(6), 1415–1423. https://doi.org/10.1111/1365-2435.12145

Kingsolver, J. G., & Gomulkiewicz, R. (2003). Environmental Variation and Selection on Performance Curves. *Integrative and Comparative Biology*, *43*(3), 470–477. https://doi.org/10.1093/icb/43.3.470

Kingsolver, J. G., & Woods, H. A. (2016). Beyond thermal performance curves: Modeling time-dependent effects of thermal stress on ectotherm growth rates. *American Naturalist*, *187*(3), 283–294. https://doi.org/10.1086/684786

Kirk, N. L., Howells, E. J., Abrego, D., Burt, J. A., & Meyer, E. (2018). Genomic and transcriptomic signals of thermal tolerance in heat-tolerant corals (Platygyra daedalea) of the Arabian/Persian Gulf. *Molecular Ecology*, *27*(24), 5180–5194. https://doi.org/10.1111/mec.14934

Klepac, C. N., & Barshis, D. J. (2022). High-resolution in situ thermal metrics coupled with acute heat stress experiments reveal differential coral bleaching susceptibility. *Coral Reefs*, *41*(4), 1045–1057. https://doi.org/10.1007/s00338-022-02276-1

Kleypas, J., Allemand, D., Anthony, K., Baker, A. C., Beck, M. W., Hale, L. Z., Hilmi, N., Hoegh-Guldberg, O., Hughes, T., Kaufman, L., Kayanne, H., Magnan, A. K., Mcleod, E., Mumby, P., Palumbi, S., Richmond, R. H., Rinkevich, B., Steneck, R. S., Voolstra, C. R., … Gattuso, J. P. (2021). Designing a blueprint for coral reef survival. *Biological Conservation*, *257*, 109107. https://doi.org/10.1016/j.biocon.2021.109107

Knowlton, N. (2001). The future of coral reefs. *Proceedings of the National Academy of Sciences of the United States of America*, *98*(10), 5419–5425. https://doi.org/10.1073/pnas.091092998

Krasowska, J., Pierzchała, K., Bzowska, A., Forró, L., Sienkiewicz, A., & Wielgus-kutrowska, B. (2021). Chromophore of an enhanced green fluorescent protein can play a photoprotective role due to photobleaching. *International Journal of Molecular Sciences*, *22*(16). https://doi.org/10.3390/ijms22168565

Krueger, T., Hawkins, T. D., Becker, S., Pontasch, S., Dove, S., Hoegh-Guldberg, O., Leggat, W., Fisher, P. L., & Davy, S. K. (2015). Differential coral bleaching-Contrasting the activity and response of enzymatic antioxidants in symbiotic partners under thermal stress. *Comparative Biochemistry and Physiology -Part A : Molecular and Integrative Physiology*, *190*, 15–25. https://doi.org/10.1016/j.cbpa.2015.08.012

Lachs, L., Humanes, A., Pygas, D. R., Bythell, J. C., Mumby, P. J., Ferrari, R., Figueira, W. F., Beauchamp, E., East, H. K., Edwards, A. J., Golbuu, Y., Martinez, H. M., Sommer, B., van der Steeg, E., & Guest, J. R. (2023). No apparent trade-offs associated with heat tolerance in a reef-building coral. *Commun*, *6*(400). https://doi.org/https://doi.org/10.1038/s42003-023-04758-6

LaJeunesse, T. C., Reyes-Bonilla, H., & Warner, M. E. (2007). Spring "bleaching" among Pocillopora in the Sea of Cortez, Eastern Pacific. *Coral Reefs*, *26*(2), 265–270. https://doi.org/10.1007/s00338-006-0189-3

LaJeunesse, Todd C., Parkinson, J. E., Gabrielson, P. W., Jeong, H. J., Reimer, J. D., Voolstra, C. R., & Santos, S. R. (2018). Systematic Revision of Symbiodiniaceae Highlights the Antiquity and Diversity of Coral Endosymbionts. *Current Biology*, *28*(16), 2570-2580.e6. https://doi.org/10.1016/j.cub.2018.07.008

Langfelder, P., & Horvath, S. (2008). WGCNA: an R package for weighted correlation network analysis. *BMC Bioinformatics*, *9*, 559. https://doi.org/10.1186/1471-2105-9-559

Langfelder, P., & Horvath, S. (2023). *WGCNA: Weighted Correlated Network Analysis*. http://horvath.genetics.ucla.edu/html/CoexpressionNetwork/Rpackages/WGCNA/

Langmead, B., & Salzberg, S. L. (2012). Fast gapped-read alignment with Bowtie 2. *Nature Methods*, *9*(4), 357–359. https://doi.org/10.1038/nmeth.1923

Latimer, C. A. L., Foley, B. R., & Chenoweth, S. F. (2015). Connecting thermal performance curve variation to the genotype: A multivariate QTL approach. *Journal of Evolutionary Biology*, *28*(1), 155–168. https://doi.org/10.1111/jeb.12552

Lee, H., Calvin, K., Dasgupta, D., Krinner, G., Mukherji, A., Thorne, P., Trisos, C., Romero, J., Aldunce, P., Barrett, K., Blanco, G., Cheung, W. W. ., Connors, S. ., Denton, F., Diongue-Niang, A., Dodman, D., Garshagen, M., Geden, O., Hayward, B., … Zommers, Z. (2023). Synthesis Report of the IPCC Sixth Asessment Report (AR6). In *IPCC*. https://report.ipcc.ch/ar6syr/pdf/IPCC_AR6_SYR_LongerReport.pdf

Leggat, W., Heron, S. F., Fordyce, A., Suggett, D. J., & Ainsworth, T. D. (2022). Experiment Degree Heating Week (eDHW) as a novel metric to reconcile and validate past and future global coral bleaching studies. *Journal of Environmental Management*, *301*(October 2021), 113919. https://doi.org/10.1016/j.jenvman.2021.113919

Leggat, W., Seneca, F. O., Wasmund, K., Ukani, L., Yellowlees, D., & Ainsworth, T. D. (2011). Differential Responses of the Coral Host and Their Algal Symbiont to Thermal Stress. *PLoS ONE*, *6*(10), e26687. https://doi.org/10.1371/journal.pone.0026687

Lenth, R. (2023). *emmeans: Estimated Marginal Means, ak Least-Squares Means* (1.8.1-1). https://cran.r-project.org/package=emmeans

Leuzinger, S., Willis, B. L., & Anthony, K. R. N. (2012). Energy allocation in a reef coral under varying resource availability. *Marine Biology*, *159*(1), 177–186. https://doi.org/10.1007/s00227-011-1797-1

Li, B., & Dewey, C. N. (2011). RSEM: accurate transcript quantification from RNA-Seq data with or without a reference genome. *BMC Bioinformatics*, *23*(323). https://doi.org/10.1186/1471-2105-12-323

Licthenthaler, H. K. (1987). Chlorophylls and Carotenoids - Pigments of Photosynthetic Biomembranes. *Methods in Enzymology*, *148*, 350–382.

Liew, Y. J., Aranda, M., & Voolstra, C. R. (2016). Reefgenomics.Org - a repository for marine genomics data. *Database*, *2016*. https://doi.org/https://doi.org/10.1093/database/baw152

Liggins, L., Treml, E. A., & Riginos, C. (2019). Seascape Genomics: Contextualizing Adaptive and Neutral Genomic Variation in the Ocean Environment. In M. F. Oleksiak & O. Rajora (Eds.), *Population Genomics: Marine Organisms* (pp. 171–218). Spinger. https://doi.org/https://doi.org/10.1007/13836_2019_68

Lirman, D., Schopmeyer, S., Manzello, D., Gramer, L. J., Precht, W. F., Muller-Karger, F., Banks, K.,

Barnes, B., Bartels, E., Bourque, A., Byrne, J., Donahue, S., Duquesnel, J., Fisher, L., Gilliam, D., Hendee, J., Johnson, M., Maxwell, K., McDevitt, E., … Thanner, S. (2011). Severe 2010 cold-water event caused unprecedented mortality to corals of the Florida reef tract and reversed previous survivorship patterns. *PLoS ONE*, *6*(8). https://doi.org/10.1371/journal.pone.0023047

Logan, C. A., Dunne, J. P., Eakin, C. M., & Donner, S. D. (2014). Incorporating adaptive responses into future projections of coral bleaching. *Global Change Biology*, *20*(1), 125–139. https://doi.org/10.1111/gcb.12390

Lohr, K. E., Camp, E. F., Kuzhiumparambil, U., Lutz, A., Leggat, W., Patterson, J. T., & Suggett, D. J. (2019). Resolving coral photoacclimation dynamics through coupled photophysiological and metabolomic profiling. *Journal of Experimental Biology*, *222*(8). https://doi.org/10.1242/jeb.195982

López-Maury, L., Marguerat, S., & Bähler, J. (2008). Tuning gene expression to changing environments: From rapid responses to evolutionary adaptation. *Nature Reviews Genetics*, *9*(8), 583–593. https://doi.org/10.1038/nrg2398

Lough, J. M., Anderson, K. D., & Hughes, T. P. (2018). Increasing thermal stress for tropical coral reefs: 1871-2017. *Scientific Reports*, *8*(1), 1–8. https://doi.org/10.1038/s41598-018-24530-9

Louis, Y. D., Bhagooli, R., Kenkel, C. D., Baker, A. C., & Dyall, S. D. (2017). Gene expression biomarkers of heat stress in scleractinian corals: Promises and limitations. *Comparative Biochemistry and Physiology Part - C: Toxicology and Pharmacology*, *191*, 63–77. https://doi.org/10.1016/j.cbpc.2016.08.007

Love, M. I., Huber, W., & Anders, S. (2014). Moderated estimation of fold change and dispersion for RNA-seq data with DESeq2. *Genome Biology*, *15*(12), 1–21. https://doi.org/10.1186/s13059-014-0550-8

Loya, Y., Sakai, K., Nakano, Y., & Woesik, R. Van. (2001). Coral bleaching: the winners and the losers. *Ecology Letters*, *4*, 122–131. https://doi.org/10.1046/j.1461-0248.2001.00203.x

Lüdecke, D., Ben-Shachar, M., Patil, I., Waggoner, P., & Makowski, D. (2021). performance: An R Package for Assessment, Comparison and Testing of Statistical Models. *Journal of Open Source Software*, *6*(60), 3139. https://doi.org/10.21105/joss.03139

Lukoschek, V., Riginos, C., & van Oppen, M. J. H. (2016). Congruent patterns of connectivity can inform management for broadcast spawning corals on the Great Barrier Reef. *Molecular Ecology*, *25*(13), 3065–3080. https://doi.org/https://doi.org/10.1111/mec.13649

Lundgren, P., Vera, J. C., Peplow, L., Manel, S., & van Oppen, M. J. H. (2013). Genotype - environment correlations in corals from the Great Barrier Reef. *BMC Genetics*, *14*(1), 9. https://doi.org/10.1186/1471-2156-14-9

Lutz, A., Raina, J. B., Motti, C. A., Miller, D. J., & Van Oppen, M. J. H. (2015). Host coenzyme Q redox state is an early biomarker of thermal stress in the coral Acropora millepora. *PLoS ONE*, *10*(10), 1–19. https://doi.org/10.1371/journal.pone.0139290

Macadam, A., Nowell, C. J., & Quigley, K. (2021). Machine learning for the fast and accurate assessment of fitness in coral early life history. *Remote Sensing*, *13*(16), 1–17. https://doi.org/10.3390/rs13163173

Madin, J. S., Baird, A. H., Dornelas, M., & Connolly, S. R. (2014). Mechanical vulnerability explains size-dependent mortality of reef corals. *Ecology Letters*, *17*(8), 1008–1015. https://doi.org/10.1111/ele.12306

Madin, J. S., Hoogenboom, M. O., Connolly, S. R., Darling, E. S., Falster, D. S., Huang, D., Keith, S. A., Mizerek, T., Pandolfi, J. M., Putnam, H. M., & Baird, A. H. (2016). A Trait-Based Approach

to Advance Coral Reef Science. *Trends in Ecology and Evolution*, *31*(6), 419–428. https://doi.org/10.1016/j.tree.2016.02.012

Magalon, H., Flot, J. F., & Baudry, E. (2007). Molecular identification of symbiotic dinoflagellates in Pacific corals in the genus Pocillopora. *Coral Reefs*, *26*(3), 551–558. https://doi.org/10.1007/s00338-007-0215-0

Magney, T. S., Barnes, M. L., & Yang, X. (2020). On the Covariation of Chlorophyll Fluorescence and Photosynthesis Across Scales. *Geophysical Research Letters*, *47*(23), 1–7. https://doi.org/10.1029/2020GL091098

Magozzi, S., & Calosi, P. (2015). Integrating metabolic performance, thermal tolerance, and plasticity enables for more accurate predictions on species vulnerability to acute and chronic effects of global warming. *Global Change Biology*, *21*(1), 181–194. https://doi.org/10.1111/gcb.12695

Maor-Landaw, K., & Levy, O. (2016). Gene expression profiles during short-term heat stress; branching vs. massive Scleractinian corals of the Red Sea. *PeerJ*, *2016*(3). https://doi.org/10.7717/peerj.1814

Marhoefer, S. R., Zenger, K. R., Strugnell, J. M., Logan, M., van Oppen, M. J. H., Kenkel, C. D., & Bay, L. K. (2021). Signatures of Adaptation and Acclimatization to Reef Flat and Slope Habitats in the Coral Pocillopora damicornis. *Frontiers in Marine Science*, *8*(September). https://doi.org/10.3389/fmars.2021.704709

Marshall, P., & Baird, A. (2000). Bleaching of corals on the Great Barrier Reef: differential susceptibilities among taxa. *Coral Reefs*, *19*, 155–163. https://doi.org/https://doi.org/10.1007/s003380000086

Marzonie, M. R., Bay, L. K., Bourne, D. G., Hoey, A. S., Matthews, S., Nielsen, J. J. V, & Harrison, H. B. (2022). *The effects of marine heatwaves on acute heat tolerance in corals*. *August*, 1–13. https://doi.org/10.1111/gcb.16473

Mason, R. A. B., Skirving, W. J., & Dove, S. G. (2020). Integrating physiology with remote sensing to advance the prediction of coral bleaching events. *Remote Sensing of Environment*, *246*(February), 111794. https://doi.org/10.1016/j.rse.2020.111794

Matias, A. M. A., Popovic, I., Thia, J. A., Cooke, I. R., Torda, G., Lukoschek, V., Bay, L. K., Kim, S. W., & Riginos, C. (2022). Cryptic diversity and spatial genetic variation in the coral Acropora tenuis and its endosymbionts across the Great Barrier Reef. *Evolutionary Applications*, *January*, 1–18. https://doi.org/10.1111/eva.13435

Matz, M. V., Treml, E. A., Aglyamova, G. V., & Bay, L. K. (2018). Potential and limits for rapid genetic adaptation to warming in a Great Barrier Reef coral. *PLoS Genetics*, *14*(4), 1–19. https://doi.org/10.1371/journal.pgen.1007220

Matz, M. V., Treml, E. A., & Haller, B. C. (2020). Estimating the potential for coral adaptation to global warming across the Indo-West Pacific. *Global Change Biology*, *26*(6), 3473–3481. https://doi.org/10.1111/gcb.15060

Mayfield, A. B., Chan, P. H., Putnam, H. M., Chen, C. S., & Fan, T. Y. (2012). The effects of a variable temperature regime on the physiology of the reef-building coral Seriatopora hystrix: Results from a laboratory-based reciprocal transplant. *Journal of Experimental Biology*, *215*(23), 4183–4195. https://doi.org/10.1242/jeb.071688

Maynard, J. A., Anthony, K. R. N., Marshall, P. A., & Masiri, I. (2008). Major bleaching events can lead to increased thermal tolerance in corals. *Marine Biology*, *155*(2), 173–182. https://doi.org/10.1007/s00227-008-1015-y

McClanahan, T. R. (2022). Coral responses to climate change exposure. *Environmental Research Letters*, *17*(7). https://doi.org/10.1088/1748-9326/ac7478

McClanahan, T. R., Baird, A. H., Marshall, P. A., & Toscano, M. A. (2004). Comparing bleaching and mortality responses of hard corals between southern Kenya and the Great Barrier Reef, Australia. *Marine Pollution Bulletin*, *48*(3–4), 327–335. https://doi.org/10.1016/j.marpolbul.2003.08.024

McClanahan, T R, Ateweberhan, M., Muhando, C., Maina, J., & Mohammed, S. M. (2007). Climate change and spatio-temporal variation in seawater temperature effects on coral bleaching and mortality in East Africa. *Ecological Monographs*, *77*(4), 503–525. https://doi.org/10.1890/06-1182.1

McClanahan, Tim R., Donner, S. D., Maynard, J. A., MacNeil, M. A., Graham, N. A. J., Maina, J., Baker, A. C., Alemu I., J. B., Beger, M., Campbell, S. J., Darling, E. S., Eakin, C. M., Heron, S. F., Jupiter, S. D., Lundquist, C. J., McLeod, E., Mumby, P. J., Paddack, M. J., Selig, E. R., & van Woesik, R. (2012). Prioritizing Key Resilience Indicators to Support Coral Reef Management in a Changing Climate. *PLoS ONE*, *7*(8). https://doi.org/10.1371/journal.pone.0042884

McClanahan, Timothy R., Maina, J. M., Darling, E. S., Guillaume, M. M. M., Muthiga, N. A., D'agata, S., Leblond, J., Arthur, R., Jupiter, S. D., Wilson, S. K., Mangubhai, S., Ussi, A. M., Humphries, A. T., Patankar, V., Shedrawi, G., Julius, P., Ndagala, J., & Grimsditch, G. (2020). Large geographic variability in the resistance of corals to thermal stress. *Global Ecology and Biogeography*, *29*(12), 2229–2247. https://doi.org/10.1111/geb.13191

McLachlan, R. H., Dobson, K. L., Schmeltzer, E. R., Thurber, R. V., & Grottoli, A. G. (2021). A review of coral bleaching specimen collection, preservation, and laboratory processing methods. *PeerJ*, *9*, 1–21. https://doi.org/10.7717/peerj.11763

McLachlan, R. H., Price, J. T., Solomon, S. L., & Grottoli, A. G. (2020). Thirty years of coral heat-stress experiments: a review of methods. *Coral Reefs*, *39*(4), 885–902. https://doi.org/10.1007/s00338-020-01931-9

McLeod, I. M., Hein, M. Y., Babcock, R., Bay, L., Bourne, D. G., Cook, N., Doropoulos, C., Gibbs, M., Harrison, P., Lockie, S., van Oppen, M. J. H., Mattocks, N., Page, C. A., Randall, C. J., Smith, A., Smith, H. A., Suggett, D. J., Taylor, B., Vella, K. J., … Boström-Einarsson, L. (2022). Coral restoration and adaptation in Australia: The first five years. *PloS One*, *17*(11), e0273325. https://doi.org/10.1371/journal.pone.0273325

McManus, L. C., Forrest, D. L., Tekwa, E. W., Schindler, D. E., Colton, M. A., Webster, M. M., Essington, T. E., Palumbi, S. R., Mumby, P. J., & Pinsky, M. L. (2021). Evolution and connectivity influence the persistence and recovery of coral reefs under climate change in the Caribbean, Southwest Pacific, and Coral Triangle. *Global Change Biology*, *27*(18), 4307–4321. https://doi.org/10.1111/gcb.15725

Mellin, C., Matthews, S., Anthony, K. R. N., Brown, S. C., Caley, M. J., Johns, K. A., Osborne, K., Puotinen, M., Thompson, A., Wolff, N. H., Fordham, D. A., & MacNeil, M. A. (2019). Spatial resilience of the Great Barrier Reef under cumulative disturbance impacts. *Global Change Biology*, *25*(7), 2431–2445. https://doi.org/10.1111/gcb.14625

Meyer, E., Aglyamova, G. V., & Matz, M. V. (2011). Profiling gene expression responses of coral larvae (Acropora millepora) to elevated temperature and settlement inducers using a novel RNA-Seq procedure. *Molecular Ecology*, *20*(17), 3599–3616. https://doi.org/10.1111/j.1365-294X.2011.05205.x

Middlebrook, R., Anthony, K. R. N., Hoegh-Guldberg, O., & Dove, S. (2010). Heating rate and symbiont productivity are key factors determining thermal stress in the reef-building coral Acropora formosa. *The Journal of Experimental Biology*, *213*(Pt 7), 1026–1034. https://doi.org/10.1242/jeb.031633

Morgan, M. B., Vogelien, D. L., & Snell, T. W. (2001). Assessing coral stress responses using molecular biomarkers of gene transcription. *Environmental Toxicology and Chemistry*, *20*(3), 537–543. https://doi.org/10.1002/etc.5620200312

Morikawa, M. K., & Palumbi, S. R. (2019). Using naturally occurring climate resilient corals to construct bleaching-resistant nurseries. *Proceedings of the National Academy of Sciences of the United States of America*, *116*(21), 10586–10591. https://doi.org/10.1073/pnas.1721415116

Morris, L. A., Voolstra, C. R., Quigley, K. M., Bourne, D. G., & Bay, L. K. (2019). Nutrient Availability and Metabolism Affect the Stability of Coral–Symbiodiniaceae Symbioses. *Trends in Microbiology*, *27*(8), 678–689. https://doi.org/10.1016/j.tim.2019.03.004

Muller, E. M., Bartels, E., & Baums, I. B. (2018). Bleaching causes loss of disease resistance within the threatened coral species acropora cervicornis. *ELife*, *7*, 1–20. https://doi.org/10.7554/eLife.35066

Muñiz-Castillo, A. I., Rivera-Sosa, A., Chollett, I., Eakin, C. M., Andrade-Gómez, L., McField, M., & Arias-González, J. E. (2019). Three decades of heat stress exposure in Caribbean coral reefs: a new regional delineation to enhance conservation. *Scientific Reports*, *9*(1), 1–14. https://doi.org/10.1038/s41598-019-47307-0

Nakagawa, S., & Schielzeth, H. (2013). A general and simple method for obtaining R2 from generalized linear mixed-effects models. *Methods in Ecology and Evolution*, *4*(2), 133–142. https://doi.org/10.1111/j.2041-210x.2012.00261.x

Naumann, M. S., Niggl, W., Laforsch, C., Glaser, C., & Wild, C. (2009). Coral surface area quantification-evaluation of established techniques by comparison with computer tomography. *Coral Reefs*, *28*(1), 109–117. https://doi.org/10.1007/s00338-008-0459-3

Newton, J. R., Smith-Keune, C., & Jerry, D. R. (2010). Thermal tolerance varies in tropical and sub-tropical populations of barramundi (Lates calcarifer) consistent with local adaptation. *Aquaculture*, *308*(SUPPL.1), S128–S132. https://doi.org/10.1016/j.aquaculture.2010.05.040

Nielsen, J. J. V., Kenkel, C. D., Bourne, D. G., Despringhere, L., Mocellin, V. J. L., & Bay, L. K. (2020). Physiological effects of heat and cold exposure in the common reef coral Acropora millepora. *Coral Reefs*, *39*(2), 259–269. https://doi.org/10.1007/s00338-019-01881-x

Nielsen, J. J. V., Matthews, G., Frith, K. R., Harrison, H. B., Marzonie, M. R., Slaughter, K. L., Suggett, D. J., & Bay, L. K. (2022). Experimental considerations of acute heat stress assays to quantify coral thermal tolerance. *Scientific Reports*, *12*(16831), 1–13. https://doi.org/10.1038/s41598-022-20138-2

Nilsson-Örtman, V., Stoks, R., De Block, M., & Johansson, F. (2012). Generalists and specialists along a latitudinal transect: Patterns of thermal adaptation in six species of damselflies. *Ecology*, *93*(6), 1340–1352. https://doi.org/10.1890/11-1910.1

Nitschke, M.R, Rossetn, S. ., Oakley, C. A., Gardner, S. G., Camp, E. F., Suggett, D. J., & Davy, S. K. (2022). The diversity and ecology of Symbiodiniaceae: A traits-based review. *Advances in Marine Biology*, *92*, 55–127. https://doi.org/https://doi.org/10.1016/bs.amb.2022.07.001.

Nitschke, Matthew R., Gardner, S. G., Goyen, S., Fujise, L., Camp, E. F., Ralph, P. J., & Suggett, D. J. (2018). Utility of photochemical traits as diagnostics of thermal tolerance amongst great barrier reef corals. *Frontiers in Marine Science*, *5*(FEB), 1–18. https://doi.org/10.3389/fmars.2018.00045

Nolan, M. K. B., Schmidt-Roach, S., Davis, A. R., Aranda, M., & Howells, E. J. (2021). Widespread bleaching in the One Tree Island lagoon (Southern Great Barrier Reef) during record-breaking temperatures in 2020. *Environmental Monitoring and Assessment*, *193*(9). https://doi.org/10.1007/s10661-021-09330-5

Oksanen, J., Blanchet, F. G., Friendly, M., Kindt, R., Legendre, P., McGlinn, D., Minchin, P. R., O'Hara, R. ., Simpson, G. L., Solymos, P., Henry, M., Stevens, H., Szoecs, E., & Wagner, H. (2020). *vegan* (2.5-7). https://cran.r-project.org/web/packages/vegan/vegan.pdf

Okubo, N., Motokawa, T., & Omori, M. (2007). When fragmented coral spawn? Effect of size and timing on survivorship and fecundity of fragmentation in Acropora formosa. *Marine Biology*, *151*(1), 353–363. https://doi.org/10.1007/s00227-006-0490-2

Oliver, T. A., & Palumbi, S. R. (2011). Do fluctuating temperature environments elevate coral thermal tolerance? *Coral Reefs*, *30*(2), 429–440. https://doi.org/10.1007/s00338-011-0721-y

Ondov, B., Bergman, N., & Phillippy, A. (2011). Interactive metagenomic visualization in a Web browser. *BMC Bioinformatics*, *12*(1), 385. https://github.com/marbl/Krona/wiki

Orejas, C., Taviani, M., Ambroso, S., Andreou, V., Bilan, Bo, M., Brooke, S., Buhl-Mortensen, P., Cordes, E., Dominguez-Carrió, Ferrier-Pagès, C., Godinho, A., Gori, A., Grinyó, J., Gutiérrez-Zárate, C., Hennige, S., Jiménez, C., Larsson, A. I., Lartaud, F., … Carreiro-Silva, M. (2019). 38 Cold-Water Coral in Aquaria: A Focus on the Mediterranean. In C. Orejas & C. Jimenes (Eds.), *Mediterranean Cold-Water Corals: Past, Present and Future*. Springer. https://doi.org/https://doi.org/10.1007/978-3-319-91608-8_38

Osman, E. O., Smith, D. J., Ziegler, M., Kürten, B., Conrad, C., El-Haddad, K. M., Voolstra, C. R., & Suggett, D. J. (2018). Thermal refugia against coral bleaching throughout the northern Red Sea. *Global Change Biology*, *24*(2), e474–e484. https://doi.org/10.1111/gcb.13895

Page, C. A., Giuliano, C., Bay, L. K., & Randall, C. J. (2023). High survival following bleaching highlights the resilience of a highly disturbed region of the Great Barrier Reef. *Ecosphere*, *14*(2), e4280. https://doi.org/https://doi.org/10.1002/ecs2.4280

Palacio-Castro, A. M., Smith, T. B., Brandtneris, V., Snyder, G. A., van Hooidonk, R., Mate, J. ., Manzello, D., Glynn, P. W., Fong, P., & Baker, A. C. (2022). Increased dominance of heat-tolerant symbionts creates resilient coral reefs in near-term ocean warming. *Proceeding of the National Academy of Sciences of the United Stated of America*, *120*(8), e2202388120. https://doi.org/https://doi.org/10.1073/pnas.2202388120

Pallarés, S., Arribas, P., Céspedes, V., Millán, A., & Velasco, J. (2012). Lethal and sublethal behavioural responses of saline water beetles to acute heat and osmotic stress. *Ecological Entomology*, *37*(6), 508–520. https://doi.org/10.1111/j.1365-2311.2012.01393.x

Palumbi, S. R., Barshis, D. J., Traylor-Knowles, N., & Bay, R. A. (2014). Mechanisms of reef resilience. *Science*, *344*(6186), 895–899.

Palumbi, Stephen R, Barshis, D. J., Traylor-Knowles, N., & Bay, R. A. (2014). Mechanisms of reef coral resistance to future climate change. *Science*, *344*(6186), 895–899.

Parkinson, J. E., Baker, A. C., Baums, I. B., Davies, S. W., Grottoli, A. G., Kitchen, S. A., Matz, M. V., Miller, M. W., Shantz, A. A., & Kenkel, C. D. (2020). Molecular tools for coral reef restoration: Beyond biomarker discovery. *Conservation Letters*, *13*(1), 1–12. https://doi.org/10.1111/conl.12687

Pausch, R. E., Williams, D. E., & Miller, M. W. (2018). Impacts of fragment genotype, habitat, and size on outplanted elkhorn coral success under thermal stress. *Marine Ecology Progress Series*, *592*, 109–117. https://doi.org/10.3354/meps12488

Pavlova, A., Beheregaray, L. B., Coleman, R., Gilligan, D., Harrisson, K. A., Ingram, B. A., Kearns, J., Lamb, A. M., Lintermans, M., Lyon, J., Nguyen, T. T. T., Sasaki, M., Tonkin, Z., Yen, J. D. L., & Sunnucks, P. (2017). Severe consequences of habitat fragmentation on genetic diversity of an endangered Australian freshwater fish: A call for assisted gene flow. *Evolutionary*

Applications, *10*(6), 531–550. https://doi.org/10.1111/eva.12484

Payet, S. D., Pratchett, M. S., Saenz-Agudelo, P., Berumen, M. L., DiBattista, J. D., & Harrison, H. B. (2022). Demographic histories shape population genomics of the common coral grouper (Plectropomus leopardus). *Evolutionary Applications*, *15*(8), 1221–1235. https://doi.org/10.1111/eva.13450

Petit, R. J., & Excoffier, L. (2009). Gene flow and species delimitation. *Trends in Ecology and Evolution*, *24*(7), 386–393. https://doi.org/10.1016/j.tree.2009.02.011

Pinheiro, J., Bates, D., DebRoy, S., Sarkar, D., & R Core Team. (2017). *nlme: Linear and Nonlinear Mixed Effects Models* (R package version 3.1-131). https://cran.r-project.org/package=nlme

Pinzón, J. H. C., Dornberger, L., Beach-Letendre, J., Weil, E., & Mydlarz, L. D. (2014). The link between immunity and life history traits in scleractinian corals. *PeerJ*, *2014*(1), 1–16. https://doi.org/10.7717/peerj.628

Pochon, X., Pawlowski, J., Zaninetti, L., & Rowan, R. (2001). High genetic diversity and relative specificity among Symbiodinium-like endosymbiotic dinoflagellates in soritid foraminiferans. *Marine Biology*, *139*(6), 1069–1078. https://doi.org/10.1007/s002270100674

Pörtner, H. O., Roberts, D. C., Masson-Delmotte, V., Zhai, P., Tignor, M., Poloczanska, E., Mintenbeck, K., Nicolai, M., Okem, A., Petzold, J., Rama, B., & Weyer, N. (2019). *IPCC Special Report on the Ocean and Cryosphere in a Changing Cimate*.

Pratchett, M. S., Caballes, C. F., Newman, S. J., Wilson, S. K., Messmer, V., & Pratchett, D. J. (2020). Bleaching susceptibility of aquarium corals collected across northern Australia. *Coral Reefs*, *39*(3), 663–673. https://doi.org/10.1007/s00338-020-01939-1

Pratchett, M. S., McCowan, D., Maynard, J. A., & Heron, S. F. (2013). Changes in Bleaching Susceptibility among Corals Subject to Ocean Warming and Recurrent Bleaching in Moorea, French Polynesia. *PLoS ONE*, *8*(7), 1–10. https://doi.org/10.1371/journal.pone.0070443

Precoda, K., Hardt, M. J., Baird, A. H., & Madin, J. S. (2020). Tissue biomass trades off with growth but not reproduction in corals. *Coral Reefs*, *39*(4), 1027–1037. https://doi.org/10.1007/s00338-020-01925-7

Qin, G., Johnson, C., Zhang, Y., Zhang, H., Yin, J., Miller, G., Turingan, R. G., Guisbert, E., & Lin, Q. (2018). Temperature-induced physiological stress and reproductive characteristics of the migratory seahorse Hippocampus erectus during a thermal stress simulation. *Biology Open*, *7*(6), 1–7. https://doi.org/10.1242/bio.032888

Quigley, K. M., Randall, C. J., van Oppen, M. J. H., & Bay, L. K. (2020). Assessing the role of historical temperature regime and algal symbionts on the heat tolerance of coral juveniles. *Biology Open*, *9*, 1–11. https://doi.org/10.1242/BIO.047316

Quigley, K., & van Oppen, M. J. (2022). Predictive models for the selection of thermally tolerant corals based on offspring survival. *Nature Communications*, *13*(1), 1–13. https://doi.org/10.1038/s41467-022-28956-8

Quigley, K.M., Davies, S. W., Kenkel, C. D., Willis, B. L., Matz, M. V., & Bay, L. K. (2014). Deep-Sequencing Method for Quantifying Background Abundances of Symbiodinium Types: Exploring the Rare Symbiodinium Biosphere in Reef-Building Corals. *PLoS ONE*, *9*(4). https://doi.org/10.1371/journal.pone.0094297

Quigley, Kate M., Bay, L. K., & van Oppen, M. J. . (2020). Genome-wide SNP analysis reveals an increase in adaptive genetic variation through selective breeding of coral. *Molecular Ecology*, *29*, 2176–2188. https://doi.org/https://doi.org/10.1111/mec.15482

Quigley, Kate M., Bay, L. K., & Willis, B. L. (2017). Temperature and water quality-related patterns

in sediment-associated Symbiodinium communities impact symbiont uptake and fitness of juveniles in the genus Acropora. *Frontiers in Marine Science*, *4*(DEC), 1–17. https://doi.org/10.3389/fmars.2017.00401

Quigley, Kate M., Bay, L. K., & Willis, B. L. (2018). Leveraging new knowledge of Symbiodinium community regulation in corals for conservation and reef restoration. *Marine Ecology Progress Series*, *600*, 245–253. https://doi.org/10.3354/meps12652

Quigley, Kate M., Hein, M., & Suggett, D. J. (2022). Translating the 10 golden rules of reforestation for coral reef restoration. *Conservation Biology*, *36*(4), 1–8. https://doi.org/10.1111/cobi.13890

Quigley, Kate M., Marzonie, M., Ramsby, B., Abrego, D., Milton, G., van Oppen, M. J. H., & Bay, L. K. (2021). Variability in Fitness Trade-Offs Amongst Coral Juveniles With Mixed Genetic Backgrounds Held in the Wild. *Frontiers in Marine Science*, *8*(February), 1–12. https://doi.org/10.3389/fmars.2021.636177

Quigley, Kate M., Ramsby, B., Laffy, P., Harris, J., Mocellin, V. J. L., & Bay, L. K. (2022). Symbioses are restructured by repeated mass coral bleaching. *Science Advances*, *8*(49), eabq8349. https://doi.org/10.1126/sciadv.abq8349

Quigley, Kate M, Bay, L. K., & van Oppen, M. J. H. Van. (2019). The active spread of adaptive variation for reef resilience. *Ecology and Evolution*, 1–14. https://doi.org/10.1002/ece3.5616

R Core Team. (2020). *R: A language and environment for statistical computing* (3.3.2). Foundation for Statistical Computing.

R Core Team. (2022). *R: A language and environment for statistical computing* (4.2.1). Foundation for Statistical Computing. https://www.r-project.org/

Radchuk, V., Reed, T., Teplitsky, C., van de Pol, M., Charmantier, A., Hassall, C., Adamík, P., Adriaensen, F., Ahola, M. P., Arcese, P., Miguel Avilés, J., Balbontin, J., Berg, K. S., Borras, A., Burthe, S., Clobert, J., Dehnhard, N., de Lope, F., Dhondt, A. A., … Kramer-Schadt, S. (2019). Adaptive responses of animals to climate change are most likely insufficient. *Nature Communications*, *10*(1), 1–14. https://doi.org/10.1038/s41467-019-10924-4

Rädecker, N., Pogoreutz, C., Gegner, H. M., Cárdenas, A., & Roth, F. (2021). Heat stress destabilizes symbiotic nutrient cycling in corals. *Proceeding of the National Academy of Sciences of the United Stated of America*, *118*(5), e2022653118. https://doi.org/10.1073/pnas.2022653118

Raftery, A. E., Zimmer, A., Frierson, D. M. W., Startz, R., & Liu, P. (2017). Less than 2 °c warming by 2100 unlikely. *Nature Climate Change*, *7*(9), 637–641. https://doi.org/10.1038/nclimate3352

Ralph, P. J., & Gademann, R. (2005). Rapid light curves: A powerful tool to assess photosynthetic activity. *Aquatic Botany*, *82*(3), 222–237. https://doi.org/10.1016/j.aquabot.2005.02.006

ReFuGe 2020 Consortium. (2015). The ReFuGe 2020 Consortium-using "omics" approaches to explore the adaptability and resilience of coral holobionts to environmental change. *Frontiers in Marine Science*, *2*(SEP). https://doi.org/10.3389/fmars.2015.00068

Richter-Boix, A., Katzenberger, M., Duarte, H., Quintela, M., Tejedo, M., & Laurila, A. (2015). Local divergence of thermal reaction norms among amphibian populations is affected by pond temperature variation. *Evolution*, *69*(8), 2210–2226. https://doi.org/10.1111/evo.12711

Ritchie, R. J. (2006). Consistent sets of spectrophotometric chlorophyll equations for acetone, methanol and ethanol solvents. *Photosynthesis Research*, *89*(1), 27–41. https://doi.org/10.1007/s11120-006-9065-9

Ritz, C., Baty, F., Streibig, J., & Gerhard, D. (2015). Doese-Response Analysis Using R. *PLoS ONE*, *30*(10). https://doi.org/10.1371/journal.pone.0146021.

Ros, M., Suggett, D. J., Edmondson, J., Haydon, T., Hughes, D. J., Kim, M., Guagliardo, P., Bougoure, J., Pernice, M., Raina, J. B., & Camp, E. F. (2021). Symbiont shuffling across environmental gradients aligns with changes in carbon uptake and translocation in the reef-building coral Pocillopora acuta. *Coral Reefs*, *40*(2), 595–607. https://doi.org/10.1007/s00338-021-02066-1

Rose, N. H., Bay, R. A., Morikawa, M. K., & Palumbi, S. R. (2018). Polygenic evolution drives species divergence and climate adaptation in corals. *Evolution*, *72*(1), 82–94. https://doi.org/10.1111/evo.13385

Rosset, S., Wiedenmann, J., Reed, A. J., & D'Angelo, C. (2017). Phosphate deficiency promotes coral bleaching and is reflected by the ultrastructure of symbiotic dinoflagellates. *Marine Pollution Bulletin*, *118*(1–2), 180–187. https://doi.org/10.1016/j.marpolbul.2017.02.044

Roth, M. S., & Deheyn, D. D. (2013). Effects of cold stress and heat stress on coral fluorescence in reef-building corals. *Scientific Reports*, *3*, 1421. https://doi.org/10.1038/srep01421

Roth, M. S., Goericke, R., & Deheyn, D. D. (2012). Cold induces acute stress but heat is ultimately more deleterious for the reef-building coral Acropora yongei. *Scientific Reports*, *2*, 240. https://doi.org/10.1038/srep00240

Rowan, R. (2004). Coral bleaching: thermal adaptation in reef coral symbionts. *Nature*, *430*(7001), 742. https://doi.org/10.1038/430742a

Ruiz-Jones, L. J., & Palumbi, S. R. (2017). Tidal heat pulses on a reef trigger a fine-tuned transcriptional response in corals to maintain homeostasis. *Science Advances*, *3*(3), 1–11. https://doi.org/10.1126/sciadv.1601298

Rustamova, S. M., Suleymanova, Z. J., Isgandarova, T. Y., Zulfugarova, S. T., Mammadov, A. C., & Huseynova, I. M. (2019). Identification of Stress Responsive Genes by Using Molecular Markers to Develop Tolerance in Wheat. In M. Hasanuzzaman, K. Nahar, & M. Hossain (Eds.), *Wheat Production in Changing Environments*. Springer. https://doi.org/https://doi.org/10.1007/978-981-13-6883-7_16

Safaie, A., Silbiger, N. J., McClanahan, T. R., Pawlak, G., Barshis, D. J., Hench, J. L., Rogers, J. S., Williams, G. J., & Davis, K. A. (2018). High frequency temperature variability reduces the risk of coral bleaching. *Nature Communications*, *9*(1), 1–12. https://doi.org/10.1038/s41467-018-04074-2

Sampayo, E. M., Ridgway, T., Franceschinis, L., Roff, G., Hoegh-Guldberg, O., & Dove, S. (2016). Coral symbioses under prolonged environmental change: living near tolerance range limits. *Scientific Reports*, *6*(November), 36271. https://doi.org/10.1038/srep36271

Sarkar, D. (2008). *Lattice: Multivariate Data Visualization with R*. Springer. http://lmdvr.r-forge.r-project.org.

Savary, R., Barshis, D. J., Voolstra, C. R., Cárdenas, A., Evensen, N. R., Banc-Prandi, G., Fine, M., & Meibom, A. (2021). Fast and pervasive transcriptomic resilience and acclimation of extremely heat-tolerant coral holobionts from the northern Red Sea. *Proceedings of the National Academy of Sciences of the United States of America*, *118*(19). https://doi.org/10.1073/pnas.2023298118

Sawall, Y., Al-Sofyani, A., Banguera-Hinestroza, E., & Voolstra, C. R. (2014). Spatio-temporal analyses of Symbiodinium physiology of the coral Pocillopora verrucosa along large-scale nutrient and temperature gradients in the Red Sea. *PLoS ONE*, *9*(8), 1–12. https://doi.org/10.1371/journal.pone.0103179

Saxby, T., Dennison, W. C., & Hoegh-Guldberg, O. (2003). Photosynthetic responses of the coral Montipora digitata to cold temperature stress. *Marine Ecology Progress Series*, *248*(April 2017), 85–97. https://doi.org/10.3354/meps248085

Scharfenstein, H. J., Chan, W. Y., Buerger, P., Humphrey, C., & van Oppen, M. J. H. (2022). Evidence for de novo acquisition of microalgal symbionts by bleached adult corals. *ISME Journal*, *16*(6), 1676–1679. https://doi.org/10.1038/s41396-022-01203-0

Scheufen, T., Krämer, W. E., Iglesias-Prieto, R., & Enríquez, S. (2017). Seasonal variation modulates coral sensibility to heat-stress and explains annual changes in coral productivity. *Scientific Reports*, *7*(1), 1–15. https://doi.org/10.1038/s41598-017-04927-8

Schoepf, V., Grottoli, A. G., Levas, S. J., Aschaffenburg, M. D., Baumann, J. H., Matsui, Y., & Warner, M. E. (2015). Annual coral bleaching and the long-term recovery capacity of coral. *Proceedings of the Royal Society B: Biological Sciences*, *282*(1819). https://doi.org/10.1098/rspb.2015.1887

Schoepf, V., Stat, M., Falter, J. L., & McCulloch, M. T. (2015). Limits to the thermal tolerance of corals adapted to a highly fluctuating, naturally extreme temperature environment. *Scientific Reports*, *5*(November), 1–14. https://doi.org/10.1038/srep17639

Schroeder, A., Mueller, O., Stocker, S., Salowsky, R., Leiber, M., Gassmann, M., Lightfoot, S., Menzel, W., Granzow, M., & Ragg, T. (2006). The RIN: An RNA integrity number for assigning integrity values to RNA measurements. *BMC Molecular Biology*, *7*, 1–14. https://doi.org/10.1186/1471-2199-7-3

Schuback, N., Tortell, P. D., Berman-Frank, I., Campbell, D. A., Ciotti, A., Courtecuisse, E., Erickson, Z. K., Fujiki, T., Halsey, K., Hickman, A. E., Huot, Y., Gorbunov, M. Y., Hughes, D. J., Kolber, Z. S., Moore, C. M., Oxborough, K., Prášil, O., Robinson, C. M., Ryan-Keogh, T. J., … Varkey, D. R. (2021). Single-Turnover Variable Chlorophyll Fluorescence as a Tool for Assessing Phytoplankton Photosynthesis and Primary Productivity: Opportunities, Caveats and Recommendations. *Frontiers in Marine Science*, *8*(July). https://doi.org/10.3389/fmars.2021.690607

Seebacher, F., Ducret, V., Little, A. G., & Adriaenssens, B. (2015). Generalist–specialist trade-off during thermal acclimation. *Royal Society Open Science*, *2*(1). https://doi.org/10.1098/rsos.140251

Selmoni, O., Rochat, E., Lecellier, G., Berteaux-Lecellier, V., & Joost, S. (2020). Seascape genomics as a new tool to empower coral reef conservation strategies: An example on north-western Pacific Acropora digitifera. *Evolutionary Applications*, *13*(8), 1923–1938. https://doi.org/10.1111/eva.12944

Seneca, F. O., & Palumbi, S. R. (2015). The role of transcriptome resilience in resistance of corals to bleaching. *Molecular Ecology*, *24*(7), 1467–1484. https://doi.org/10.1111/mec.13125

Sharkey, T. D. (2005). Effects of moderate heat stress on photosynthesis: Importance of thylakoid reactions, rubisco deactivation, reactive oxygen species, and thermotolerance provided by isoprene. *Plant, Cell and Environment*, *28*(3), 269–277. https://doi.org/10.1111/j.1365-3040.2005.01324.x

Shenkar, N., Fine, M., & Loya, Y. (2005). Size matters: Bleaching dynamics of the coral Oculina patagonica. *Marine Ecology Progress Series*, *294*(2001), 181–188. https://doi.org/10.3354/meps294181

Siebeck, U. E., Marshall, N. J., Klüter, A., & Hoegh-Guldberg, O. (2006). Monitoring coral bleaching using a colour reference card. *Coral Reefs*, *25*(3), 453–460. https://doi.org/10.1007/s00338-006-0123-8

Silverstein, R. N., Cunning, R., & Baker, A. C. (2015). Change in algal symbiont communities after bleaching, not prior heat exposure, increases heat tolerance of reef corals. *Global Change Biology*, *21*(1), 236–249. https://doi.org/10.1111/gcb.12706

Sinclair, B. J., Marshall, K. E., Sewell, M. A., Levesque, D. L., Willett, C. S., Slotsbo, S., Dong, Y., Harley, C. D. G., Marshall, D. J., Helmuth, B. S., & Huey, R. B. (2016). Can we predict ectotherm responses to climate change using thermal performance curves and body temperatures? *Ecology Letters*, *19*(11), 1372–1385. https://doi.org/10.1111/ele.12686

Sing Wong, A., Vrontos, S., & Taylor, M. L. (2022). An assessment of people living by coral reefs over space and time. *Global Change Biology*, *28*(23), 7139–7153. https://doi.org/10.1111/gcb.16391

Skirving, W., Marsh, B., De La Cour, J., Liu, G., Harris, A., Maturi, E., Geiger, E., & Mark Eakin, C. (2020). Coraltemp and the coral reef watch coral bleaching heat stress product suite version 3.1. *Remote Sensing*, *12*(23), 1–10. https://doi.org/10.3390/rs12233856

Smith-Keune, C., & Van Oppen, M. (2006). Genetic structure of a reef-building coral from thermally distinct environments on the Great Barrier Reef. *Coral Reefs*, *25*(3), 493–502. https://doi.org/10.1007/s00338-006-0129-2

Smith, E. G., D'Angelo, C., Salih, A., & Wiedenmann, J. (2013). Screening by coral green fluorescent protein (GFP)-like chromoproteins supports a role in photoprotection of zooxanthellae. *Coral Reefs*, *32*(2), 463–474. https://doi.org/10.1007/s00338-012-0994-9

Smith, G., & Spillman, C. (2019). New high-resolution sea surface temperature forecasts for coral reef management on the Great Barrier Reef. *Coral Reefs*, *38*(5), 1039–1056. https://doi.org/10.1007/s00338-019-01829-1

Smith, L. W., Barshis, D., & Birkeland, C. (2007). Phenotypic plasticity for skeletal growth, density and calcification of Porites lobata in response to habitat type. *Coral Reefs*, *26*(3), 559–567. https://doi.org/10.1007/s00338-007-0216-z

Soneson, C., Love, M. I., & M.D., R. (2015). Differential analyses for RNA-seq: transcript-level estimates improve gene-level inferences. *F1000Research*, *4*(1521). https://doi.org/https://doi.org/10.12688/f1000research.7563.2

Song, M., Zhao, J., Wen, H. S., Li, Y., Li, J. F., Li, L. M., & Tao, Y. X. (2019). The impact of acute thermal stress on the metabolome of the black rockfish (Sebastes schlegelii). *PLoS ONE*, *14*(5), 1–23. https://doi.org/10.1371/journal.pone.0217133

Souter, D., Planes, S., Wicquart, J., Logan, M., Obura, D., & Staub, F. (2020). *Status of Coral Reefs of the World:2020*.

Spady, B. L., Skirving, W. J., Liu, G., De La Cour, J. L., McDonald, C. J., & Manzello, D. P. . (2022). *Unprecedented early-summer heat stress and forecast of coral bleaching on the Great Barrier Reef, 2021-2022 [version 4]*. https://doi.org/https://doi.org/10.12688/f1000research.108724.4

Starcevic, A., Dunlap, W. C., Cullum, J., Malcolm Shick, J., Hranueli, D., & Long, P. F. (2010). Gene expression in the scleractinian Acropora microphthalma exposed to high solar irradiance reveals elements of photoprotection and coral bleaching. *PLoS ONE*, *5*(11). https://doi.org/10.1371/journal.pone.0013975

Strader, M. E., & Quigley, K. M. (2022). The role of gene expression and symbiosis in reef-building coral acquired heat tolerance. *Nature Communications*, *13*(1), 1–8. https://doi.org/10.1038/s41467-022-32217-z

Suggett, D. J., Camp, E., Edmondson, J., Boström-Einarsson, L., Ramler, L., Lohr, K., & Patterson, J. T. (2019). Optimizing return-on-effort for coral nursery and outplanting practices to aid restoration of the Great Barrier Reef. *Restoration Ecology*, *27*, 683–693. https://doi.org/https://doi.org/10.1111/rec.12916

Suggett, D. J., Goyen, S., Evenhuis, C., Szabó, M., Pettay, D. T., Warner, M. E., & Ralph, P. J. (2015). Functional diversity of photobiological traits within the genus Symbiodinium appears to

be governed by the interaction of cell size with cladal designation. *New Phytologist*, *208*(2), 370–381. https://doi.org/10.1111/nph.13483

Suggett, D. J., Nitschke, M. R., Hughes, D. J., Bartels, N., Camp, E. F., Dilernia, N., Edmondson, J., Fitzgerald, S., Grima, A., Sage, A., & Warner, M. E. (2022). Toward bio-optical phenotyping of reef-forming corals using Light-Induced Fluorescence Transient-Fast Repetition Rate fluorometry. *Limnology and Oceanography: Methods*. https://doi.org/10.1002/lom3.10479

Suggett, D. J., & Smith, D. J. (2011). Interpreting the sign of coral bleaching as friend vs. foe. *Global Change Biology*, *17*(1), 45–55. https://doi.org/10.1111/j.1365-2486.2009.02155.x

Suggett, D. J., & Smith, D. J. (2020). Coral bleaching patterns are the outcome of complex biological and environmental networking. *Global Change Biology*, *26*(1), 68–79. https://doi.org/10.1111/gcb.14871

Sully, S., Burkepile, D. E., Donovan, M. K., Hodgson, G., & van Woesik, R. (2019). A global analysis of coral bleaching over the past two decades. *Nature Communications*, *10*(1), 1–5. https://doi.org/10.1038/s41467-019-09238-2

Sweet, M., Bulling, M., Varshavi, D., Lloyd, G. R., Jankevics, A., Najdekr, L., Weber, R. J. M., Viant, M. R., & Craggs, J. (2021). Species-Specific Variations in the Metabolomic Profiles of Acropora hyacinthus and Acropora millepora Mask Acute Temperature Stress Effects in Adult Coral Colonies. *Frontiers in Marine Science*, *8*(March), 1–15. https://doi.org/10.3389/fmars.2021.574292

Tallarida, R. (1992). Statistical analysis of drug combinations for synergism. *Pain*, *49*(1), 93–97. https://doi.org/10.1016/0304-3959(92)90193-F

Tang, J., Ni, X., Wen, J., Wang, L., Luo, J., & Zhou, Z. (2020). Increased Ammonium Assimilation Activity in the Scleractinian Coral Pocillopora damicornis but Not Its Symbiont After Acute Heat Stress. *Frontiers in Marine Science*, *7*(September), 1–10. https://doi.org/10.3389/fmars.2020.565068

Teague, J., Willans, J., Allen, M. J., Scott, T. B., & Day, J. C. C. (2019). Applied marine hyperspectral imaging; coral bleaching from a spectral viewpoint. *Spectroscopy Europe*, *31*(1), 13–17.

Teixeira, T., Diniz, M., Calado, R., & Rosa, R. (2013). Coral physiological adaptations to air exposure: Heat shock and oxidative stress responses in Veretillum cynomorium. *Journal of Experimental Marine Biology and Ecology*, *439*, 35–41. https://doi.org/10.1016/j.jembe.2012.10.010

Thomas, L., Rose, N. H., Bay, R. A., López, E. H., Morikawa, M. K., Ruiz-Jones, L., & Palumbi, S. R. (2018). Mechanisms of Thermal Tolerance in Reef-Building Corals across a Fine-Grained Environmental Mosaic: Lessons from Ofu, American Samoa. *Frontiers in Marine Science*, *4*(February), 1–14. https://doi.org/10.3389/fmars.2017.00434

Thomas, L., Underwood, J. N., Rose, N. H., Fuller, Z. L., Richards, Z. T., Dugal, L., Grimaldi, C. M., Cooke, I. R., Palumbi, S. R., & Gilmour, J. P. (2022). Spatially varying selection between habitats drives physiological shifts and local adaptation in a broadcast spawning coral on a remote atoll in Western Australia. *Science Advances*, *8*(17), 1–12. https://doi.org/10.1126/sciadv.abl9185

Thompson, R. M., Beardall, J., Beringer, J., Grace, M., & Sardina, P. (2013). Means and extremes: Building variability into community-level climate change experiments. *Ecology Letters*, *16*(6), 799–806. https://doi.org/10.1111/ele.12095

Thornton, S., & Richardson, L. . (2022). *Coral Reefs*. National Geographic.

https://education.nationalgeographic.org/resource/coral-reefs

Tisthammer, K. H., Timmins-Schiffman, E., Seneca, F. O., Nunn, B. L., & Richmond, R. H. (2021). Physiological and molecular responses of lobe coral indicate nearshore adaptations to anthropogenic stressors. *Scientific Reports*, *11*(1), 1–11. https://doi.org/10.1038/s41598-021-82569-7

Tolosa, I., Treignier, C., Grover, R., & Ferrier-Pagès, C. (2011). Impact of feeding and short-term temperature stress on the content and isotopic signature of fatty acids, sterols, and alcohols in the scleractinian coral Turbinaria reniformis. *Coral Reefs*, *30*(3), 763–774. https://doi.org/10.1007/s00338-011-0753-3

Torres, A. F., Valino, D. A. M., & Ravago-Gotanco, R. (2021). Zooxanthellae Diversity and Coral-Symbiont Associations in the Philippine Archipelago: Specificity and Adaptability Across Thermal Gradients. *Frontiers in Marine Science*, *8*(October), 1–15. https://doi.org/10.3389/fmars.2021.731023

Traylor-Knowles, N., Rose, N. H., Sheets, E. A., & Palumbi, S. R. (2017). Early transcriptional responses during heat stress in the coral Acropora hyacinthus. *Biological Bulletin*, *232*(2), 91–100. https://doi.org/10.1086/692717

Tsang, R. H. L., & Ang, P. (2015). Cold temperature stress and predation effects on corals: their possible roles in structuring a nonreefal coral community. *Coral Reefs*, *34*(1), 97–108. https://doi.org/10.1007/s00338-014-1210-x

Turnham, K. E., Wham, D. C., Sampayo, E., & LaJeunesse, T. C. (2021). Mutualistic microalgae co-diversify with reef corals that acquire symbionts during egg development. *ISME Journal*, *15*(11), 3271–3285. https://doi.org/10.1038/s41396-021-01007-8

van Oppen, M. J.H., Palstra, F. P., Piquet, A. M. T., & Miller, D. J. (2001). Patterns of coral-dinoflagellate associations in Acropora: Significance of local availability and physiology of Symbiodinium strains and host-symbiont selectivity. *Proceedings of the Royal Society B: Biological Sciences*, *268*(1478), 1759–1767. https://doi.org/10.1098/rspb.2001.1733

van Oppen, M. J H, Souter, P., Howells, E. J., Heyward, A., & Berkelmans, R. (2011). Novel genetic diversity through somatic mutations: Fuel for adaptation of reef corals? *Diversity*, *3*(3), 405–423. https://doi.org/10.3390/d3030405

van Oppen, Madeleine J. H., & Quigley, K. M. (2022). Enhancing corals using assisted evolution. In P. Hutchings, S. Hamylton, & O. Hoegh-Guldberg (Eds.), *Coral Reefs of Australia: Perspectives from Beyond the Water's Edge* (pp. 291–295). CSIRO Publishing.

van Oppen, Madeleine J H, Oliver, J. K., Putnam, H. M., & Gates, R. D. (2015). Building coral reef resilience through assisted evolution. *Proceedings of the National Academy of Sciences*, *112*(8), 1–7. https://doi.org/10.1073/pnas.1422301112

van Woesik, R., Shlesinger, T., Grottoli, A. G., Toonen, R. J., Thurber, R. V., Warner, Mark, E., Hulver, A. M., Chapron, L., Mclachlan, R. H., Albright, R., Crandall, E., Decarlo, T. M., Donovan, M. ., Eirin-Lopez, J., Harrison, H. B., Heron, S. F., Huang, D., Humanes, A., Krueger, T., … Zaneveld, J. (2022). Coral-bleaching responses to climate change across biological scales. *Global Change Biology*, 1–22. https://doi.org/10.1111/gcb.16192

Veal, C. J., Carmi, M., Fine, M., & Hoegh-Guldberg, O. (2010). Increasing the accuracy of surface area estimation using single wax dipping of coral fragments. *Coral Reefs*, *29*(4), 893–897. https://doi.org/10.1007/s00338-010-0647-9

Vidal-Dupiol, J., Harscouet, E., Shefy, D., Toulza, E., Rey, O., Allienne, J. F., Mitta, G., & Rinkevich, B. (2022). Frontloading of stress response genes enhances robustness to environmental change in chimeric corals. *BMC Biology*, *20*(1), 1–18.

https://doi.org/10.1186/s12915-022-01371-7

Voolstra, C. R., Buitrago-López, C., Perna, G., Cárdenas, A., Hume, B. C. C., Rädecker, N., & Barshis, D. J. (2020). Standardized short-term acute heat stress assays resolve historical differences in coral thermotolerance across microhabitat reef sites. *Global Change Biology*, *26*(8), 4328–4343. https://doi.org/10.1111/gcb.15148

Voolstra, C. R., Peixoto, R. S., & Ferrier-pag, C. (2023). Mitigating the ecological collapse of coral Effective strategies to preserve coral reef ecosystems. *EMBO Reports*, e56826. https://doi.org/10.15252/embr.202356826

Voolstra, C. R., Suggett, D. J., Peixoto, R. S., Parkinson, J. E., Quigley, K. M., Silveira, C. B., Sweet, M., Muller, E. M., Barshis, D. J., Bourne, D. G., & Aranda, M. (2021). Extending the natural adaptive capacity of coral holobionts. *Nature Reviews Earth & Environment*, *0123456789*. https://doi.org/10.1038/s43017-021-00214-3

Voolstra, C. R., Valenzuela, J. J., Turkarslan, S., Cárdenas, A., Hume, B. C. C., Perna, G., Buitrago-López, C., Rowe, K., Orellana, M. V., Baliga, N. S., Paranjape, S., Banc-Prandi, G., Bellworthy, J., Fine, M., Frias-Torres, S., & Barshis, D. J. (2021). Contrasting heat stress response patterns of coral holobionts across the Red Sea suggest distinct mechanisms of thermal tolerance. *Molecular Ecology*, *30*(18), 4466–4480. https://doi.org/10.1111/mec.16064

Walker, N. S., Cornwell, B. H., Nestor, V., Armstrong, K. C., Golbuu, Y., & Palumbi, S. R. (2022). Persistence of phenotypic responses to short-term heat stress in the tabletop coral Acropora hyacinthus. *PLoS ONE*, *17*(9 September), 1–20. https://doi.org/10.1371/journal.pone.0269206

Wall, C. B., Kaluhiokalani, M., Popp, B. N., Donahue, M. J., & Gates, R. D. (2020). Divergent symbiont communities determine the physiology and nutrition of a reef coral across a light-availability gradient. *ISME Journal*, *14*(4), 945–958. https://doi.org/10.1038/s41396-019-0570-1

Waltham, N. J., & Sheaves, M. (2017). Acute thermal tolerance of tropical estuarine fish occupying a man-made tidal lake, and increased exposure risk with climate change. *Estuarine, Coastal and Shelf Science*, *196*, 173–181. https://doi.org/10.1016/j.ecss.2017.06.032

Wang, J. T., Wang, Y. T., Keshavmurthy, S., Meng, P. J., & Chen, C. A. (2019). The coral Platygyra verweyi exhibits local adaptation to long-term thermal stress through host-specific physiological and enzymatic response. *Scientific Reports*, *9*(1), 1–11. https://doi.org/10.1038/s41598-019-49594-z

Wangpraseurt, D., Lichtenberg, M., Jacques, S. L., Larkum, A. W. D., & Kühl, M. (2019). Optical properties of corals distort variable chlorophyll fluorescence measurements. *Plant Physiology*, *179*(4), 1608–1619. https://doi.org/10.1104/pp.18.01275

Warner, M. E., Fitt, W. K., & Schmidt, G. W. (1996). The effects of elevated temperature on the photosynthetic efficiency of zooxanthellae in hospite from four different species of reef coral: A novel approach. *Plant, Cell and Environment*, *19*(3), 291–299. https://doi.org/10.1111/j.1365-3040.1996.tb00251.x

Warner, Mark E, Fittt, W. K., & Schmidt, G. W. (1999). Damage to Photosystem II in Symbiotic Dinoflagellates . A Determinant of Coral Bleaching Author (s): Mark E . Warner , William K . Fitt and Gregory W . Schmidt Source : Proceedings of the National Academy of Sciences of the United States of America , Pu. *Pnas*, *96*(14), 8007–8012.

Weis, V. (2008). Cellular mechanisms of Cnidarian bleaching: stress cause the collapse of symbiosis. *Journal of Experimental Biology*, *211*, 3059–3066. https://doi.org/10.1242/jeb.009597

Weis, V. M. (2010). The susceptibility and resilience of corals to thermal stress: Adaptation, acclimatization or both?: NEWS and VIEWS. *Molecular Ecology*, *19*(8), 1515–1517.

https://doi.org/10.1111/j.1365-294X.2010.04575.x

White, A. J., & Critchley, C. (1999). Rapid light curves: A new fluorescence method to assess the state of the photosynthetic apparatus. *Photosynthesis Research*, *59*, 63–72. https://doi.org/https://doi.org/10.1023/A:1006188004189

Whitehead, A., & Crawford, D. L. (2006). Neutral and adaptive variation in gene expression. *Proceedings of the National Academy of Sciences of the United States of America*, *103*(14), 5425–5430. https://doi.org/10.1073/pnas.0507648103

Whitlock, M. C., & Schluter, D. (2009). *The Analysis of Biological Data*. Roberts and Comapny Publishers.

Wiedenmann, J., D'Angelo, C., Smith, E. ., Hunt, A. ., Legiret, F.-E., Postle, A. ., & Actherberg, E. . (2013). Nutrient enrichment can increase the susceptibility of reef corals to bleaching. *Nature Climate Change*, *3*, 160–164. https://doi.org/https://doi.org/10.1038/nclimate1661

Wikelski, M., & Cooke, S. J. (2006). Conservation physiology. *Trends in Ecology and Evolution*, *21*(1), 38–46. https://doi.org/10.1016/j.tree.2005.10.018

Wilson, S. G., Carleton, J. H., & Meekan, M. G. (2003). Spatial and temporal patterns in the distribution and abundance of macrozooplankton on the southern North West Shelf, Western Australia. *Estuarine, Coastal and Shelf Science*, *56*(5–6), 897–908. https://doi.org/10.1016/S0272-7714(02)00285-8

Winters, G., Holzman, R., Blekhman, A., Beer, S., & Loya, Y. (2009). Photographic assessment of coral chlorophyll contents : Implications for ecophysiological studies and coral monitoring. *Journal of Experimental Marine Biology and Ecology*, *380*(1–2), 25–35. https://doi.org/10.1016/j.jembe.2009.09.004

Wood, D., & Salz. (2014). Kraken: ultrafast metagenomic sequence classification using exact alignments. *Genome Biology*, *15*(R46).

Wooldridge, S. A. (2009). Water quality and coral bleaching thresholds: Formalising the linkage for the inshore reefs of the Great Barrier Reef, Australia. *Marine Pollution Bulletin*, *58*(5), 745–751. https://doi.org/10.1016/j.marpolbul.2008.12.013

Wright, R. M., Aglyamova, G. V., Meyer, E., & Matz, M. V. (2015). Gene expression associated with white syndromes in a reef building coral, Acropora hyacinthus. *BMC Genomics*, *16*(1), 1–12. https://doi.org/10.1186/s12864-015-1540-2

Wright, R. M., Mera, H., Kenkel, C. D., Nayfa, M., Bay, L. K., & Matz, M. V. (2019). Positive genetic associations among fitness traits support evolvability of a reef-building coral under multiple stressors. *Global Change Biology*, *25*(10), 3294–3304. https://doi.org/10.1111/gcb.14764

Wyatt, A. S. J., Leichter, J. J., Washburn, L., Kui, L., Edmunds, P. J., & Burgess, S. C. (2023). Hidden heatwaves and severe coral bleaching linked to mesoscale eddies and thermocline dynamics. *Nature Communications*, *14*(1), 1–17. https://doi.org/10.1038/s41467-022-35550-5

Yuyama, I., & Higuchi, T. (2014). Comparing the effects of symbiotic algae (Symbiodinium) clades C1 and D on early growth stages of Acropora tenuis. *PLoS ONE*, *9*(6), 1–8. https://doi.org/10.1371/journal.pone.0098999

Zanuzzo, F. S., Bailey, J. A., Garber, A. F., & Gamperl, A. K. (2019). Comparative Biochemistry and Physiology , Part A The acute and incremental thermal tolerance of Atlantic cod (Gadus morhua) families under normoxia and mild hypoxia ☆. *Comparative Biochemistry and Physiology, Part A*, *233*(September 2018), 30–38. https://doi.org/10.1016/j.cbpa.2019.03.020

Zhang, B., & Horvath, S. (2005). A General Framework for Weighted Gene Co-Expression Network

Analysis. *Statistical Applications in Genetics and Molecular Biology*, *4*(1).

Ziegler, M., Arif, C., Burt, J. A., Dobretsov, S., Roder, C., LaJeunesse, T. C., & Voolstra, C. R. (2017). Biogeography and molecular diversity in the genus Symbiodinium around the Arabian Peninsula. *Journal of Biogeography*. https://doi.org/10.1111/jbi.12913

Ziegler, Maren, Roder, C. M., Büchel, C., & Voolstra, C. R. (2014). Limits to physiological plasticity of the coral Pocillopora verrucosa from the central Red Sea. *Coral Reefs*, *33*(4), 1115–1129. https://doi.org/10.1007/s00338-014-1192-8

Ziegler, Maren, Seneca, F. O., Yum, L. K., Palumbi, S. R., & Voolstra, C. R. (2017). Bacterial community dynamics are linked to patterns of coral heat tolerance. *Nature Communications*, *8*, 1–8. https://doi.org/10.1038/ncomms14213

Appendix A – Supplementary materials for Chapter 2

Supplementary Table A.1 Treatment temperature (High and Mid) achieved during each acute heat stress experimental run compared to the ambient sea-water temperature.

Experiment	Reef	Treatment combo	Mean heated temperature	Heated SE	Mean ambient temperature	Ambient SE	Temperature difference
1	13-123 *A. tenuis*	High/Ambient	34.89	0.059	29.94	0.026	4.952381
	13-123 *P. damicornis*	High/Ambient	35.02	0.068	30.03	0.049	4.990476
2	Creech	High/Ambient	34.63	0.097	29.59	0.029	5.038889
3	11-049	High/Ambient	34.99	0.12	29.96	0.020	5.035714
	13-124	High/Ambient	34.98	0.061	30.55	0.013128	4.433333
	13-124	Mid/Ambient	33.44	0.027	30.2	0.040237	3.24
	Corbett	High/Ambient	35.23	0.037	30.8	0.016903	4.433333
	Corbett	Mid/Ambient	32.99	0.060	30.39	0.015065	2.594444
	Davie	High/Ambient	34.99	0.034	30.87	0.062994	4.12
	Davie	Mid/Ambient	34.21	0.031	29.96	0.066898	4.255556
	Lagoon	High/Ambient	35.09	0.089	29.53	0.023035	5.561905
	Lagoon	Mid/Ambient	33.37	0.049	29.46	0.013436	3.911111
	Mantis	High/Ambient	35.28	0.085	30.37	0.027021	4.913333
	Mantis	Mid/Ambient	33.53	0.079	29.84	0.082896	3.688889

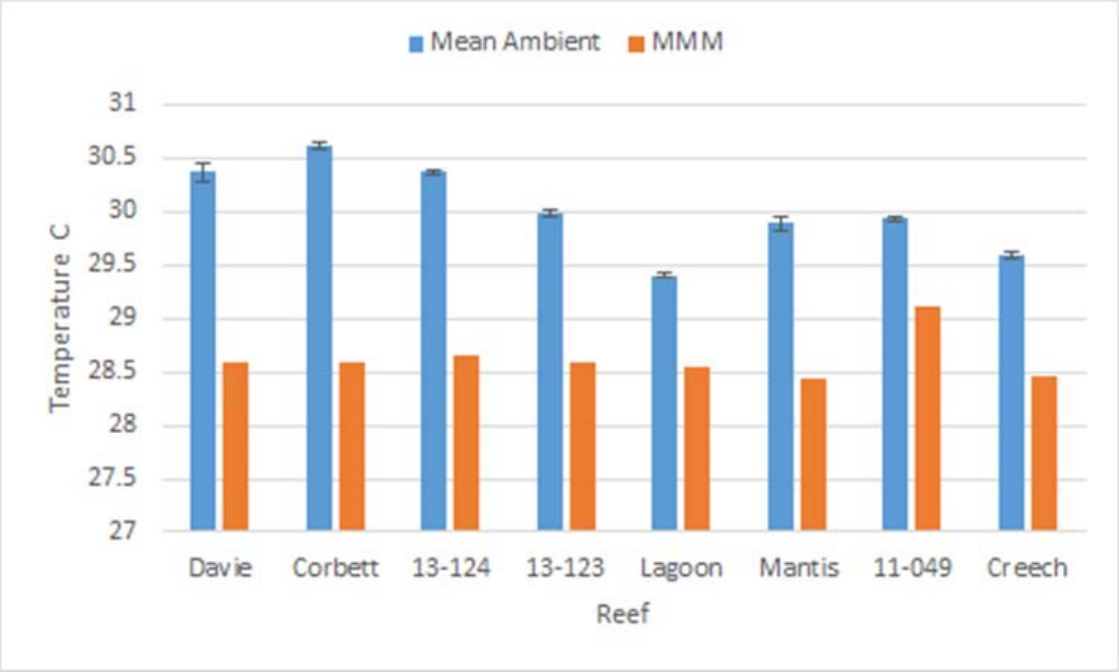

Supplementary Figure A.1 Difference between mean (±SE) ambient temperature at time of experiment and the reef-specific Max Monthly Mean (MMM) temperature obtained from NOAA.

Supplementary Table A.2 Statistical outputs for size and treatment effects in *A. tenuis* and *P. damicornis*. Significant effects are indicated in **bold**.

Species	Trait	Transformation	Term	df	Z	p
A. tenuis	Colour change	Cube root	Treatment	106	-6.714	**1.89E-11**
			Size	106	4.231	**2.32E-05**
			Treatment*Size	106	-3.255	**0.00114**
	Chlorophyll *a*	NA	Treatment	104	-6.236	**< 0.0001**
			Size	104	1.19	0.234
			Treatment*Size	104	-0.079	0.937
	Catalase activity	log	Treatment	93	2.382	**0.0172**
			Size	93	-1.309	0.1904
			Treatment*Size	93	-1.281	0.2003
	Protein content	log	Treatment	91	-5.112	**< 0.0001**
			Size	91	-0.775	0.438
			Treatment*Size	91	0.882	0.378
	F_v/F_m	NA	Treatment	212	-10.13	**< 0.0001**
			Size	212	0.82	0.413
			Treatment*Size	212	1.26	0.207
P. damicornis	Colour change	Cube root	Treatment	106	-9.273	**< 0.0001**
			Size	106	-2.631	**0.0085**
			Treatment*Size	106	2.499	**0.0125**
	Chlorophyll *a*	NA	Treatment	96	-2.776	**0.0055**
			Size	96	2.653	**0.00797**
			Treatment*Size	96	-1.975	**0.04827**
	Catalase activity	log	Treatment	86	-4.546	**< 0.0001**
			Size	86	-1.851	0.064175
			Treatment*Size	86	2.82	**0.004804**
	Protein content	log	Treatment	102	-3.173	**0.00151**
			Size	102	-2.761	**0.00577**
			Treatment*Size	102	0.136	0.89186
	F_v/F_m	NA	Treatment	195	-8.15	**< 0.0001**
			Size	195	-1.31	0.192
			Treatment*Size	195	0.27	0.785

Supplementary Table A.3 Post-hoc contrasts of physiological traits for both *A. tenuis* and *P. damicornis* with respect to fragment size. Significant contrasts are indicated in **bold**.

Species	Trait	Contrast	df	T ratio	p
A. tenuis	Colour change	Large Heated - Large Ambient	106	6.714	**< 0.0001**
		Small Ambient - Large Ambient	106	-4.231	**< 0.0001**
		Small Heated - Large Heated	106	0.371	0.7114
		Small Heated - Small Ambient	106	11.316	**< 0.0001**
P. damicornis	Chlorophyll *a*	Large Heated - Large Ambient	96	2.776	**0.0066**
		Small Ambient - Large Ambient	96	5.586	**< 0.0001**
		Small Heated - Large Heated	96	-2.653	**0.0093**
		Small Heated - Small Ambient	96	0.177	0.8603
	Colour change	Large Heated - Large Ambient	106	9.279	**< 0.0001**
		Small Ambient - Large Ambient	106	5.745	**< 0.0001**
		Small Heated - Large Heated	106	2.631	**0.0098**
		Small Heated - Small Ambient	106	-0.902	0.3689
	Catalase activity	Large Heated - Large Ambient	86	4.546	**< 0.0001**
		Small Ambient - Large Ambient	86	0.225	0.8228
		Small Heated - Large Heated	86	1.851	0.0676
		Small Heated - Small Ambient	86	-2.146	**0.0347**

Supplementary Table A.4 Statistical outputs for sampling time effect in *A. tenuis*. Significant effects are indicated in **bold**.

Trait	Term	estimate	d. error	z	p
Catalase	Intercept	-9.22	26.014	-0.35	0.72
	T_1	-56.85	33.85	-1.68	**0.093**
	T_2	109.48	33.8	3.24	**0.0012**
	T_3	40.42	34.34	1.18	0.24
	T_4	-34.53	34.56	-1.00	0.32
	T_5	-88.38	35.40	-2.50	**0.013**
	T_6	-74.58	32.88	-2.27	**0.023**
Chlorophyll	Intercept	-24.18	9.90	-2.44	**0.015**
	T_1	-17.29	14.57	-1.19	0.24
	T_2	-27.73	13.55	-2.05	**0.041**
	T_3	-41.19	13.20	-3.12	**0.0018**
	T_4	-35.25	13.55	-2.60	**0.0093**
	T_5	-59.65	14.00	-4.26	**< 0.0001**
	T_6	-54.06	13.20	-4.10	**< 0.0001**
Colour change	Intercept	-9.98	3.14	-3.18	**0.0015**
	T_1	-4.49	2.93	-1.53	0.13
	T_2	-8.96	2.93	-3.05	**0.0023**
	T_3	-15.33	2.93	-5.23	**< 0.0001**
	T_4	-24.73	2.93	-8.43	**< 0.0001**
	T_5	-30.70	2.93	-10.46	**< 0.0001**
	T_6	-37.81	2.93	-12.89	**< 0.0001**
Protein	Intercept	-26.44	11.25	-2.35	**0.019**
	T_1	-10.89	16.56	-0.66	0.51
	T_2	-24.05	16.91	-1.51	0.13
	T_3	-57.61	16.56	-3.48	**0.0005**
	T_4	-58.08	15.91	-3.65	**0.0003**
	T_5	-73.56	15.91	-4.62	**< 0.0001**
	T_6	-73.56	15.41	-4.78	**< 0.0001**
$\boldsymbol{F_v/F_m}$	Intercept	-5.85	2.43	-2.40	**0.016**
	T_1	-3.85	3.01	-1.28	0.20
	T_2	-1.61	3.01	-0.54	0.59
	T_3	0.60	3.01	0.20	0.84

	T_4	0.40	3.01	0.13	0.90
	T_5	-4.43	3.11	-1.43	0.154
	T_6	-32.10	3.01	-10.65	**< 0.0001**

Supplementary Table A.5 Post-hoc contrasts of physiological traits over time, *A. tenuis*. Significant contrasts are indicated in **bold**.

Traits	contrast	estimate	SE	df	t ratio	p value
Protein	T0 - T1	10.88921	16.6	39	0.658	0.9942
	T0 - T2	24.04836	15.9	39	1.511	0.7364
	T0 - T3	57.61369	16.6	39	3.479	**0.0196**
	T0 - T4	58.07697	15.9	39	3.65	**0.0124**
	T0 - T5	73.55848	15.9	39	4.623	**0.0008**
	T0 - T6	73.55836	15.4	39	4.775	**0.0005**
	T1 - T2	13.15916	16.6	39	0.795	0.9842
	T1 - T3	46.72448	17.2	39	2.719	0.1204
	T1 - T4	47.18777	16.6	39	2.849	0.0908
	T1 - T5	62.66928	16.6	39	3.784	**0.0086**
	T1 - T6	62.66915	16.1	39	3.898	**0.0063**
	T2 - T3	33.56532	16.6	39	2.027	0.415
	T2 - T4	34.02861	15.9	39	2.139	0.3513
	T2 - T5	49.51012	15.9	39	3.112	**0.0495**
	T2 - T6	49.50999	15.4	39	3.214	**0.0386**
	T3 - T4	0.46329	16.6	39	0.028	1
	T3 - T5	15.9448	16.6	39	0.963	0.959
	T3 - T6	15.94467	16.1	39	0.992	0.9528
	T4 - T5	15.48151	15.9	39	0.973	0.9569
	T4 - T6	15.48138	15.4	39	1.005	0.9498
	T5 - T6	-0.00012	15.4	39	0	1
Chlorophyll	T0 - T1	17.29	14.6	45	1.187	0.8955
	T0 - T2	27.73	13.6	45	2.046	0.4014
	T0 - T3	41.19	13.2	45	3.121	**0.0457**
	T0 - T4	35.24	13.6	45	2.601	0.15
	T0 - T5	59.65	14	45	4.262	**0.0018**
	T0 - T6	54.06	13.2	45	4.097	**0.0031**
	T1 - T2	10.44	14.1	45	0.738	0.9893
	T1 - T3	23.9	13.8	45	1.732	0.599

	T1 - T4	17.96	14.1	45	1.27	0.8618
	T1 - T5	42.36	14.6	45	2.908	0.0764
	T1 - T6	36.77	13.8	45	2.665	0.1313
	T2 - T3	13.46	12.7	45	1.058	0.9369
	T2 - T4	7.52	13.1	45	0.574	0.9972
	T2 - T5	31.92	13.6	45	2.356	0.2412
	T2 - T6	26.33	12.7	45	2.07	0.3876
	T3 - T4	-5.94	12.7	45	-0.467	0.9991
	T3 - T5	18.46	13.2	45	1.399	0.7993
	T3 - T6	12.87	12.3	45	1.043	0.941
	T4 - T5	24.4	13.6	45	1.801	0.5544
	T4 - T6	18.81	12.7	45	1.479	0.7556
	T5 - T6	-5.59	13.2	45	-0.424	0.9995

Traits	**contrast**	**estimate**	**SE**	**df**	**t ratio**	**p value**
Colour change	T0 - T1	4.49	2.93	53	1.532	0.7249
	T0 - T2	8.96	2.93	53	3.054	0.0513
	T0 - T3	15.33	2.93	53	5.225	**0.0001**
	T0 - T4	24.73	2.93	53	8.429	**<.0001**
	T0 - T5	30.7	2.93	53	10.462	**<.0001**
	T0 - T6	37.81	2.93	53	12.887	**<.0001**
	T1 - T2	4.47	2.83	53	1.577	0.6971
	T1 - T3	10.84	2.83	53	3.826	**0.006**
	T1 - T4	20.24	2.83	53	7.145	**<.0001**
	T1 - T5	26.2	2.83	53	9.251	**<.0001**
	T1 - T6	33.32	2.83	53	11.763	**<.0001**
	T2 - T3	6.37	2.83	53	2.249	0.2878
	T2 - T4	15.77	2.83	53	5.568	**<.0001**
	T2 - T5	21.74	2.83	53	7.674	**<.0001**

	T2 - T6	28.85	2.83	53	10.186	**<.0001**
	T3 - T4	9.4	2.83	53	3.318	0.0257
	T3 - T5	15.37	2.83	53	5.425	**<.0001**
	T3 - T6	22.48	2.83	53	7.937	**<.0001**
	T4 - T5	5.97	2.83	53	2.106	0.3641
	T4 - T6	13.08	2.83	53	4.619	**0.0005**
	T5 - T6	7.12	2.83	53	2.512	0.1758
F_v/F_m	T0 - T1	3.849	3.01	51	1.277	0.8591
	T0 - T2	1.612	3.01	51	0.535	0.9982
	T0 - T3	-0.597	3.01	51	-0.198	1
	T0 - T4	-0.396	3.01	51	-0.131	1
	T0 - T5	4.428	3.11	51	1.426	0.7855
	T0 - T6	32.099	3.01	51	10.651	**<.0001**
	T1 - T2	-2.237	2.8	51	-0.798	0.9841
	T1 - T3	-4.446	2.8	51	-1.586	0.6916
	T1 - T4	-4.245	2.8	51	-1.514	0.735
	T1 - T5	0.579	2.9	51	0.2	1
	T1 - T6	28.25	2.8	51	10.078	**<.0001**
	T2 - T3	-2.209	2.8	51	-0.788	0.9851
	T2 - T4	-2.008	2.8	51	-0.716	0.991
	T2 - T5	2.816	2.9	51	0.972	0.9578
	T2 - T6	30.488	2.8	51	10.876	**<.0001**
	T3 - T4	0.201	2.8	51	0.072	1
	T3 - T5	5.025	2.9	51	1.734	0.5969
	T3 - T6	32.696	2.8	51	11.664	**<.0001**
	T4 - T5	4.824	2.9	51	1.665	0.6417
	T4 - T6	32.496	2.8	51	11.592	**<.0001**
	T5 - T6	27.672	2.9	51	9.551	**<.0001**

Traits	contrast	estimate	SE	df	t ratio	p value
Catalase	T0 - T1	56.8	33.8	37	1.679	0.6334
	T0 - T2	-109.5	33.8	37	-3.239	**0.0371**
	T0 - T3	-40.4	34.3	37	-1.177	0.8983
	T0 - T4	34.5	34.6	37	0.999	0.951
	T0 - T5	88.4	35.4	37	2.497	0.1899
	T0 - T6	74.6	32.9	37	2.268	0.2861
	T1 - T2	-166.3	33.8	37	-4.921	**0.0003**
	T1 - T3	-97.3	34.3	37	-2.832	0.0956
	T1 - T4	-22.3	34.6	37	-0.646	0.9947
	T1 - T5	31.5	35.4	37	0.891	0.9717
	T1 - T6	17.7	32.9	37	0.539	0.998
	T2 - T3	69.1	33.1	37	2.089	0.38
	T2 - T4	144	31.9	37	4.51	**0.0011**
	T2 - T5	197.9	33	37	6.002	**<.0001**
	T2 - T6	184.1	30.6	37	6.006	**<.0001**
	T3 - T4	74.9	33.7	37	2.223	0.3083
	T3 - T5	128.8	34.6	37	3.726	**0.0105**
	T3 - T6	115	32.3	37	3.562	**0.0163**
	T4 - T5	53.9	33.1	37	1.629	0.6649
	T4 - T6	40.1	30.5	37	1.312	0.842
	T5 - T6	-13.8	31.9	37	-0.433	0.9994

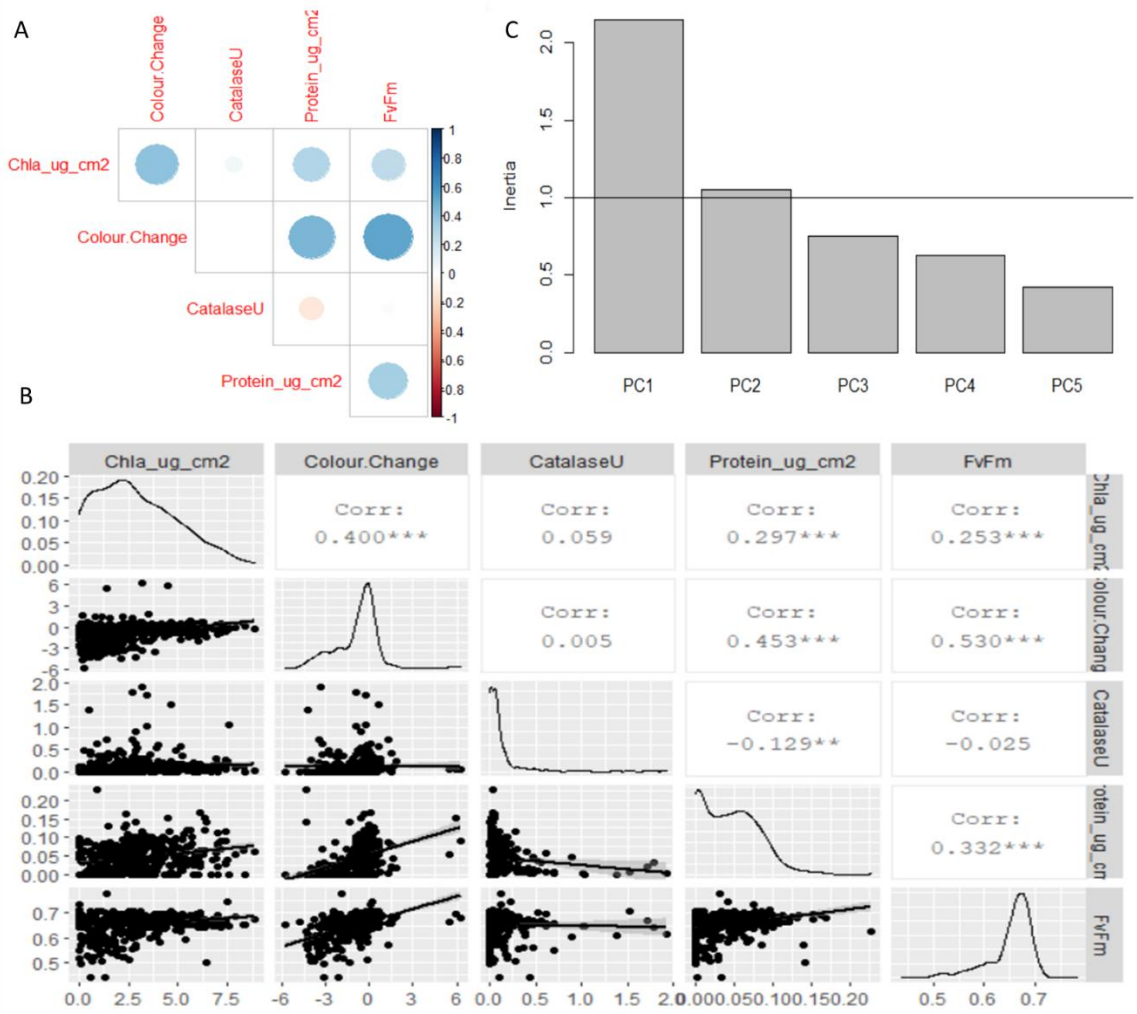

Supplementary Figure A.6 Support graphs for Principal Component Analysis of alternative physiological measurements. (A and B); some of the physiological measurements were correlated to each other. C; Screeplot showing the Eigen values of the five principle components generated. Principle components were plotted only for those where inertia > 1 (PC1 and PC2, specifically).

Supplementary Table A.7 The cost of equipment use per 100 samples was based on an approximation of how many samples were likely to be processed over a conservative lifespan of the respective item. For example, I assumed that a refrigerated centrifuge would have a lifespan of at least 10,000 samples whereas an icebox would only last for 1,000 samples However, within this calculation I did not consider differences in centrifuge times across different physiological measurements, where the centrifuge is used once for chlorophyll extractions as opposed to three times successively for tissue blasting.

Equipment	Assays required for	Cost	Lifespan (# samples)
Diving-PAM	Photosynthesis efficiency	$49,074	100,000
Camera + memory card	Tissue colour change	$1,800	100,000
Memory card (SD)	Tissue colour change	$55	100,000
Coral Health Colour Chart	Tissue colour change	$5	1,000
Airgun	Tissue blasting	$63.72	10,000
Centrifuge, refrigerated	Tissue blasting, chlorophyll, protein	$11,720	10,000
Styrofoam coolers	Tissue blasting, chlorophyll, protein, catalase	$10	1,000
Homogeniser	Tissue blasting	$927	10,000
Pipette, single channel	Tissue blasting, chlorophyll, protein, catalase, symbiont density	$432	10,000
Vortex	Tissue blasting, chlorophyll, catalase, symbiont density	$369	10,000
Oven	Protein	$2,220	100,000
Pipette, multi-channel	Protein, catalase	$1,420	10,000
Sonicator	Chlorophyll, protein	$1,500	10,000
Spectrophotometer	Chlorophyll, protein, catalase	$25,000	100,000
Stopwatch	Chlorophyll, protein, catalase, surface area	$12	1,000
Scale	Surface area, chemical preparations	$995	10,000
Forceps	Tissue blasting, surface area	$1.58	1,000
Waterbath	Surface area	$1,115	10,000
Ultralow freezer	Sample storage	$50,000	100,000

Supplementary Table A.8 Overview of other costs, special consideration, and benefits for each assay examined here.

Assay	Other costs/special considerations	Benefit
Photosynthetic efficiency	Expensive initial outlay for instrument	In-field data gathering
		Range of photo-physiological data available
Tissue colour change		In-field data gathering
		Rapid processing - especially with more automation coming online
		Accessible technology
Tissue blasting	Samples require special storage to be viable	Leg-work for a wide range of physiological measurements
	Requires multiple pieces of laboratory equipment	
Chlorophyll	Ethanol (hazardous chemical) or other solvent	Specific measurement of symbiont bleaching response
	Specialist training - spectrophotometer	
Protein	Specialist training - spectrophotometer	Specific measurement of either symbiont and/or host physiological response to heat stress
	Requires extraction kits	
Catalase	Long downstream data processing	Specific measurement of either symbiont and/or host physiological response to heat stress
	Expensive microwell plates required	
	Specialist training - spectrophotometer	
Surface area	Required for most assays listed	Cheaper than 3D photogrammetry methods
	Prone to operator error	
	Less accurate than 3D photogrammetry methods	

Supplementary material A.9 Pricing for Cost Benefit Analysis. This material consists of direct links to pages where the consumables and equipment required for the assays presented here can be purchased. These prices formed the basis of Appendix A.10 below.

Ethanol – absolute, 2.5L

Ethanol | Sigma-Aldrich (sigmaaldrich.com)

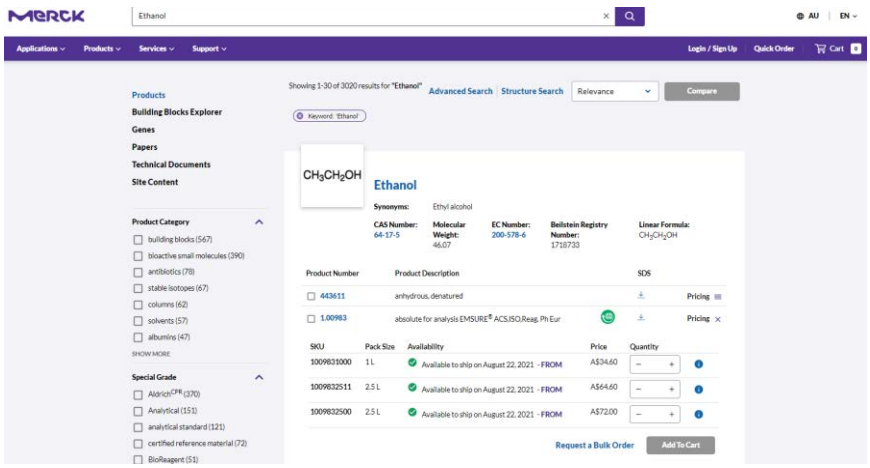

Pipette tips – red, green, and blue used

SpaceSaver Pipette Tip Refills | Made from recycled PETE (mt.com)

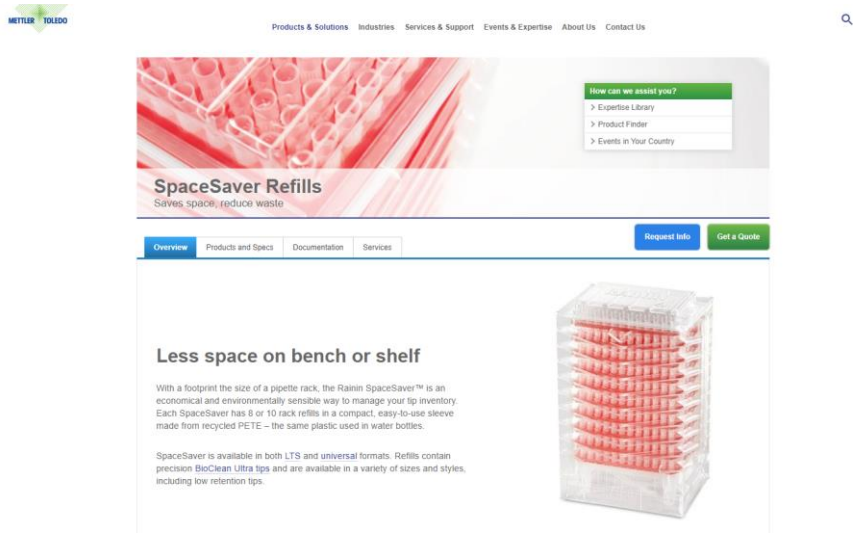

BioClean Ultra Pipette Tips

BioClean™ has long been the standard for assuring customers that Rainin tips are high quality and free of biological contaminants.

Benefits of RAININ BioClean Ultra tips:

No additives are added to the tips during the manufacturing process
Tips are free from any biological contaminants
Tested to very low detection levels using sensitive techniques
RAININ pipette and RAININ tips are very compatible in terms of fit
Fine point tip designed ensures complete sample delivery
The tip plastic doesn't have any defects ; quality checks during manufacturing process

Green-Pak SpaceSaver with LTS Tips:

Item(s)	Catalogue no	Quantity	Price
GPS-LTS-A-10µL-960/10	30389291	1	$57
GPS-LTS-A-250µL-960/10	30389299	1	$57
GPS-LTS-A-1000µL-768/8	30389292	1	$57

prices listed are subjected to price changes

Spec plates – Chlorophyll and protein assays only

Immulon® Immunoassay Plates and Strip Assemblies | Krackeler Scientific, Inc.

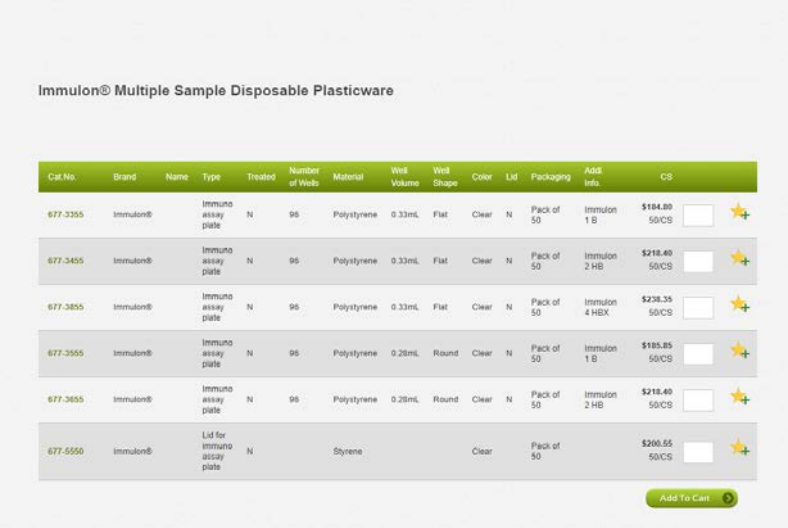

Immulon® Multiple Sample Disposable Plasticware

Cat.No.	Brand	Name	Type	Treated	Number of Wells	Material	Well Volume	Well Shape	Color	Lid	Packaging	Addl. Info.	CS
677-3355	Immulon®		Immuno assay plate	N	96	Polystyrene	0.33mL	Flat	Clear	N	Pack of 50	Immulon 1 B	$184.80 50/CS
677-3455	Immulon®		Immuno assay plate	N	96	Polystyrene	0.33mL	Flat	Clear	N	Pack of 50	Immulon 2 HB	$218.40 50/CS
677-3855	Immulon®		Immuno assay plate	N	96	Polystyrene	0.33mL	Flat	Clear	N	Pack of 50	Immulon 4 HBX	$238.35 50/CS
677-3555	Immulon®		Immuno assay plate	N	96	Polystyrene	0.28mL	Round	Clear	N	Pack of 50	Immulon 1 B	$185.85 50/CS
677-3655	Immulon®		Immuno assay plate	N	96	Polystyrene	0.28mL	Round	Clear	N	Pack of 50	Immulon 2 HB	$218.40 50/CS
677-5550	Immulon®		Lid for immuno assay plate	N		Styrene			Clear		Pack of 50		$200.55 50/CS

Add To Cart

Deep well plates

SSI Deep Well Plate - 2.0 mL, 96-well, Square, V Bottom (5/pack) | LabGear Australia - Laboratory Equipment and Consumables for the Australian Scientific and Research Community

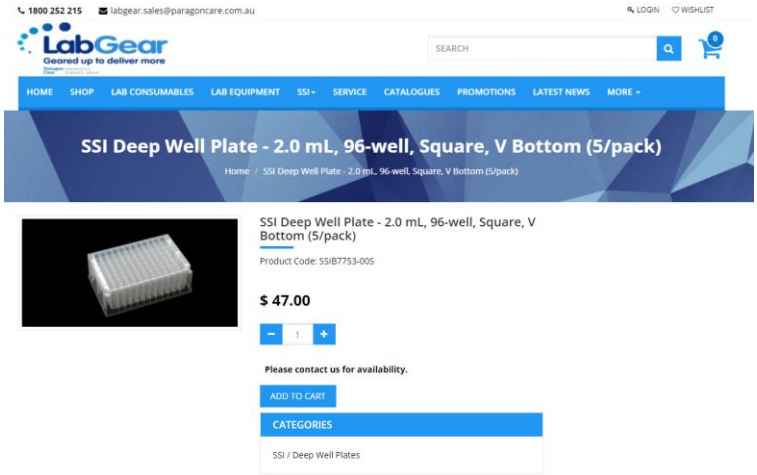

Air blow gun

[MettleAir AG2-100 4" Compressed Air Blow Gun, 1/4" NPT, Inlet Commercial Grade, AG2-100 (Pack of 10): Amazon.com: Tools & Home Improvement]

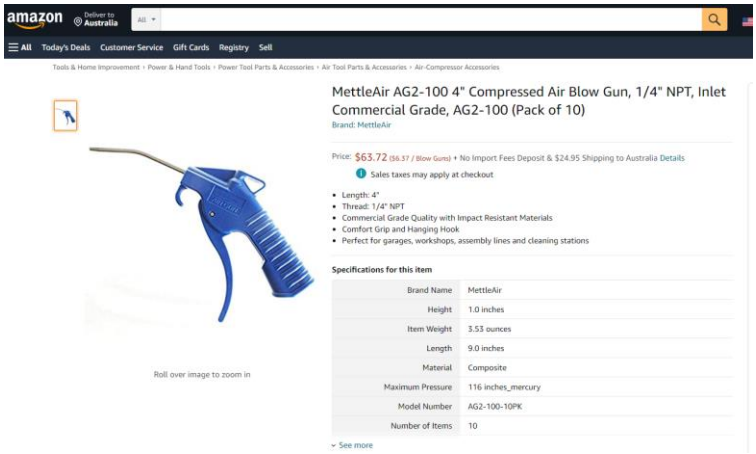

Aluminium foil

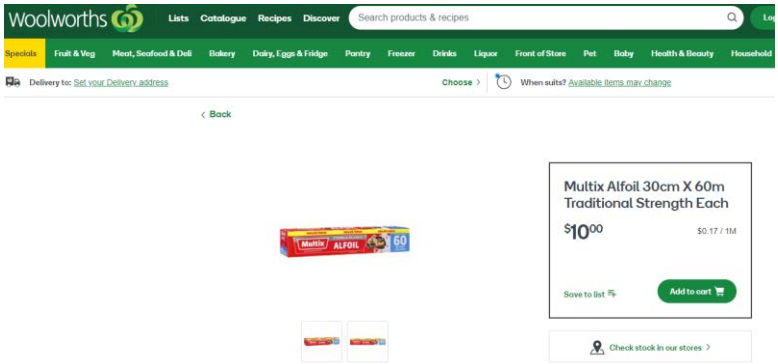

Refrigerated centrifuge with falcon-tube capacity

[Centrifuge 5804/ 5804 R - Multipurpose Centrifuges, Centrifugation - Eppendorf South Pacific]

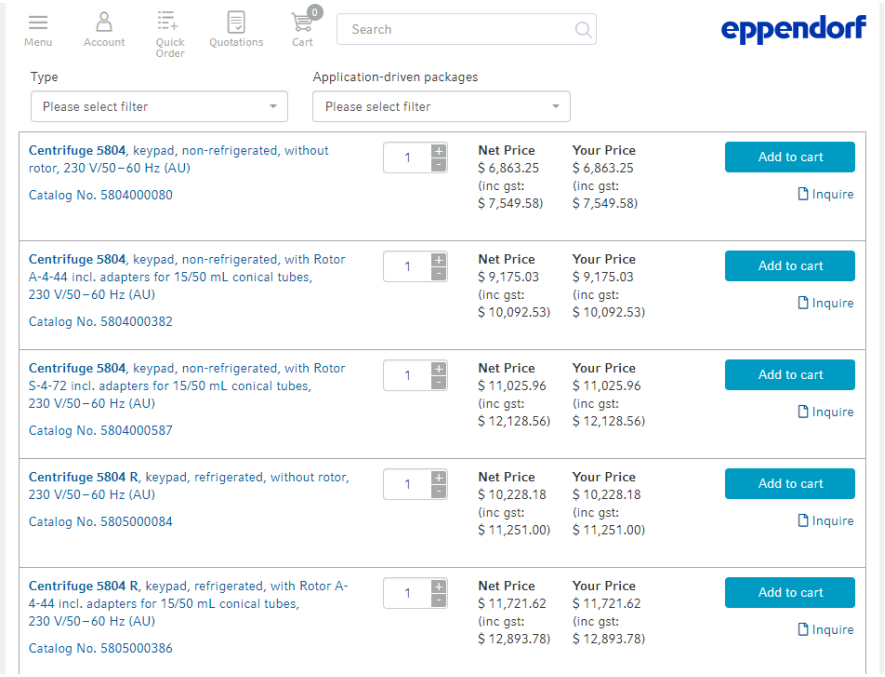

EDTA

[EDTA | Sigma-Aldrich (sigmaaldrich.com)]

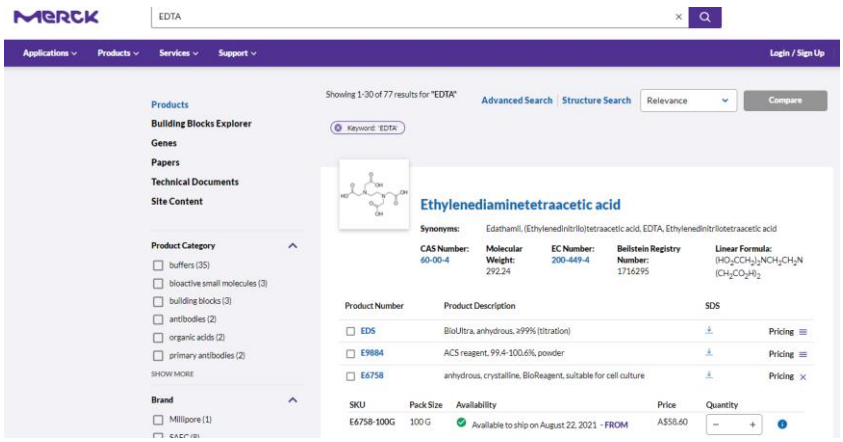

Styrofoam coolers

[Polystyrene Six Pack Esky - Rope Handle for Carrying - Foam Sales](#)

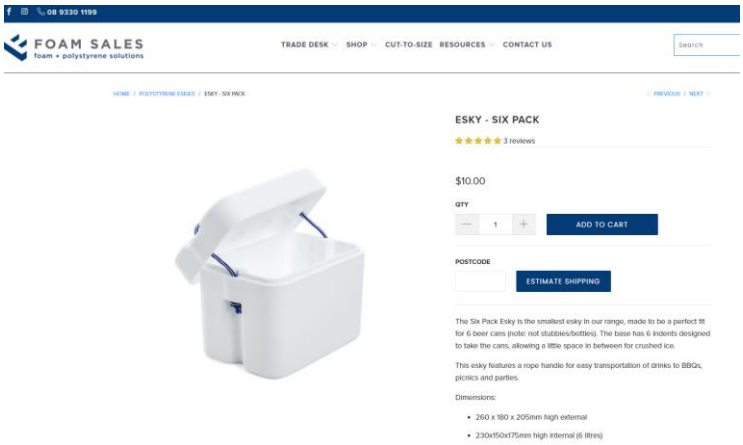

15ml Centrifuge tubes

[Conical Centrifuge Tubes, Screw Cap, Graduated, Sterile, 15ml - Buy Online at LabDirect](#)

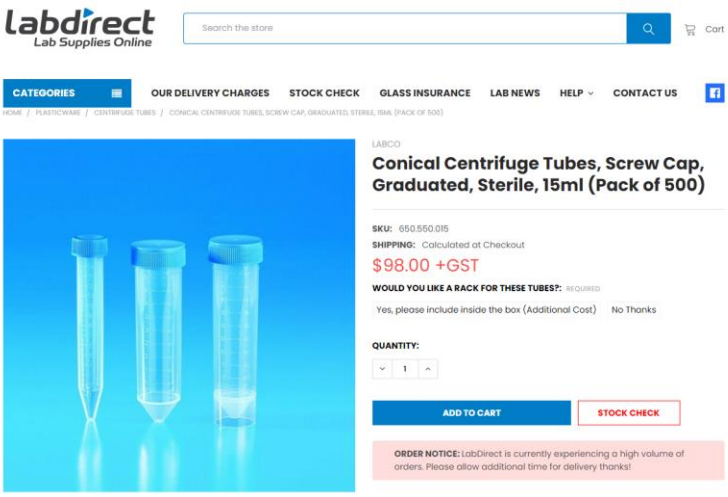

Formaldehyde solution

[Formaldehyde solution for molecular biology, 36.5-38% in H2O | 50-00-0 (sigmaaldrich.com)](#)

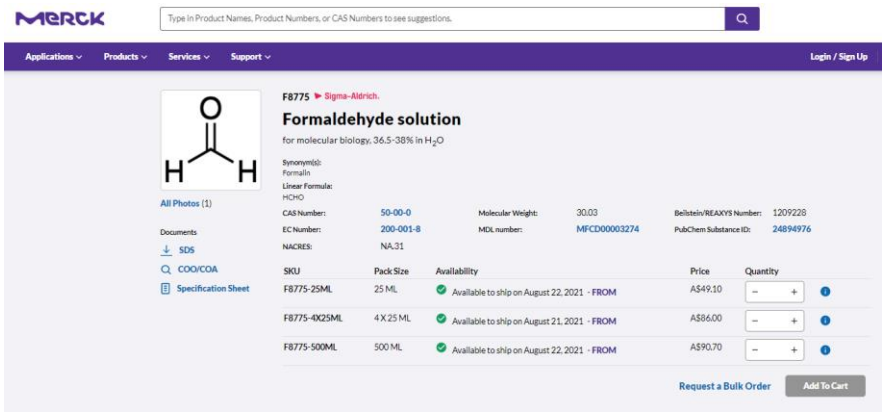

H2O2 solution

[Hydrogen peroxide solution 30 % (w/w) in H2O, contains stabilizer | 7722-84-1 (sigmaaldrich.com)]

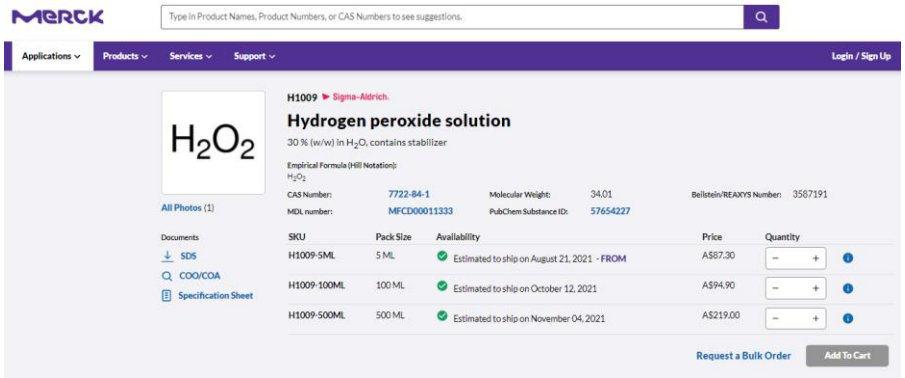

Homogeniser

[PRO Scientific Bio-Gen PRO200 Homogenizer]

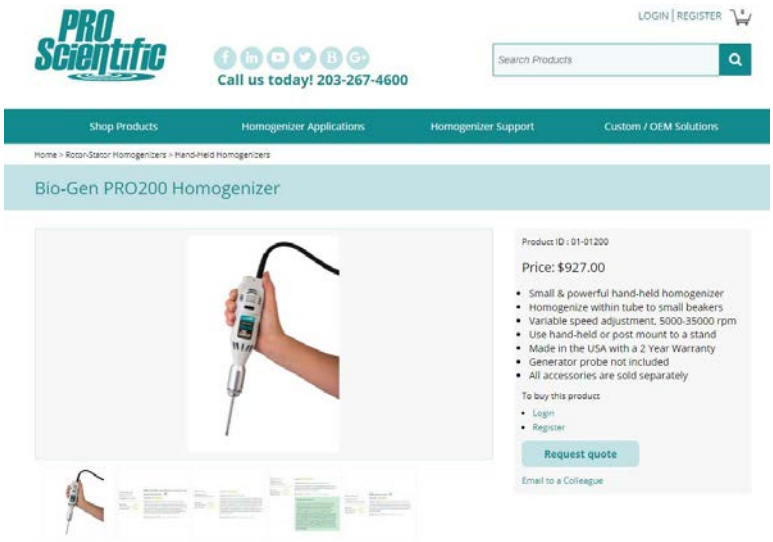

KimWipes

[Kimtech® Science™ 34120A KimWipes™ Delicate Task Wipers -
 White - 280 Sheets/Box - Case of 30 Boxes | KIMTECH SCIENCE* Wipers | Cleaning Cloths, Wipers & Sponges | Hygiene & Cleaning | Blackwoods]

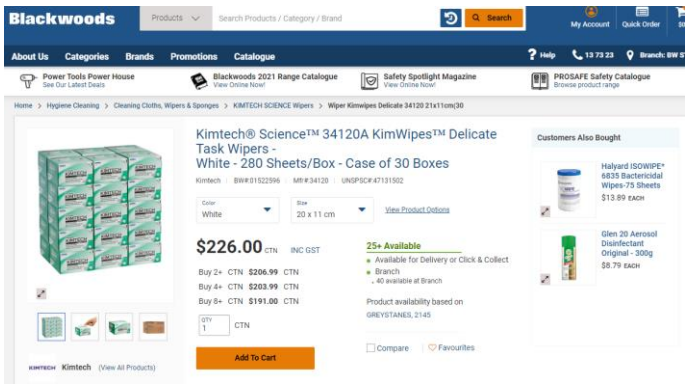

Zip-lock bags – 4x6”

[Econo-Zip Reclosable Bags (thomassci.com)]

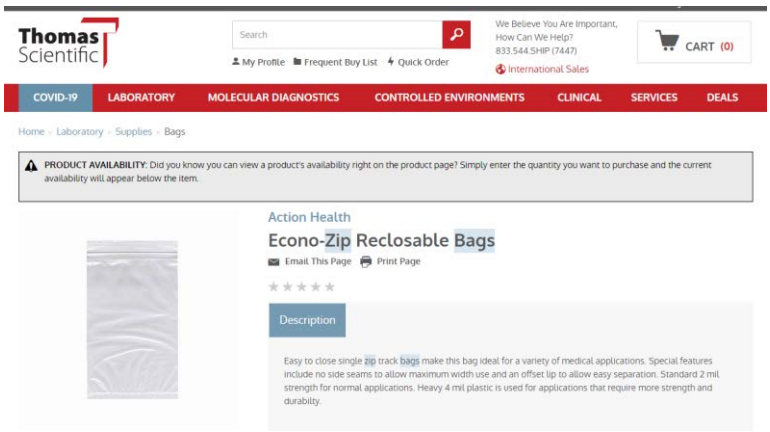

Microcentrifuge tubes, 1.5ml

[1.5ml MICROCENTRIFUGE TUBE | Interpath]

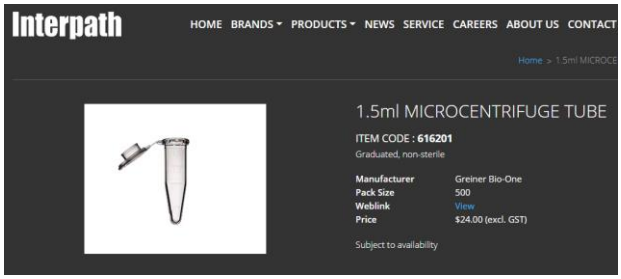

Multichannel pipettes

20uL

Ln#	Item No	Description	Unit Price
3	17013803	L8-20XLS+PIPET-LITE XLS+ LTS 8-CH PIPET 2-20	$1,420.00

200uL

Ln#	Item No	Description	Unit Price
4	17013805	L8-200XLS+PIPET-LITE XLS+ LTS 8-CH PIPET 20-200	$1,420.00

Sodium Hydroxide pellets

[Sodium hydroxide - 'Caustic soda', Sodium hydroxide solution (sigmaaldrich.com)]

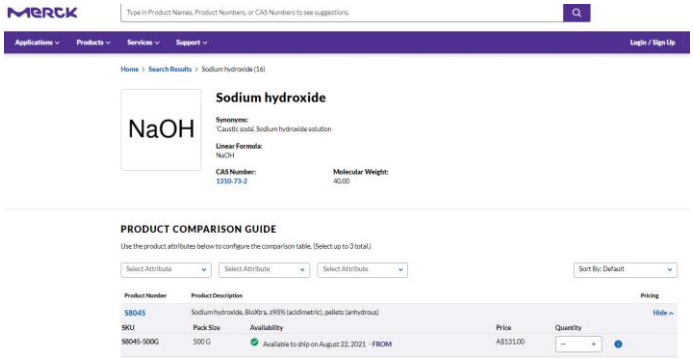

Oven

PBS tablets

[Phosphate buffered saline - PBS, Phosphate buffered saline (sigmaaldrich.com)]

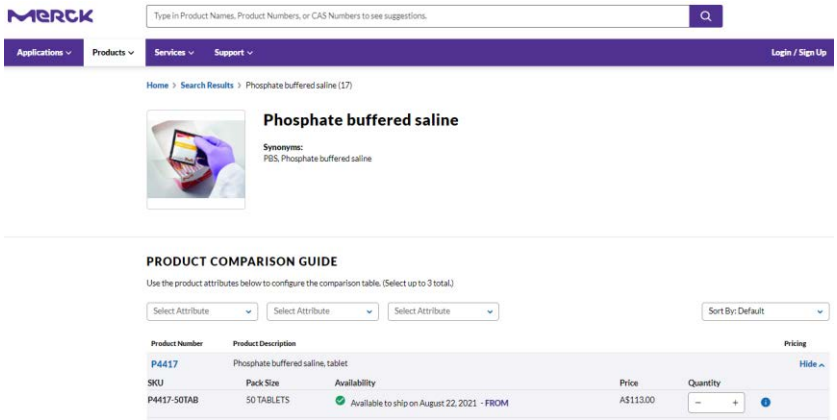

Single-channel pipettes

Ln#	Item No	Description	Unit Price
1	17014406	L-STARTXLS+ STARTER KIT L-20XLS+.L-200XLS+.L-1000XLS+	$1,295.00

Protein kit – BD BioRad

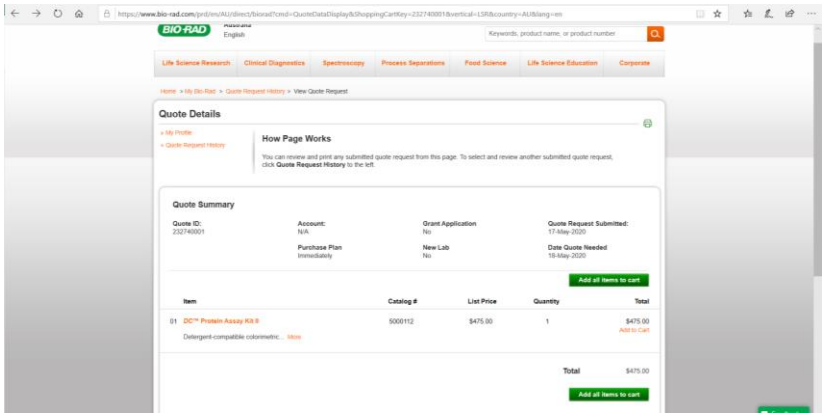

Small zip-lock bags

[Small Resealable Bags 90 x 60mm | Seal Bags Small | QIS Packaging]

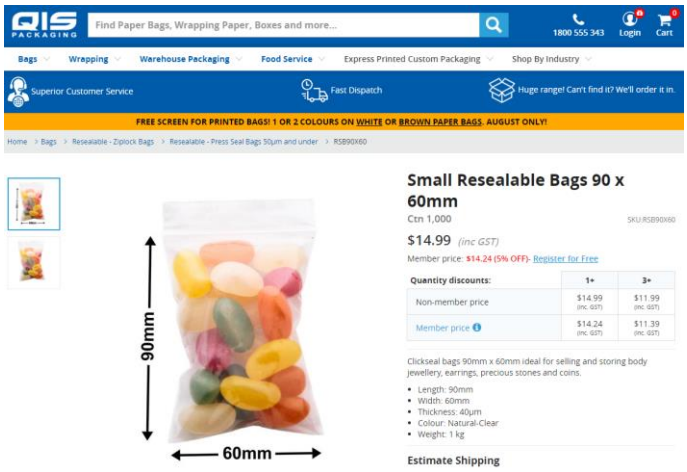

Digital timer

[Wiltshire Digital Timer | BIG W]

Vortex mixer

[Personal Vortex Mixer - VM1 (instrumentchoice.com.au)]

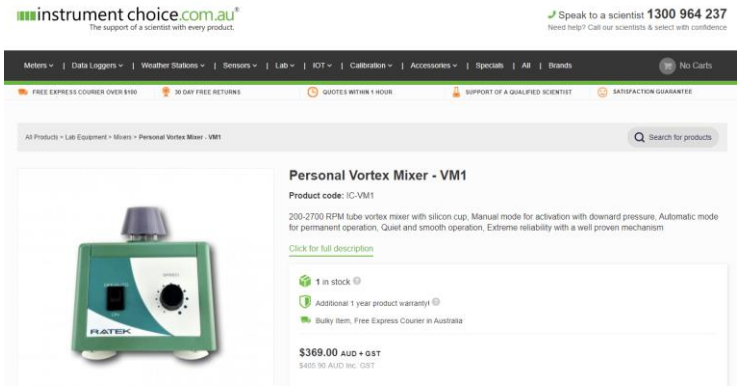

Multi-channel reservoirs

[Reagent Reservoirs (thomassci.com)]

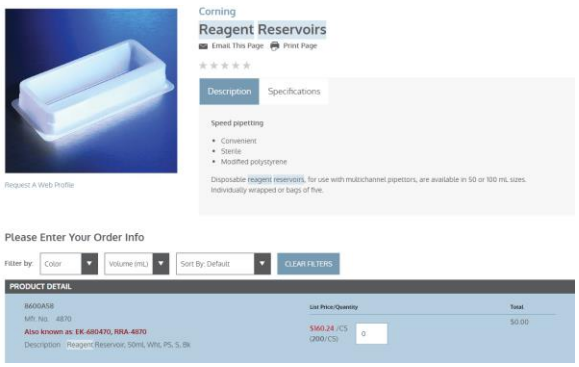

BD CS&T beads

[CS&T Research Beads (bdbiosciences.com)]

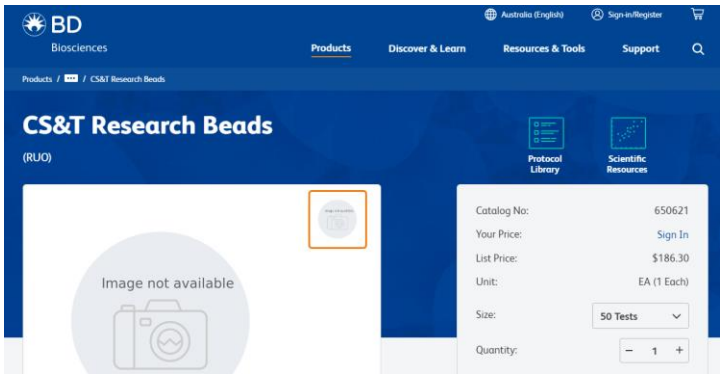

Colour chart

[Coral Health Chart – CoralWatch]

SD card

[SanDisk Extreme SDXC Memory Card 128GB Black | Officeworks]

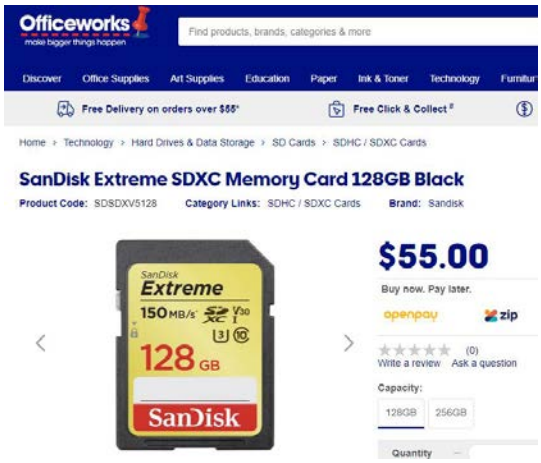

Camera

[Discontinued - DSLR D300 - Nikon Australia Pty Ltd]

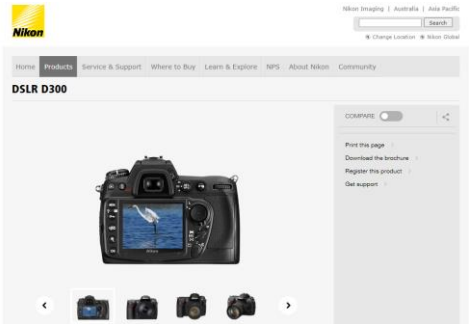

Scales

[A&D FX-i Best Ammunition Reloading Scales - Shop Online (scaleshop.com.au)]

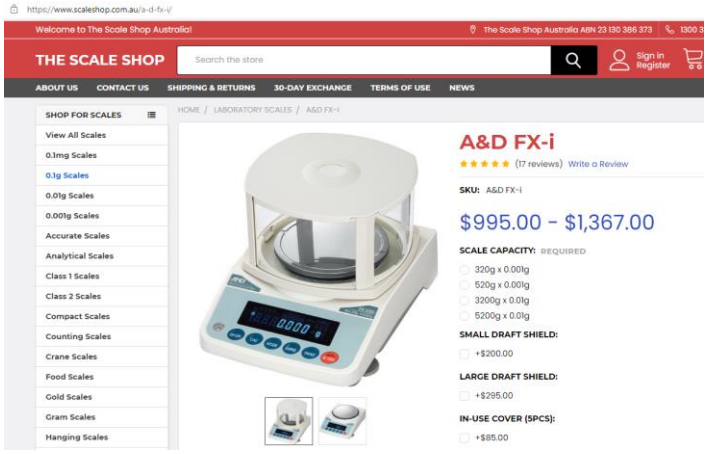

Forceps

[Aaxis SM Forceps Stainless Steel Splinter 12.5cm — Medshop Australia]

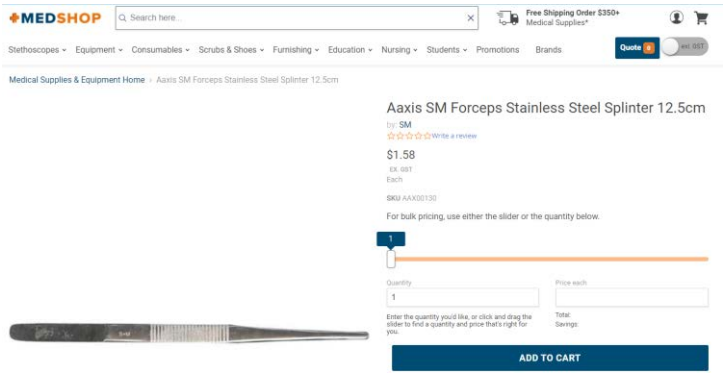

Paraffin wax

[We R Memory Keepers 1.3 Kg Wick Paraffin Wax (spotlightstores.com)]

Waterbath

[Digital Thermostatic Water Bath 4L (westlab.com.au)]

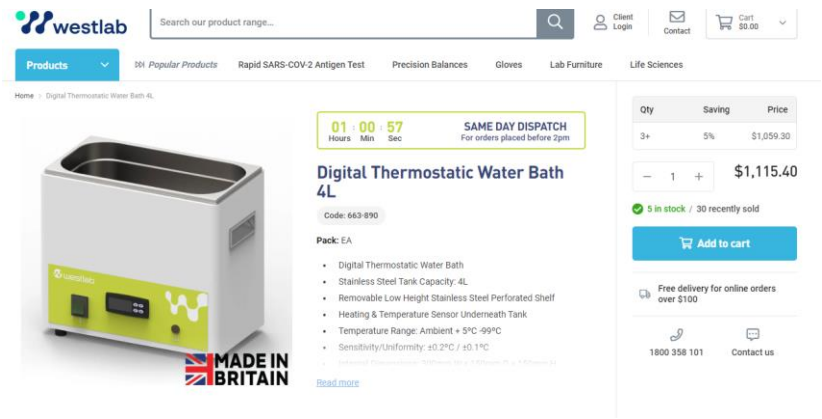

Supplementary Table A.10 Overview of consumables, quantities required, costs, lifespan of equipment and cost per sample for each assay.

Assay	Consumables	Quantity supplied	Cost supplied	Quantity required per sample	# samples possible with supplied quantity	Cost per sample	Equipment	Quantity needed/supplied	Cost	Assumed lifespan # samples	Cost per sample over lifespan
Tissue blasting	Ethanol (100%)	2.5L	$64.60	1 mL	2500	$0.03	Air gun	1	$62.72	10,000	$0.01
Tissue blasting	Formalin	25 mL (36%)	$49.10	0.25 mL (10%)	360.231	$0.14	Centrifuge, refrigerated	1	$11,720	10,000	$1.17
Tissue blasting	Seawater (filtered)						Esky	2	$20	1,000	$0.02
Tissue blasting	96-well tissue culture plate	5	$47.00	0.015	480	$0.10	Homogeniser	1	$927	10,000	$0.09
Tissue blasting	Aluminium foil	60 m	$10.00	0.00625 m2	2880	$0.00	Pipettes	2; different sizes	$864	10,000	$0.09
Tissue blasting	Conical centrifuge tubes	500	$98.00	1	500	$0.20	Ultralow freezer	1	$50,000	100,000	$0.50
Tissue blasting	Sample storage boxes	5	$34.92	0.013	405	$0.08	Vortex	1	$369	10,000	$0.04
Tissue blasting	Ice										
Tissue blasting	KimWipes	30 boxes (280 sheets each)	$226.00	3 sheets	2790	$0.08					
Tissue blasting	Zip-lock bags (A5)	100	$11.29	1	100	$0.11					
Tissue blasting	Microcentrifuge tubee (1.5 mL)	500	$24.00	4	125	$0.19					
Tissue blasting	Pipette tipes	768	$57.00	7	109.714	$0.52					
Tissue blasting	Zip-lock bags, small	1000	$15.00	1	1000	$0.02					
Tissue blasting	Liquid nitrogen	20L	$68.20	50mL	400	$0.17					
Chlorophyll	Ethanol	2.5L	$64.60	0.8	3125	$0.02	Centrifuge	1	$11,720	10,000	$1.17
Chlorophyll	Spec plate	50	$184.80	0.033	1550	$0.12	Pipette, 200ul	1	$432.00	10,000	$0.04
Chlorophyll	Pipette tips blue	768	$57.00	1	768	$0.07	Sonicator	1	$1,500.00	10,000	$0.15
Chlorophyll	Pipette tips green	960	$57.00	1	960	$0.06	Spectrophotometer	1	$25,000.00	100,000	$0.25
Chlorophyll	KimWipes	30 boxes (280 sheets each)	$226.00	0.03 (sheets)	280000	$0.00	Vortex	1	$369.00	10,000	$0.04
Protein	NaOH	500g	$131.00	0.3ml (1M)	4167	$0.03	Centrifuge	1	$11,720.00	10000	$1.17
Protein	Bio-Rad protein kit	1	$484.00		5000	$0.10	Multichannel Pipette, 200ul	1	$1,420.00	10000	$0.14
Protein	Spec plate	50	$184.80	0.033	1550	$0.12	Pipette, 20ul	1	$432.00	10000	$0.04
Protein	Pipette tips green/red	960	$57.00	4	240	$0.24	Sonicator	1	$1,500.00	10000	$0.15
Protein	Alufoil	60m	$10.00	0.0083	7228.915663	$0.00	Spectrophotometer	1	$25,000.00	100,000	$0.25
Protein							Stopwatch	1	$12.00	1000	$0.01
Protein							Multichannel reservoirs	200	$160.24	100000	$0.00
Protein							Oven	1	$2,230.00	100,000	$0.02
Catalase	EDTA	100g	$58.60	0.02ml (0.1mM)	17,000,000	$0.00	Multichannel Pipette, 200ul	1	$1,420.00	10000	$0.14
Catalase	H2O2	100ml (30%)	$94.90	0.12ml (50mM)	166,666	$0.00	Pipette, 200ul	1	$432.00	10000	$0.04
Catalase	PBS	50 tablets	$113.00	0.06ml (50mM)	33333.33333	$0.00	Spectrophotometer	1	$25,000.00	100,000	$0.25
Catalase	Spec plate	40	$751.00	0.033	1240	$0.61	Stopwatch	1	$12.00	1000	$0.01
Catalase	Pipette tips	960	$57.00	4	240	$0.24	Multichannel reservoirs	200	$160.24	100000	$0.00
Catalase	KimWipes	30 boxes (280 sheets each)	$226.00	0.03 (sheets)	280000	$0.00					
Surface area	Wax	1.3 kg	$27.00	2 grams	650	$0.04	Scale	1	$995.00	10000	$0.10
Surface area							Stopwatch	1	$12.00	1000	$0.01
Surface area							Forceps	1	$1.58	1000	$0.00
Surface area							Waterbath	1	$1,115.40	10000	$0.11
Tissue Colour							Camera	1	$1,800.00	100,000	$0.02
							SD card	1	$50.00	100,000	$0.00
							scale bar	1	$5.00	1,000	$0.01
FvFm							Diving-PAM	1	$49,074	100,000	0.49074

Supplementary Table A.10 continued: time requirements, samples per week, capital and consumable costs, along with total costs of each assay.

Assay	Time	Samples possible per 7h day	Minutes per sample	Labour cost per sample	Capital cost per sample	Consumable cost per sample	Time requirement per sample (min)	Labour cost per sample	Total cost per sample (capital + consumable + labour)
Tissue blasting	Blasting	36	11.667	$6.78	$1.91	$1.63	12.37	$7.19	$10.74
	Data entry	600	0.7	$0.41					
Tissue blasting									
Tissue blasting									
Tissue blasting									
Tissue blasting									
Tissue blasting									
Tissue blasting									
Tissue blasting									
Tissue blasting									
Tissue blasting									
Tissue blasting									
Tissue blasting									
Tissue blasting									
Tissue blasting									
Chlorophyll	Assay	150	2.8	$1.62	$1.65	$0.27	3.05	$1.77	$3.70
Chlorophyll	data entry	1680	0.25	$0.15					
Chlorophyll									
Chlorophyll									
Chlorophyll									
Protein	assay	96	4.375	$2.54	$1.79	$0.49	4.625	$2.68	$9.10
Protein	data entry	1680	0.25	$0.15					
Protein									
Protein									
Protein									
Protein									
Protein									
Protein									
Catalase	Assay	150	2.8	$1.62	$0.45	$0.85	3	$2.79	$4.08
Catalase	data entry	210	2	$1.16					
Catalase									
Catalase									
Catalase									
Catalase									
Surface area	Assay	75	5.6	$3.25	$0.22	$0.04	5.85	$3.39	$3.66
Surface area	Data entry	1680	0.25	$0.15					
Surface area									
Surface area									
Tissue Colour	Taking photos	2,800	0.15	$0.09	$0.02	$0.00	1.02	$0.59	$0.62
	Data entry	482	0.87	$0.50					
FvFm	Zapping	1400	1.5	$0.87	0.49074	0	1.65	$0.96	$1.45
	Transcription	2800	0.15	$0.09					

Appendix B – Supplementary material for Chapter 3

Supplementary Table B.1 Collection and experimental treatment details.

Reef	Latitude	Longitude	Collection month/Year	Collection dates	MMM ºC	Treatments	Species	n colonies
Lady Musgrave	-23.9074	152.3865	Jan-20	03/01/2020	27.07	MMM, +3ºC, +6ºC, +9ºC	*A. tenuis*	14
							P. meandrina	10
							P. other	5
							P. verrucosa	1
Fairfax	-23.8697	152.3611	Jan-20	04/01/2020	27.08	MMM, +3ºC, +6ºC, +9ºC	*A. tenuis*	18
							P. meandrina	8
							P. other	7
							P. verrucosa	0
Hoskyns	-23.808	152.2836	Jan-20	05/01/2020	27.06	MMM, +3ºC, +6ºC, +9ºC	*A. tenuis*	15
							P. meandrina	9
							P. other	4
							P. verrucosa	2
Boult	-23.7482	152.2715	Jan-20	06/01/2020	27.1	MMM, +3ºC, +6ºC, +9ºC	*A. tenuis*	15
							P. meandrina	7
							P. other	12
							P. verrucosa	0
Masthead	-23.5322	151.7228	Jan-20	10/01/2020	27.17	MMM, +3ºC, +6ºC, +9ºC	*A. tenuis*	15
Erskine	-23.5085	151.7685	Jan-20	10/01/2020	27.42	MMM, +3ºC, +6ºC, +9ºC	*A. tenuis*	15
Chinaman	-22.0137	152.6543	Jan-20	18/01/2020	27.42	MMM, +3ºC, +6ºC, +9ºC	*P. meandrina*	25
							P. other	12
							P. verrucosa	3
22-084	-22.0028	152.457	Jan-20	14/01/2020	27.52	MMM, +3ºC, +6ºC, +9ºC	*A. tenuis*	15
							P. meandrina	3
							P. other	3
							P. verrucosa	1

21-550	-21.9618	152.3124	Jan-20	14/01/2020	27.56	MMM, +3ºC, +6ºC, +9ºC	*A. tenuis*	15
							P. meandrina	2
							P. other	0
							P. verrucosa	0
Davies	-18.4962	147.3761	Apr-21	21/04/2021	28.45	MMM, +3ºC, +6ºC, +9ºC	*A. tenuis*	15
							P. meandrina	3
							P. other	3
							P. verrucosa	9
Chicken	-18.402	147.424	Apr-21	20/04/2021	28.37	MMM, +3ºC, +6ºC, +9ºC	*A. tenuis*	15
							P. meandrina	3
							P. other	5
							P. verrucosa	7
Kelso	-18.2541	146.5907	Apr-21	11/04/2021	28.63	MMM, +3ºC, +6ºC, +9ºC	*A. tenuis*	15
							P. meandrina	1
							P. other	0
							P. verrucosa	14
Mackay	-16.2306	145.3908	Apr-21	16/04/2021	28.63	MMM, +3ºC, +6ºC, +9ºC	*A. tenuis*	15
							P. meandrina	2
							P. other	5
							P. verrucosa	8
Sandbank_1	-14.198	144.9055	Jan-19	06/01/2019	28.55	MMM, +3ºC, +6ºC	*A. tenuis*	17
							P. meandrina	0
							P. other	0
							P. verrucosa	12
Davie	-13.9677	144.4455	Jan-19	09/01/2019	28.58	MMM, +3ºC, +6ºC	*A. tenuis*	19
							P. meandrina	3
							P. other	4
							P. verrucosa	9
Corbett	-13.9227	144.2405		11/01/2019	28.58		*A. tenuis*	18

			Jan 2019 and Dec-19	07/12/2019		MMM, +3ºC, +6ºC, +9ºC (*Pocillopora* only)	*P. meandrina*	13
							P. other	10
							P. verrucosa	15
13-124	-13.8517	144.0906	Jan-19	13/01/2019	28.66	MMM, +3ºC, +6ºC	*A. tenuis*	15
							P. meandrina	3
							P. other	1
							P. verrucosa	12
Lagoon	-12.3922	143.7394	Jan-19	18/01/2019	28.54	MMM, +3ºC, +6ºC	*A. tenuis*	15
							P. meandrina	1
							P. other	0
							P. verrucosa	15
Mantis	-12.3384	143.8608	Jan-19 (*A. tenuis* only) and Dec-19	20/01/2019	28.44	MMM, +3ºC, +6ºC, +9ºC (*Pocilloporas* only)	*A. tenuis*	15
				01/12/2019			*P. meandrina*	4
							P. other	2
							P. verrucosa	33

Supplementary Table B.2 Primers used

ORF primers from Johnston et al., 2018

Forward	5'-TTTGGGSATTCGTTTAGCAG-3'
Reverse	5'-SCCAATATGTTAAACASCATGTCA-3'

ITS2 primers from Pochon et al., 2001.

Forward	5'-TCGTCGGCAGCGTCAGATGTGTATAAGAGACAGGTGAATTGCAGAACTCCGTG-3'
Reverse	5'-GTCTCGTGGGCTCGGAGATGTGTATAAGAGACAGCCTCCGCTTACTTATATGCTT-3'

Supplementary Table B.3 – Overview of environmental and thermal history variables used. All thermal history data obtained from NOAA Coral Reef Watch Operational Daily Near-Real-Time Global 5-km Satellite Coral Bleaching Monitoring Products, accessed through ERDDAP - NOAA Coral Reef Watch Operational Daily Near-Real-Time Global 5-km Satellite Coral Bleaching Monitoring Products - Data Access Form (hawaii.edu) for each reef coordinate.

Variable	Comment
Recent.min_SST	Minimum SST in the last 5 years prior to collection
Recent.mean_SST	Average SST in the last 5 years prior to collection
Recent.mean_DHW	Average heat stress (DHW) during heatwaves in the last 5 years prior to collection
Recent.max_SST	Maximum SST recorded in the last 5 years prior to collection
Recent.max_DHW	Maximum heat stress (DHW) recorded in the last 5 years prior to collection
Range_SST	Annual difference between the highest and lowest SST recorded
MMM	NOAA climatology
Min_SST	The minimum SST recorded
Mean_SST	The average SST recorded
Mean_DHW	The average heat stress (DHW) recorded during heatwaves
Max_SST	The maximum SST recorded.
Max_DHW	The highest heat stress loading (DHW) recorded
Long	Reef longitude, recorded on site by GPS
Lat	Reef latitude, recorded on site by GPS
DHW8	Number of heatwave events where heat stress exceeded 8 DHW. DHW > 8 commonly recognised as indicator of severe bleaching and mortality.
DHW6	Number of heatwave events where heat stress exceeded 6 DHW
DHW4	Number of heatwave events where heat stress exceeded 4 DHW. DHW 3 and 4 commonly recognised as alert level for bleaching.
DHW3	Number of heatwave events where heat stress exceeded 3 DHW. DHW 3 and 4 commonly recognised as alert level for bleaching.
DHW2	Number of heatwave events where heat stress exceeded 2 DHW

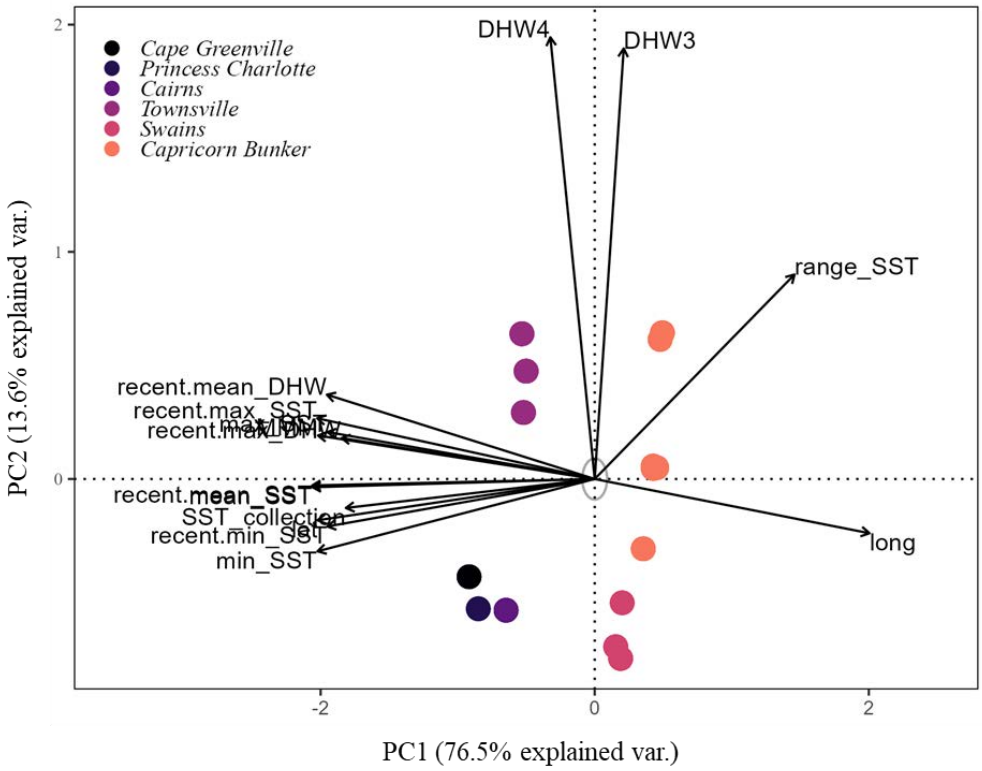

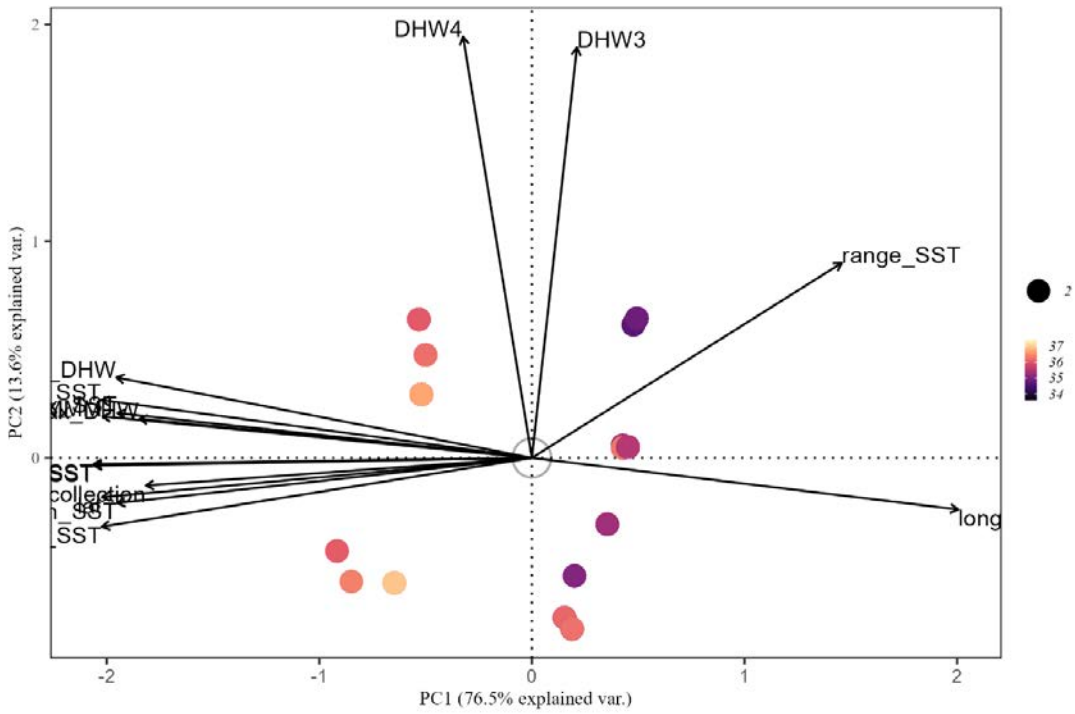

Supplementary Figure B.4 A) PCA of environmental variables and reef sectors. B) Environmental variables and their Principal Component association with absolute ED50s.

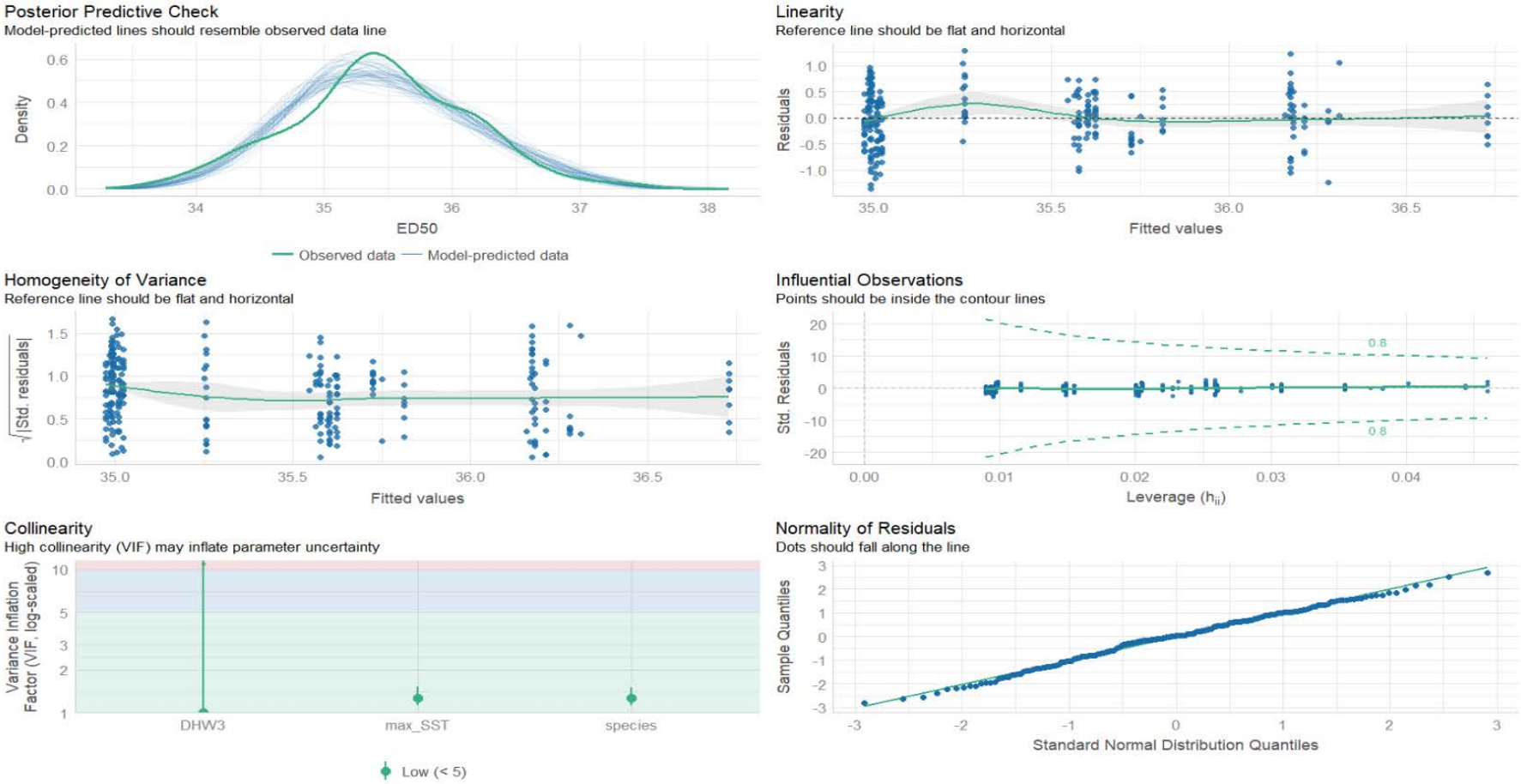

Supplementary Figure B.5 Model checking for the linear model that best predicted ED50 from thermal variables (ED50 ~ species + max_SST + DHW3).

Supplementary material B.6 Statistical outputs for assessment of F_v/F_m by species, treatment, and their interaction.

Statistical test of FvFm in treatments * species, Wald's test

	numDF <int>	denDF <dbl>	F-value <chr>	p-value <chr>
(Intercept)	1	3176	139320.67	<.0001
species	3	571	7.82	<.0001
treatment	3	3176	1349.43	<.0001
species:treatment	9	3176	9.23	<.0001

Supplementary table Table B.6 Mean F_v/F_m (± SE) values per species by treatment, averaged across all reefs.

Species	F_v/F_m MMM	F_v/F_m +3ºC	F_v/F_m +6ºC	F_v/F_m +9ºC
A. tenuis	0.669 ± 0.0007	0.660 ± 0.001	0.625 ± 0.0025	0.447 ± 0.013
P. meandrina	0.667 ± 0.0001	0.663 ± 0.0018	0.631 ± 0.0036	0.406 ± 0.024
P. verrucosa	0.671 ± 0.0012	0.671 ± 0.002	0.626 ± 0.0046	0.356 ± 0.028

Supplementary material B.7 Absolute ED50s by host species statistical outputs

```
Nonlinear mixed-effects model fit by maximum likelihood
  Model: mean.FvFm ~ meLL.3(TreatmentTemp, b, d, e)
  Data: data

Random effects:
 Formula: e ~ 1 | colonyID
        e.(Intercept)   Residual
StdDev:      0.722752 0.02889441

Fixed effects:  list(b ~ species - 1, d ~ species - 1, e ~ species - 1)
 Correlation:
                   b.spcsm b.spcst b.spcsv d.spcsm d.spcst d.spcsv e.spcsm e.spcst
b.speciestenuis     0.000
b.speciesverrucosa  0.000   0.000
d.speciesmeandrina -0.311   0.000   0.000
d.speciestenuis     0.000  -0.276   0.000   0.000
d.speciesverrucosa  0.000   0.000  -0.169   0.000   0.000
e.speciesmeandrina -0.203   0.000   0.000  -0.054   0.000   0.000
e.speciestenuis     0.000  -0.468   0.000   0.000  -0.003   0.000   0.000
e.speciesverrucosa  0.000   0.000  -0.175   0.000   0.000  -0.056   0.000   0.000

Standardized Within-Group Residuals:
        Min          Q1         Med          Q3         Max
-6.88483620 -0.33490805  0.06394375  0.41105626  7.02270829

Number of Observations: 981
Number of Groups: 278
```

	Value <chr>	Std.Error <chr>	DF <chr>	t-value <chr>	p-value <chr>
b.speciesmeandrina	82.38376	5.110428	695	16.1207	0
b.speciestenuis	69.98497	4.406040	695	15.8839	0
b.speciesverrucosa	71.66758	8.451204	695	8.4802	0
d.speciesmeandrina	0.66171	0.002540	695	260.4911	0
d.speciestenuis	0.66080	0.001440	695	459.0097	0
d.speciesverrucosa	0.66313	0.002691	695	246.4314	0
e.speciesmeandrina	35.21934	0.108648	695	324.1593	0
e.speciestenuis	35.31381	0.076576	695	461.1632	0
e.speciesverrucosa	36.20909	0.132002	695	274.3064	0

9 rows

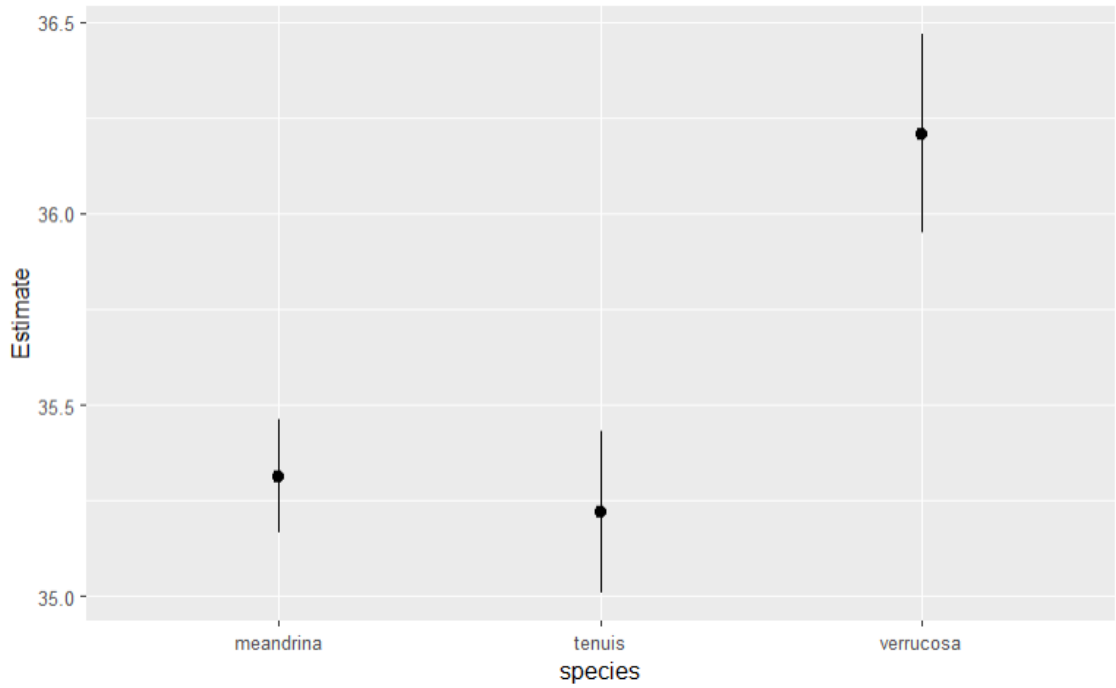

Supplementary Figure B.7 Absolute ED50 temperatures were significantly higher in *P. verrucosa* than in *P. meandrina* and *A. tenuis* yet, did not differ between the two latter species. Statistical groupings were assessed by emmeans() (Hartig & Lohse, 2021).

Post-hoc Tukey's for differences in ED50s between species

```
 contrast              estimate     SE  df t.ratio p.value
 meandrina - tenuis     -0.0108 0.0956 255  -0.113  0.9929
 meandrina - verrucosa  -0.5686 0.1532 255  -3.712  0.0007
 tenuis - verrucosa     -0.5577 0.1349 255  -4.135  0.0001

Results are averaged over the levels of: Sector
Degrees-of-freedom method: containment
P value adjustment: tukey method for comparing a family of 3 estimates
 species    emmean    SE df lower.CL upper.CL .group
 meandrina    35.5 0.120 11     35.1     35.8  a
 tenuis       35.5 0.102 11     35.2     35.8  a
 verrucosa    36.1 0.156 11     35.6     36.5   b
```

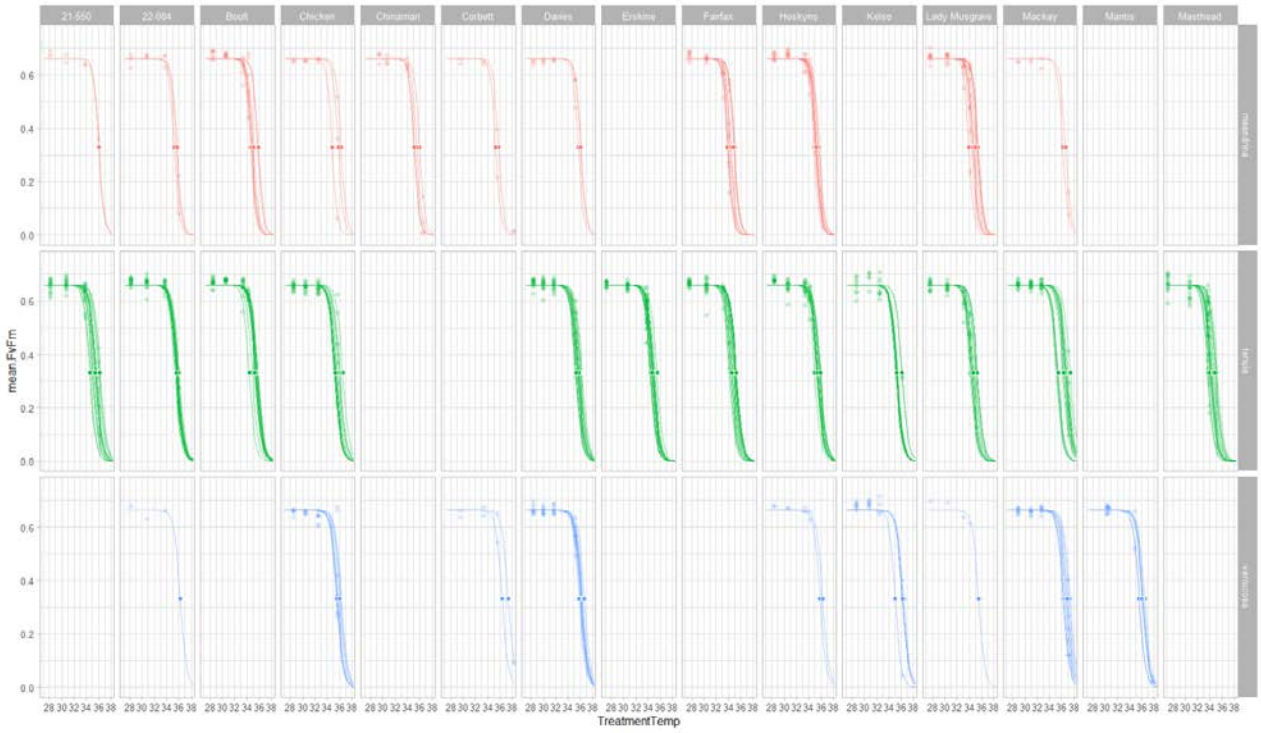

Supplementary figure B.7.1 ED50 curves per species per reef.

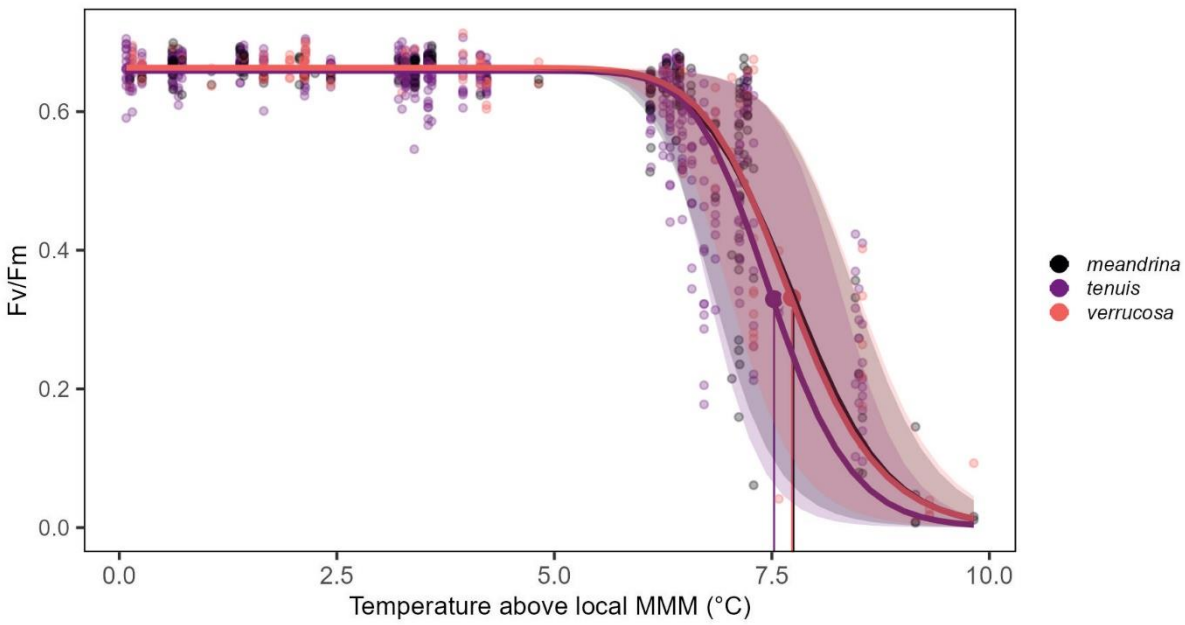

Supplementary Figure B.8 Relative ED50 (temperature above local MMM) did not significantly differ between the three species.

Supplementary material B.9 Absolute ED50 values by reef sector

```
Linear mixed-effects model fit by REML
  Data: dat

Random effects:
 Formula: ~1 | site
        (Intercept)  Residual
StdDev:   0.3268465 0.4188848

Fixed effects:  ED50 ~ Sector * species
 Correlation:
                                      (Intr) SctrTw SctrSw SctrCB spcstn spcsvr
SectorTownsville                      -0.747
SectorSwains                          -0.774  0.578
SectorCapricorn Bunker                -0.882  0.659  0.683
speciestenuis                         -0.608  0.454  0.471  0.536
speciesverrucosa                      -0.680  0.508  0.526  0.600  0.771
SectorTownsville:speciestenuis         0.496 -0.615 -0.384 -0.437 -0.815 -0.628
SectorSwains:speciestenuis             0.492 -0.367 -0.565 -0.434 -0.809 -0.623
SectorCapricorn Bunker:speciestenuis   0.575 -0.430 -0.445 -0.574 -0.946 -0.729
SectorTownsville:speciesverrucosa      0.538 -0.651 -0.417 -0.475 -0.610 -0.792
SectorSwains:speciesverrucosa          0.329 -0.246 -0.366 -0.290 -0.373 -0.484
SectorCapricorn Bunker:speciesverrucosa 0.477 -0.357 -0.370 -0.463 -0.541 -0.702
                                      SctrTwnsvll:spcst SctrSwns:spcst
```

	numDF <int>	denDF <dbl>	F-value <chr>	p-value <chr>
(Intercept)	1	255	157256.51	<.0001
Sector	3	11	9.98	0.0018
species	2	255	22.03	<.0001
Sector:species	6	255	1.03	0.4049

Post hoc contrasts of absolute ED50 between sectors

```
 contrast                      estimate    SE df t.ratio p.value
 Northern - Townsville           0.2555 0.293 11   0.871  0.8197
 Northern - Swains               0.3330 0.326 11   1.022  0.7404
 Northern - Capricorn Bunker     0.9568 0.268 11   3.576  0.0194
 Townsville - Swains             0.0775 0.317 11   0.244  0.9946
 Townsville - Capricorn Bunker   0.7013 0.257 11   2.729  0.0795
 Swains - Capricorn Bunker       0.6237 0.293 11   2.126  0.2042

Results are averaged over the levels of: species
Degrees-of-freedom method: containment
P value adjustment: tukey method for comparing a family of 4 estimates
 Sector           emmean    SE df lower.CL upper.CL .group
 Capricorn Bunker   35.1 0.160 11     34.6     35.6  a
 Swains             35.7 0.246 11     35.0     36.5  ab
 Townsville         35.8 0.201 11     35.2     36.4  ab
 Northern           36.1 0.214 14     35.4     36.7   b

Results are averaged over the levels of: species
Degrees-of-freedom method: containment
Confidence level used: 0.95
Conf-level adjustment: bonferroni method for 4 estimates
P value adjustment: bonferroni method for 6 tests
significance level used: alpha = 0.05
NOTE: If two or more means share the same grouping symbol,
      then we cannot show them to be different.
      But we also did not show them to be the same.
```

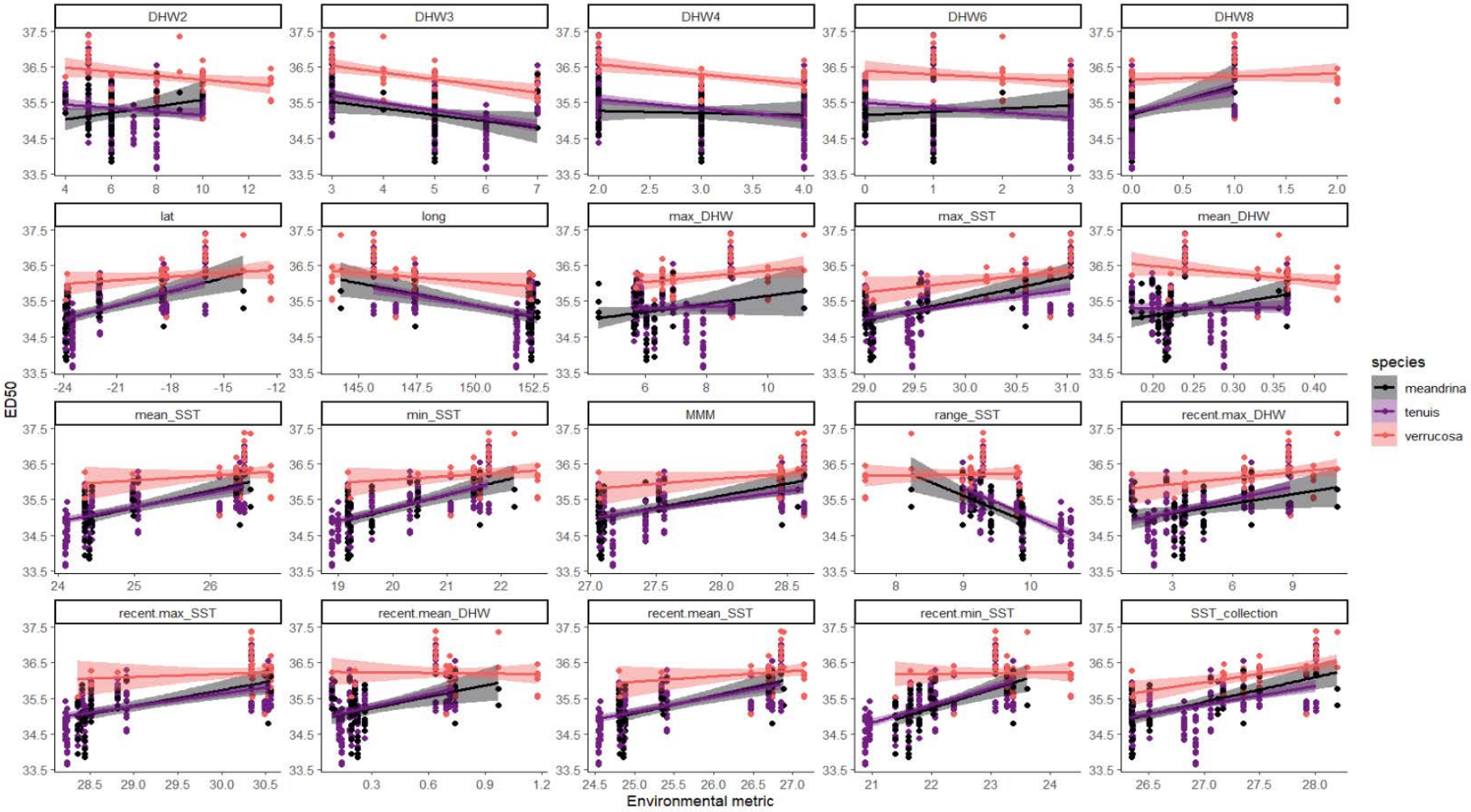

Supplementary Figure B.10 Correlations between absolute ED50 values and 20 thermal history metrics, coloured by species (P. *meandrina* = black, *A. tenuis* = purple, *P. verrucosa* = orange).

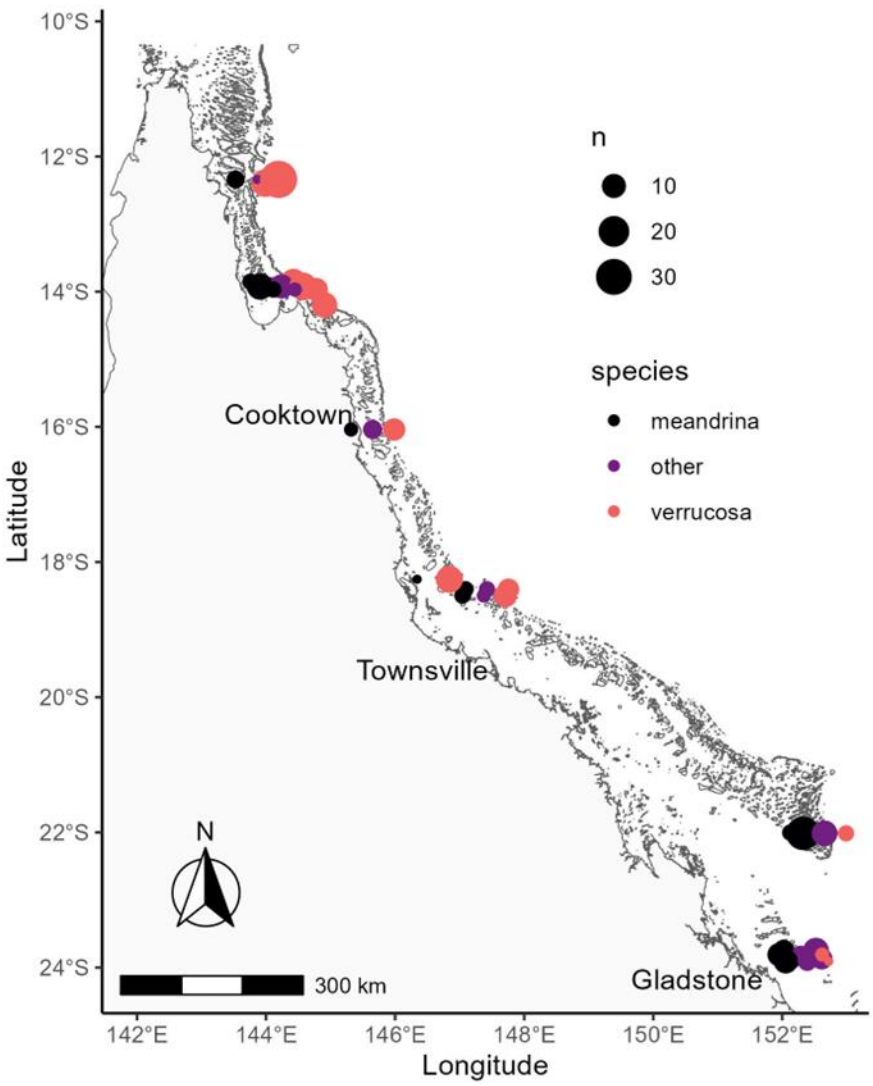

Supplementary Figure B.11 Map of collected *Pocillopora* colonies by RFLP-confirmed species (*P. verrucosa* = orange, *P. meandrina* = black, *P. others* = purple). Dot size indicates number of colonies collected within species per reef.

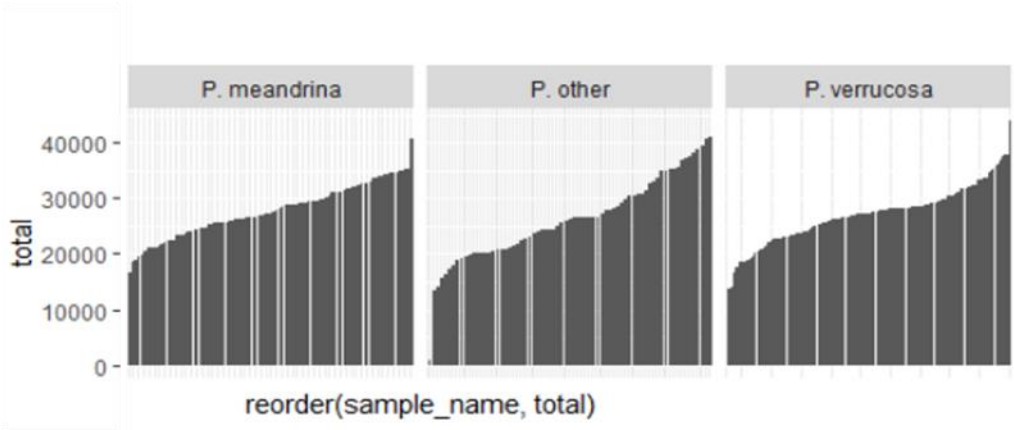

Supplementary Figure B.12 Sequencing read depth per sample per species, ordered from least number of reads to highest.

Supplementary Table B.12 Library statistics overview from ITS2 sequencing of *P. meandrina* and *P. verrucosa* samples.

Library statistics	***P. meandrina***	***P. verrucosa***
Samples (n)	96	141
Average reads per sample	27,715.07	26,989.94
Proportion non-profile sequences	0.187	0.155
Unique type profiles (n)	11	17

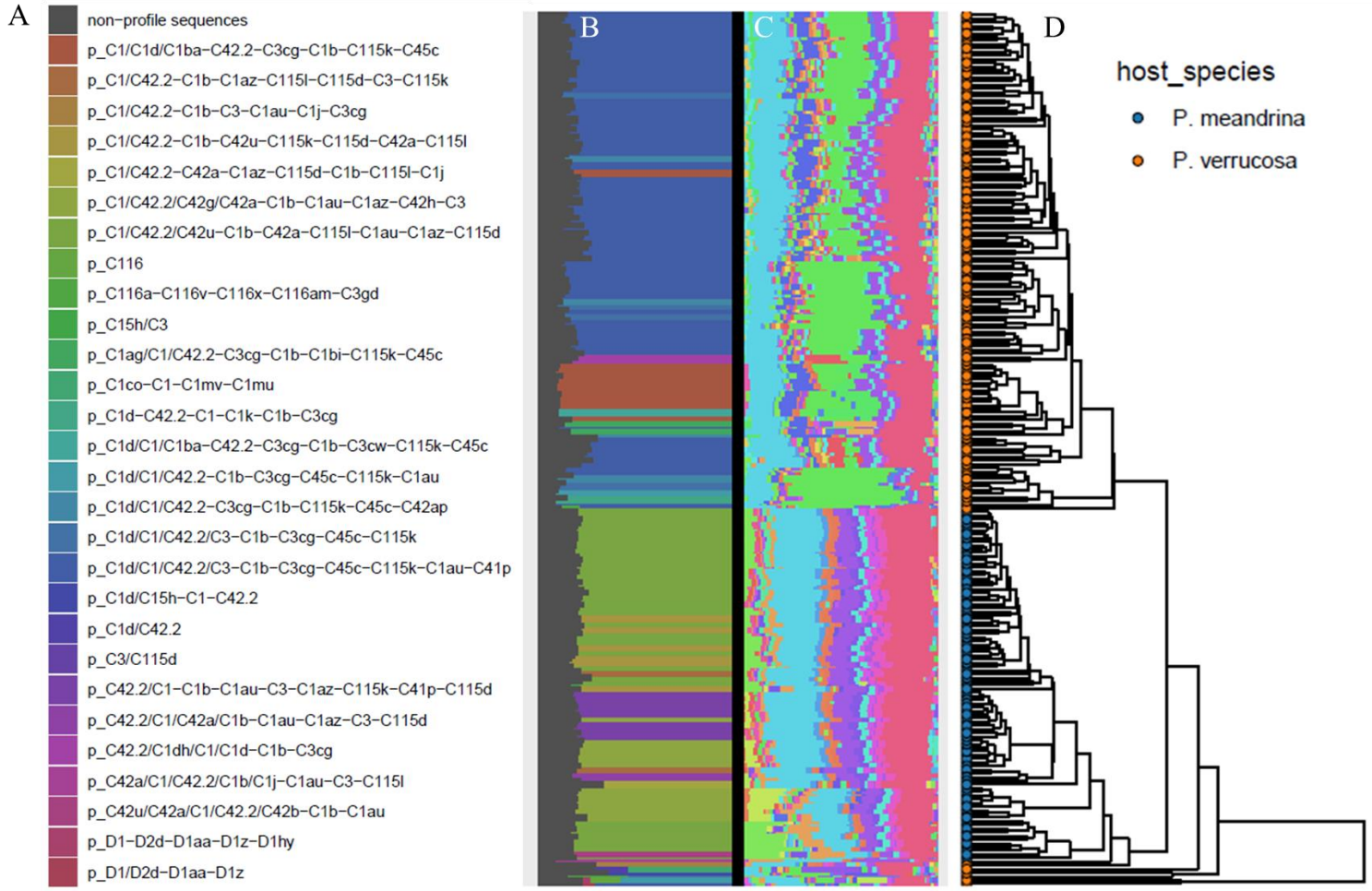

Supplementary Figure B.13 ITS2 profiles: Phylogenetic tree of sample relatedness based on k-mer hierarchical clustering and generalised UniFrac distances (GUniFrac). The tree highlights the clear split in symbiont composition between *P. meandrina* (blue) and *P. verrucosa* (orange) colonies.

Supplementary Table B.14 Most abundant (relative abundance) ITS2-type profile by species and sector. The dominant types within *P. meandrina* were all C1/C42.2/C42u-C1b-C42a-C115l-C1au-C1az-C115d except for in the Capricorn Bunker Group which recorded the C3 DIV. In *P. verrucosa*, a similar trend was recorded where the most dominant ITS2-type profile was C1d/C1/C42.2/C3-C1b-C3cg-C45c-C115k-C1au-C41p except in the Capricorn Bunker Group where all three sampled colonies of this species recorded different ITS2-type profiles.Interestingly, only one of the colonies sampled from this species in this sector recorded the *C. pacificum* diagnostic ITS2 sequence (C1d) which was absent from the profiles of the other two samples.

Sector	**Species**	**Most abundant ITS2-type profile**
Cape Greenville	*P. verrucosa*	C1d/C1/C42.2/C3-C1b-C3cg-C45c-C115k-C1au-C41p
	P. meandrina	C1/C42.2/C42u-C1b-C42a-C115l-C1au-C1az-C115d
Princess Charlotte Bay	*P. verrucosa*	C1d/C1/C42.2/C3-C1b-C3cg-C45c-C115k-C1au-C41p
	P. meandrina	C1/C42.2/C42u-C1b-C42a-C115l-C1au-C1az-C115d
Cairns	*P. verrucosa*	C1d/C1/C42.2/C3-C1b-C3cg-C45c-C115k-C1au-C41p
	P. meandrina	C1/C42.2/C42u-C1b-C42a-C115l-C1au-C1az-C115d
Townsville	*P. verrucosa*	C1d/C1/C42.2/C3-C1b-C3cg-C45c-C115k-C1au-C41p
	P. meandrina	C1/C42.2/C42u-C1b-C42a-C115l-C1au-C1az-C115d
Swains	*P. verrucosa*	C1d/C1/C42.2/C3-C1b-C3cg-C45c-C115k-C1au-C41p
	P. meandrina	C1/C42.2/C42u-C1b-C42a-C115l-C1au-C1az-C115d
Capricorn Bunkers	*P. verrucosa*	C1d/C1/C42.2/C3-C1b-C3cg-C45c-C115k-C1au-C41p C1ag/C1/C42.2-C3cg-C1b-C1bi-C115k-C45c C1/C42.2-C1b-C3-C1au-C1j-C3cg
	P. meandrina	C1/C42.2/C42g/C42a-C1b-C1au-C1az-C42h-C3

Supplementary Figure B.14 Most abundant ITS2-type profiles by species (green hues = *P. meandrina*, purple hues = *P. verrucosa*) and reef sector

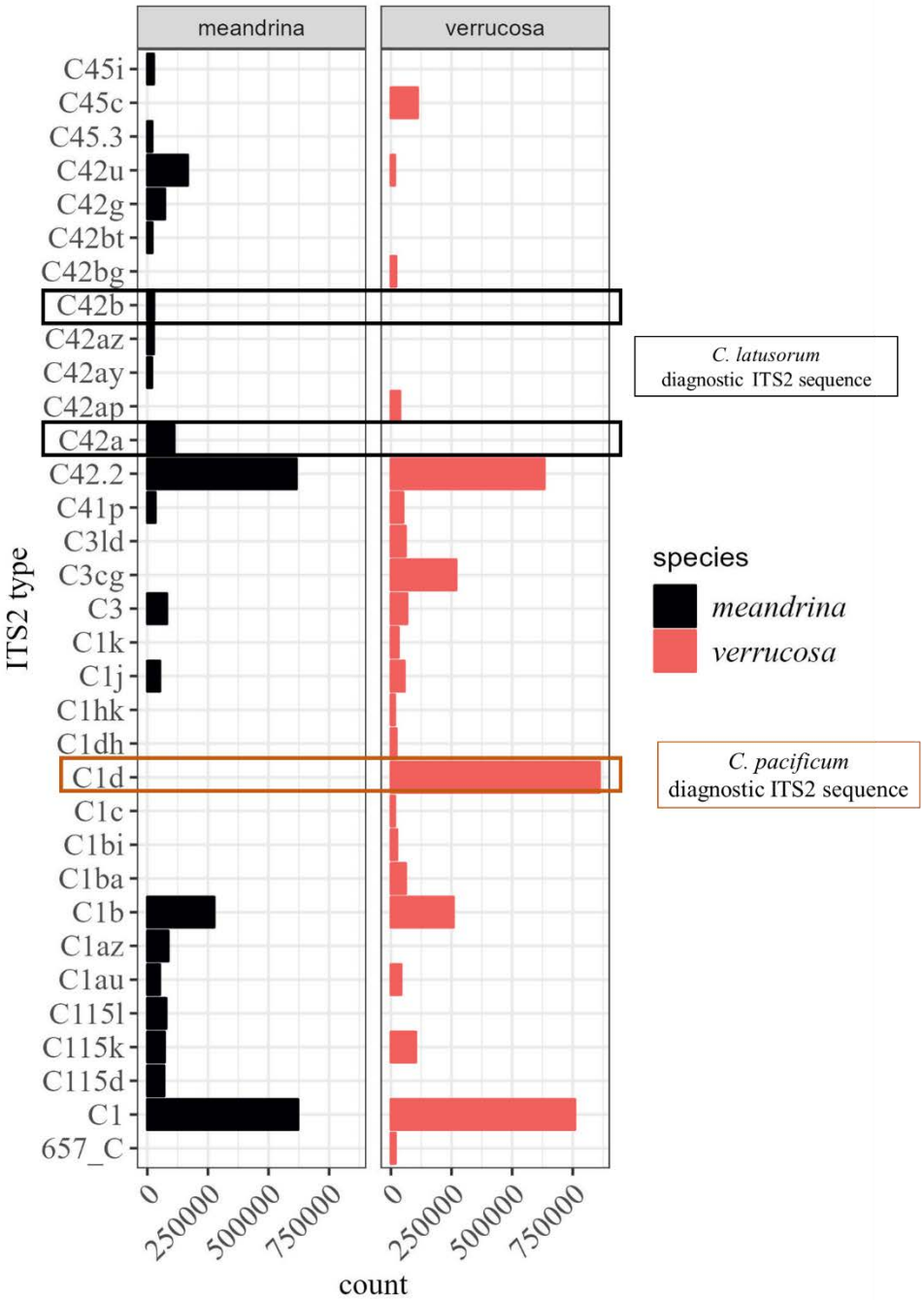

Supplementary Figure B.15 Bar chart of absolute DIV (ITS2 sequence) abundance from SymPortal in *P. meandrina* (black) and *P. verrucosa* (orange). The boxes indicate the diagnostic ITS2 sequences for *Cladocopium latusorum* (black, *P. meandrina*) and *C. pacificum* (orange, *P. verrucosa*).

Supplementary Table B.16 Statistical outputs from PERMANOVAs of symbiont community, thermal history, geography, and acute heat tolerance (ED50)

Terms	Variable	Species	Df	Sums of Squares	R2	F	P	***
Ecology	Species	NA	1	0.62	0.49	230.27	0.0001	***
	Coral cover	*P. verrucosa*	2	0.014	0.032	2.32	0.041	*
		P. meandrina	2	0.02	0.01	5.45	0.001	***
Geography	Latitude	*P. verrucosa*	1	0.027	0.064	9.95	0.001	***
		P. meandrina	1	0.017	0.097	10.85	0.001	***
	Longitude	*P. verrucosa*	1	0.024	0.056	8.79	0.001	**
		P. meandrina	1	0.013	0.071	7.99	0.001	***
	Region	*P. verrucosa*	2	0.071	0.17	13.70	0.001	***
		P. meandrina	2	0.05	0.28	18.11	0.001	***
	Sector	*P. verrucosa*	5	0.083	0.19	6.46	0.001	***
		P. meandrina	5	0.057	0.33	8.71	0.001	***
	Reef	*P. verrucosa*	13	0.10	0.24	3.10	0.001	***
		P. meandrina	15	0.082	0.47	4.67	0.001	***
Thermal history	MMM	*P. verrucosa*	1	0.008	0.02	3.12	0.027	*
		P. meandrina	1	0.025	0.14	16.90	0.001	***
	Max_SST	*P. verrucosa*	1	0.025	0.059	8.92	0.001	***
		P. meandrina	1	0.009	0.053	5.62	0.001	***
	Range_SST	*P. verrucosa*	1	0.045	0.10	16.46	0.001	***
		P. meandrina	1	0.014	0.081	9.73	0.001	***
	Mean_DHW	*P. verrucosa*	1	0.009	0.021	3.11	0.004	**
		P. meandrina	1	0.014	0.079	8.42	0.001	***
	DHW2	*P. verrucosa*	1	0.006	0.013	2.00	0.044	*
		P. meandrina	1	0.011	0.060	6.60	0.002	***
	DHW3	*P. verrucosa*	1	0.013	0.030	4.48	0.001	***
		P. meandrina	1	0.011	0.061	6.64	0.001	***
	DHW4	*P. verrucosa*	1	0.021	0.047	7.07	0.001	***
		P. meandrina	1	0.006	0.036	3.93	0.006	**
	Fv/Fm ED50	*P. verrucosa*	1	0.14	0.044	2.04	0.072	NS

Thermal tolerance		*P. meandrina*	1	0.38	0.17	10.17	0.001	***

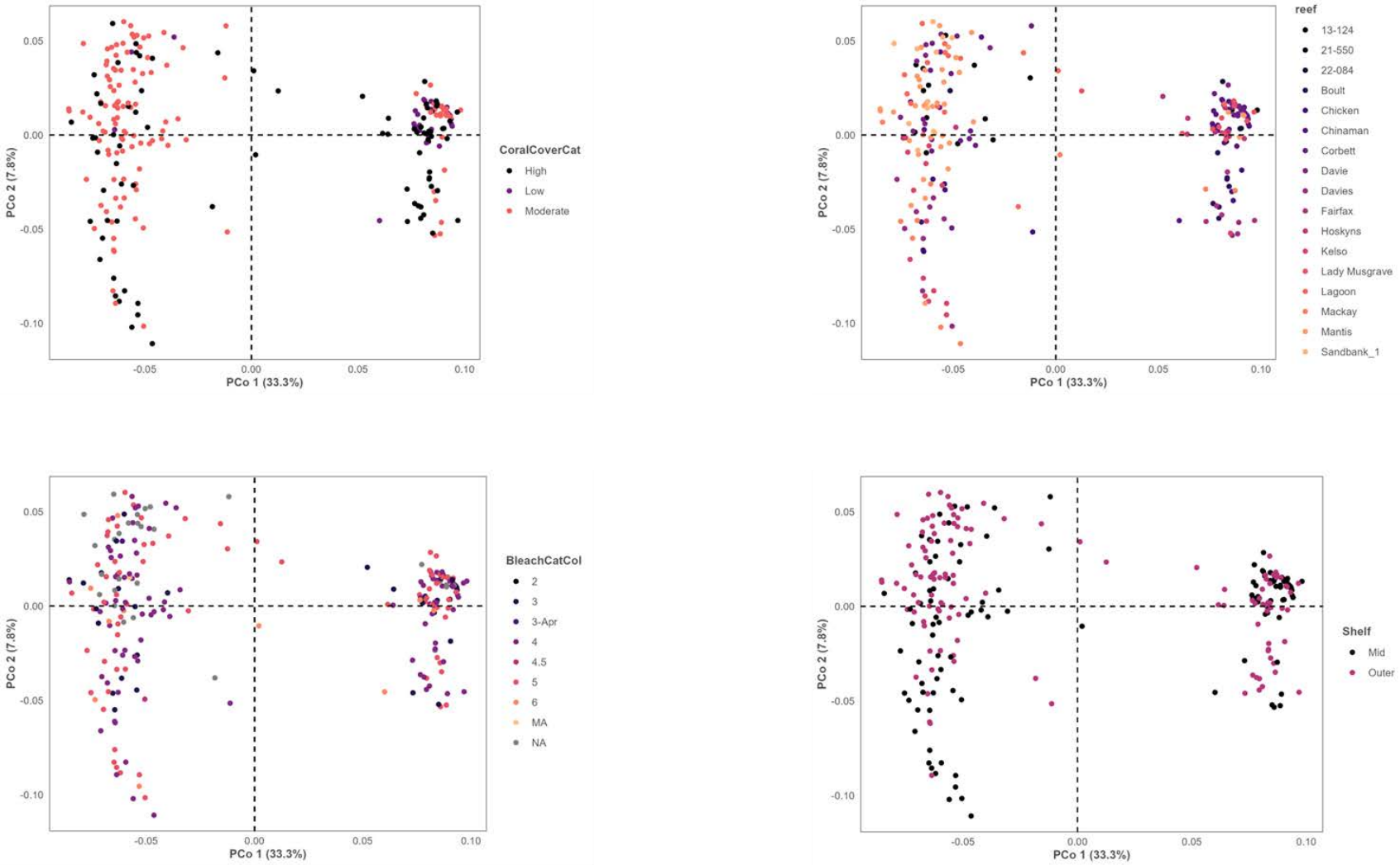

Supplementary Figure B. 17.a Symbiont community composition shows a strong split between the two coral host species but do not show evidence of clustering by reef, bleaching category, shelf position, or coral cover category.

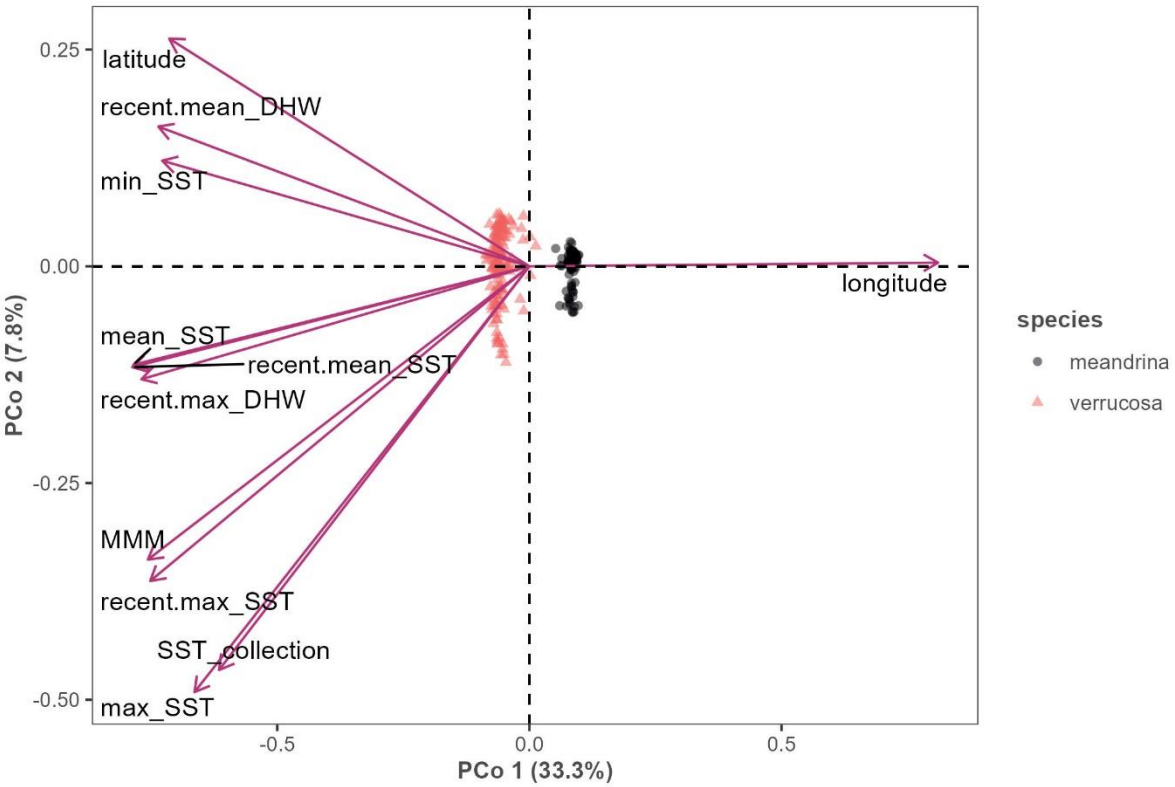

Supplementary Figure B.17.b PCoA of symbiont communities between the two species (*P. verrucosa* = orange, *P. meandrina* = black) with vectors indicating different thermal variables associated with each reef.

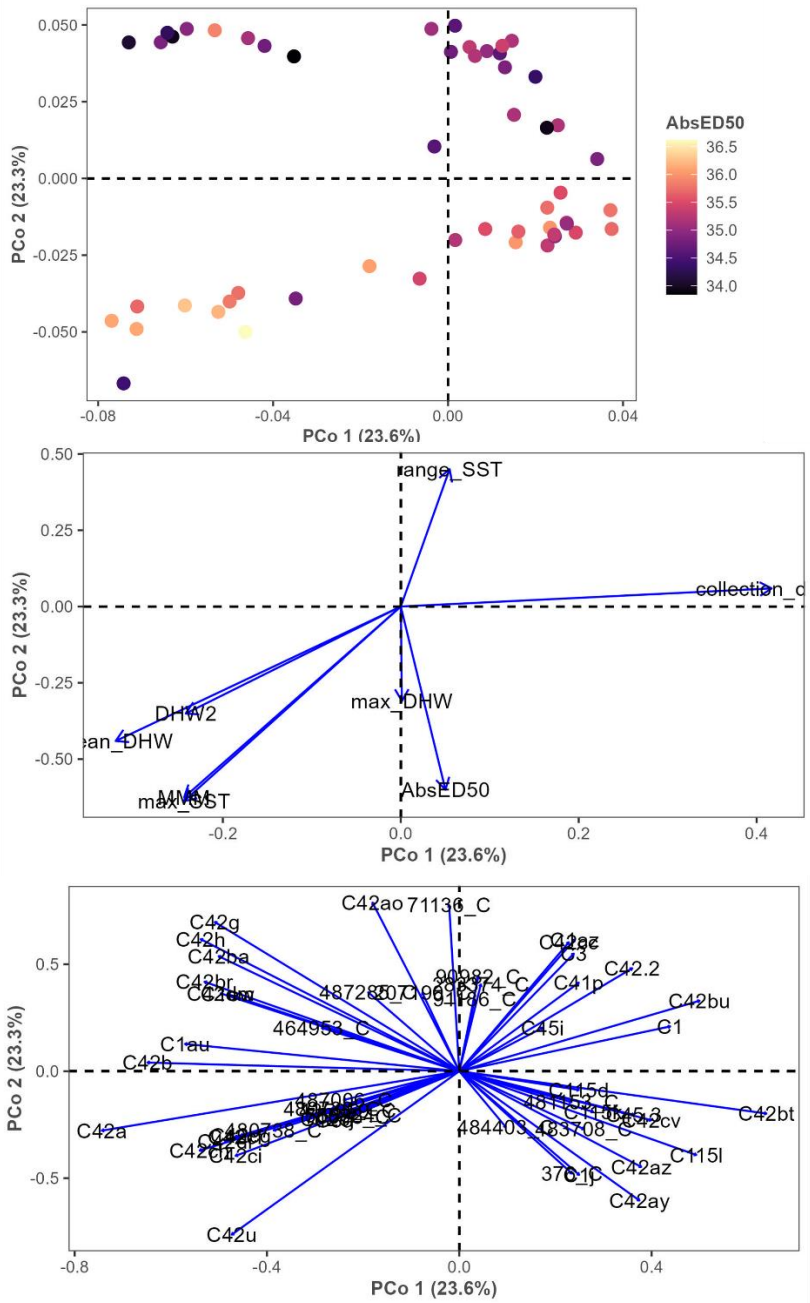

Supplementary Figure B.18 A) PCoA of *P. meandrina* symbiont communities with respect to ED50. B) Association of environmental variables with ED50. C) No single ITS2 DIV was significantly associated with higher ED50.

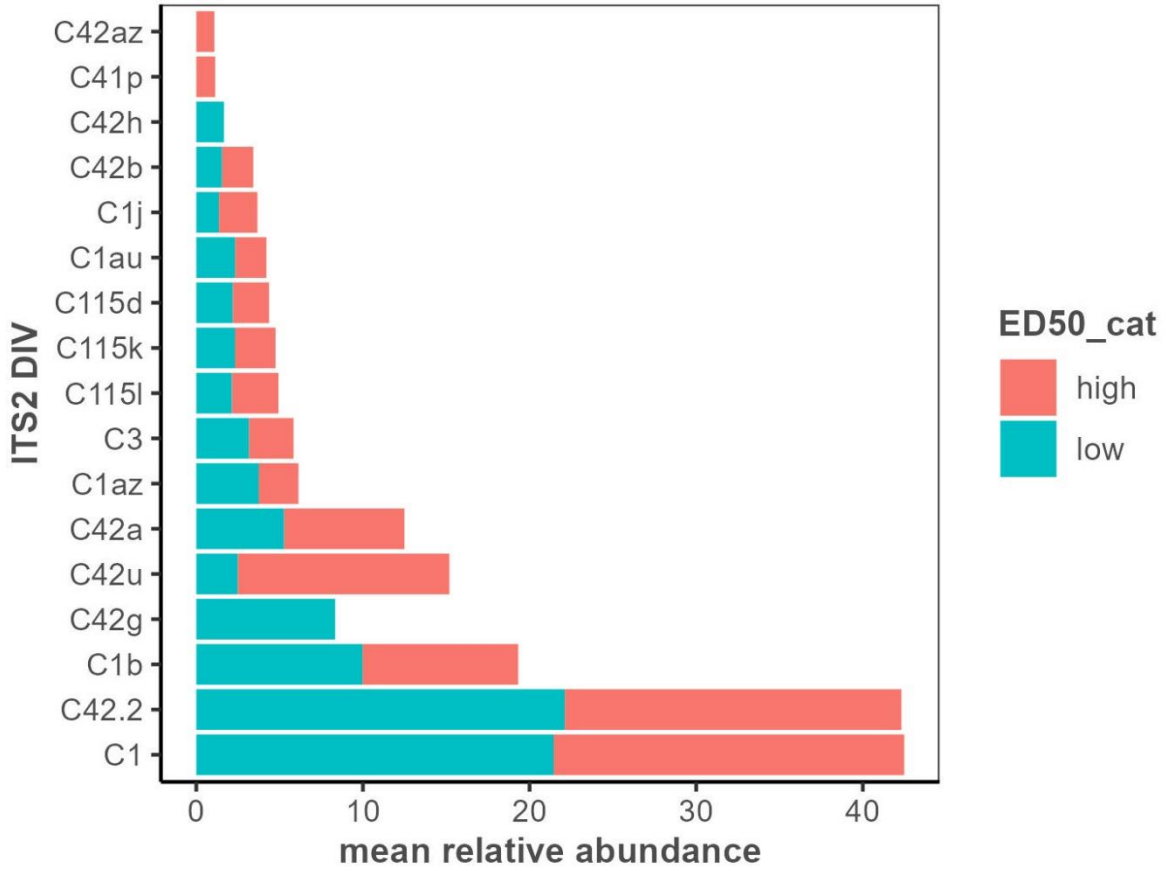

Supplementary Figure B.19 Overview of the most abundant DIVs associated with high (red) and low (blue) acute heat tolerance (ED50).

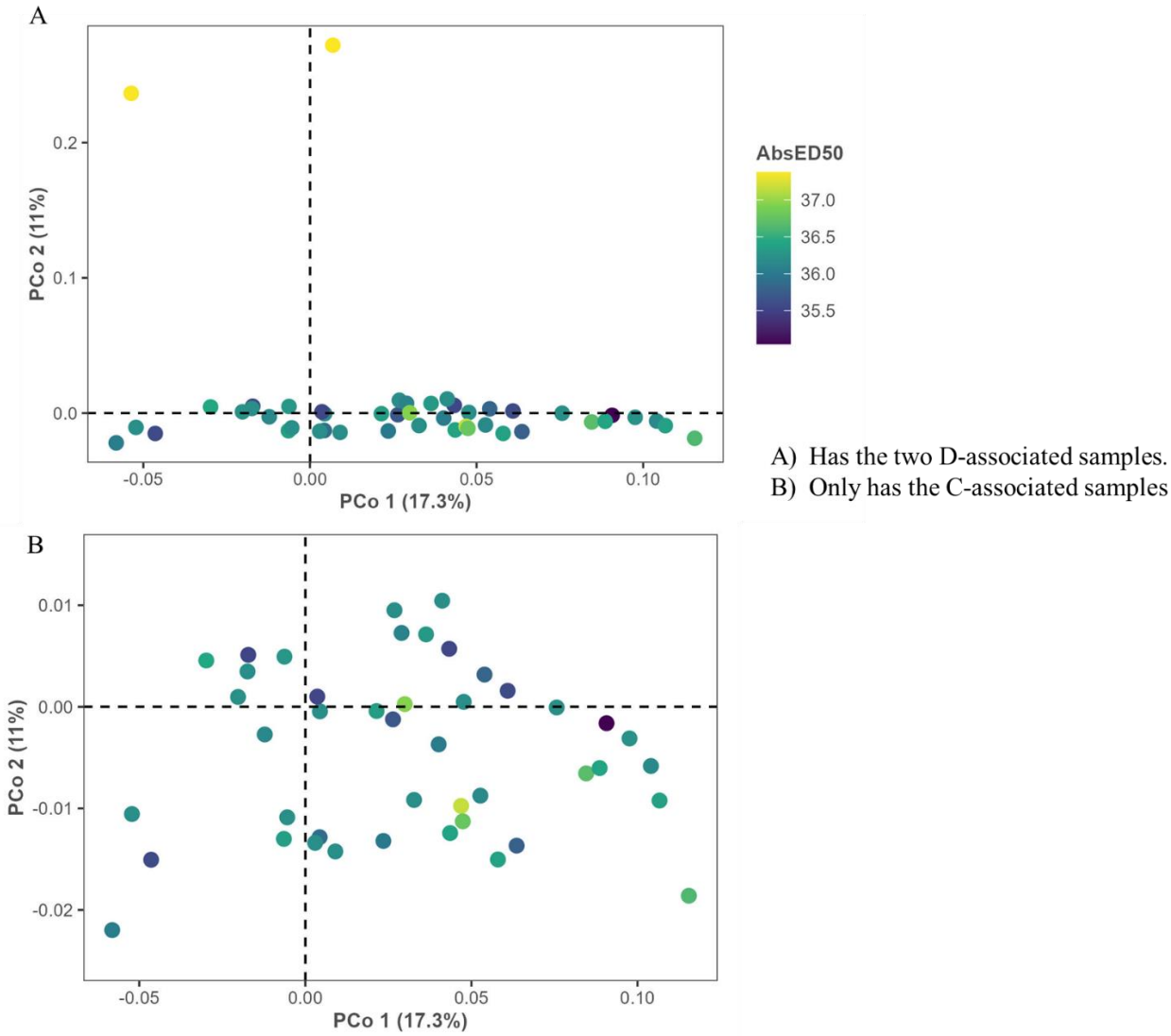

Supplementary Figure B.20 A) ED50 was higher (by 0.2ºC) in the two samples hosting *Durusdinium*-genus symbionts but (B) there was no effect of *Cladocopium* community of ED50s.

Supplementary material B.21 Statistical outputs for physiological traits

S21a - Fv/Fm

	numDF <int>	denDF <dbl>	F-value <chr>	p-value <chr>
(Intercept)	1	3176	139320.67	<.0001
species	3	571	7.82	<.0001
treatment	3	3176	1349.43	<.0001
species:treatment	9	3176	9.23	<.0001

S21b – Chlorophyll content

	numDF <int>	denDF <dbl>	F-value <chr>	p-value <chr>
(Intercept)	1	185	2691.3747	<.0001
species	2	111	0.0685	0.9339
Treatment	2	185	119.8849	<.0001
species:Treatment	4	185	7.9479	<.0001

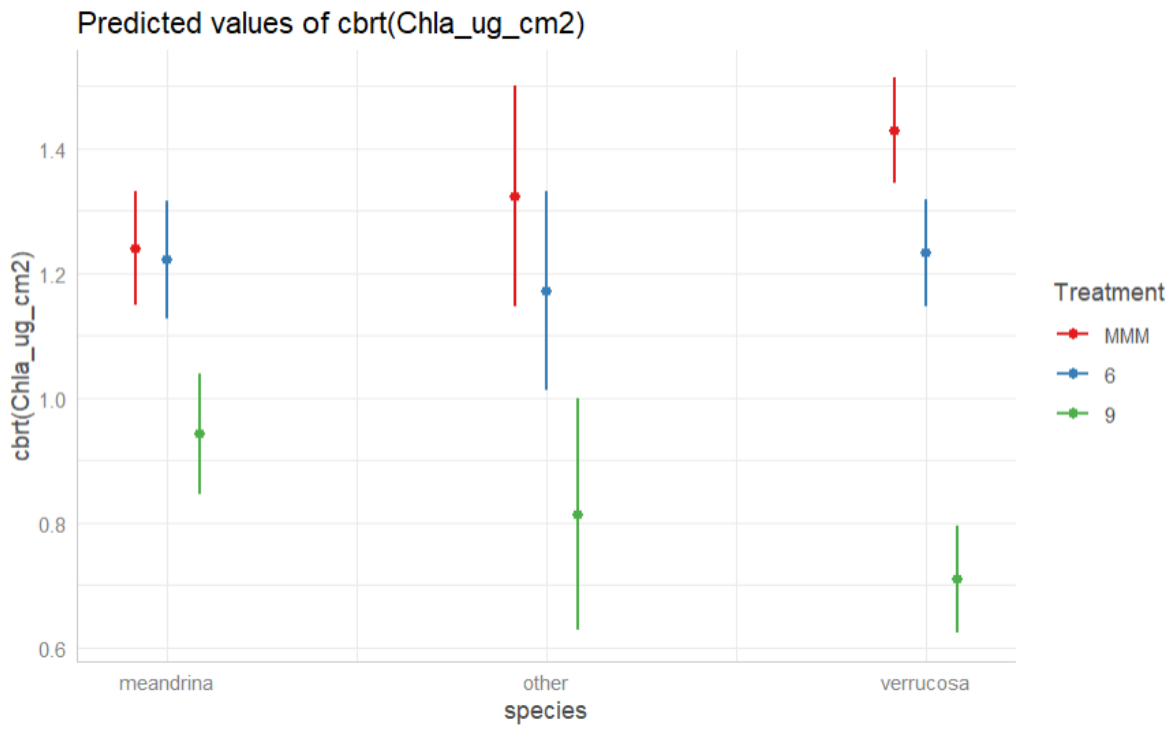

Factor	Level	contrast	estimate	SE	df	t.ratio	p.value	Sig code
Treatment	MMM	Meandrina – other	-0.0834	0.1007	111	-0.828	0.6864	
		Meandrina - verrucosa	-0.1887	0.0628	111	-3.002	0.0092	**
		Other - verrucosa	-0.1053	0.0994	111	-1.059	0.5412	
	6	Meandrina – other	0.0499	0.0936	111	0.533	0.8553	
		Meandrina - verrucosa	-0.0107	0.0645	111	-0.166	0.9849	
		Other - verrucosa	-0.0606	0.0915	111	-0.663	0.7856	
	9	Meandrina – other	0.1289	0.1056	111	1.220	0.4439	
		Meandrina - verrucosa	0.2333	0.0653	111	3.574	0.0015	**
		Other - verrucosa	0.1044	0.1032	111	1.012	0.5710	
Species	Meandrina	MMM - 6	0.0186	0.0552	185	0.337	0.9393	
		MMM - 9	0.2983	0.0559	185	5.337	<0.0001	***
		6 - 9	0.2797	0.0578	185	4.840	<0.0001	***
	Other	MMM - 6	0.1519	0.1082	185	1.403	0.3414	
		MMM - 9	0.5105	0.1167	185	4.376	0.0001	***
		6 - 9	0.3586	0.1061	185	3.38	0.0025	**
	Verrucosa	MMM - 6	0.1965	0.0505	185	3.894	0.0004	**
		MMM - 9	0.7202	0.0505	185	14.27	<0.0001	***
		6 - 9	0.5237	0.0508	185	10.311	<0.0001	***

S21c – Protein content

	numDF <int>	denDF <dbl>	F-value <chr>	p-value <chr>
(Intercept)	1	205	5121.201	<.0001
species	2	135	10.188	0.0001
Treatment	2	205	141.838	<.0001
species:Treatment	4	205	0.851	0.4942

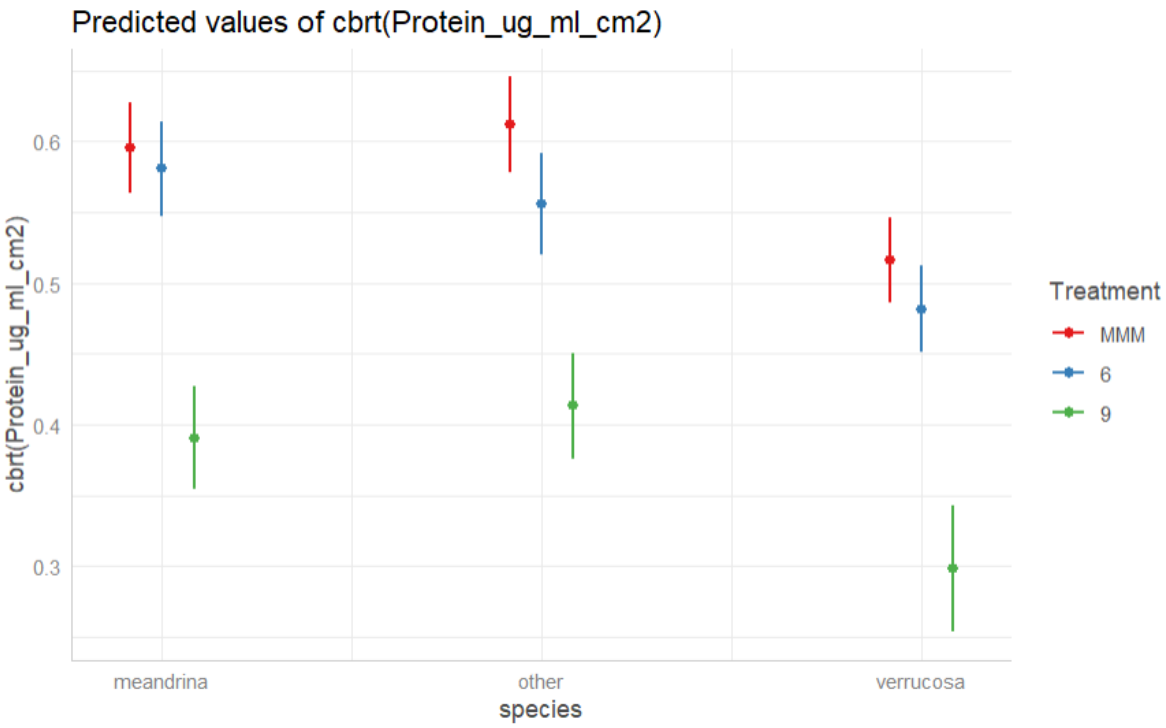

Factor	Level	contrast	estimate	SE	df	t.ratio	p.value	Sig code
Treatment	MMM	Meandrina – other	-0.0166	0.0235	135	-0.707	0.7601	
		Meandrina - verrucosa	0.0793	0.0221	135	3.582	0.0014	**
		Other - verrucosa	0.0959	0.0228	135	4.202	0.0001	***
	6	Meandrina – other	0.0246	0.0247	135	0.995	0.5813	
		Meandrina - verrucosa	0.0992	0.0227	135	4.371	0.0001	***
		Other - verrucosa	0.0747	0.0237	135	3.153	0.0057	**
	9	Meandrina – other	-0.0226	0.0262	135	-0.862	0.6653	
		Meandrina - verrucosa	0.0928	0.0289	135	3.210	0.0047	**
		Other - verrucosa	0.1154	0.0293	135	3.936	0.0004	***
Species	meandrina	MMM - 6	0.0148	0.0193	205	0.767	0.7236	
		MMM - 9	0.2049	0.0205	205	9.973	<0.0001	***
		6 - 9	0.1901	0.0211	205	8.992	<0.0001	***
	Other	MMM - 6	0.0560	0.0209	205	2.681	0.0215	*
		MMM - 9	0.1989	0.0216	205	9.215	<0.0001	***
		6 - 9	0.1430	0.022	205	6.487	<0.0001	***
	verrucosa	MMM - 6	0.0348	0.0177	205	1.961	0.1246	
		MMM - 9	0.2185	0.0242	205	9.026	<0.0001	***
		6 - 9	0.1837	0.0242	205	7.576	<0.0001	***

S21d – Catalase activity

	numDF <int>	denDF <dbl>	F-value <chr>	p-value <chr>
(Intercept)	1	202	3782.281	<.0001
species	2	135	20.010	<.0001
Treatment	2	202	4.469	0.0126
species:Treatment	4	202	4.987	0.0007

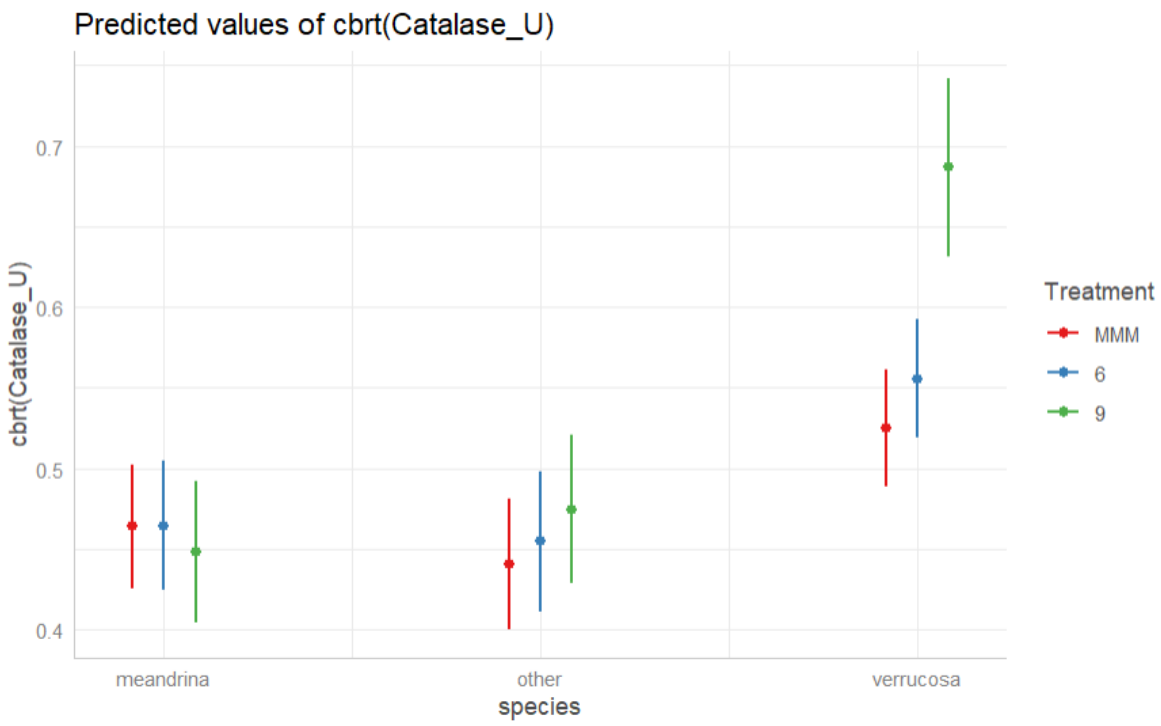

Factor	Level	contrast	estimate	SE	df	t.ratio	p.value	Sig code
Treatment	MMM	Meandrina – other	0.0236	0.0283	135	0.834	0.6829	
		Meandrina - verrucosa	-0.0607	0.0268	135	-2.268	0.0639	
		Other - verrucosa	-0.0843	0.0276	135	-3.052	0.0077	**
	6	Meandrina – other	0.0100	0.0299	135	0.336	0.9399	
		Meandrina - verrucosa	-0.0910	0.0275	135	-3.306	0.0035	**
		Other - verrucosa	-0.1010	0.0288	135	-3.512	0.0017	**
	9	Meandrina – other	-0.0263	0.0321	135	-0.818	0.6927	
		Meandrina - verrucosa	-0.2385	0.0356	135	-6.694	<0.0001	***
		Other - verrucosa	-0.2122	0.0363	135	-5.847	<0.0001	***
Species	Meandrina	MMM - 6	-0.000445	0.0253	202	-0.018	0.9989	
		MMM - 9	0.015892	0.0268	202	0.593	0.8240	
		6 - 9	0.016337	0.0275	202	0.594	0.8235	
	Other	MMM - 6	-0.014006	0.0272	202	-0.514	0.8644	
		MMM - 9	-0.033961	0.0284	202	-1.197	0.4561	
		6 - 9	-0.019955	0.0291	202	-0.687	0.7715	
	Verrucosa	MMM - 6	-0.030742	0.0235	202	-1.308	0.3924	
		MMM - 9	-0.161892	0.0314	202	-5.153	<0.0001	***
		6 - 9	-0.131150	0.0314	202	-4.176	0.0001	***

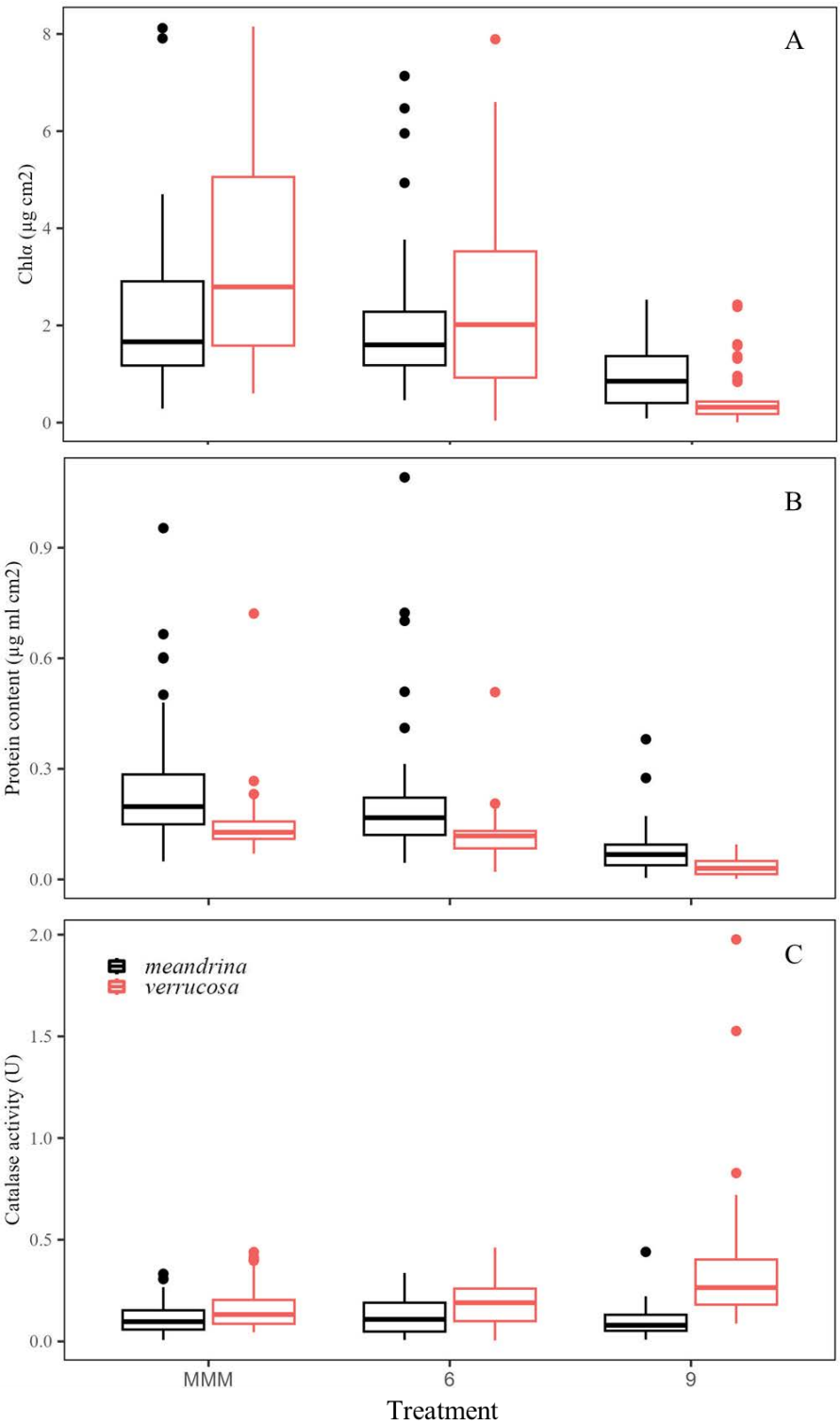

Supplementary Figure B.21 Declines are widely recorded across coral species in response to increasing treatment temperatures during acute heat stress assays in A) chlorophyll-α, B) protein content, and C) catalase activity. The boxplots are coloured by species (*P. meandrina* = black, *P. verrucosa* = orange) and outline the interquartile range, the whiskers indicate 1 SD, the line inside the boxes indicates the mean per group, and the dots indicate data outliers.

Additional results for chapter 3

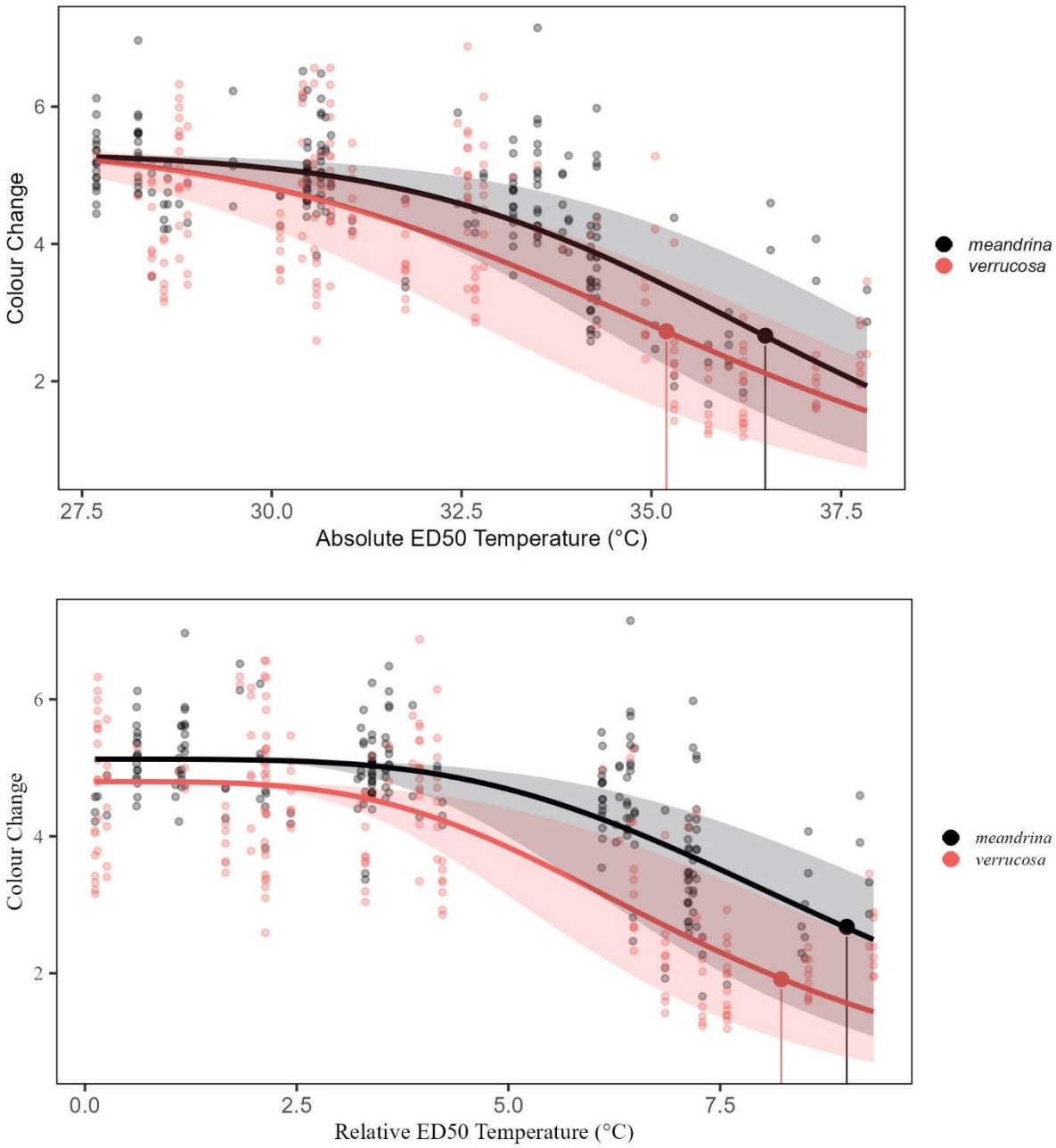

Supplementary Figure B.22 ED50 values derived from coral tissue colour change. Top) Absolute ED50s did not differ between species, with *P. meandrina* (black) recording a colour-change ED50 of 36.54ºC and *P. verrucosa* (orange) of 35.50ºC. Bottom) there were also no significant differences in the relative ED50 values derived from tissue colour change between the two species. The bands indicate 95% confidence intervals.

Statistical outputs for absolute colour-derived ED50s

```
Estimated effective doses

                Estimate Std. Error    Lower    Upper
e:meandrina:50 36.53850    0.44659 35.66062 37.41639
e:verrucosa:50 35.49791    0.48616 34.54222 36.45359
```

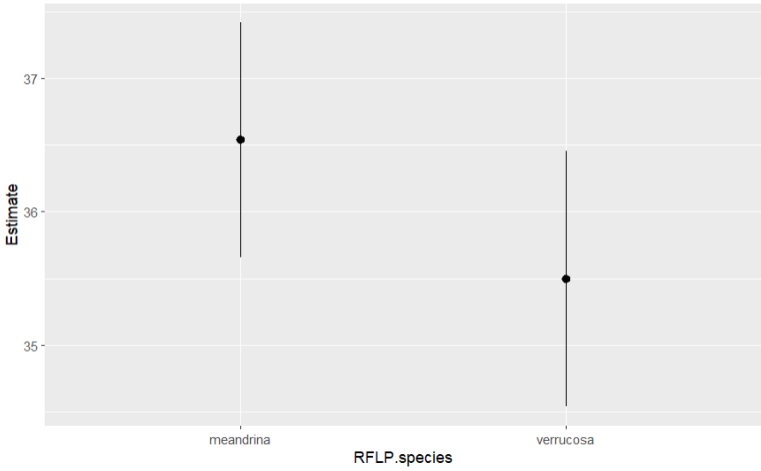

Statistical outputs for relative colour-derived ED50s

```
Estimated effective doses

                Estimate Std. Error   Lower   Upper
e:meandrina:50  8.90763    0.55238 7.82167 9.99358
e:verrucosa:50  8.36760    0.53258 7.32056 9.41465
```

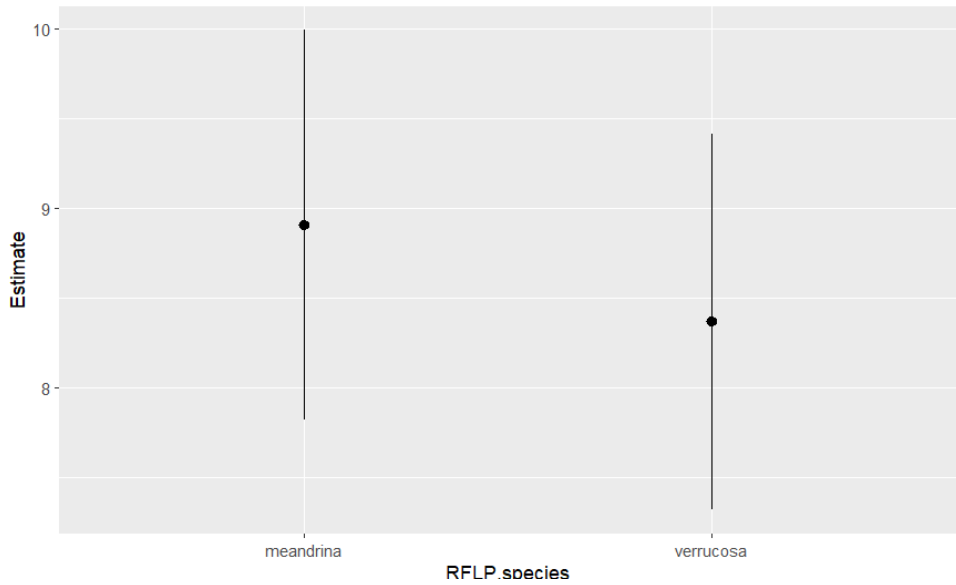

Supplementary material B.23 Model selection process. Here, I tested 16 different linear models with various combinations of thermal history variables, species, sector, and interaction terms. I compare them to a fully naïve dredge() model void of biological information.

```{r}

# need to widen the data frame

thermal.subset2<- thermal.subset %>%

  spread(key = variable, value = value) %>%

  ungroup() %>% # ungroup() was necessary to remove site

  dplyr::select(-Sector, -colonyID, -site, -meanSite_ED50)


options(na.action = "na.fail")

dredge.mod1 <- dredge(lm(ED50~species +., data = thermal.subset2), rank = "AIC", m.lim = c(1,4))


#just look at the top 20 scoring models

head(dredge.mod1, 20)


#extracting the best fit model using AIC score

bestmodel1 <- get.models(dredge.mod1, 1)[[1]]

lm.dredge1 <- lm(bestmodel1, data = dredge.sub)

summary(lm.dredge1)


# but I should probably consider that the species need an interaction term, especially in range_SST where verrucosa shows a very different relationship to meandrina/tenuis

lm.1 <- lm(ED50 ~ species + range_SST+ recent.mean_SST, data = thermal.subset2 )

lm.2 <- lm(ED50 ~ species * range_SST+ recent.mean_SST, data = thermal.subset2)

# does forcing recent.max_DHW add explanatory power?

lm.11 <- lm(ED50 ~ species * range_SST+ recent.mean_SST + recent.max_DHW, data = thermal.subset2)

# no, adding recent.max_DHW does not significantly improve the fit.


AICc(lm.1, lm.2)

# model 2 is the better model based on AICc

anova(lm.2) #

summary(lm.2) # interaction is significant, so worth modelling



# should check variance inflation

vif(lm.2) # ok, that's not great...
```

```
vif(lm.1)

#re-dredge with the interaction now specified
dredge.mod2 <- dredge(lm(ED50~species*range_SST +., data = thermal.subset2), rank = "AIC", m.lim = c(1,4))
head(dredge.mod2, 10)
#extracting the best fit model using AIC score
bestmodel2 <- get.models(dredge.mod2, 1)[[1]]
lm.dredge2 <- lm(bestmodel2, data = thermal.subset2)
summary(lm.dredge2)

library(performance)
check_model(lm.2)
check_model(lm.1)
check_model(lm.dredge2)

# compare trends in the model interaction
emtrends(lm.2, pairwise~species, var = "range_SST")

# what are the relative importance of each predictor?
library(relaimpo)
calc.relimp(lm.2, type = "lmg")
# so species accounts for 12.9%, range_SST = 17.2%, recent.mean_SST = 17.3%, and the interaction for 5.8% = 53.2% of total variation.
calc.relimp(lm.dredge2, type = "lmg")
calc.relimp(lm.11, type = "lmg")

r.squaredGLMM(lm.dredge2) # = 52.7% variation explained.
r.squaredGLMM(lm.6) # so a complete dredge model has some variance inflation issues but ultimately, explains 7% more variability within the data.
```

What would happen if I dredged from the very beginning without any pre-conceived ideas of co-linear variables?

```{r}
# need to widen the data frame
dredge.sub<- meta.long3 %>%
  spread(key = variable, value = value) %>%
  ungroup() %>% # ungroup() was necessary to remove site
```

```
  dplyr::select(-Sector, -colonyID, -site)

options(na.action = "na.fail")
dredge.mod3 <- dredge(lm(ED50~species +., data = dredge.sub), rank = "AIC", m.lim = c(1,4))

#just look at the top 20 scoring models
head(dredge.mod3, 20)

#extracting the best fit model using AIC score
bestmodel3 <- get.models(dredge.mod3, 1)[[1]]
lm.dredge3 <- lm(bestmodel3, data = dredge.sub)
summary(lm.dredge3)

# but I should probably consider that the species need an interaction term, especially in range_SST where verrucosa shows a very different relationship to meandrina/tenuis
lm.6 <- lm(ED50 ~ species + recent.max_DHW + recent.mean_DHW + recent.min_SST, data = dredge.sub )
lm.7 <- lm(ED50 ~ species * recent.max_DHW + recent.mean_DHW + recent.min_SST, data = dredge.sub)
lm.8 <- lm(ED50 ~ species * recent.mean_DHW + recent.max_DHW + recent.min_SST, data = dredge.sub)
lm.9 <- lm(ED50 ~ species + recent.mean_DHW + recent.max_DHW + recent.min_SST, data = dredge.sub)

AICc(lm.6, lm.7, lm.8, lm.9)
# model 6 and 9 are the best fit from AIC scores with same DFs,
# are model 6 and 9 significantly different to each other?
anova(lm.6, lm.9) # no, they are the exact some.
# should check variance inflation
vif(lm.6) # ok, that's alright

library(performance)
check_model(lm.6)

# what are the relative importance of each predictor?
library(relaimpo)
calc.relimp(lm.6, type = "lmg")
# so species accounts for 12.9%, range_SST = 17.2%, recent.mean_SST = 17.3%, and the interaction for 5.8% = 53.2% of total variation.
calc.relimp(lm.5, type = "lmg")
calc.relimp(lm.dredge3, type = "lmg")
r.squaredGLMM(lm.dredge3) # = 59.8% variation explained.
```

r.squaredGLMM(lm.6) # so a complete dredge model has some variance inflation issues but ultimately, explains 7% more variability within the data.

```

**# Adding sector**

Can I add in sector to help soak up more of the variability? Answer: Yes, I can. Takes me up to a total variance epxlained of 62%

```{r}

# need to widen the data frame

dredge.sub2<- meta.long3 %>%

  spread(key = variable, value = value) %>%

  ungroup() %>% # ungroup() was necessary to remove site

  dplyr::select(-colonyID, -site)


options(na.action = "na.fail")

dredge.mod4 <- dredge(lm(ED50~species +., data = dredge.sub2), rank = "AIC", m.lim = c(1,4))


#just look at the top 20 scoring models

head(dredge.mod4, 20)


#extracting the best fit model using AIC score

bestmodel4 <- get.models(dredge.mod4, 1)[[1]]

lm.dredge4 <- lm(bestmodel4, data = dredge.sub2)

summary(lm.dredge4)


# but I should probably consider that the species need an interaction term, especially in range_SST where verrucosa shows a very different relationship to meandrina/tenuis

lm.12 <- lm(ED50 ~ max_SST + recent.mean_SST + Sector + species, data = dredge.sub2 )

lm.13 <- lm(ED50 ~ species + max_SST + recent.mean_SST + Sector, data = dredge.sub2)

lm.14 <- lm(ED50 ~ species * Sector + max_SST + recent.mean_SST, data = dredge.sub2)



AICc(lm.12, lm.13, lm.14)

# model 12 and 13 are best fit, and likely identical

# are model 6 and 9 significantly different to each other?

anova(lm.12, lm.13) # no, they are the exact some.

summary(lm.13)

```
should check variance inflation

vif(lm.13) # ok, that's alright

check_model(lm.13)

what are the relative importance of each predictor?

library(relaimpo)

calc.relimp(lm.13, type = "lmg")

so species accounts for 12.9%, range_SST = 17.2%, recent.mean_SST = 17.3%, and the interaction for 5.8% = 53.2% of total variation.

calc.relimp(lm.5, type = "lmg")

calc.relimp(lm.dredge3, type = "lmg")

r.squaredGLMM(lm.dredge3) # = 59.8% variation explained.

r.squaredGLMM(lm.6) # so a complete dredge model has some variance inflation issues but ultimately, explains 7% more variability within the data.
```

 # Does variance explained significantly improve if I include latitude?

```{r}
# need to widen the data frame

dredge.sub2<- meta.long3 %>%

  spread(key = variable, value = value) %>%

  ungroup() %>% # ungroup() was necessary to remove site

  dplyr::select(-colonyID, -site)


options(na.action = "na.fail")

dredge.mod5 <- dredge(lm(ED50~lat + ., data = dredge.sub2), rank = "AIC", m.lim = c(1,4))

#just look at the top 10 scoring models

head(dredge.mod5, 10)


#extracting the best fit model using AIC score

bestmodel5 <- get.models(dredge.mod5, 1)[[1]]

lm.dredge5 <- lm(bestmodel5, data = dredge.sub2)

summary(lm.dredge5)


# but I should probably consider that the species need an interaction term, especially in range_SST where verrucosa shows a very different relationship to meandrina/tenuis

lm.15 <- lm(ED50 ~ max_SST + recent.mean_SST + Sector + species, data = dredge.sub2 )
```

```
lm.16 <- lm(ED50 ~ lat + max_SST + recent.mean_SST + Sector + species, data = dredge.sub2)

AICc(lm.15, lm.16)
# model 16 is a better model according to AICc
# are the models significantly different to each other?
anova(lm.15, lm.16) # yes, they are different
summary(lm.16)
# should check variance inflation
vif(lm.16) # ok, there are issues here which are inherint when including latitude

check_model(lm.16)

# what are the relative importance of each predictor?
calc.relimp(lm.16, type = "lmg")
# so species accounts for 9.4%, sector = 21%, latitude = 10%, max_SST = 11%, recent.mean_SST = 12%
r.squaredGLMM(lm.16) # this model describes ~ 63% of total variation
```

Supplementary Material B.24 Within-sector differences in acute tolerance (ED50) between the three coral species.

	species	Sector	mean	sd	n	se
1	meandrina	Northern	35.97358	0.5642391	4	0.28211955
2	meandrina	Townsville	35.80475	0.5364455	6	0.21900297
3	meandrina	Swains	35.58126	0.3872892	9	0.12909639
4	meandrina	Capricorn Bunker	34.93149	0.5375813	34	0.09219444
5	tenuis	Northern	36.22536	0.7357440	15	0.18996828
6	tenuis	Townsville	35.57479	0.3743058	41	0.05845674
7	tenuis	Swains	35.55289	0.3903892	30	0.07127498
8	tenuis	Capricorn Bunker	34.97460	0.5369886	93	0.05568312
9	verrucosa	Northern	36.45767	0.5373518	17	0.13032694
10	verrucosa	Townsville	36.07732	0.3414409	25	0.06828818
11	verrucosa	Swains	36.21989	NA	1	NA
12	verrucosa	Capricorn Bunker	35.89497	0.3772095	3	0.21778200

```
Degrees-of-freedom method: containment
Confidence level used: 0.95

$contrasts
Sector = Northern:
 contrast              estimate     SE  df t.ratio p.value
 meandrina - tenuis      -0.129 0.2610 255  -0.496  0.8732
 meandrina - verrucosa   -0.657 0.2523 255  -2.602  0.0264
 tenuis - verrucosa      -0.527 0.1740 255  -3.029  0.0076

Sector = Townsville:
 contrast              estimate     SE  df t.ratio p.value
 meandrina - tenuis       0.207 0.1854 255   1.115  0.5057
 meandrina - verrucosa   -0.296 0.1945 255  -1.520  0.2831
 tenuis - verrucosa      -0.502 0.1069 255  -4.701  <.0001

Sector = Swains:
 contrast              estimate     SE  df t.ratio p.value
 meandrina - tenuis       0.100 0.1895 255   0.529  0.8569
 meandrina - verrucosa   -0.503 0.4567 255  -1.100  0.5147
 tenuis - verrucosa      -0.603 0.4312 255  -1.398  0.3433

Sector = Capricorn Bunker:
 contrast              estimate     SE  df t.ratio p.value
 meandrina - tenuis      -0.221 0.0891 255  -2.481  0.0365
 meandrina - verrucosa   -0.819 0.2557 255  -3.204  0.0043
 tenuis - verrucosa      -0.598 0.2520 255  -2.375  0.0478

Degrees-of-freedom method: containment
P value adjustment: tukey method for comparing a family of 3 estimates
```

Supplementary Material B.25 Comparison of ED50 and ED25.

The proposed ED25 trait was nearly perfectly correlated with ED50 (spearman's rank, S = 74836, $p < 0.0001$, rho = 0.979). Interestingly, this high correlation suggests that resilient corals record high ED traits, regardless of looking at the ED25 or the ED50 response. In contrast, a high ED25 followed by a low ED50 would have been characteristic of a tipping point response, while this indicates a more linear decline in photosynthesis.

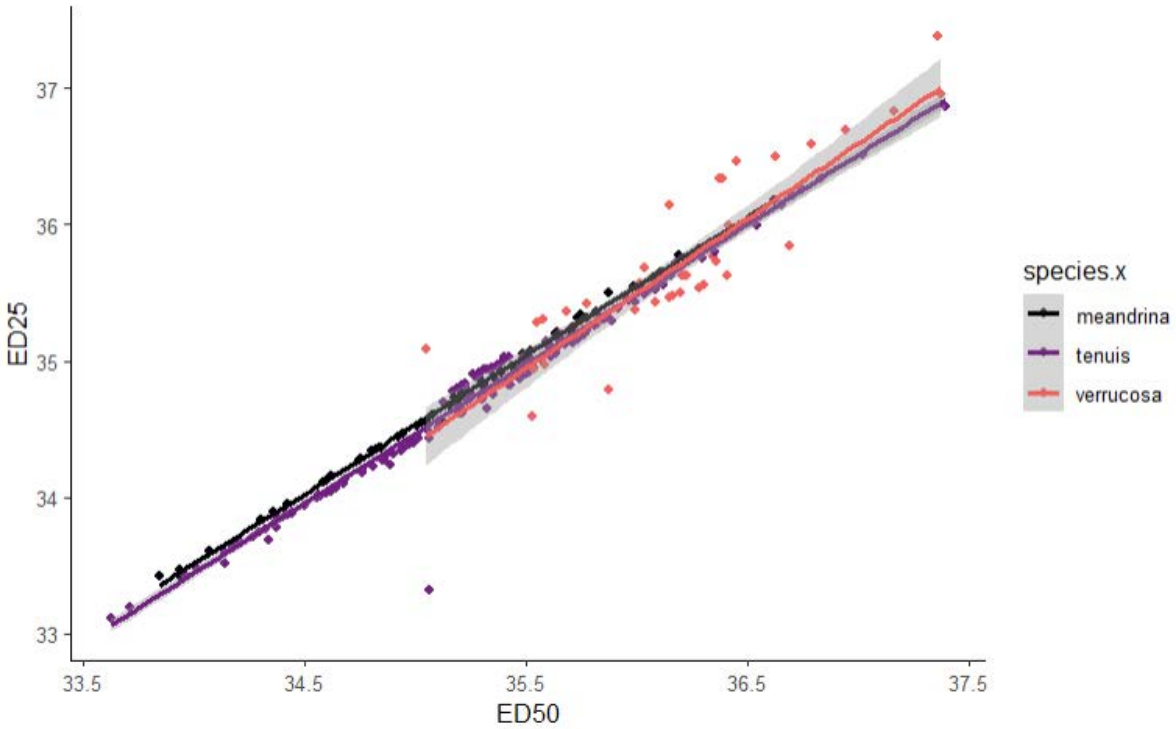

Appendix C – Supplementary material for Chapter 4

Continues next page.

Supplementary Table C.1a Rapid Light Curve (RLC) and photosynthesis terminology used.

Term	***Definition***	***Equation***	***Reference***
PSII	Algal photosystem 2		
E_k	Minimum saturating irradiance of PSII		Nitschke et al 2018
rETR	Relative Electron Transport Rate		Ralph & Gademann, 2005
[1-Q]	Light-dependent non-photochemical quenching	$(F_m` - F`)/(F_m` - F_o`)$	(Suggett et al., 2015)
[1-C]	Light-dependent photochemical quenching	$(F_v`/F_m`)/(F_v/F_m)$	(White & Critchley, 1999)
Fq'/F_m'	Effective photochemical efficiency of PSII (dimensionless)	$(F_m` - F`)/F_m`$	Nitschke et al 2018
F_o	minimum dark-acclimated fluorescence yield		
$F_o`$	minimum fluorescence yield under actinic light		
F_m	maximum dark-acclimated fluorescence yield		
$F_m`$	maximum fluorescence yield under actinic light		
$F`$	minimum fluorescence yield under actinic light		
F_v/F_m	Maximum photochemical yield of PSII (dimensionless)	$(F_m - F_o)/F_m$	

Supplementary Table C.1b Actinic light steps for each treatment.

Actinic light step #	Ambient	30°C	32, 34, and 35.5°C
0	0	0	0
1	99	106	78
2	190	201	150
3	291	294	233
4	419	422	339
5	563	564	455
6	804	808	653
7	1086	1071	875
8	1557	1567	1286

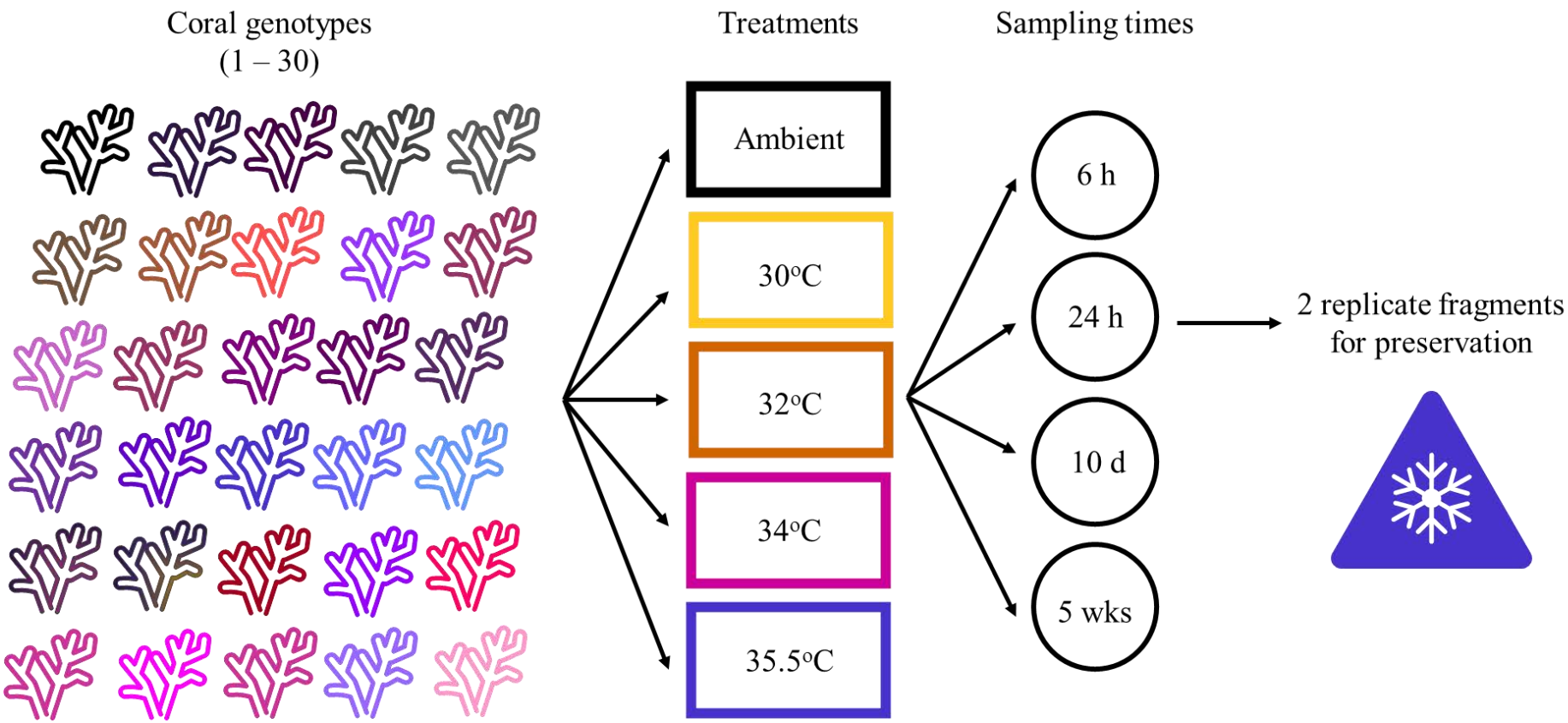

Supplementary Figure C.2 Experimental design diagram. 30 coral genotypes were fragmented into 40 fragments each, and distributed across five treatments, such that each genotype was present in each treatment by 8 fragments. At each of the four sampling time points, two fragments per genotype per treatment were collected (n = 60 fragments total per sampling point per treatment) and preserved in liquid nitrogen for downstream processing.

Supplementary Table C.3 Overview of total number of coral fragments available for physiological assays.

Time point	Fragments in system	Sampling activity
T0	1200	Prior photographs and weighing
6 h	1200	Photographs post heating RLC 2 fragments removed per genotype per treatment
24 h	900	Photographs post heating RLC 2 fragments removed per genotype per treatment
10 d	600	Photographs post heating RLC Weighing 2 fragments removed per genotype per treatment
5 wks	300	Photographs post heating RLC Weighing 2 fragments removed per genotype per treatment (all frags collected

Supplementary Table C.4 Sampling details for physiological maintenance (PM) trait. All values derived from the 34°C treatment. The highest genotype trait mean is the most desirable state and this genotype recorded the highest PM score (30). The lowest genotype trait mean was the least desirable physiological state and this genotype recorded the lowest PM score (1).

Trait	Time point	Genotypes (n)	Fragments per genotype	Total fragments available	Highest genotype trait mean	Lowest genotype trait mean
Colour change	24 h	30	4 - 6	174	0.608	-3.05
F_q/F_m	24 h	23	1 – 2	44	0.70	0.53
E_k	24 h	23	1 - 2	44	199.6	63.7
Buoyant weight changes	10 d	30	3 - 4	115	$1.79 * 10^{-4}$ g d^{-1} g^{-1}	$-7.04 * 10^{-4}$ g d^{-1} g^{-1}

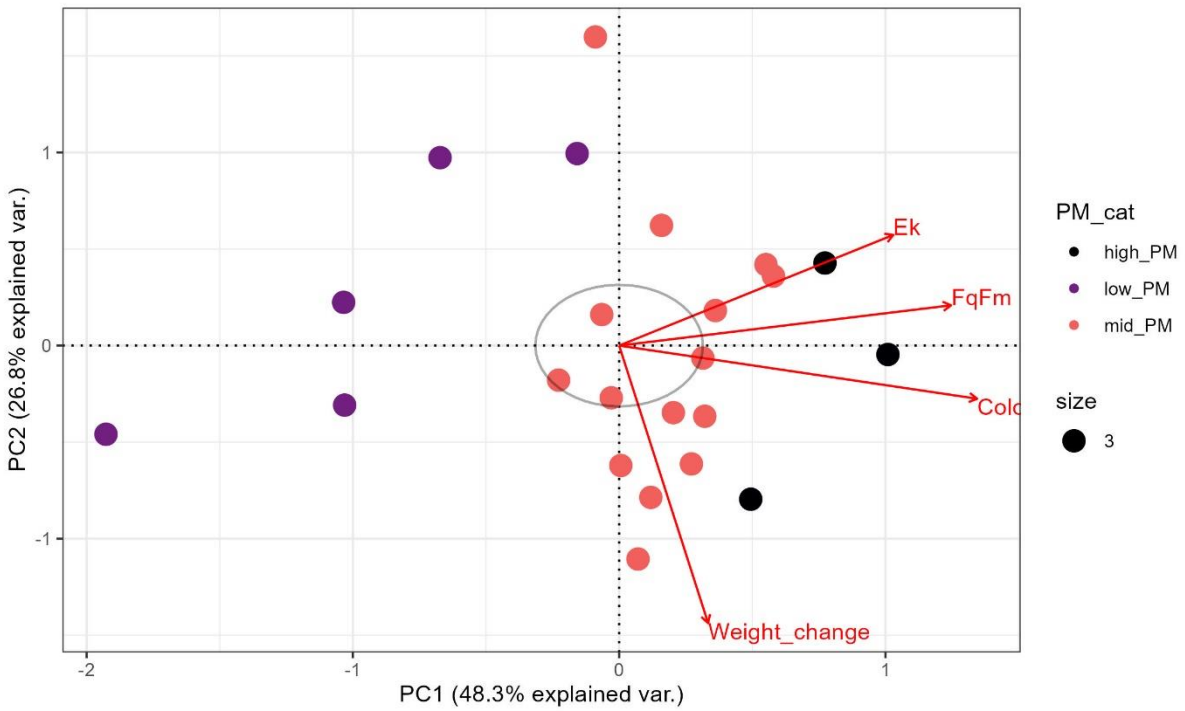

Supplementary Figure C.5 PCA of genotype-level trait responses in high PM(black) vs low PM (purple) scoring colonies.

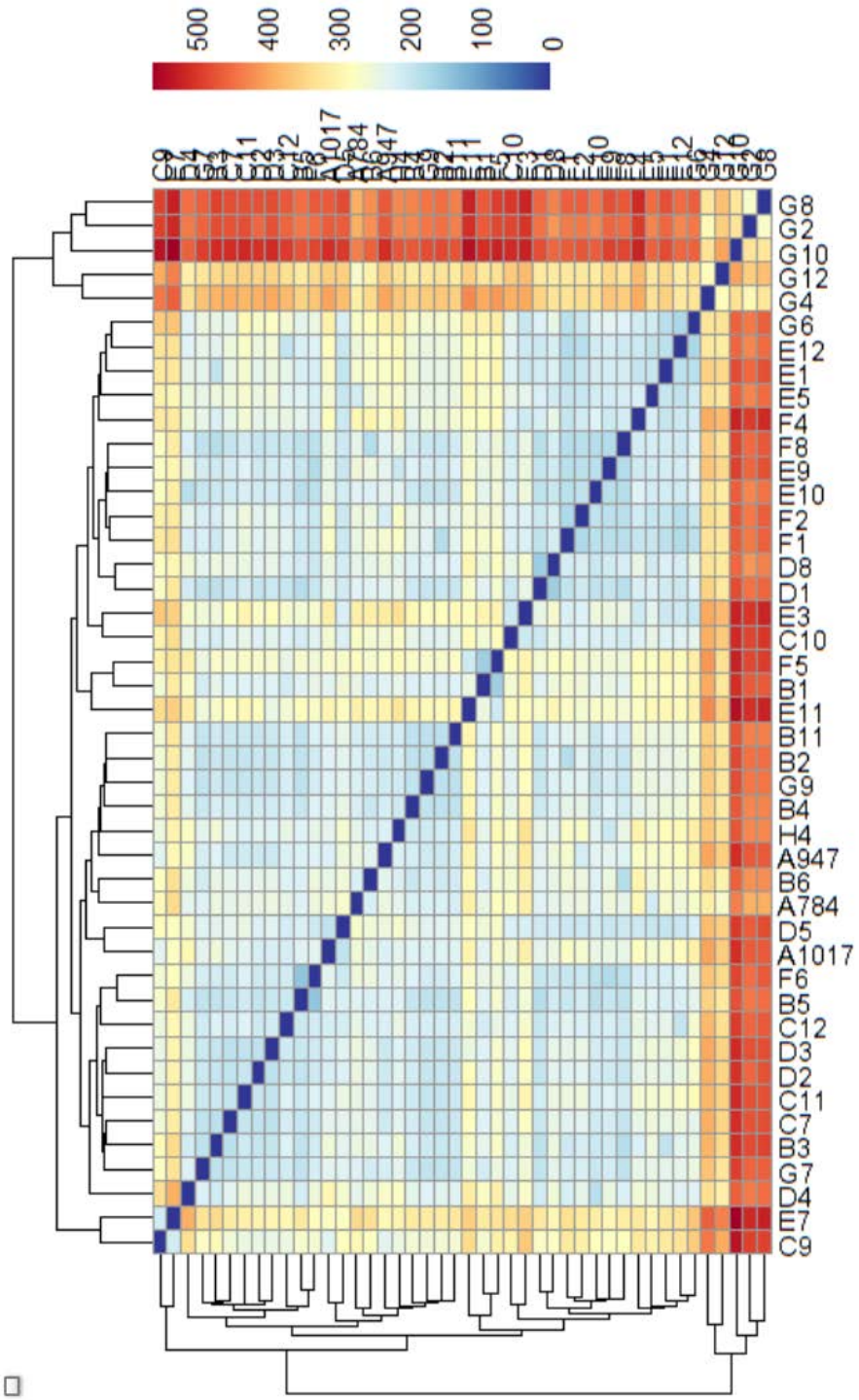

Supplementary Figure C.6.1 Sample-sample distance matrix based on normalised gene read counts including all 44 samples.

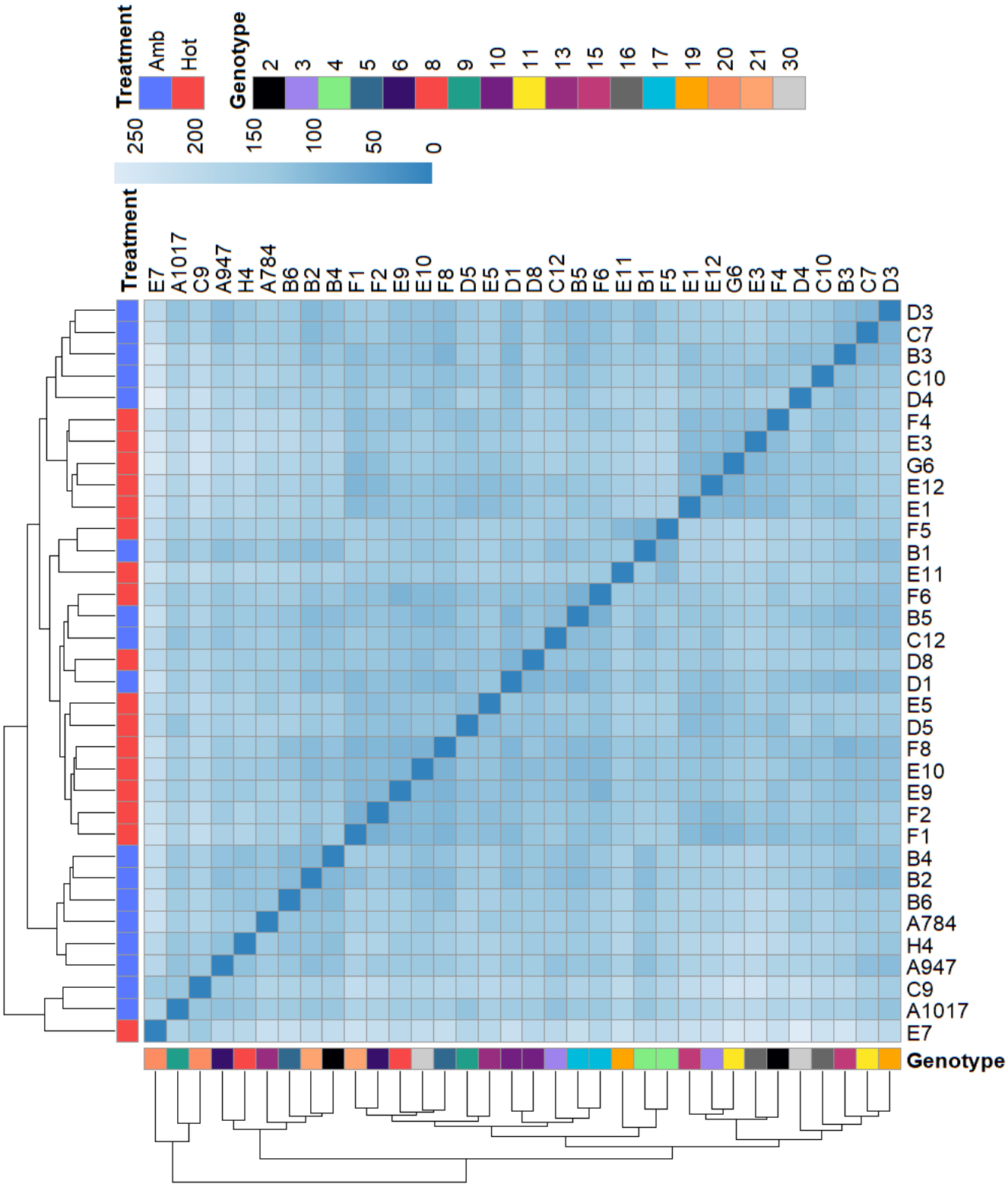

Supplementary Figure C.6.2 Sample-Sample distance matrix based on 34 samples after exclusion of outliers and unpaired samples.

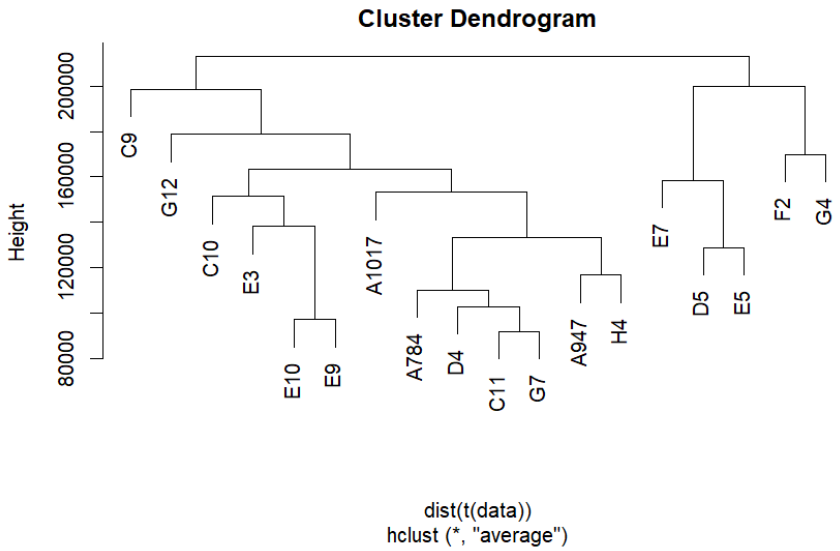

Supplementary Figure C.7.1 Cluster dendrogram of samples included in the WGCNA. No samples were identified as outliers.

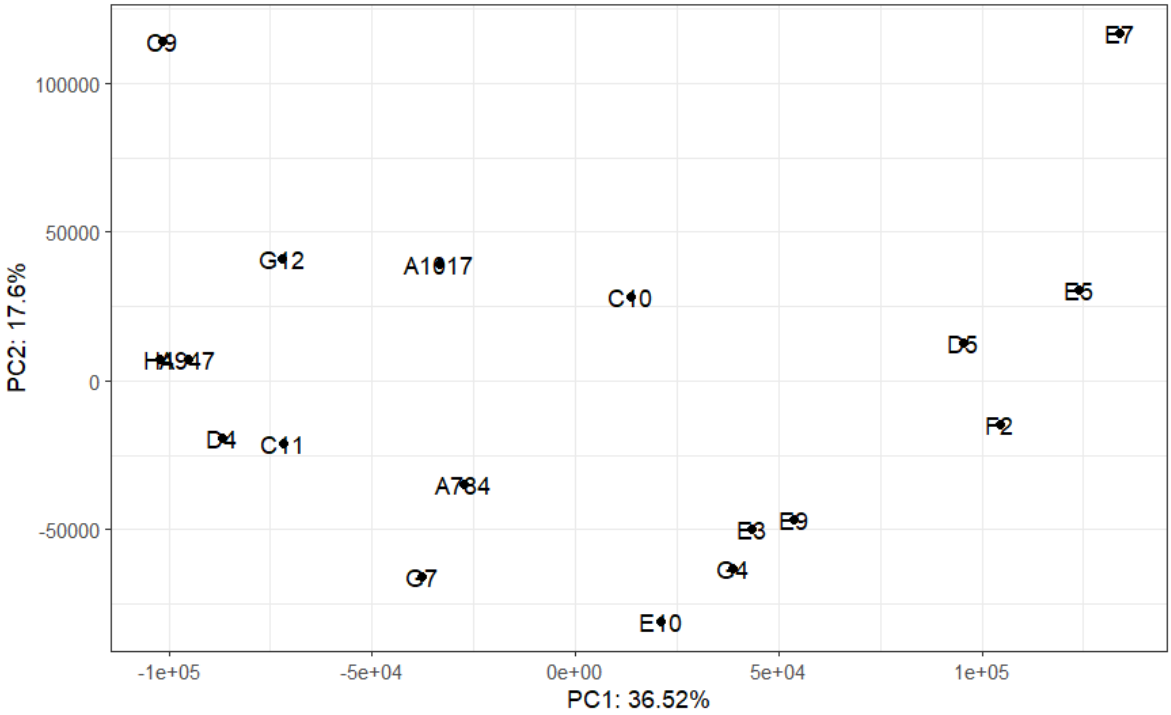

Supplementary Figure C.7.2 PCA of samples included in the WGCNA. No samples were identified as outliers.

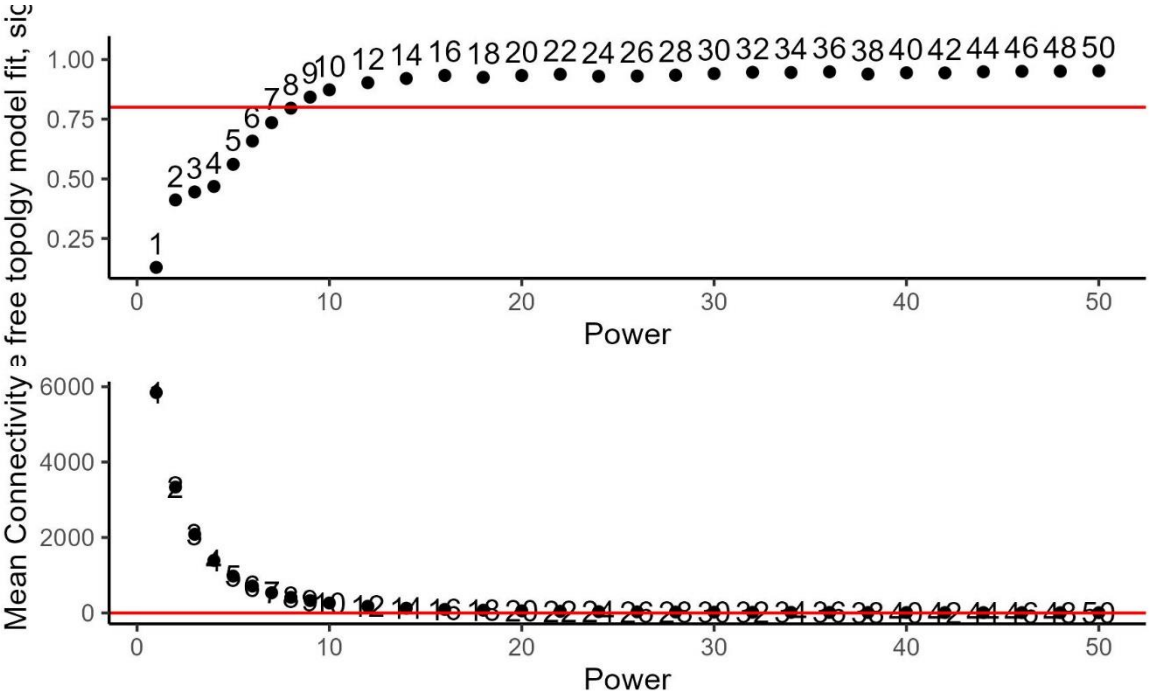

Supplementary Figure C.7.3 Soft threshold power selection for the WGCNA. Top = free topology where red line indicates that this is greater than 0.8. Bottom = mean connectivity of the model where the red line indicates that this value is < 0.1.

Supplementary material C.8 Physiological responses to acute heat stress across treatments

Photosynthetic performance and tissue colour change showed significant effects of heating 24h after the end of thermal stress (Supplementary Figure C.8.A and C.8.B). The initial coral tissue colour was significantly lower in the 30ºC treatment than in the other four treatments (df =1165, z = 108.23, p < 0.0001. Supplementary Figure C.8.C). After 24 h, colour change was significantly affected by temperature treatment (df = 4, F = 544.15, p < 0.0001, Supplementary Figure C.8.A), with corals exposed to the highest treatment (35.5 ºC) showing the greatest decline colour. Similarly, photosynthetic efficiency (F_v/F_m) was also significantly reduced in the extreme treatment (Wald's test, df = 4, F = 489, p < 0.001, Supplementary Figure C.8.B) but there were no effects of heating on F_v/F_m in any of the other treatments. Raw F_v/F_m values per fragment are shown in C.

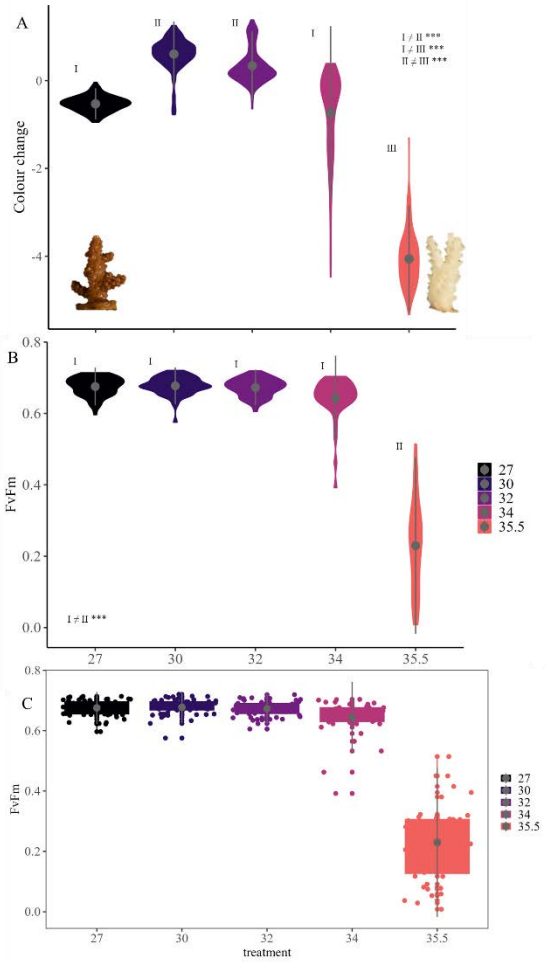

Supplementary Figure C.8. Colony-level variation in physiological responses to acute heat stress 24h after heating. A) Tissue colour change (final – initial colour score) and B) maximum photochemical efficiency (F_v/F_m) show violin plots of responses across five treatments. C) The raw Fv/Fm data points. Grey circles show the treatment means and the whiskers indicate the interquartile range. Roman numerals indicate post-hoc comparisons between treatments with Bonferroni adjustments for multiple comparisons. Asterisks show significance level (p < 0.05 *, p < 0.001 **, p < 0.0001 ***). Inserts on A) show fragments of mean colour score at ambient (5.06 ± 0.05) and 35.5ºC treatment (1.41 ± 0.06).

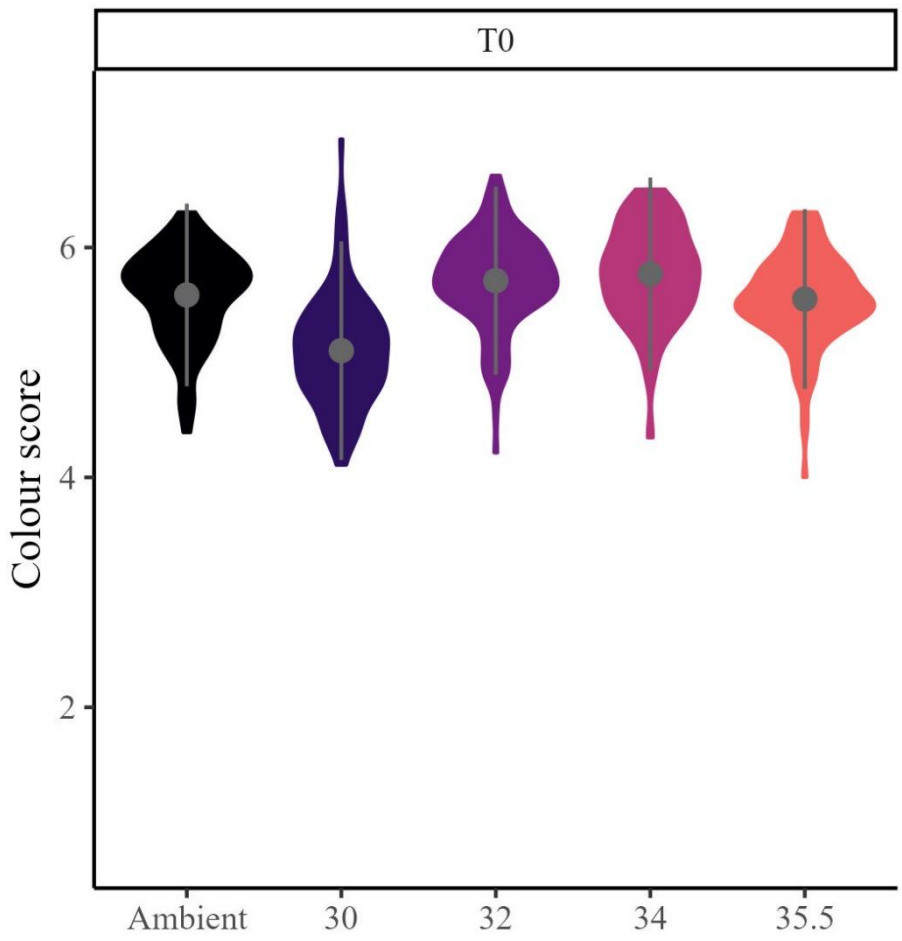

Supplementary Figure C.8.C Initial colour score differed significantly between treatments, with the 30°C treatment recording a much lower starting colour than the other four treatments.

Supplementary material C. 9 Colour change differed between treatments.

Initial colour score differed in the 30C treatment, so therefore it was necessary to use colour change for all subsequent analyses.

```
 Family: gaussian  ( identity )
Formula:          T0.colour.score ~ Treatment + (1 | Tank)
Data: dat

     AIC      BIC   logLik deviance df.resid
  1662.5   1698.0   -824.3   1648.5     1165

Random effects:

Conditional model:
 Groups   Name        Variance Std.Dev.
 Tank     (Intercept) 0.006703 0.08187
 Residual             0.233323 0.48304
Number of obs: 1167, groups:  Tank, 20

Dispersion estimate for gaussian family (sigma^2): 0.233

Conditional model:
              Estimate Std. Error z value Pr(>|z|)
(Intercept)    5.58689    0.05162  108.23  < 2e-16 ***
Treatment30   -0.49776    0.07315   -6.80 1.01e-11 ***
Treatment32    0.12049    0.07306    1.65   0.0991 .
Treatment34    0.18449    0.07306    2.53   0.0116 *
Treatment35.5 -0.04293    0.07312   -0.59   0.5571
---
Signif. codes:  0 ‘***’ 0.001 ‘**’ 0.01 ‘*’ 0.05 ‘.’ 0.1 ‘ ’ 1
# R2 for Mixed Models
```

Relative colour change across all treatments at 24h.

```
> summary(Col_lme)
Linear mixed-effects model fit by REML
  Data: dat

Random effects:
 Formula: ~1 | Tank
        (Intercept)  Residual
StdDev:   0.1349839 0.5639907

Fixed effects:  T0.T24h.colour.change ~ Treatment
 Correlation:
              (Intr) Trtm30 Trtm32 Trtm34
Treatment30   -0.706
Treatment32   -0.706  0.499
Treatment34   -0.707  0.499  0.499
Treatment35.5 -0.706  0.498  0.499  0.499

Standardized Within-Group Residuals:
        Min          Q1         Med          Q3         Max
-6.73679396 -0.38339462  0.02516243  0.46177050  4.91937014

Number of Observations: 868
Number of Groups: 20
```

	numDF <int>	denDF <dbl>	F-value <chr>	p-value <chr>
(Intercept)	1	848	600.5147	<.0001
Treatment	4	15	544.1532	<.0001

```
> # emmeans for treatment comparisons
> marginal = emmeans(Col_lme, ~ Treatment)
> pairs(marginal, adjust="tukey")
 contrast       estimate    SE df t.ratio p.value
 Ambient - 30     -1.127 0.113 15  -9.975  <.0001
 Ambient - 32     -0.870 0.113 15  -7.708  <.0001
 Ambient - 34      0.205 0.113 15   1.814  0.4014
 Ambient - 35.5    3.532 0.113 15  31.253  <.0001
 30 - 32           0.257 0.113 15   2.272  0.2074
 30 - 34           1.332 0.113 15  11.778  <.0001
 30 - 35.5         4.659 0.113 15  41.158  <.0001
 32 - 34           1.075 0.113 15   9.514  <.0001
 32 - 35.5         4.402 0.113 15  38.921  <.0001
 34 - 35.5         3.327 0.113 15  29.415  <.0001

Degrees-of-freedom method: containment
P value adjustment: tukey method for comparing a family of 5 estimates
> cld(marginal, alpha=0.05, Letters=letters, adjust="bonferroni")
 Treatment emmean     SE df lower.CL upper.CL .group
 35.5      -4.061 0.0800 15   -4.297   -3.825  a
 34        -0.734 0.0799 15   -0.970   -0.499   b
 Ambient   -0.529 0.0798 19   -0.758   -0.301   b
 32         0.341 0.0799 15    0.105    0.576    c
 30         0.598 0.0801 15    0.362    0.834    c

Degrees-of-freedom method: containment
Confidence level used: 0.95
Conf-level adjustment: bonferroni method for 5 estimates
P value adjustment: bonferroni method for 10 tests
significance level used: alpha = 0.05
```

Supplementary material C. 10 Colour change statistics for genotype effect in the 34ºC and ambient treatment.

34 ºC

	numDF <int>	denDF <dbl>	F-value <chr>	p-value <chr>
(Intercept)	1	136	272.94641	<.0001
Genotype_ID	29	136	37.55863	<.0001

2 rows

```
Degrees-of-freedom method: containment
P value adjustment: tukey method for comparing a family of 30 estimates
 Genotype_ID   emmean    SE df lower.CL upper.CL .group
 16          -3.65527 0.154  3    -5.32   -1.986  a
 13          -2.41541 0.154  3    -4.09   -0.746   b
 20          -2.07515 0.154  3    -3.74   -0.405   bc
 3           -1.92800 0.154  3    -3.60   -0.258   bc
 6           -1.51573 0.154  3    -3.19    0.154    cd
 2           -1.46036 0.154  3    -3.13    0.209    cd
 9           -1.37273 0.168  3    -3.19    0.448    cde
 11          -1.36037 0.154  3    -3.03    0.309    cd
 28          -1.29384 0.154  3    -2.96    0.376    cde
 15          -1.19854 0.168  3    -3.02    0.623    cdef
 23          -1.02312 0.168  3    -2.84    0.798     defg
 19          -0.49192 0.154  3    -2.16    1.178      efgh
 12          -0.39312 0.154  3    -2.06    1.277       fgh
 31          -0.30393 0.168  3    -2.13    1.522       fgh
 7           -0.29302 0.154  3    -1.96    1.377        gh
 21          -0.28504 0.154  3    -1.95    1.385        gh
 24          -0.26026 0.154  3    -1.93    1.409        gh
 22          -0.20602 0.168  3    -2.03    1.615        gh
 14          -0.20419 0.168  3    -2.03    1.622        gh
 5           -0.17828 0.154  3    -1.85    1.491        gh
 18          -0.07335 0.168  3    -1.89    1.748         h
 1            0.00559 0.154  3    -1.66    1.675         h
 30           0.01726 0.186  3    -2.01    2.043         h
 8            0.02306 0.168  3    -1.80    1.849         h
 17           0.02907 0.154  3    -1.64    1.699         h
 29           0.02987 0.154  3    -1.64    1.700         h
 4            0.05132 0.154  3    -1.62    1.721         h
 10           0.11259 0.168  3    -1.71    1.934         h
 25           0.12879 0.154  3    -1.54    1.798         h
 27           0.13460 0.154  3    -1.54    1.804         h

Degrees-of-freedom method: containment
Confidence level used: 0.95
Conf-level adjustment: bonferroni method for 30 estimates
P value adjustment: bonferroni method for 435 tests
significance level used: alpha = 0.05
NOTE: If two or more means share the same grouping symbol,
      then we cannot show them to be different.
      But we also did not show them to be the same.
```

No significant genotype effect in **ambient** colour change after 24 hours

```
Linear mixed-effects model fit by REML
  Data: dat24amb

Random effects:
 Formula: ~1 | Tank
        (Intercept)  Residual
StdDev:   0.0997004 0.1856031

Fixed effects:  (T0.T24h.colour.change) ~ Genotype_ID
 Correlation:
              (Intr) Gn_ID2 Gn_ID3 Gn_ID4 Gn_ID5 Gn_ID6 Gn_ID7 Gn_ID8 Gn_ID9 G_ID10 G_ID11 G_ID12
Genotype_ID2  -0.675
Genotype_ID3  -0.662  0.508
Genotype_ID4  -0.675  0.535  0.508
Genotype_ID5  -0.661  0.505  0.499  0.505
Genotype_ID6  -0.650  0.482  0.490  0.482  0.492
```

	numDF <int>	denDF <dbl>	F-value <chr>	p-value <chr>
(Intercept)	1	26	94.67044	<.0001
Genotype_ID	29	26	1.39218	0.1985

Supplementary material C.11 F_q'/F_m' statistics for treatment effect after 24 hours.

	numDF <int>	denDF <dbl>	F-value <chr>	p-value <chr>
(Intercept)	1	239	25269.568	<.0001
treatment	4	15	489.008	<.0001

```
> marginal = emmeans(FvFm_lme, ~ treatment)
> pairs(marginal, adjust="bonferroni")
 contrast                    estimate     SE df t.ratio p.value
 treatment27 - treatment30   -0.00194 0.0113 15  -0.172  1.0000
 treatment27 - treatment32    0.00260 0.0112 15   0.232  1.0000
 treatment27 - treatment34    0.03217 0.0119 15   2.703  0.1635
 treatment27 - treatment35.5  0.44579 0.0120 15  37.220  <.0001
 treatment30 - treatment32    0.00454 0.0114 15   0.398  1.0000
 treatment30 - treatment34    0.03411 0.0121 15   2.822  0.1287
 treatment30 - treatment35.5  0.44773 0.0122 15  36.815  <.0001
 treatment32 - treatment34    0.02957 0.0120 15   2.456  0.2670
 treatment32 - treatment35.5  0.44319 0.0121 15  36.587  <.0001
 treatment34 - treatment35.5  0.41362 0.0127 15  32.445  <.0001

Degrees-of-freedom method: containment
P value adjustment: bonferroni method for 10 tests
> cld(marginal, alpha=0.05, Letters=letters, adjust="bonferroni")
 treatment emmean      SE df lower.CL upper.CL .group
 35.5       0.230 0.00906 15    0.203    0.256  a
 34         0.643 0.00896 15    0.617    0.670   b
 32         0.673 0.00804 15    0.649    0.696   b
 27         0.675 0.00783 19    0.653    0.698   b
 30         0.677 0.00811 15    0.653    0.701   b

Degrees-of-freedom method: containment
Confidence level used: 0.95
Conf-level adjustment: bonferroni method for 5 estimates
P value adjustment: bonferroni method for 10 tests
significance level used: alpha = 0.05
```

Supplementary Material C.12 F_q'/F_m' statistics for genotype effect in the 34ºC treatment.

	numDF <int>	denDF <dbl>	F-value <chr>	p-value <chr>
(Intercept)	1	17	50459.76	<.0001
genotype	22	17	6.96	1e-04

2 rows

genotype	emmean	SE	df	lower.CL	upper.CL	.group
20	0.549	0.0125	3	0.425	0.672	a
17	0.615	0.0125	3	0.491	0.739	ab
25	0.622	0.0125	3	0.498	0.746	ab
31	0.623	0.0125	3	0.499	0.747	ab
13	0.626	0.0125	3	0.502	0.750	ab
16	0.630	0.0177	3	0.455	0.805	ab
10	0.638	0.0125	3	0.514	0.762	b
7	0.644	0.0125	3	0.520	0.768	b
3	0.646	0.0125	3	0.523	0.770	b
2	0.655	0.0125	3	0.532	0.779	b
22	0.657	0.0125	3	0.533	0.781	b
23	0.661	0.0126	3	0.536	0.786	b
1	0.664	0.0125	3	0.540	0.788	b
11	0.666	0.0125	3	0.542	0.790	b
6	0.669	0.0125	3	0.545	0.793	b
9	0.673	0.0176	3	0.498	0.848	b
14	0.676	0.0125	3	0.552	0.799	b
24	0.676	0.0125	3	0.552	0.800	b
27	0.681	0.0125	3	0.557	0.805	b
8	0.687	0.0125	3	0.563	0.811	b
5	0.694	0.0125	3	0.570	0.817	b
18	0.695	0.0125	3	0.571	0.819	b
30	0.704	0.0176	3	0.529	0.879	b

```
Degrees-of-freedom method: containment
Confidence level used: 0.95
Conf-level adjustment: bonferroni method for 23 estimates
P value adjustment: bonferroni method for 253 tests
significance level used: alpha = 0.05
NOTE: If two or more means share the same grouping symbol,
      then we cannot show them to be different.
      But we also did not show them to be the same.
```

Supplementary Material C.13 Buoyant weight changes across treatments at 10 days and 5 weeks post heating.

10 Days

	numDF <int>	denDF <dbl>	F-value <chr>	p-value <chr>
(Intercept)	1	136	19.47925	<.0001
Treatment	3	84	13.61813	<.0001

```
$emmeans
 Treatment    emmean       SE df  lower.CL  upper.CL
 Ambient    0.000110 8.33e-05 87 -5.55e-05  2.75e-04
 30         0.000454 8.30e-05 84  2.89e-04  6.19e-04
 32         0.000398 8.44e-05 84  2.31e-04  5.66e-04
 34        -0.000205 8.10e-05 84 -3.66e-04 -4.37e-05

Degrees-of-freedom method: containment
Confidence level used: 0.95

$contrasts
 contrast      estimate       SE df t.ratio p.value
 Ambient - 30 -3.44e-04 0.000118 84  -2.927  0.0224
 Ambient - 32 -2.88e-04 0.000119 84  -2.433  0.0787
 Ambient - 34  3.15e-04 0.000116 84   2.709  0.0400
 30 - 32       5.58e-05 0.000118 84   0.471  0.9652
 30 - 34       6.59e-04 0.000116 84   5.679  <.0001
 32 - 34       6.03e-04 0.000117 84   5.156  <.0001

Degrees-of-freedom method: containment
P value adjustment: tukey method for comparing a family of 4 estimates
```

No difference in weight changes between treatments after 5 weeks

	numDF <int>	denDF <dbl>	F-value <chr>	p-value <chr>
(Intercept)	1	136	35.27831	<.0001
Treatment	3	84	1.04392	0.3775

Summary table for weight changes

Variable	Treatment	N	Mean	Std	SE
Mass change, 10 days	Ambient	54	$1.26 * 10^{-4}$	$3.50 * 10^{-4}$	$0.96 * 10^{-4}$
	30	52	$4.46 * 10^{-4}$	$4.44 * 10^{-4}$	$0.62 * 10^{-4}$
	32	58	$4.82 * 10^{-4}$	$5.40 * 10^{-4}$	$0.71 * 10^{-4}$
	34	60	$-1.78 * 10^{-4}$	$3.27 * 10^{-4}$	$0.42 * 10^{-4}$
5 weeks	Ambient	54	$0.89 * 10^{-4}$	$1.61 * 10^{-4}$	$0.22 * 10^{-4}$
	30	52	$1.52 * 10^{-4}$	$1.39 * 10^{-4}$	$0.19 * 10^{-4}$
	32	58	$0.96 * 10^{-4}$	$1.34 * 10^{-4}$	$0.18 * 10^{-4}$
	34	60	$1.05 * 10^{-4}$	$2.51 * 10^{-4}$	$0.32 * 10^{-4}$

Supplementary material C. 14 Buoyant weight changes differed between genotypes in the 34°C treatment 10 days after heating.

	numDF <int>	denDF <dbl>	F-value <chr>	p-value <chr>
(Intercept)	1	27	1.778480	0.1935
Genotype_ID	29	27	2.212974	0.0206

```
Degrees-of-freedom method: containment
P value adjustment: tukey method for comparing a family of 30 estimates
> cld(marginal, alpha=0.05, Letters=letters, adjust="bonferroni")
 Genotype_ID    emmean      SE df lower.CL upper.CL .group
 11          -5.89e-04 0.00018  3 -0.00254  0.00137  a
 6           -4.57e-04 0.00018  3 -0.00242  0.00150  a
 13          -4.43e-04 0.00018  3 -0.00240  0.00152  ab
 2           -3.28e-04 0.00018  3 -0.00228  0.00162  ab
 9           -3.23e-04 0.00018  3 -0.00228  0.00164  ab
 16          -2.73e-04 0.00018  3 -0.00223  0.00168  ab
 4           -2.67e-04 0.00018  3 -0.00223  0.00169  ab
 1           -2.63e-04 0.00018  3 -0.00222  0.00169  ab
 17          -2.57e-04 0.00018  3 -0.00222  0.00170  ab
 12          -2.55e-04 0.00018  3 -0.00221  0.00170  ab
 15          -2.45e-04 0.00018  3 -0.00220  0.00171  ab
 7           -2.43e-04 0.00018  3 -0.00220  0.00171  ab
 28          -2.08e-04 0.00018  3 -0.00217  0.00175  ab
 21          -1.99e-04 0.00018  3 -0.00216  0.00176  ab
 10          -1.94e-04 0.00018  3 -0.00215  0.00176  ab
 29          -1.86e-04 0.00018  3 -0.00214  0.00177  ab
 22          -1.85e-04 0.00018  3 -0.00214  0.00177  ab
 18          -1.57e-04 0.00018  3 -0.00211  0.00180  ab
 19          -1.50e-04 0.00018  3 -0.00211  0.00181  ab
 30          -1.39e-04 0.00018  3 -0.00209  0.00182  ab
 23          -1.31e-04 0.00018  3 -0.00209  0.00182  ab
 24          -1.17e-04 0.00018  3 -0.00208  0.00184  ab
 25          -9.97e-05 0.00018  3 -0.00205  0.00185  ab
 14          -7.68e-05 0.00018  3 -0.00203  0.00188  ab
 20          -7.13e-05 0.00018  3 -0.00203  0.00189  ab
 3           -6.35e-05 0.00018  3 -0.00202  0.00189  ab
 5           -2.78e-05 0.00018  3 -0.00198  0.00193  ab
 27          -5.78e-06 0.00018  3 -0.00196  0.00195  ab
 8            5.57e-05 0.00018  3 -0.00190  0.00201  ab
 31           2.29e-04 0.00018  3 -0.00173  0.00219   b

Degrees-of-freedom method: containment
Confidence level used: 0.95
Conf-level adjustment: bonferroni method for 30 estimates
P value adjustment: bonferroni method for 435 tests
significance level used: alpha = 0.05
NOTE: If two or more means share the same grouping symbol,
      then we cannot show them to be different.
      But we also did not show them to be the same.
```

Supplementary material C. 15 Statistical outputs for assessment of ED50 between genotypes.

ED50 emmeans outputs

	Estimate	Std. Error	Lower	Upper	genotype
e:1:50	35.33688	0.04330695	35.25084	35.42292	1
e:2:50	35.32119	0.04356988	35.23463	35.40775	2
e:3:50	35.28899	0.04420945	35.20116	35.37682	3
e:5:50	35.47674	0.04424833	35.38883	35.56464	5
e:6:50	35.11664	0.04960644	35.01808	35.21519	6
e:7:50	34.83686	0.06312143	34.71146	34.96227	7
e:8:50	35.51657	0.04551915	35.42614	35.60700	8
e:9:50	35.44929	0.04437994	35.36112	35.53746	9
e:10:50	35.29443	0.04419666	35.20663	35.38224	10
e:11:50	35.05773	0.05232411	34.95378	35.16168	11
e:13:50	35.23763	0.04584249	35.14655	35.32870	13
e:14:50	35.27036	0.04425883	35.18243	35.35829	14
e:16:50	35.49314	0.04518124	35.40338	35.58290	16
e:17:50	35.25962	0.04533552	35.16955	35.34969	17
e:18:50	35.64994	0.05291918	35.54481	35.75507	18
e:20:50	34.82233	0.07352506	34.67626	34.96840	20
e:22:50	34.91316	0.05942151	34.79511	35.03121	22
e:23:50	35.44883	0.04375273	35.36190	35.53575	23
e:24:50	34.79527	0.06131867	34.67345	34.91709	24
e:25:50	35.07484	0.05295978	34.96963	35.18006	25
e:27:50	35.29665	0.04369760	35.20984	35.38346	27
e:30:50	35.74304	0.06120083	35.62145	35.86462	30
e:31:50	35.43622	0.04373099	35.34935	35.52310	31

Supplementary material C. 16 Minimum saturating intensities (E_k) did not differ between genotypes within the 34°C treatment 24 h after heat stress.

	numDF <int>	denDF <dbl>	F-value <chr>	p-value <chr>
(Intercept)	1	21	60.26949	<.0001
genotype	22	21	1.09797	0.4166

Supplementary material C. 17. There were no significant differences in rank-normalised PM scores between genotypes.

```
> # Wald Test for terms within model
> anova(modelTT)
Analysis of Variance Table

Response: Rank_norm
            Df Sum Sq  Mean Sq F value  Pr(>F)
Genotype_ID 29 3.2104 0.110703  1.4995 0.08251 .
Residuals   76 5.6108 0.073827
---
Signif. codes:  0 ‘***’ 0.001 ‘**’ 0.01 ‘*’ 0.05 ‘.’ 0.1 ‘ ’ 1
```

Supplementary figure C17.b Correlation between physiological trait across genotypes. Correlations were spearman rank correlations and performed on the genotype trait values from the 34ºC treatment at 24 h post heating, except for weight changes which represent data collected 10 days post heating.

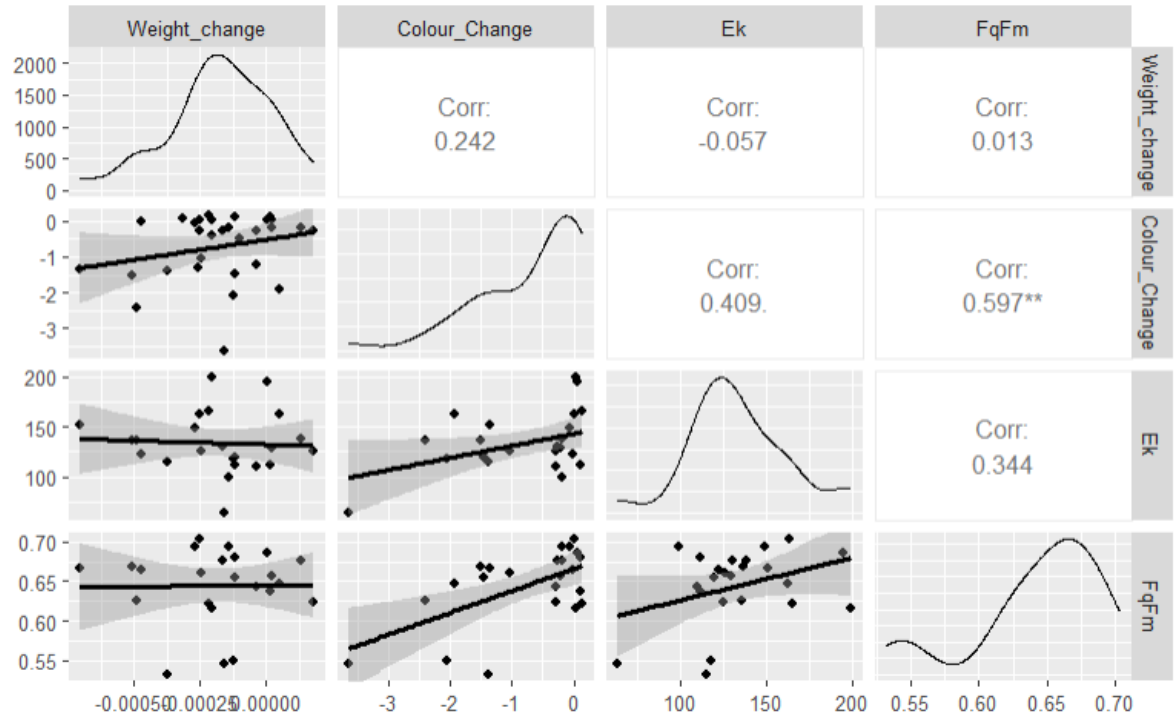

Supplementary Material C. 18 Krona output from KrakenUniq

Component	Mean % of reads	SE
Acorpora tenuis	64	1.39
Cladocopium goreaui	18.23	0.72
No hits	14.14	0.58
Bacteria	0.23	0.086
viruses	0.012	0.001
Breviolum mintum	0.89	0.025
Fugacium kawagutii	0.69	0.025
Durusdinium trenchii	0.56	0.023
Symbiodinium microadriaticum	0.196	0.0095

2 samples showing presence of human reads (G8 shown below, and G10 which also had high bacteria content).

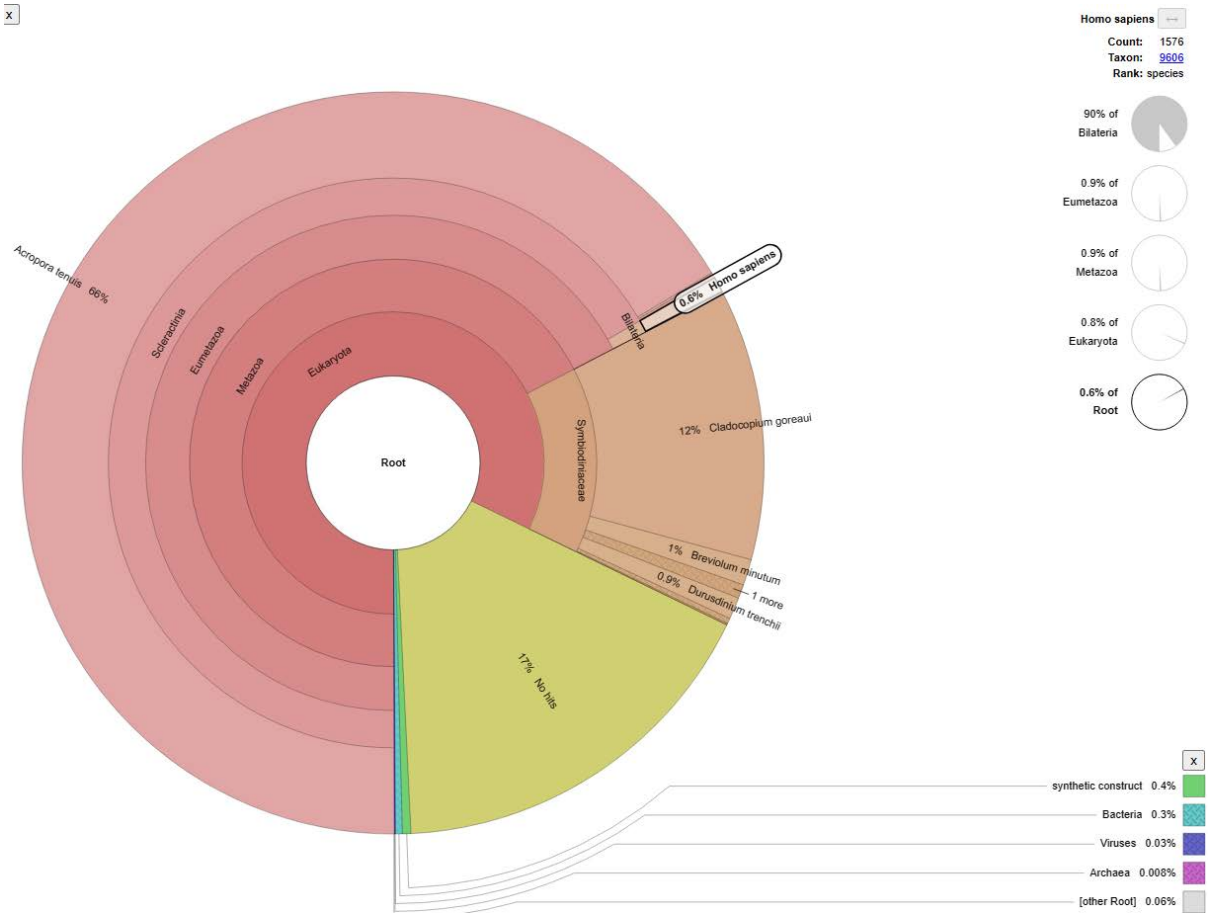

Sample G10 high (4%) content of bacteria

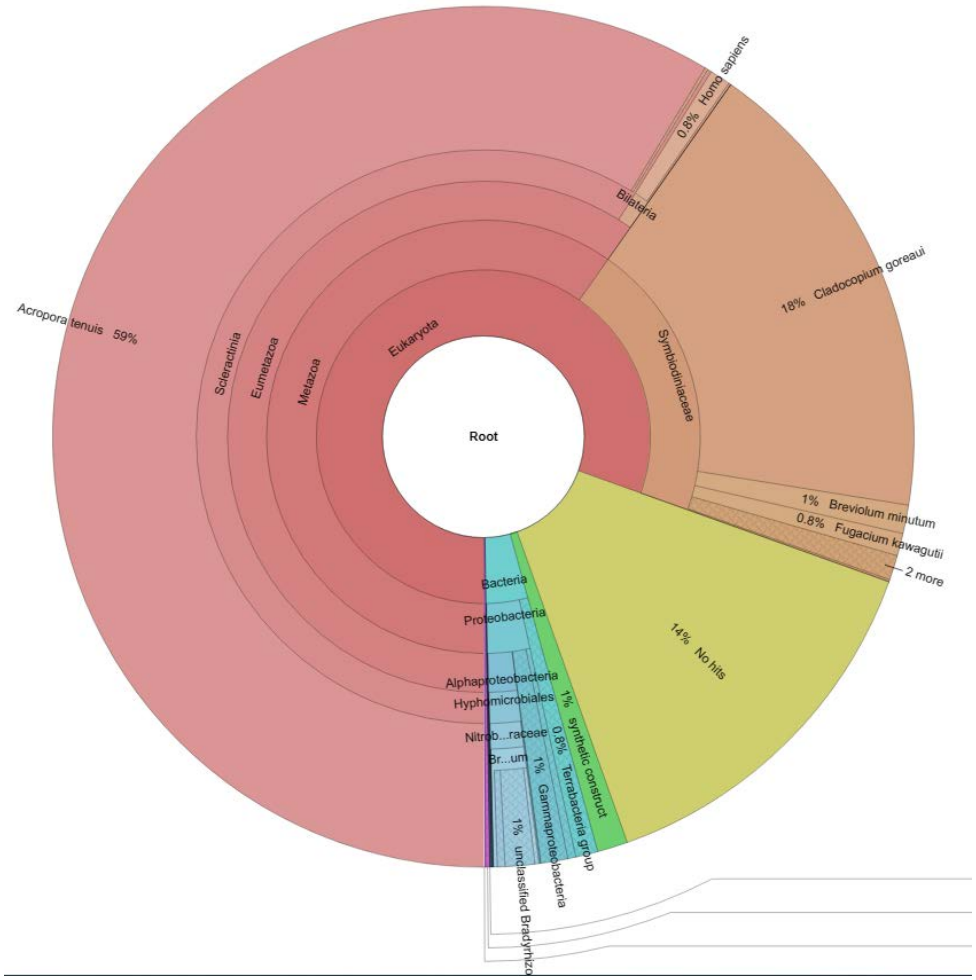
Root
Eukaryota
Metazoa
Eumetazoa
Scleractinia
Acropora tenuis 59%
Bilateria
Homo sapiens
0.8%
Symbiodiniaceae
18% Cladocopium goreaui
1% Breviolum minutum
0.8% Fugacium kawagutii
2 more
14% No hits
Bacteria
Proteobacteria
Alphaproteobacteria
Hyphomicrobiales
Nitrob...raceae
Br...um
1% unclassified Bradyrhizo
1% Gammaproteobacteria
0.8% Terrabacteria group
1% synthetic construct

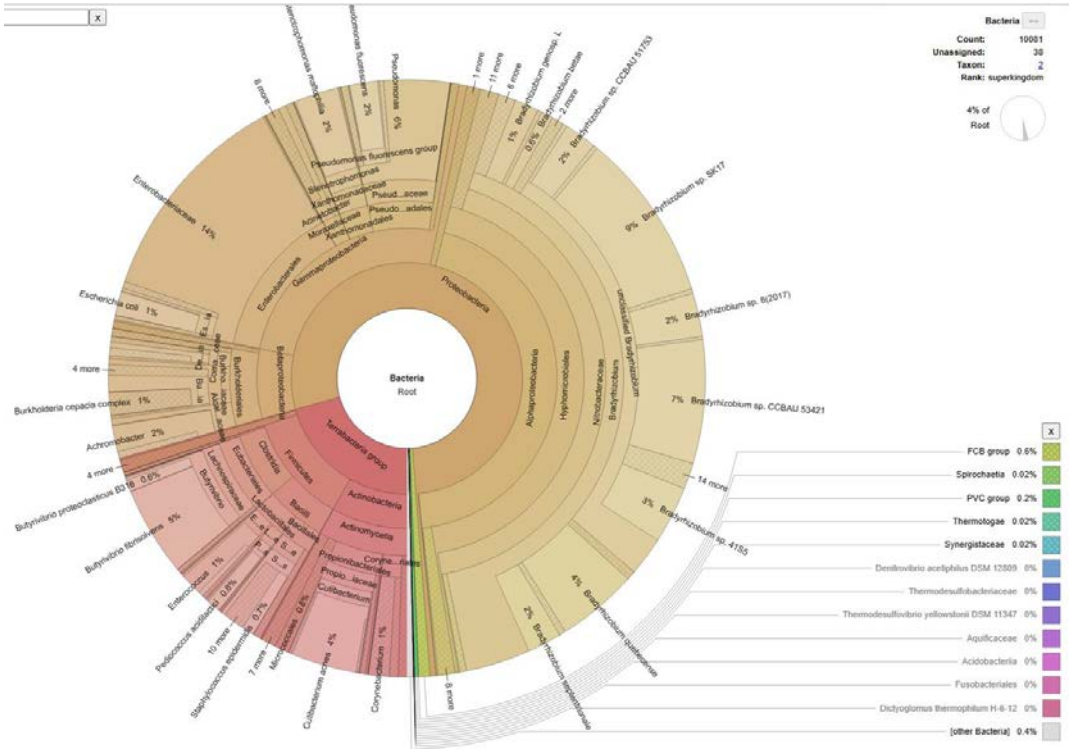
Bacteria
Root
Count: 10081
Unassigned: 38
Taxon: 2
Rank: superkingdom
4% of Root
Proteobacteria
Alphaproteobacteria
Hyphomicrobiales
Nitrobacteraceae
Bradyrhizobium
unclassified Bradyrhizobium
Terrabacteria group
Firmicutes
Bacilli
Bacillales
Actinobacteria
Actinomycetia
Enterobacteriales
Enterobacteriaceae 14%
Gammaproteobacteria
Pseudomonas 6%
Pseudomonas fluorescens group
Burkholderiales
Burkholderia cepacia complex 1%
Achromobacter 2%
Bradyrhizobium sp. SK17
Bradyrhizobium sp. BI(2017)
Bradyrhizobium sp. CCBAU 53421
Bradyrhizobium sp. 4155
Bradyrhizobium guangdongense
Bradyrhizobium liaoningense
Bradyrhizobium sp. CCBAU 51753
14 more
FCB group 0.6%
Spirochaetia 0.02%
PVC group 0.2%
Thermotogae 0.02%
Synergistaceae 0.02%
Denitrovibrio acetiphilus DSM 12809 0%
Thermodesulfobacteriaceae 0%
Thermodesulfovibrio yellowstonii DSM 11347 0%
Aquificaceae 0%
Acidobacteriia 0%
Fusobacteriales 0%
Dictyoglomus thermophilum H-6-12 0%
[other Bacteria] 0.4%

Supplementary Table C. 19 RNA library statistics

Item	Value	se
Mean reads per sample	47.265 million	± 1.017 million
Min reads	40.007 million	
Max reads	67.084 million	
Mean unique alignment	38.51 %	0.59 %
Max alignment rate	46.3 %	
Min alignment rate	26.0 %	

Supplementary material C. 20 Gene expression differences with respect to treatment

Supplementary Table C.20.1 Overview of number of differentially expressed genes after filtering low abundance genes.

Level	Description	# genes
Host	Total genes identified	13,293
	Upregulated	569
	Downregulated	266
Symbiont	Total genes identified	20,270
	Upregulated	17
	Downregulated	7

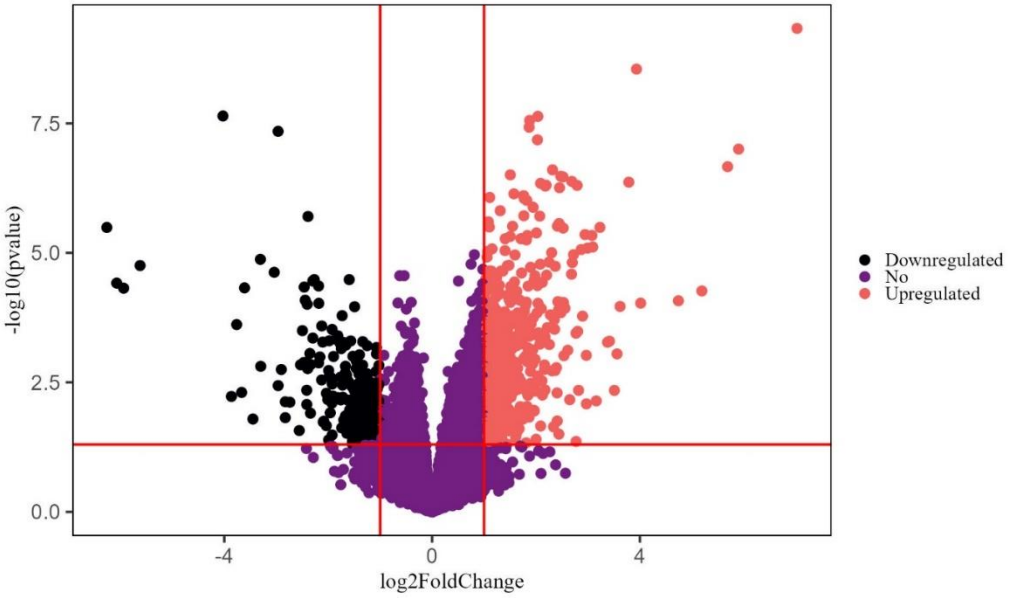

Supplementary Figure C.20.2 Combined volcano plot (both coral and symbiont DEGs).

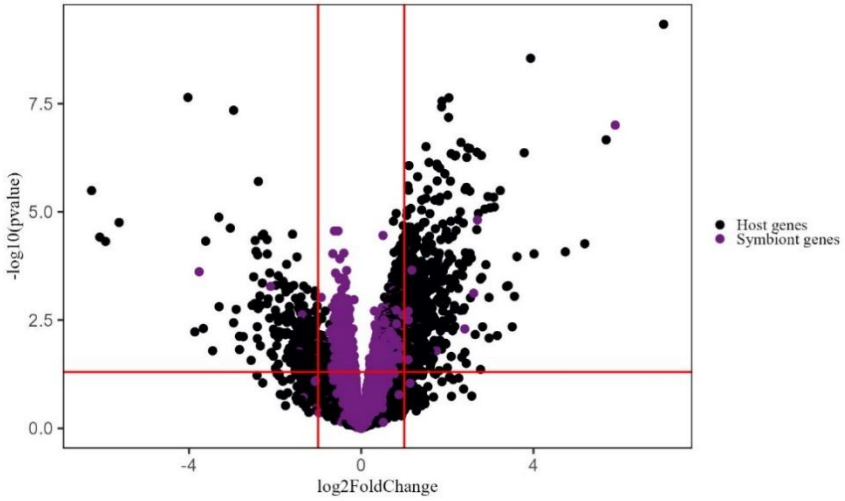

Supplementary Figure C.20.3 Combined volcano plot by gene origin.

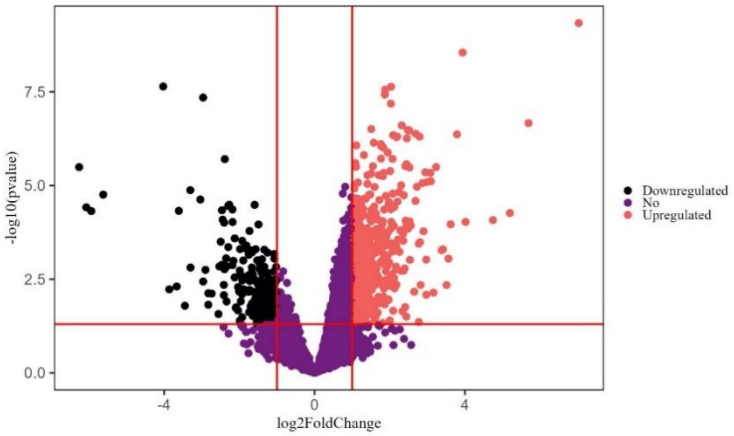

Supplementary Figure C.20.4 Host-read volcano plot.

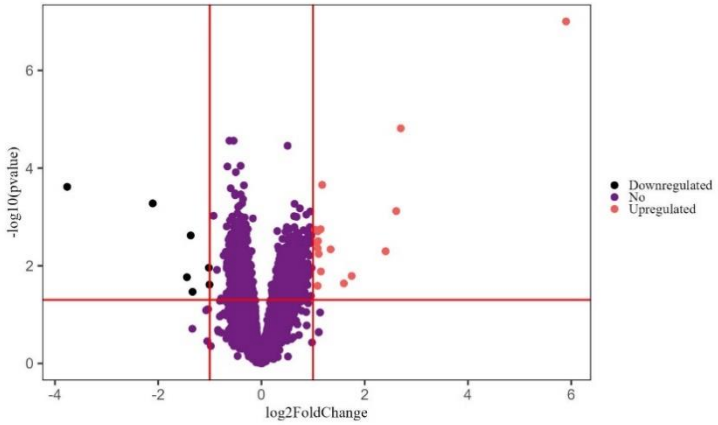

Supplementary Figure C.20.5 Symbiont-read volcano plot.

Supplementary Table C.21 Up- and downregulated host DEGs in response to treatment. A total of 609 contigs were included. Any contig without a Uniprot accession ID was excluded. The base mean, log2FoldChange (L2FC) and p value from DESeq() output is shown. Direction indicated whether gene was up- or downregulated in response to treatment. Finally, gene name is given for those where this information was available. If no gene name was available, the protein name was used instead (prefix ProteinName_).

Uniprot	baseMean	L2FC	p	Direction	gene name
Q9BZC7	680.97	1.01	0.0002	Up	ABCA2 ABC2 KIAA1062
Q8R420	2496.53	1.31	0.0000	Up	Abca3
O94929	99.53	1.14	0.0000	Up	ABLIM3 KIAA0843 HMFN1661
Q10751	141.19	-1.42	0.0138	Down	ACE DCP1
Q2UPB1	496.59	1.08	0.0132	Up	aclC AO090001000041
A5D6U8	425.27	-1.27	0.0169	Down	acp7 papl zgc:162913
P41216	1214.88	1.47	0.0015	Up	Acsl1 Acsl2 Facl2
P27041	643.16	1.02	0.0005	Up	acvr2b
Q61824	1250.06	1.14	0.0001	Up	Adam12 Mltna
Q9ZSK4	67.29	1.25	0.0066	Up	ADF3 At5g59880 MMN10.12
A6QLU6	31.00	1.38	0.0010	Up	ADGRD1 GPR133
Q8IZF6	375.70	1.05	0.0003	Up	ADGRG4 GPR112
O95490	841.14	1.33	0.0006	Up	ADGRL2 KIAA0786 LEC1 LPHH1 LPHN2
Q9HAR2	95.47	1.16	0.0018	Up	ADGRL3 KIAA0768 LEC3 LPHN3
Q9HAR2	333.31	1.18	0.0017	Up	ADGRL3 KIAA0768 LEC3 LPHN3
Q9HAR2	1242.89	1.29	0.0035	Up	ADGRL3 KIAA0768 LEC3 LPHN3
Q9HAR2	130.18	2.09	0.0000	Up	ADGRL3 KIAA0768 LEC3 LPHN3
Q6GNL7	744.83	1.09	0.0003	Up	aldh1l1
Q8K009	211.27	1.23	0.0004	Up	Aldh1l2
R1CW23	92.20	2.69	0.0000	Up	ALMA7 EMIHUDRAFT_114859
Q94K49	157.74	-1.73	0.0002	Down	ALP1 At3g63270 F16M2.120
Q9CXB8	267.77	1.64	0.0277	Up	Alpk1 Kiaa1527
P16157	52.45	1.65	0.0128	Up	ANK1 ANK
Q01484	629.00	1.28	0.0006	Up	ANK2 ANKB

Q5F478	102.98	2.17	0.0044	Up	ANKRD44 RCJMB04_2g14
Q99JG3	568.03	1.39	0.0014	Up	Anxa13
P36633	147.20	-1.13	0.0107	Down	Aoc1 Abp1
Q8NKE2	128.24	2.52	0.0000	Up	AOX1 CNAG_00162
P55088	1208.88	1.26	0.0006	Up	Aqp4
O43315	28.76	-1.20	0.0044	Down	AQP9 SSC1
B2RQE8	58.59	1.01	0.0028	Up	Arhgap42 Graf3
Q9FFU6	1165.46	1.18	0.0000	Up	At5g54830 MBG8_9
Q6NRQ1	138.91	-1.49	0.0001	Down	b3galnt2
O94766	29.08	-1.21	0.0286	Down	B3GAT3
Q91X34	130.42	3.62	0.0001	Up	Baat
Q497V6	581.49	1.50	0.0000	Up	Bahd1 Gm117 Kiaa0945
M9NDE3	55.28	1.22	0.0049	Up	bark aka CG3921
Q9XWB9	52.25	-1.55	0.0103	Down	bath-36 Y75B12B.4
Q9QYN5	376.43	1.45	0.0140	Up	Bcl10
Q9JJS6	1290.31	1.62	0.0002	Up	Bco1 Bcdo Bcdo1 Bcmo1
Q1IG70	748.22	-2.18	0.0013	Down	betA PSEEN0372
P80057	176.82	1.69	0.0093	Up	blaSE mpr BLi00340 BL01804
Q8K2J9	131.32	1.40	0.0003	Up	Btbd6
P21180	271.71	-1.19	0.0078	Down	C2
Q8UWA5	2899.76	-1.34	0.0005	Down	ca2
Q5VU97	242.19	1.77	0.0000	Up	CACHD1 KIAA1573 VWCD1
Q6PDJ1	143.64	2.16	0.0015	Up	Cachd1 Kiaa1573 Vwcd1
Q6PDJ1	258.25	2.18	0.0004	Up	Cachd1 Kiaa1573 Vwcd1
Q5VU97	308.79	2.25	0.0000	Up	CACHD1 KIAA1573 VWCD1
Q9VBW3	91.29	-1.11	0.0257	Down	Cad96Ca HD-14 CG10244
Q9VBW3	101.94	-1.07	0.0069	Down	Cad96Ca HD-14 CG10244
Q9VBW3	99.65	-1.04	0.0173	Down	Cad96Ca HD-14 CG10244
Q9VBW3	156.49	-1.03	0.0073	Down	Cad96Ca HD-14 CG10244
Q60431	828.91	2.41	0.0000	Up	CASP3 CPP32
P54965	945.38	-1.49	0.0124	Down	cbh CPE0709

Q8VC31	86.95	1.39	0.0026	Up	Ccdc9
P28648	777.85	-2.09	0.0177	Down	Cd63
P28648	664.57	1.73	0.0005	Up	Cd63
Q5VXM1	92.69	-1.36	0.0051	Down	CDCP2
Q8BQH6	49.16	1.15	0.0146	Up	Cdcp2
Q8BQH6	118.02	1.37	0.0023	Up	Cdcp2
Q9H251	78.61	1.13	0.0039	Up	CDH23 KIAA1774 KIAA1812 UNQ1894/PRO4340
Q6RT24	29.97	1.57	0.0234	Up	Cenpe
F1NPG5	51.47	-1.18	0.0217	Down	CENPT
Q6ZTR5	51.40	1.44	0.0005	Up	CFAP47 CHDC2 CXorf22 CXorf30 CXorf59
P04186	817.01	1.65	0.0017	Up	Cfb Bf H2-Bf
B2ZGJ1	205.69	1.15	0.0004	Up	chat
Q95M17	20.80	-1.91	0.0058	Down	CHIA
Q13231	217.14	-1.34	0.0090	Down	CHIT1
P9WMV9	2978.89	1.20	0.0092	Up	choD Rv3409c
P49582	86.74	1.83	0.0099	Up	Chrna7 Acra7
Q5IS75	144.44	1.13	0.0129	Up	CHRNB3
G5EBQ8	37.59	1.60	0.0013	Up	chs-2 F48A11.1
Q9UDT6	241.85	1.03	0.0058	Up	CLIP2 CYLN2 KIAA0291 WBSCR3 WBSCR4 WSCR4
Q7F0J0	869.94	2.37	0.0000	Up	CML13 Os07g0618800 LOC_Os07g42660 P0552F09.133 P0560B08.106
O23184	465.38	1.98	0.0000	Up	CML19 CEN2 At4g37010 AP22.11 C7A10.350
Q96M20	270.89	1.00	0.0232	Up	CNBD2 C20orf152
Q32L92	419.63	-1.13	0.0428	Down	CNN3
Q9UIV1	286.24	5.69	0.0000	Up	CNOT7 CAF1
P97846	101.24	1.04	0.0001	Up	Cntnap1 Caspr Nrxn4
O54991	270.81	-1.93	0.0003	Down	Cntnap1 Nrxn4
Q60847	34.00	1.20	0.0205	Up	Col12a1
P02466	3811.32	-1.22	0.0111	Down	Col1a2
Q17RW2	1975.48	-1.11	0.0171	Down	COL24A1
Q91VF6	91.16	-1.28	0.0072	Down	Col26a1 Col26a Emid2 Emu2

P08120	2184.97	1.05	0.0004	Up	Col4a1 Cg25C DCg1 CG4145
P12109	97.82	1.98	0.0011	Up	COL6A1
P15988	36.16	-1.63	0.0030	Down	COL6A2
P15989	410.13	1.33	0.0027	Up	COL6A3
A6NMZ7	2648.65	1.22	0.0003	Up	COL6A6
P34340	144.23	1.71	0.0006	Up	col-90 C29E4.1
Q5R5F2	57.97	-1.55	0.0072	Down	COPZ1 COPZ
P43510	108.07	-1.00	0.0192	Down	cpr-6 C25B8.3
Q9BSW2	134.16	1.01	0.0006	Up	CRACR2A EFCAB4B
Q80T79	206.72	1.02	0.0202	Up	Csmd3 Kiaa1894
Q62908	284.89	-1.30	0.0045	Down	Csrp2 Smlim
Q9TU53	159.51	-1.74	0.0240	Down	CUBN
O70244	176.91	-3.31	0.0000	Down	Cubn Ifcr
O70244	264.92	1.46	0.0001	Up	Cubn Ifcr
O73853	309.65	1.14	0.0163	Up	cyp17a1 cyp17
P05183	827.76	1.14	0.0001	Up	Cyp3a2 Cyp3a-2 Cyp3a11
Q9WVK8	38.21	1.27	0.0459	Up	Cyp46a1 Cyp46
Q964T1	228.15	1.09	0.0004	Up	CYP4C21
Q9Y4B6	149.50	1.21	0.0019	Up	DCAF1 KIAA0800 RIP VPRBP
Q9Y4B6	111.06	1.36	0.0019	Up	DCAF1 KIAA0800 RIP VPRBP
Q80TR8	161.81	1.46	0.0206	Up	Dcaf1 Kiaa0800 Vprbp
Q58A42	66.59	-1.33	0.0103	Down	DD3-3 DDB_G0283095
Q62371	1452.31	1.74	0.0002	Up	Ddr2 Ntrkr3 Tkt Tyro10
P04753	67.14	-1.16	0.0094	Down	DHFR
Q9Z207	953.03	1.08	0.0000	Up	Diaph3 Diap3
O42412	50.90	1.13	0.0205	Up	DIO3
Q9UBP4	73.82	-1.42	0.0041	Down	DKK3 REIC UNQ258/PRO295
P53454	389.86	1.33	0.0000	Up	dl
P09623	103.55	-1.11	0.0236	Down	DLD LAD
Q9UGM3	471.01	1.74	0.0038	Up	DMBT1 GP340
Q566X8	470.24	1.20	0.0002	Up	dmbx1b mbx2 zgc:112395

E9Q8T7	212.87	1.20	0.0005	Up	Dnah1 Dhc7 Dnahc1
Q2MHE5	323.40	1.02	0.0003	Up	Dok6
P31429	142.87	-1.41	0.0050	Down	DPEP1
P16444	176.61	-1.14	0.0178	Down	DPEP1 MDP RDP
Q4VSN2	174.92	2.26	0.0006	Up	dstyk ripk5
Q94464	177.70	-3.67	0.0049	Down	dymA DDB_G0277849
Q86Y13	1019.89	-2.19	0.0000	Down	DZIP3 KIAA0675
Q86Y13	55.84	1.19	0.0119	Up	DZIP3 KIAA0675
Q5THR3	190.77	1.08	0.0006	Up	EFCAB6 DJBP KIAA1672
P10079	212.34	1.36	0.0048	Up	EGF1
P10079	179.37	2.09	0.0220	Up	EGF1
Q8NDI1	135.20	1.42	0.0024	Up	EHBP1 KIAA0903 NACSIN
P41969	1619.43	1.19	0.0010	Up	Elk1
Q8IZ81	69.55	1.21	0.0008	Up	ELMOD2
Q28CX0	31.15	-1.08	0.0407	Down	elp6 tmem103 TTpA007a13.1
P09759	99.93	1.34	0.0403	Up	Ephb1 Elk Epth2
Q5BIM8	43.99	1.04	0.0004	Up	ERCC8
P29773	2168.02	1.42	0.0007	Up	ETS-2
Q06194	353.24	1.10	0.0006	Up	F8 Cf8 F8c
Q5RA50	649.26	1.49	0.0003	Up	FAM124A
Q5HY64	104.22	1.87	0.0122	Up	FAM47C
Q91VS8	94.59	1.26	0.0209	Up	Farp2 Kiaa0793
Q91VS8	79.23	1.68	0.0039	Up	Farp2 Kiaa0793
O94887	30.06	-1.43	0.0034	Down	FARP2 KIAA0793 PLEKHC3
Q14517	4692.28	1.03	0.0003	Up	FAT1 CDHF7 FAT
Q6V0I7	44.94	1.49	0.0002	Up	FAT4 CDHF14 FATJ Nbla00548
Q2PZL6	53.45	-1.77	0.0006	Down	Fat4 Fatj
P98133	171.98	-1.29	0.0347	Down	FBN1
Q96IG2	253.75	1.72	0.0000	Up	FBXL20 FBL2
Q7TSL3	184.37	1.21	0.0005	Up	Fbxo11

Q9UKT5	327.87	1.09	0.0001	Up	FBXO4 FBX4
P20693	143.06	-1.99	0.0019	Down	Fcer2 Fcer2a
B4J6M4	44.04	-2.42	0.0013	Down	Fen1 GH21157
Q6I6M7	167.62	1.01	0.0018	Up	fgf1 fgf-1
Q6I6M7	478.50	1.02	0.0003	Up	fgf1 fgf-1
Q7SIF8	517.61	1.20	0.0015	Up	fgf1 fgf-1
Q7SIF8	513.47	2.18	0.0000	Up	fgf1 fgf-1
Q9ESL9	321.83	1.34	0.0028	Up	Fgf20
P48804	807.35	1.10	0.0237	Up	FGF4 FGF-4
Q86PM4	3413.90	1.19	0.0003	Up	FGFR
P22607	3790.66	1.17	0.0002	Up	FGFR3 JTK4
A6QLR4	162.20	2.11	0.0029	Up	FLOT2
Q95V55	474.95	1.26	0.0012	Up	foxo Afx CG3143
Q6INU7	115.43	1.54	0.0026	Up	frrs1
Q96I24	98.60	-3.45	0.0161	Down	FUBP3 FBP3
E1BWM5	400.13	-1.55	0.0106	Down	FUNDC1
O93274	180.71	1.09	0.0132	Up	fzd8 fz8
P61315	68.20	-2.10	0.0184	Down	Gal3st3
O08726	75.09	1.26	0.0052	Up	Galr2 Galnr2
Q8MVR1	82.13	1.04	0.0298	Up	gbpC gefT rasGEFT DDB_G0291079
Q8MVR1	130.35	1.04	0.0108	Up	gbpC gefT rasGEFT DDB_G0291079
Q8MVR1	28.42	1.10	0.0397	Up	gbpC gefT rasGEFT DDB_G0291079
Q8MVR1	61.45	1.48	0.0051	Up	gbpC gefT rasGEFT DDB_G0291079
Q8MVR1	199.33	1.61	0.0004	Up	gbpC gefT rasGEFT DDB_G0291079
Q8MVR1	88.93	1.83	0.0092	Up	gbpC gefT rasGEFT DDB_G0291079
Q8MVR1	42.02	2.31	0.0019	Up	gbpC gefT rasGEFT DDB_G0291079
Q8IWJ2	32.98	1.21	0.0025	Up	GCC2 KIAA0336 RANBP2L4
Q5I3Q2	146.31	2.03	0.0024	Up	gdf-8
P43793	227.92	-1.52	0.0010	Down	gdhA HI_0189
Q3UPY5	73.17	1.04	0.0094	Up	Glb1l2
Q9H4G4	3552.27	1.10	0.0189	Up	GLIPR2 C9orf19 GAPR1

Q9H4G4	1407.42	1.17	0.0011	Up	GLIPR2 C9orf19 GAPR1
Q9H4G4	176.49	1.29	0.0000	Up	GLIPR2 C9orf19 GAPR1
Q9CYL5	250.14	-1.75	0.0007	Down	Glipr2 Gapr1
Q9CYL5	48.36	-1.05	0.0405	Down	Glipr2 Gapr1
Q8VDU0	38.01	1.82	0.0000	Up	Gpsm2 Lgn Pins
Q9JJA9	571.27	1.16	0.0004	Up	Grasp MNCb-4428
Q9SZJ2	641.78	1.94	0.0000	Up	GRDP2 At4g37900 F20D10.20
A4D2P6	240.39	1.04	0.0009	Up	GRID2IP
A0A1L8F5J9	35.44	-1.20	0.0053	Down	grin1
P28799	182.30	-2.83	0.0152	Down	GRN
P28799	262.38	-1.25	0.0315	Down	GRN
P28799	858.45	-1.05	0.0488	Down	GRN
Q5ZKH0	100.98	-1.07	0.0300	Down	GTF2H5 RCJMB04_10n20
A1Z6E0	2190.61	1.11	0.0012	Up	gus CG2944
Q7Z2Y8	110.00	-3.04	0.0000	Down	GVINP1 GVIN1 VLIG1
Q8BR93	40.83	1.49	0.0217	Up	Harbi1
P58308	243.64	1.10	0.0035	Up	Hcrtr2 Mox2r
V6CLA2	52.95	1.34	0.0331	Up	hecd-1 C34D4.14
Q6DFV5	124.57	1.35	0.0018	Up	Helz Kiaa0054
Q15751	34.81	1.31	0.0022	Up	HERC1
Q0V8S0	1119.95	1.04	0.0003	Up	HGS
D3YXG0	48.30	1.07	0.0374	Up	Hmcn1
Q96RW7	934.74	-1.15	0.0344	Down	HMCN1 FIBL6
Q96RW7	2045.87	1.06	0.0014	Up	HMCN1 FIBL6
Q96RW7	130.30	1.15	0.0394	Up	HMCN1 FIBL6
A2AJ76	133.45	-2.83	0.0075	Down	Hmcn2
A2AJ76	157.35	1.08	0.0116	Up	Hmcn2
Q8NDA2	441.75	1.41	0.0015	Up	HMCN2
Q8NDA2	868.10	1.50	0.0001	Up	HMCN2
Q8NDA2	111.22	2.22	0.0003	Up	HMCN2

A2AJ76	167.03	2.49	0.0001	Up	Hmcn2
Q9YGT6	148.14	-1.24	0.0176	Down	hoxa5a
P17124	549.63	1.25	0.0001	Up	HRH2
P17124	120.27	1.49	0.0004	Up	HRH2
P06581	267.20	1.11	0.0051	Up	hsp-16.41 hsp16-41 Y46H3A.2
O97125	256.47	1.13	0.0055	Up	Hsp68 CG5436
Q8K0U4	254.13	-2.01	0.0068	Down	Hspa12a Kiaa0417
Q25197	64.06	1.13	0.0010	Up	HTK7
Q8TDY8	2382.47	1.03	0.0001	Up	IGDCC4 DDM36 KIAA1628 NOPE
A6NGN9	70.53	3.38	0.0005	Up	IGLON5
Q921Y2	69.52	1.97	0.0112	Up	Imp3
B8JK39	376.97	1.11	0.0001	Up	Itga9
B8JK39	1337.53	1.11	0.0000	Up	Itga9
P18870	2256.84	1.31	0.0008	Up	JUN
A2CG49	43.39	2.12	0.0000	Up	Kalrn
Q7T199	28.73	-1.15	0.0304	Down	KCNA10
Q3U0V1	49.22	-2.96	0.0036	Down	Khsrp Fubp2
Q8K135	383.24	1.00	0.0001	Up	Kiaa0319l Aavr
Q6UXG2	207.89	1.12	0.0037	Up	KIAA1324 EIG121 UNQ2426/PRO4985
Q6DDW2	256.71	1.20	0.0014	Up	kiaa1324l eig121l
Q96L93	73.35	1.46	0.0004	Up	KIF16B C20orf23 KIAA1590 SNX23
Q9FZ06	476.19	1.07	0.0004	Up	KINUA ARK3 PAK At1g12430 F5O11.15
Q53HC5	45.02	1.31	0.0204	Up	KLHL26
Q96PQ7	363.00	1.11	0.0000	Up	KLHL5
O15229	182.93	-1.02	0.0015	Down	KMO
Q071E0	114.83	-1.05	0.0211	Down	kmt5aa set8a setd8 setd8a zgc:153719
Q498E6	76.70	-1.27	0.0048	Down	kmt5a-b mp36 setd8-b
P70168	69.77	1.07	0.0458	Up	Kpnb1 Impnb
P07942	1057.26	1.12	0.0000	Up	LAMB1
Q00174	354.44	1.48	0.0000	Up	LanA lamA CG10236
Q5SW96	657.16	1.31	0.0009	Up	LDLRAP1 ARH

Q8QGW7	155.31	1.14	0.0014	Up	LITAF SIMPLE
Q5F464	903.44	1.07	0.0002	Up	LPP RCJMB04_2l20
O75096	183.50	1.17	0.0087	Up	LRP4 KIAA0816 LRP10 MEGF7
O75581	136.16	1.02	0.0353	Up	LRP6
Q80WG5	215.72	-1.15	0.0473	Down	Lrrc8a Lrrc8
Q8CI17	28.96	1.15	0.0084	Up	Mab21L3
A2VDU3	295.57	1.81	0.0010	Up	MAP3K7
Q61532	2058.93	1.45	0.0000	Up	Mapk6 Erk3 Prkm4 Prkm6
Q8BJ34	53.52	1.21	0.0043	Up	Marf1 Kiaa0430 Lkap
Q29RI9	47.11	-1.05	0.0389	Down	MAT2B
Q6Q2B2	517.01	1.59	0.0000	Up	mbnl2a
P55023	23.62	-1.16	0.0153	Down	melC2 mel
P21956	201.32	1.84	0.0007	Up	Mfge8
P70490	60.86	-1.40	0.0084	Down	Mfge8 Ags
O27188	295.03	-2.96	0.0000	Down	mfnA MTH_1116
O27188	5842.44	-1.07	0.0009	Down	mfnA MTH_1116
Q6NUT3	7913.97	1.86	0.0002	Up	MFSD12 C19orf28
Q5ZIJ9	642.91	1.00	0.0009	Up	MIB2 RCJMB04_25j24
Q5ZIJ9	106.31	1.14	0.0015	Up	MIB2 RCJMB04_25j24
Q5UQ50	230.94	1.84	0.0056	Up	MIMI_L668
Q9CD89	611.76	-2.41	0.0001	Down	ML0127
Q99542	52.16	-1.27	0.0228	Down	MMP19 MMP18 RASI
Q3U435	7435.85	1.85	0.0000	Up	Mmp25
Q3U435	4600.72	2.01	0.0000	Up	Mmp25
Q10738	8322.93	1.47	0.0017	Up	Mmp7
Q98ST7	2833.60	1.24	0.0022	Up	MOXD1 DBHR MOX
Q98ST7	210.21	1.98	0.0000	Up	MOXD1 DBHR MOX
P22897	24.46	1.17	0.0036	Up	MRC1 CLEC13D CLEC13DL MRC1L1
Q9H2W6	22.88	-1.65	0.0023	Down	MRPL46 C15orf4 LIECG2
Q9H2W6	47.84	-1.46	0.0307	Down	MRPL46 C15orf4 LIECG2

Q9H2W6	144.01	-1.06	0.0122	Down	MRPL46 C15orf4 LIECG2
O43196	460.64	1.57	0.0001	Up	MSH5
A1R8N8	52.68	1.24	0.0070	Up	mshA AAur_2891
A1R8N8	41.84	2.82	0.0045	Up	mshA AAur_2891
A0LQY9	36.11	2.09	0.0004	Up	mshA Acel_0073
A0LQY9	140.23	2.36	0.0003	Up	mshA Acel_0073
A0LQY9	38.58	3.41	0.0005	Up	mshA Acel_0073
D5UJ42	69.59	-1.60	0.0000	Down	mshA Cfla_0653
B1VEI4	46.09	-1.00	0.0463	Down	mshA cu0213
B1VEI4	360.91	1.30	0.0208	Up	mshA cu0213
B1VEI4	32.40	1.59	0.0235	Up	mshA cu0213
C7R101	40.85	1.87	0.0004	Up	mshA Jden_2087
Q5YP47	83.86	1.62	0.0319	Up	mshA NFA_51920
Q0SF06	44.41	3.08	0.0000	Up	mshA RHA1_ro02073
C7Q4Y6	480.00	1.96	0.0109	Up	mshA1 Caci_5074
C7Q4Y6	69.52	2.48	0.0001	Up	mshA1 Caci_5074
Q91955	138.75	-1.94	0.0026	Down	MTPN RCJMB04_23o21 RCJMB04_35l16
Q3THE2	180.48	-1.12	0.0242	Down	Myl12b Mrlc2 Mylc2b
Q5E9E2	970.93	-1.27	0.0313	Down	MYL9 MYRL2
Q28970	289.96	1.22	0.0039	Up	MYO7A
P07207	141.12	1.04	0.0019	Up	N CG3936
D8VNT0	82.54	-2.50	0.0003	Down	ProteinName_Ryncolin-4
P83553	1602.26	-2.40	0.0017	Down	ProteinName_Dermatopontin (Tyrosine-rich acidic matrix protein) (TRAMP)
P81018	422.85	-2.30	0.0000	Down	ProteinName_Ladderlectin
P35068	2793.20	-2.18	0.0001	Down	ProteinName_Histone H2B.1/H2B.2
B3EX02	184.21	-2.13	0.0028	Down	ProteinName_MAM and fibronectin type III domain-containing protein 1 (Fragment)
P86982	2790.85	-2.12	0.0003	Down	ProteinName_Insoluble matrix shell protein 1 (IMSP1) (Fragment)
Q01528	6820.01	-2.04	0.0216	Down	ProteinName_Hemagglutinin/amebocyte aggregation factor (18K-LAF)
D9IQ16	434.46	-2.04	0.0051	Down	ProteinName_Galaxin
Q9U8W7	112.03	-1.96	0.0122	Down	ProteinName_Techylectin-5B
C0H691	1587.92	-1.93	0.0080	Down	ProteinName_Small cysteine-rich protein 2 (Amil-SCRiP2) (SCRiP2)

G8HTB6	142.91	-1.52	0.0116	Down	ProteinName_ZP domain-containing protein
G8HTB6	168.27	-1.44	0.0050	Down	ProteinName_ZP domain-containing protein
Q01528	211.86	-1.43	0.0355	Down	ProteinName_Hemagglutinin/amebocyte aggregation factor (18K-LAF)
P81018	91.31	-1.42	0.0428	Down	ProteinName_Ladderlectin
B8UU51	653.21	-1.33	0.0320	Down	ProteinName_Galaxin-2
C0H691	20140.28	-1.24	0.0075	Down	ProteinName_Small cysteine-rich protein 2 (Amil-SCRiP2) (SCRiP2)
B8V7S0	128.69	-1.20	0.0066	Down	ProteinName_CUB and peptidase domain-containing protein 1 (Fragment)
B8V7S0	25.06	-1.19	0.0248	Down	ProteinName_CUB and peptidase domain-containing protein 1 (Fragment)
C0H691	803.39	-1.16	0.0494	Down	ProteinName_Small cysteine-rich protein 2 (Amil-SCRiP2) (SCRiP2)
B8VIV4	182.84	-1.13	0.0440	Down	ProteinName_CUB and peptidase domain-containing protein 2 (Fragment)
B8V7S0	435.56	-1.13	0.0046	Down	ProteinName_CUB and peptidase domain-containing protein 1 (Fragment)
B3EWZ8	311.26	-1.13	0.0397	Down	ProteinName_Ectin (Fragment)
B3EX01	319.13	-1.11	0.0361	Down	ProteinName_CUB domain-containing protein
Q76DT2	29.18	-1.07	0.0056	Down	ProteinName_DELTA-thalatoxin-Avl2a (DELTA-TATX-Avl2a) (Toxin AvTX-60A) (Av60A)
O16025	385.44	-1.06	0.0442	Down	ProteinName_Allene oxide synthase-lipoxygenase protein [Includes: Allene oxide synthase (EC 4.2.1.92) (Hydroperoxidehydrase); Arachidonate 8-lipoxygenase (EC 1.13.11.40)]
P29241	58.28	-1.05	0.0379	Down	ProteinName_ADP-ribosyl cyclase/cyclic ADP-ribose hydrolase (EC 3.2.2.6) (2'-phospho-ADP-ribosyl cyclase) (2'-phospho-ADP-ribosyl cyclase/2'-phospho-cyclic-ADP-ribose transferase) (EC 2.4.99.20) (2'-phospho-cyclic-ADP-ribose transferase) (ADP-ribosyl cyclase) (ADPRC) (ADRC) (NAD glycohydrolase) (NAD(+) nucleosidase) (NADase)
B3EWY6	221.32	-1.05	0.0421	Down	ProteinName_Skeletal aspartic acid-rich protein 1
B3EWY7	424.36	-1.03	0.0206	Down	ProteinName_Acidic skeletal organic matrix protein (Acidic SOMP)
P12027	1325.99	1.00	0.0404	Up	ProteinName_Polysialoglycoprotein (PSGP) (Apopolysialoglycoprotein) (apoPSGP)
P55807	53.45	1.06	0.0005	Up	ProteinName_NAD(P)(+)--arginine ADP-ribosyltransferase 2 (EC 2.4.2.31) (Mono(ADP-ribosyl)transferase 2) (AT2)
P13908	227.51	1.08	0.0077	Up	ProteinName_Neuronal acetylcholine receptor subunit non-alpha-2 (GFN-alpha-2)
Q3UZV7	51.86	1.17	0.0252	Up	ProteinName_UPF0577 protein KIAA1324-like homolog (Estrogen-induced gene 121-like protein) (EIG121L)
B3EX00	36.97	1.19	0.0048	Up	ProteinName_Uncharacterized skeletal organic matrix protein 1 (Uncharacterized SOMP-1) (Fragment)
O16025	1090.14	1.20	0.0063	Up	ProteinName_Allene oxide synthase-lipoxygenase protein [Includes: Allene oxide synthase (EC 4.2.1.92) (Hydroperoxidehydrase); Arachidonate 8-lipoxygenase (EC 1.13.11.40)]
P35409	117.63	1.21	0.0026	Up	ProteinName_Probable glycoprotein hormone G-protein coupled receptor
Q17232	38.68	1.25	0.0047	Up	ProteinName_Octopamine receptor
B3EWZ3	39.52	1.27	0.0022	Up	ProteinName_Coadhesin (Fragment)
B3EWZ2	127.74	1.30	0.0030	Up	ProteinName_Uncharacterized skeletal organic matrix protein 8 (Uncharacterized SOMP-8)

B3EWZ7	73.99	1.31	0.0017	Up	ProteinName_Threonine-rich protein (Fragment)
P55143	1949.22	1.37	0.0015	Up	ProteinName_Glutaredoxin
Q9I928	34.76	1.43	0.0005	Up	ProteinName_Fucolectin-4
B3EX02	243.41	1.44	0.0009	Up	ProteinName_MAM and fibronectin type III domain-containing protein 1 (Fragment)
Q03278	22.13	1.50	0.0004	Up	ProteinName_Retrovirus-related Pol polyprotein from type-1 retrotransposable element R2 (Retrovirus-related Pol polyprotein from type I retrotransposable element R2) [Includes: Reverse transcriptase (EC 2.7.7.49); Endonuclease] (Fragment)
P16273	83.29	1.52	0.0256	Up	ProteinName_Pathogen-related protein
B3EX02	214.64	1.59	0.0000	Up	ProteinName_MAM and fibronectin type III domain-containing protein 1 (Fragment)
Q7SIC1	44.15	1.61	0.0369	Up	ProteinName_Fucolectin
Q9I929	431.41	1.69	0.0003	Up	ProteinName_Fucolectin-3
B8V7S0	520.74	1.76	0.0000	Up	ProteinName_CUB and peptidase domain-containing protein 1 (Fragment)
Q9I927	208.50	1.91	0.0002	Up	ProteinName_Fucolectin-5
B3EX00	650.83	1.96	0.0000	Up	ProteinName_Uncharacterized skeletal organic matrix protein 1 (Uncharacterized SOMP-1) (Fragment)
Q9I929	53.01	1.98	0.0047	Up	ProteinName_Fucolectin-3
B8VIW9	402.08	2.01	0.0000	Up	ProteinName_Fibronectin type III domain-containing protein (Neuroglian-like protein)
Q94743	79.54	2.02	0.0001	Up	ProteinName_Sorcin
P18320	401.95	2.07	0.0006	Up	ProteinName_Profilin
B8VIU6	23.18	2.41	0.0176	Up	ProteinName_Uncharacterized skeletal organic matrix protein 5 (Uncharacterized SOMP-5)
O16025	486.03	2.43	0.0001	Up	ProteinName_Allene oxide synthase-lipoxygenase protein [Includes: Allene oxide synthase (EC 4.2.1.92) (Hydroperoxidehydrase); Arachidonate 8-lipoxygenase (EC 1.13.11.40)]
D9IQ16	774.18	2.47	0.0001	Up	ProteinName_Galaxin
Q8WPD0	465.19	2.77	0.0004	Up	ProteinName_Alpha-N-acetylgalactosamine-specific lectin (Alpha-N-acetylgalactosamine-binding lectin) (GalNAc-specific lectin) (Lectin) (ApL) (Tn antigen-specific lectin)
P16049	204.99	2.80	0.0003	Up	ProteinName_Trypsin-1 (EC 3.4.21.4) (Trypsin I)
Q9U6Y3	37.50	3.16	0.0072	Up	ProteinName_GFP-like fluorescent chromoprotein cFP484
P55115	135.24	-1.50	0.0044	Down	nas-15 T04G9.2
P55115	305.38	1.14	0.0002	Up	nas-15 T04G9.2
P55115	1001.27	1.57	0.0000	Up	nas-15 T04G9.2
O35136	490.98	1.82	0.0000	Up	Ncam2 Ocam Rncam
O14594	36.53	-1.22	0.0477	Down	NCAN CSPG3 NEUR
Q6PBH5	152.03	-1.21	0.0030	Down	ndufa4 zgc:73405
P18519	132.61	1.42	0.0014	Up	NGFR TNFRSF16

P14543	314.14	-1.12	0.0325	Down	NID1 NID
Q6ZUT1	46.27	1.01	0.0037	Up	NKAPD1 C11orf57
Q5DU56	208.31	1.03	0.0104	Up	Nlrc3
Q5DU56	139.63	1.83	0.0047	Up	Nlrc3
Q7RTR2	48.92	1.03	0.0286	Up	NLRC3 NOD3
Q7RTR2	43.96	1.04	0.0194	Up	NLRC3 NOD3
Q7RTR2	89.69	1.06	0.0070	Up	NLRC3 NOD3
Q7RTR2	250.34	1.16	0.0061	Up	NLRC3 NOD3
Q7RTR2	109.29	1.37	0.0174	Up	NLRC3 NOD3
Q7RTR2	151.60	1.40	0.0001	Up	NLRC3 NOD3
Q7RTR2	57.01	1.42	0.0079	Up	NLRC3 NOD3
Q7RTR2	95.09	1.50	0.0146	Up	NLRC3 NOD3
Q7RTR2	42.13	1.55	0.0032	Up	NLRC3 NOD3
Q7RTR2	181.89	1.91	0.0010	Up	NLRC3 NOD3
Q7RTR2	93.50	2.12	0.0055	Up	NLRC3 NOD3
Q7RTR2	176.80	2.16	0.0018	Up	NLRC3 NOD3
Q7RTR2	51.27	2.44	0.0316	Up	NLRC3 NOD3
Q7RTR2	223.57	2.53	0.0001	Up	NLRC3 NOD3
Q9NPP4	177.69	1.89	0.0019	Up	NLRC4 CARD12 CLAN CLAN1 IPAF UNQ6189/PRO20215
Q3UP24	60.49	1.90	0.0033	Up	Nlrc4 Card12 Ipaf
F1MHT9	168.30	1.40	0.0044	Up	NLRC4 IPAF
F1MHT9	297.61	1.75	0.0002	Up	NLRC4 IPAF
F6R2G2	47.36	-1.22	0.0402	Down	nlrc4 ipaf TGas028l14.1
F6R2G2	180.53	2.00	0.0004	Up	nlrc4 ipaf TGas028l14.1
F6R2G2	53.51	2.03	0.0000	Up	nlrc4 ipaf TGas028l14.1
F6R2G2	91.34	2.72	0.0000	Up	nlrc4 ipaf TGas028l14.1
C6FG12	439.11	4.01	0.0001	Up	nlrc5
Q86WI3	176.77	1.55	0.0050	Up	NLRC5 NOD27 NOD4
Q8K3Z0	60.39	1.18	0.0101	Up	Nod2 Card15
Q8K3Z0	46.35	1.95	0.0012	Up	Nod2 Card15

C5H5C4	185.54	1.34	0.0021	Up	notum1a
Q924V1	169.36	1.51	0.0011	Up	Nox4 Kox
Q99743	36.04	-1.10	0.0149	Down	NPAS2 BHLHE9 MOP4 PASD4
Q99743	48.60	1.84	0.0003	Up	NPAS2 BHLHE9 MOP4 PASD4
Q9EQD2	44.39	-1.22	0.0056	Down	Npffr2 Gpr74 Npff2 Npgpr
Q9Y5X5	72.61	1.62	0.0002	Up	NPFFR2 GPR74 NPFF2 NPGPR
Q99J85	275.19	1.31	0.0413	Up	Nptxr Npr
Q9GK74	87.30	1.19	0.0026	Up	NPY2R
O35375	298.63	2.07	0.0000	Up	Nrp2
A6H603	272.87	1.27	0.0002	Up	Nwd1
Q39575	64.59	1.65	0.0001	Up	ODA2 ODA-2
Q29RU2	476.15	1.35	0.0063	Up	OIT3
Q8R4V5	76.54	1.20	0.0003	Up	Oit3 Lzp
Q6V0K7	2149.23	1.27	0.0006	Up	Oit3 Lzp
Q9VCA2	48.13	-1.77	0.0005	Down	Orct CG6331
Q9VCA2	46.58	-1.05	0.0354	Down	Orct CG6331
P29341	39.60	-1.09	0.0080	Down	Pabpc1 Pabp1
Q8R4K8	1733.93	1.28	0.0001	Up	Pappa
Q460N5	47.57	1.47	0.0037	Up	PARP14 BAL2 KIAA1268
Q2EMV9	240.76	-1.51	0.0185	Down	Parp14 Kiaa1268
Q8BH04	7881.56	1.04	0.0009	Up	Pck2
P41413	77.57	-1.27	0.0063	Down	Pcsk5
Q9DE49	968.83	1.20	0.0083	Up	pdgfra
Q6NU98	44.96	1.07	0.0082	Up	pdik1-b
Q8N165	48.16	-1.38	0.0476	Down	PDIK1L CLIK1L
Q5U318	302.07	1.14	0.0017	Up	Pea15
Q5U318	66.67	1.61	0.0044	Up	Pea15
O70597	548.72	1.01	0.0012	Up	Pex11a Pex11
P0C0R5	41.10	2.01	0.0031	Up	Pik3r4
Q99570	48.15	1.35	0.0178	Up	PIK3R4 VPS15
Q4GZT3	620.05	1.10	0.0002	Up	PKD2 TRPP2

P70208	89.28	1.39	0.0003	Up	Plxna3
P29590	37.14	1.42	0.0108	Up	PML MYL PP8675 RNF71 TRIM19
Q6P8U6	4681.38	2.10	0.0001	Up	Pnlip
Q80TC5	39.85	1.46	0.0274	Up	Pogk Kiaa1513
A6QNP3	110.26	1.03	0.0073	Up	PPP1R3B
O95685	165.67	1.04	0.0029	Up	PPP1R3D PPP1R6
P20664	140.50	-1.67	0.0140	Down	Prim1
P33610	123.66	-1.14	0.0120	Down	Prim2
P09215	690.04	1.03	0.0001	Up	Prkcd Pkcd
Q6MG82	223.39	1.16	0.0016	Up	Prrt1 Ng5
Q9NQE7	71.75	-1.86	0.0005	Down	PRSS16 TSSP
Q9NQE7	48.98	-1.67	0.0236	Down	PRSS16 TSSP
P26779	2116.33	-1.24	0.0022	Down	PSAP
Q64487	736.48	1.11	0.0000	Up	Ptprd
P0C5E4	114.22	1.38	0.0027	Up	Ptprq
O88488	122.93	2.44	0.0000	Up	Ptprq Ptpgmc1
Q3UQ28	174.27	1.03	0.0023	Up	Pxdn Kiaa0230
Q92626	5542.88	2.54	0.0010	Up	PXDN KIAA0230 MG50 PRG2 VPO VPO1
A4IGL7	43544.15	1.09	0.0090	Up	pxdn pxn
A4IGL7	319.06	1.26	0.0382	Up	pxdn pxn
C3ZQF9	312.04	1.12	0.0027	Up	QRFPR BRAFLDRAFT_74637
C3ZQF9	132.79	1.22	0.0001	Up	QRFPR BRAFLDRAFT_74637
Q96P65	213.21	1.10	0.0014	Up	QRFPR GPR103
Q4R5Y0	55.94	1.28	0.0015	Up	QtsA-19889
Q923S9	1564.44	1.05	0.0006	Up	Rab30 Rsb30
G0FUS0	348.35	1.34	0.0028	Up	RAM_03320
Q9CR50	53.35	1.44	0.0071	Up	Rchy1 Arnip Chimp Zfp363 Znf363
P55006	3102.54	1.07	0.0018	Up	Rdh7 Rdh3
Q9N126	32.72	1.68	0.0248	Up	RDH8 PRRDH
Q0DXS3	145.51	1.02	0.0086	Up	RDR1 Os02g0736200 LOC_Os02g50330

Q0DXS3	32.36	1.14	0.0039	Up	RDR1 Os02g0736200 LOC_Os02g50330
Q9FT72	90.75	2.39	0.0016	Up	RECQL3 RECQ3 RQL3 At4g35740 F8D20.250
G3V9H8	95.72	1.70	0.0030	Up	Ret
P07949	61.49	1.24	0.0000	Up	RET CDHF12 CDHR16 PTC RET51
E9Q555	83.59	1.62	0.0136	Up	Rnf213 Mystr
A0A0R4IBK5	150.81	1.44	0.0059	Up	rnf213a
A0A0R4IBK5	270.40	1.65	0.0043	Up	rnf213a
A0A0R4IBK5	47.96	2.44	0.0001	Up	rnf213a
Q9Y6N7	1973.85	1.38	0.0002	Up	ROBO1 DUTT1
Q9HCK4	138.74	1.02	0.0374	Up	ROBO2 KIAA1568
Q6XHB2	83.02	2.00	0.0397	Up	roco4 DDB_G0288251
O44252	84.88	1.58	0.0004	Up	rost CG9552
Q6NU95	62.62	1.35	0.0074	Up	rpap3
Q8VEE0	57.99	1.44	0.0010	Up	Rpe
P04052	977.25	1.05	0.0003	Up	RpII215 CG1554
P04646	2402.35	-1.14	0.0153	Down	Rpl35a
Q3SVL8	90.42	-1.25	0.0459	Down	rpmB Nwi_0406
Q9GT45	204.19	-2.41	0.0045	Down	RpS26 AGAP012100
P18654	4458.69	1.09	0.0001	Up	Rps6ka3 Mapkapk1b Rps6ka-rs1 Rsk2
P9WLL5	257.82	1.06	0.0010	Up	Rv2075c MTCY49.14c
Q9PVX0	112.16	1.36	0.0000	Up	RX2 RAX2
Q4J9D2	62.67	1.21	0.0033	Up	Saci_1252
Q9NZJ4	85.51	-1.26	0.0431	Down	SACS KIAA0730
Q9NZJ4	261.24	1.18	0.0343	Up	SACS KIAA0730
Q9NZJ4	234.20	1.55	0.0041	Up	SACS KIAA0730
Q9NZJ4	78.29	1.62	0.0020	Up	SACS KIAA0730
Q9NZJ4	126.07	2.97	0.0082	Up	SACS KIAA0730
A3KN83	168.54	1.01	0.0052	Up	SBNO1 MOP3
Q8SQC1	23.25	1.07	0.0346	Up	SCARB1
H1AFJ5	46.42	-1.41	0.0062	Down	scnn1a enacalpha
Q6V4S5	646.71	1.07	0.0000	Up	Sdk2 Kiaa1514

Q58EX2	257.24	2.56	0.0001	Up	SDK2 KIAA1514
D3ZTD8	69.75	1.11	0.0017	Up	Sema5a
D3ZTD8	219.74	1.55	0.0000	Up	Sema5a
Q13591	126.13	1.12	0.0012	Up	SEMA5A SEMAF
Q9GZR1	127.96	-6.07	0.0000	Down	SENP6 KIAA0797 SSP1 SUSP1 FKSG6
Q9DEQ4	1769.32	1.19	0.0001	Up	SFRP1
A2AAY5	1158.74	1.49	0.0001	Up	Sh3pxd2b Fad49 Tks4
P07768	86.51	-1.57	0.0005	Down	SI
Q6Q3F5	29.79	1.01	0.0007	Up	Sidt1
Q9NXL6	120.57	1.01	0.0029	Up	SIDT1
Q6A4L1	203.12	1.08	0.0019	Up	slc12a8
Q9Z0Z5	35.59	1.02	0.0040	Up	Slc13a3 Nadc3 Sdct2
Q68F72	164.85	-1.03	0.0094	Down	slc15a4
A1L1W9	31.94	1.49	0.0007	Up	slc16a10 si:ch211-241j12.1 zgc:158478
Q90632	1011.86	1.06	0.0004	Up	SLC16A3 MCT3 REMP
Q9DB41	617.76	1.27	0.0000	Up	Slc25a18 Gc2
Q6DIV6	318.56	1.44	0.0019	Up	slc32a1 viaat
P23978	97.81	-1.01	0.0217	Down	Slc6a1 Gabt1 Gat-1 Gat1
Q9QXA6	497.06	-1.02	0.0311	Down	Slc7a9 Bat1
Q8K078	329.22	1.16	0.0000	Up	Slco4a1 Oatp4a1 Oatpe Slc21a12
Q499Z3	38.05	1.05	0.0102	Up	SLFNL1
Q5R5X9	2344.40	1.17	0.0011	Up	SMYD4
Q7JR71	3685.42	1.35	0.0023	Up	Sod3 CG9027
P41962	302.40	-1.17	0.0082	Down	SODC
Q9WTP3	7947.50	1.26	0.0003	Up	Spdef Pdef Pse
P54735	299.41	2.37	0.0019	Up	spkD sll0776
Q10LI1	490.21	1.24	0.0008	Up	SRFP1 Os03g0348900 LOC_Os03g22680 OsJ_10832
Q10LI1	664.12	1.37	0.0268	Up	SRFP1 Os03g0348900 LOC_Os03g22680 OsJ_10832
Q9Y2M2	809.70	1.26	0.0009	Up	SSUH2 C3orf32 FLS485
Q9UBI4	91.99	1.20	0.0004	Up	STOML1 SLP1 UNC24 MSTP019

Q6ZWJ1	120.30	-1.01	0.0453	Down	STXBP4
Q8JG30	52.59	-1.10	0.0122	Down	SULT1B1 SULT1B
A2AVA0	233.48	3.79	0.0000	Up	Svep1
O62732	271.12	1.34	0.0106	Up	SYN1
Q5R4U3	2625.65	1.19	0.0005	Up	TAX1BP1
Q3MII6	250.57	1.03	0.0001	Up	TBC1D25 OATL1
Q6DFJ6	422.80	1.04	0.0008	Up	tbk1
O95935	448.50	1.29	0.0011	Up	TBX18
Q5ZMS6	19.53	1.18	0.0070	Up	TDRD3 RCJMB04_1e24
Q02858	44.01	1.82	0.0048	Up	Tek Hyk Tie-2 Tie2
Q06807	82.25	1.50	0.0024	Up	TEK TIE-2 TIE2
O93429	2727.86	-2.74	0.0077	Down	tf
B5XCB8	23.34	1.37	0.0014	Up	thap1
B5XCB8	23.34	1.37	0.0014	Up	thap1
Q6PFL8	139.74	1.17	0.0016	Up	thyn1 zgc:66269
Q9USM7	274.64	-2.46	0.0000	Down	tim23 SPCC16A11.09c
Q9W6B4	303.98	-3.61	0.0000	Down	TIMP3
Q9R088	40.34	-1.08	0.0020	Down	Tk2
Q9WVM6	147.27	2.04	0.0000	Up	Tll2
O57382	627.59	-1.37	0.0272	Down	tll2 xld
O57382	307.59	1.23	0.0003	Up	tll2 xld
Q15399	36.14	1.02	0.0019	Up	TLR1 KIAA0012
Q68Y56	185.64	1.50	0.0001	Up	TLR4
Q99MX7	71.72	1.07	0.0005	Up	Tmem121b Cecr6
A3KN95	59.01	2.94	0.0000	Up	tmem151b
Q9BSE2	134.51	1.08	0.0010	Up	TMEM79 MATT
Q3MHQ7	1511.82	1.20	0.0003	Up	TMEM86A
P69526	41.21	-1.34	0.0015	Down	Tmprss9
P69525	48.95	-1.16	0.0429	Down	Tmprss9
P16599	514.21	-1.14	0.0441	Down	Tnf Tnfa Tnfsf2
P19438	105.30	1.24	0.0002	Up	TNFRSF1A TNFAR TNFR1

Q9WUU8	3046.80	1.30	0.0009	Up	Tnip1 Abin Naf1
Q3SYU7	276.94	1.08	0.0013	Up	TNPO1 KPNB2
Q92752	77.77	-1.44	0.0116	Down	TNR
Q05546	437.30	1.87	0.0003	Up	Tnr
D2IYS2	359.88	1.17	0.0055	Up	tor
O88898	147.30	-1.38	0.0264	Down	Tp63 P63 P73l Tp73l Trp63
Q13114	360.09	1.02	0.0004	Up	TRAF3 CAP1 CRAF1
Q60803	265.97	1.03	0.0070	Up	Traf3 Craf1 Trafamn
Q60803	316.76	1.09	0.0154	Up	Traf3 Craf1 Trafamn
Q60803	175.29	1.30	0.0039	Up	Traf3 Craf1 Trafamn
Q60803	1916.01	1.76	0.0011	Up	Traf3 Craf1 Trafamn
P70191	190.34	1.80	0.0001	Up	Traf5
B6CJY5	180.53	1.13	0.0057	Up	TRAF6
P70196	339.96	1.25	0.0016	Up	Traf6
B5DF45	135.81	1.44	0.0015	Up	Traf6
Q5BIM1	57.98	1.50	0.0007	Up	TRIM45
E7FAM5	34.76	-1.54	0.0482	Down	trim71 lin41
E7FAM5	55.23	-1.16	0.0472	Down	trim71 lin41
O75762	1045.81	1.04	0.0077	Up	TRPA1 ANKTM1
Q9R244	117.67	1.04	0.0088	Up	Trpc2 Trp2 Trrp2
Q13507	57.71	1.03	0.0041	Up	TRPC3 TRP3
O35119	42.98	1.11	0.0264	Up	Trpc4
Q9BX84	264.43	1.21	0.0464	Up	TRPM6 CHAK2
Q96AY4	56.02	-2.56	0.0269	Down	TTC28 KIAA1043 TPRBK
Q96AY4	39.17	1.04	0.0187	Up	TTC28 KIAA1043 TPRBK
Q96AY4	288.98	1.08	0.0027	Up	TTC28 KIAA1043 TPRBK
Q96AY4	23.87	1.09	0.0434	Up	TTC28 KIAA1043 TPRBK
Q96AY4	89.28	1.11	0.0259	Up	TTC28 KIAA1043 TPRBK
Q96AY4	231.47	1.15	0.0003	Up	TTC28 KIAA1043 TPRBK
Q96AY4	31.10	1.30	0.0002	Up	TTC28 KIAA1043 TPRBK

Q96AY4	25.58	1.37	0.0054	Up	TTC28 KIAA1043 TPRBK
Q96AY4	150.67	3.23	0.0000	Up	TTC28 KIAA1043 TPRBK
Q96AY4	118.30	4.74	0.0001	Up	TTC28 KIAA1043 TPRBK
A2ASS6	2353.79	1.10	0.0035	Up	Ttn
G4SLH0	39.35	-1.67	0.0015	Down	ttn-1 W06H8.8
O73787	88.41	-1.20	0.0036	Down	tubgcp3
H9D1R1	82.66	-1.40	0.0009	Down	Txndc12
Q969M7	119.57	-1.02	0.0035	Down	UBE2F NCE2
O95164	133.89	1.04	0.0005	Up	UBL3 PNSC1
Q9VL06	39.55	1.37	0.0083	Up	Ufd4 CG5604
Q91X17	124.12	1.15	0.0174	Up	Umod
Q9Z1N9	674.80	1.06	0.0000	Up	Unc13b Unc13a
C5IAW9	170.65	1.05	0.0166	Up	unc5b-b
Q7T2Z5	68.77	-1.46	0.0012	Down	UNC5C
O95185	114.68	-1.17	0.0276	Down	UNC5C UNC5H3
Q9VB11	65.94	1.25	0.0017	Up	unc80 CG18437
O75445	46.92	-1.34	0.0201	Down	USH2A
A7SFB5	168.43	3.56	0.0009	Up	v1g211400
A7SLZ2	109.41	1.44	0.0495	Up	v1g246111
A7SLZ2	207.92	1.69	0.0001	Up	v1g246111
Q9NHV9	21.67	-1.76	0.0069	Down	Vav CG7893
Q9JHA8	2730.65	1.25	0.0006	Up	Vwa7 D17h6s56e-3 G7c
Q8N2E2	116.46	-1.83	0.0005	Down	VWDE
Q5ZMC3	100.39	1.05	0.0002	Up	WDSUB1 RCJMB04_2i21
Q9Y6F9	74.59	-1.06	0.0486	Down	WNT6
Q14191	163.42	2.32	0.0000	Up	WRN RECQ3 RECQL2
O54975	52.29	-1.66	0.0006	Down	Xpnpep1 App
O31463	47.00	-2.27	0.0000	Down	ybgG BSU02410
Q04336	3042.48	2.02	0.0004	Up	YMR196W YM9646.09
O34918	38.34	-1.27	0.0191	Down	yoaJ BSU18630
Q9C0D7	679.33	1.15	0.0000	Up	ZC3H12C KIAA1726 MCPIP3

Q94BZ1	305.63	1.02	0.0017	Up	ZIFL1 At5g13750 MXE10.2
Q9XTR8	35.33	-1.48	0.0069	Down	ZK262.3
Q96NB3	84.43	1.09	0.0093	Up	ZNF830 CCDC16
Q8R151	215.16	1.94	0.0002	Up	Znfx1
Q9P2E3	73.73	-2.41	0.0085	Down	ZNFX1 KIAA1404
Q9P2E3	82.96	-1.20	0.0177	Down	ZNFX1 KIAA1404
Q9P2E3	101.20	1.81	0.0001	Up	ZNFX1 KIAA1404
Q5ZLX5	41.84	1.60	0.0168	Up	ZRANB2 RCJMB04_4i6

Supplementary Table C.22 All gene ontologies (GO terms) identified in response to treatment in the host reads. GO terms identified with the GO_MWU pipeline (Wright et al., 2015). Significant GO terms ($P_{adj} < 0.05$) are shown in **bold.** Divisions are Biological Process (BP), Cellular Component (CC), and Molecular Function (MF). Nseqs represents the number of genes contained in each term. The term represents the most abundant GO term returned; name of the term, and adjusted p value (P_{adj}).

Division	delta.rank	nseqs	term	name	p.adj
BP	52	4	GO:0002526	acute inflammatory response	0.891971
BP	216	5	GO:0000380	alternative mRNA splicing	
BP	164	9	GO:0001755	ameboidal-type cell migration	0.565048
BP	501	4	GO:0071695	anatomical structure maturation	0.246624
BP	30	50	GO:0048513	animal organ development	0.778058
BP	152	7	GO:0006915	apoptotic process	0.63562
BP	690	4	GO:0001662	behavioral fear response	0.072994
BP	**-236**	**62**	**GO:0044249**	**biosynthetic process**	**0.009984**
BP	0	108	GO:1901565	branching morphogenesis of an epithelial tube	0.99422
BP	-179	4	GO:1901137	carbohydrate derivative biosynthetic process	0.673928
BP	-133	8	GO:1901135	carbohydrate derivative metabolic process	0.66367
BP	-82	12	GO:0005975	carbohydrate metabolic process	0.720346
BP	27	13	GO:0003333	carboxylic acid transmembrane transport	0.897696
BP	-95	70	GO:0009057	catabolic process	0.348878
BP	234	15	GO:0030001	cation transport	0.295558
BP	50	39	GO:0007389	cell activation	0.714083
BP	-142	40	GO:0000278	cell cycle	0.298444
BP	-40	38	GO:0000086	cell cycle G2/M phase transition	0.743772
BP	84	7	GO:0002064	cell development	0.768007
BP	**-267**	**36**	**GO:1901566**	**cellular amide metabolic process**	**0.030337**
BP	-73	8	GO:0006520	cellular amino acid metabolic process	0.778058
BP	**-143**	**131**	**GO:0022618**	**cellular component assembly**	**0.030337**
BP	119	69	GO:0048869	cellular developmental process	0.250477
BP	-47	53	GO:0000184	cellular macromolecule catabolic process	0.691414
BP	**-319**	**33**	**GO:0044271**	**cellular nitrogen compound biosynthetic process**	**0.009984**

BP	292	7	GO:0022412	cellular process involved in reproduction in multicellular organism	0.350055
BP	125	18	GO:0003006	developmental process involved in reproduction	0.548176
BP	388	5	GO:0070838	divalent metal ion transport	0.308791
BP	**-184**	**82**	**GO:0006281**	**DNA metabolic process**	**0.02899**
BP	**-575**	**7**	**GO:0000076**	**DNA replication checkpoint**	**0.041465**
BP	-335	8	GO:0000447	endonucleolytic cleavage of tricistronic rRNA transcript (SSU-rRNA	
BP	314	10	GO:0003351	epithelial cilium movement involved in extracellular fluid movement	0.246624
BP	-68	9	GO:0001654	eye development	0.778058
BP	-99	16	GO:0006631	fatty acid metabolic process	0.639263
BP	-260	13	GO:0001732	formation of cytoplasmic translation initiation complex	0.272571
BP	309	7	GO:0001704	formation of primary germ layer	0.325742
BP	-110	7	GO:0001731	formation of translation preinitiation complex	0.714405
BP	-73	5	GO:0010467	gene expression	0.832631
BP	206	6	GO:0001835	hatching	0.556731
BP	348	9	GO:0001947	heart looping	0.213022
BP	299	18	GO:0002244	hematopoietic progenitor cell differentiation	0.11283
BP	-106	28	GO:0000723	homeostatic process	0.540046
BP	-167	10	GO:0008610	lipid biosynthetic process	0.548176
BP	-356	6	GO:0016042	lipid catabolic process	0.308791
BP	-86	37	GO:0044255	lipid metabolic process	0.550398
BP	20	14	GO:0001889	liver development	0.925755
BP	412	4	GO:0001676	long-chain fatty acid metabolic process	0.325742
BP	-263	26	GO:0034645	macromolecule biosynthetic process	0.08487
BP	-151	8	GO:0001510	macromolecule methylation	0.614051
BP	-394	9	GO:0000470	maturation of LSU-rRNA	0.143334
BP	-375	6	GO:0000463	maturation of LSU-rRNA from tricistronic rRNA transcript (SSU-rRNA	
BP	-378	13	GO:0000462	maturation of SSU-rRNA from tricistronic rRNA transcript (SSU-rRNA	
BP	-331	9	GO:1903046	meiotic cell cycle process	0.246624
BP	231	7	GO:0001656	metanephros development	0.494505
BP	118	5	GO:0001578	microtubule bundle formation	0.738608

BP	**346**	**28**	**GO:0003341**	**microtubule-based movement**	**0.009984**
BP	**240**	**80**	**GO:0007017**	**microtubule-based process**	**0.003268**
BP	-68	8	GO:0000002	mitochondrial genome maintenance	0.790758
BP	-59	22	GO:0007005	mitochondrion organization	0.728943
BP	29	163	GO:0051656	mitotic sister chromatid segregation	0.673928
BP	223	7	GO:0015672	monovalent inorganic cation transport	0.501283
BP	**203**	**65**	**GO:0016477**	**movement of cell or subcellular component**	**0.030097**
BP	-49	111	GO:0016071	mRNA metabolic process	0.556731
BP	150	30	GO:0001701	multicellular organism development	0.325742
BP	**-335**	**50**	**GO:0034470**	**ncRNA processing**	**0.001383**
BP	-192	24	GO:0031570	negative regulation of cell cycle	0.272571
BP	365	5	GO:0006469	negative regulation of molecular function	0.325742
BP	62	84	GO:0000186	negative regulation of multicellular organismal process	0.540046
BP	109	10	GO:0001933	negative regulation of protein phosphorylation	0.690906
BP	117	8	GO:0009968	negative regulation of response to stimulus	0.691473
BP	148	5	GO:0051051	negative regulation of transport	0.691473
BP	237	8	GO:0050877	nervous system process	0.454292
BP	267	6	GO:0000289	nuclear-transcribed mRNA poly(A) tail shortening	0.456921
BP	-329	12	GO:0000469	nucleic acid phosphodiester bond hydrolysis	0.157676
BP	-197	9	GO:0000054	nucleobase-containing compound transport	0.501283
BP	-387	5	GO:0009117	nucleobase-containing small molecule metabolic process	0.308791
BP	104	34	GO:0000045	organelle assembly	0.497304
BP	-38	10	GO:0000266	organelle fission	0.877324
BP	-79	26	GO:0019752	organic acid metabolic process	0.63562
BP	-238	14	GO:0034654	organic cyclic compound biosynthetic process	0.298444
BP	-161	9	GO:0090407	organophosphate biosynthetic process	0.565865
BP	9	17	GO:0001649	osteoblast differentiation	0.963802
BP	**-356**	**18**	**GO:0006518**	**peptide metabolic process**	**0.04222**
BP	-380	11	GO:0000413	peptidyl-amino acid modification	0.11283
BP	-180	6	GO:0008654	phospholipid metabolic process	0.60493
BP	-161	16	GO:0006796	phosphorus metabolic process	0.467114

BP	-2	5	GO:0010608	posttranscriptional regulation of gene expression	0.99422
BP	-112	13	GO:0006486	protein glycosylation	0.63562
BP	-59	26	GO:0008104	protein localization	0.714083
BP	114	7	GO:0000338	protein modification by small protein removal	0.714083
BP	65	421	GO:0000082	protein modification process	0.147421
BP	157	18	GO:0006508	proteolysis	0.456921
BP	314	7	GO:0006511	proteolysis involved in cellular protein catabolic process	0.325742
BP	-219	41	GO:0051726	regulation of cell cycle	0.072994
BP	237	11	GO:0001558	regulation of cell growth	0.346245
BP	97	7	GO:0042127	regulation of cell population proliferation	0.738608
BP	239	25	GO:0051128	regulation of cellular component organization	0.141933
BP	904	4	GO:0001868	regulation of complement activation	
BP	-289	16	GO:0000079	regulation of cyclin-dependent protein serine/threonine kinase activity	0.152753
BP	-209	6	GO:0000018	regulation of DNA recombination	0.550398
BP	-60	4	GO:0016486	regulation of hormone levels	0.877324
BP	37	167	GO:0051641	regulation of immune system process	0.594204
BP	258	17	GO:0051049	regulation of localization	0.20435
BP	8	24	GO:0000381	regulation of mRNA processing	0.963802
BP	233	6	GO:0001919	regulation of receptor recycling	0.52247
BP	97	133	GO:0071900	regulation of response to stimulus	0.195097
BP	186	14	GO:0051130	regulation of vesicle-mediated transport	0.42374
BP	-11	33	GO:0022414	reproductive process	0.940157
BP	-149	9	GO:0001541	reproductive structure development	0.60493
BP	-491	4	GO:0000712	resolution of meiotic recombination intermediates	0.248555
BP	113	29	GO:0001666	response to abiotic stimulus	0.497304
BP	3	15	GO:0000302	response to chemical	0.99422
BP	126	4	GO:0010035	response to inorganic substance	0.741315
BP	-154	8	GO:0002931	response to ischemia	0.60493
BP	-29	119	GO:0006950	response to stress	0.714083
BP	99	6	GO:0001523	retinoid metabolic process	0.743772

BP	**-420**	**19**	**GO:0000027**	**ribosomal large subunit assembly**	**0.009984**
BP	-189	8	GO:0000028	ribosomal small subunit assembly	0.548176
BP	-328	4	GO:0000966	RNA 5'-end processing	0.456921
BP	-124	6	GO:0032774	RNA biosynthetic process	0.714083
BP	-268	22	GO:0009451	RNA modification	0.11283
BP	**-179**	**127**	**GO:0006396**	**RNA processing**	**0.008011**
BP	-71	77	GO:0000375	RNA splicing	0.494505
BP	**-407**	**31**	**GO:0006364**	**rRNA metabolic process**	**0.001486**
BP	-466	7	GO:0000154	rRNA modification	0.120059
BP	11	147	GO:0051276	signal transduction	0.873843
BP	-313	6	GO:0000012	single strand break repair	0.351531
BP	-258	10	GO:0044283	small molecule biosynthetic process	0.325742
BP	-108	44	GO:0044281	small molecule metabolic process	0.419528
BP	-239	5	GO:0000491	small nucleolar ribonucleoprotein complex assembly	0.548176
BP	-250	6	GO:0000245	spliceosomal complex assembly	0.494505
BP	-296	24	GO:0000387	spliceosomal snRNP assembly	0.058187
BP	-183	8	GO:0000244	spliceosomal tri-snRNP complex assembly	0.550398
BP	-370	4	GO:0002223	stimulatory C-type lectin receptor signaling pathway	0.379151
BP	53	5	GO:0000096	sulfur amino acid metabolic process	0.877324
BP	-162	11	GO:0006790	sulfur compound metabolic process	0.548176
BP	-377	5	GO:0000722	telomere maintenance via recombination	0.325742
BP	255	3	GO:0001894	tissue homeostasis	0.60493
BP	29	81	GO:0006811	transport	0.738608
BP	-112	11	GO:0006400	tRNA modification	0.664779
BP	-203	16	GO:0008033	tRNA processing	0.327682
BP	-263	7	GO:0002097	tRNA wobble base modification	0.42374
BP	-491	5	GO:0002098	tRNA wobble uridine modification	0.183369
BP	218	13	GO:0035148	tube formation	0.346245
BP	-103	8	GO:0000050	urea metabolic process	0.714405
BP	-196	5	GO:0000038	very long-chain fatty acid metabolic process	0.60493
CC	123	14	GO:0001669	acrosomal vesicle	0.51182

CC	118	6	GO:0000421	autophagosome membrane	0.698628
CC	337	7	GO:0005930	axoneme	0.233027
CC	-3	181	GO:1902494	catalytic complex	0.979233
CC	403	6	GO:0070161	cell junction	0.188393
CC	191	14	GO:0005814	centriole	0.294018
CC	-54	23	GO:0000785	chromatin	0.746087
CC	-125	25	GO:0000775	chromosomal region	0.377425
CC	-166	24	GO:0000228	chromosome	0.240349
CC	201	12	GO:0005929	cilium	0.296627
CC	-494	6	GO:0005680	cullin-RING ubiquitin ligase complex	0.08464
CC	13	80	GO:0005829	cytosol	0.941936
CC	24	82	GO:0005783	endoplasmic reticulum	0.79939
CC	-89	11	GO:0005788	endoplasmic reticulum lumen	0.698628
CC	12	53	GO:0005789	endoplasmic reticulum membrane	0.941936
CC	-169	19	GO:0140534	endoplasmic reticulum protein-containing complex	0.279339
CC	176	4	GO:0010008	endosome membrane	0.628703
CC	6	15	GO:0036452	ESCRT complex	0.981437
CC	5	6	GO:0000813	ESCRT I complex	0.99025
CC	197	6	GO:0000815	ESCRT III complex	0.51182
CC	-224	13	GO:0000176	exosome (RNase complex)	0.240349
CC	-154	39	GO:0005615	extracellular space	0.201803
CC	-96	22	GO:0001650	fibrillar center	0.51182
CC	41	5	GO:0000506	glycosylphosphatidylinositol-N-acetylglucosaminyltransferase (GPI-GnT) complex	0.941936
CC	81	27	GO:0005794	Golgi apparatus	0.541518
CC	93	23	GO:0098791	Golgi apparatus subcompartment	0.51182
CC	315	5	GO:0000137	Golgi cis cisterna	0.294018
CC	158	13	GO:0031985	Golgi cisterna	0.446224
CC	110	7	GO:0000138	Golgi trans cisterna	0.698628
CC	87	27	GO:0000123	histone acetyltransferase complex	0.51182
CC	-54	19	GO:0000118	histone deacetylase complex	0.78676

CC	2	4	GO:0000836	Hrd1p ubiquitin ligase complex	0.992468
CC	-146	4	GO:0001772	immunological synapse	0.698628
CC	-398	5	GO:0031301	integral component of organelle membrane	0.233027
CC	-99	110	GO:0099080	integral component of plasma membrane	0.183414
CC	78	119	GO:0140535	intracellular protein-containing complex	0.240349
CC	**-260**	**41**	**GO:0000776**	**kinetochore**	**0.011395**
CC	318	6	GO:0002177	manchette	0.247884
CC	-374	4	GO:0016592	mediator complex	0.278232
CC	**-194**	**68**	**GO:0098796**	**membrane protein complex**	**0.011395**
CC	151	13	GO:0005777	microbody	0.454647
CC	70	9	GO:0005874	microtubule	0.79939
CC	336	4	GO:0005875	microtubule associated complex	0.319948
CC	-42	23	GO:0005813	microtubule organizing center	0.812648
CC	-277	7	GO:0005759	mitochondrial matrix	0.279339
CC	-79	53	GO:0019866	mitochondrial membrane	0.446224
CC	-155	13	GO:0005741	mitochondrial outer membrane	0.446224
CC	**-371**	**34**	**GO:0098800**	**mitochondrial protein-containing complex**	**0.000191**
CC	-109	135	GO:0005739	mitochondrion	0.08464
CC	-82	146	GO:0043232	non-membrane-bounded organelle	0.201803
CC	17	5	GO:0005643	nuclear pore	0.979233
CC	-110	99	GO:0140513	nuclear protein-containing complex	0.146082
CC	-216	29	GO:0005730	nucleolus	0.088558
CC	89	84	GO:0005654	nucleoplasm	0.247855
CC	71	4	GO:0000109	nucleotide-excision repair complex	0.913472
CC	26	12	GO:0005623	obsolete cell	0.941936
CC	30	14	GO:0005635	organelle envelope	0.941936
CC	157	8	GO:0031970	organelle envelope lumen	0.51182
CC	-88	27	GO:0043233	organelle lumen	0.51182
CC	-378	6	GO:0098799	outer mitochondrial membrane protein complex	0.216375
CC	-80	34	GO:1905368	peptidase complex	0.51182
CC	296	5	GO:0000242	pericentriolar material	0.323772

CC	80	17	GO:0000779	phagocytic cup	0.661181
CC	-11	21	GO:0000793	photoreceptor inner segment	0.979233
CC	159	9	GO:0001750	photoreceptor outer segment	0.51182
CC	**159**	**100**	**GO:0005886**	**plasma membrane**	**0.011395**
CC	222	36	GO:0001726	plasma membrane bounded cell projection	0.053045
CC	**523**	**9**	**GO:0002102**	**podosome**	**0.011395**
CC	-110	19	GO:0000502	proteasome complex	0.51182
CC	287	6	GO:0000164	protein phosphatase type 1 complex	0.294018
CC	178	6	GO:0000159	protein phosphatase type 2A complex	0.515959
CC	233	12	GO:0008287	protein serine/threonine phosphatase complex	0.240349
CC	66	64	GO:0099512	protein-DNA complex	0.486956
CC	-382	5	GO:0033177	proton-transporting two-sector ATPase complex	
CC	-207	7	GO:0033178	proton-transporting two-sector ATPase complex	
CC	-316	14	GO:0098803	respiratory chain complex	0.088558
CC	-260	10	GO:0005747	respiratory chain complex I	0.240349
CC	-231	14	GO:1990904	ribonucleoprotein complex	0.240349
CC	161	6	GO:0090576	RNA polymerase III transcription regulator complex	0.572014
CC	114	11	GO:0000124	SAGA complex	0.591687
CC	-297	7	GO:0005681	spliceosomal complex	0.247855
CC	240	12	GO:0001725	stress fiber	0.240349
CC	-55	15	GO:0005667	transcription regulator complex	0.79939
CC	-46	5	GO:1902554	transferase complex	
CC	7	10	GO:0005802	trans-Golgi network	0.981437
CC	122	54	GO:0000151	ubiquitin ligase complex	0.233027
CC	13	41	GO:0098852	vacuolar membrane	0.941936
CC	16	27	GO:0000323	vacuole	0.941936
CC	163	52	GO:0031410	vesicle	0.088558
CC	-18	11	GO:0000145	vesicle tethering complex	0.972527
CC	265	3	GO:0019012	virion	0.51182
MF	-28	6	GO:0016706	2-oxoglutarate-dependent dioxygenase activity	0.973487

MF	-237	5	GO:0003899	5'-3' RNA polymerase activity	0.855211
MF	-306	4	GO:0003988	acetyl-CoA C-acyltransferase activity	0.821499
MF	101	14	GO:0016407	acetyltransferase activity	0.921163
MF	-629	9	GO:0003993	acid phosphatase activity	0.212146
MF	65	32	GO:0022853	active transmembrane transporter activity	0.921163
MF	6	978	GO:0016788	adenyl nucleotide binding	0.965643
MF	-653	7	GO:0070566	adenylyltransferase activity	0.267862
MF	6	162	GO:0015179	adrenergic receptor activity	0.973487
MF	-731	4	GO:0004032	aldo-keto reductase (NADP) activity	0.383826
MF	219	32	GO:0033218	amide binding	0.469436
MF	-394	14	GO:0004177	aminopeptidase activity	0.383826
MF	22	61	GO:0008509	anion transmembrane transporter activity	0.965643
MF	210	6	GO:0001671	ATPase activator activity	0.855211
MF	-113	14	GO:0016887	ATPase activity	0.908846
MF	102	10	GO:0060590	ATPase regulator activity	0.954641
MF	373	11	GO:0000993	basal RNA polymerase II transcription machinery binding	0.469436
MF	-48	6	GO:0005227	calcium activated cation channel activity	0.965643
MF	91	408	GO:0000981	calcium ion binding	0.267862
MF	45	5	GO:0004198	calcium-dependent cysteine-type endopeptidase activity	0.965643
MF	-98	5	GO:0005544	calcium-dependent phospholipid binding	0.965643
MF	229	10	GO:0005516	calmodulin binding	0.765322
MF	449	8	GO:0004683	calmodulin-dependent protein kinase activity	0.469436
MF	-138	8	GO:0019200	carbohydrate kinase activity	0.921163
MF	355	5	GO:0015144	carbohydrate transmembrane transporter activity	0.711972
MF	-70	20	GO:0016831	carbon-carbon lyase activity	0.954641
MF	477	4	GO:0016884	carbon-nitrogen ligase activity	
MF	51	5	GO:0016840	carbon-nitrogen lyase activity	0.965643
MF	-580	19	GO:0140097	catalytic activity	
MF	-205	52	GO:0140098	catalytic activity	
MF	-37	21	GO:0140101	catalytic activity	
MF	126	61	GO:0000978	cis-regulatory region sequence-specific DNA binding	0.627982

MF	-74	5	GO:0009975	cyclase activity	0.965643
MF	796	7	GO:0004112	cyclic-nucleotide phosphodiesterase activity	0.149556
MF	775	5	GO:0004869	cysteine-type endopeptidase inhibitor activity	0.267862
MF	-106	27	GO:0004197	cysteine-type peptidase activity	0.855211
MF	-867	5	GO:0005125	cytokine activity	0.197316
MF	**515**	**65**	**GO:0003779**	**cytoskeletal protein binding**	**0.000991**
MF	-378	8	GO:0003684	damaged DNA binding	0.580341
MF	-271	12	GO:0051213	dioxygenase activity	0.627982
MF	337	10	GO:0140297	DNA-binding transcription factor binding	0.580341
MF	-346	4	GO:0004952	dopamine neurotransmitter receptor activity	0.777975
MF	-47	124	GO:1990837	double-stranded DNA binding	0.855211
MF	-12	5	GO:0003725	double-stranded RNA binding	0.978652
MF	-134	10	GO:0004129	electron transfer activity	0.908846
MF	382	6	GO:0000014	endodeoxyribonuclease activity	0.627982
MF	328	59	GO:0008047	enzyme activator activity	0.07869
MF	258	32	GO:0019899	enzyme binding	0.383826
MF	155	34	GO:0004857	enzyme inhibitor activity	0.638377
MF	-62	23	GO:0004540	exonuclease activity	0.958212
MF	-407	34	GO:0008238	exopeptidase activity	0.095321
MF	413	11	GO:0000062	fatty-acyl-CoA binding	0.434508
MF	-554	5	GO:0000400	four-way junction DNA binding	0.469436
MF	-65	6	GO:0001640	G protein-coupled glutamate receptor activity	0.965643
MF	-460	7	GO:0004890	GABA-A receptor activity	0.476838
MF	-323	65	GO:0016863	galactosidase activity	0.070119
MF	-939	4	GO:0015926	glucosidase activity	0.212146
MF	-49	4	GO:0046527	glucosyltransferase activity	0.965643
MF	-788	9	GO:0004364	glutathione transferase activity	0.095321
MF	151	8	GO:0005104	growth factor receptor binding	0.908846
MF	**836**	**20**	**GO:0005085**	**guanyl-nucleotide exchange factor activity**	**0.00399**
MF	-238	45	GO:0004553	hydrolase activity	

MF	-978	7	GO:0016799	hydrolase activity	
MF	-452	21	GO:0016811	hydrolase activity	
MF	-609	6	GO:0016814	hydrolase activity	
MF	219	157	GO:0017111	hydrolase activity	
MF	-553	17	GO:0016836	hydro-lyase activity	0.10914
MF	136	22	GO:0005254	inorganic anion transmembrane transporter activity	0.814586
MF	145	7	GO:0005229	intracellular calcium activated chloride channel activity	0.921163
MF	-559	12	GO:0003756	intramolecular oxidoreductase activity	
MF	-757	5	GO:0016861	intramolecular oxidoreductase activity	
MF	-34	14	GO:0022839	ion gated channel activity	0.965643
MF	**-517**	**34**	**GO:0016860**	**isomerase activity**	**0.038546**
MF	654	4	GO:0004860	kinase inhibitor activity	0.465489
MF	63	21	GO:0030594	ligand-gated ion channel activity	0.958323
MF	18	32	GO:0016874	ligase activity	0.965643
MF	-212	6	GO:0004812	ligase activity	
MF	205	9	GO:0016405	ligase activity	
MF	-394	6	GO:0016421	ligase activity	
MF	411	9	GO:0016879	ligase activity	
MF	109	47	GO:0052689	lipase activity	0.759142
MF	801	8	GO:0004622	lysophospholipase activity	0.109669
MF	-477	4	GO:0005384	manganese ion transmembrane transporter activity	0.627982
MF	816	8	GO:0004559	mannosidase activity	0.103424
MF	-109	20	GO:0000030	mannosyltransferase activity	0.866951
MF	443	8	GO:0004181	metallocarboxypeptidase activity	0.469436
MF	**1202**	**7**	**GO:0000146**	**microfilament motor activity**	**0.022927**
MF	**719**	**26**	**GO:0003777**	**microtubule motor activity**	**0.00399**
MF	392	14	GO:0072341	modified amino acid binding	0.383826
MF	-15	5	GO:0140104	molecular carrier activity	0.977919
MF	223	173	GO:0030234	molecular function regulator	0.051478
MF	-42	46	GO:0004497	monooxygenase activity	0.958323
MF	**653**	**52**	**GO:0003774**	**motor activity**	**8.94E-05**

MF	-172	6	GO:0003730	mRNA 3'-UTR binding	0.908846
MF	-359	14	GO:0003729	mRNA binding	0.450651
MF	29	9	GO:0008080	N-acetyltransferase activity	0.970314
MF	669	6	GO:0003951	NAD+ kinase activity	0.307941
MF	-250	5	GO:0003954	NADH dehydrogenase activity	0.855211
MF	574	5	GO:0005042	netrin receptor activity	0.469436
MF	437	5	GO:0005328	neurotransmitter:sodium symporter activity	0.627982
MF	-821	9	GO:0008170	N-methyltransferase activity	0.083266
MF	-398	24	GO:0016776	nucleobase-containing compound kinase activity	0.197316
MF	65	9	GO:0015932	nucleobase-containing compound transmembrane transporter activity	0.965643
MF	10	25	GO:0001882	nucleoside binding	0.977919
MF	-382	6	GO:0004550	nucleoside diphosphate kinase activity	0.627982
MF	-1042	7	GO:0019206	nucleoside kinase activity	0.055174
MF	**398**	**87**	**GO:0060589**	**nucleoside-triphosphatase regulator activity**	**0.00399**
MF	-272	4	GO:0005338	nucleotide-sugar transmembrane transporter activity	0.855211
MF	-262	21	GO:0016779	nucleotidyltransferase activity	0.487111
MF	46	12	GO:0016411	O-acyltransferase activity	0.965643
MF	-140	223	GO:0016491	oxidoreductase activity	0.172109
MF	-206	39	GO:0016616	oxidoreductase activity	
MF	-220	8	GO:0016620	oxidoreductase activity	
MF	-12	18	GO:0016627	oxidoreductase activity	
MF	50	6	GO:0016634	oxidoreductase activity	
MF	121	9	GO:0016638	oxidoreductase activity	
MF	20	5	GO:0016641	oxidoreductase activity	
MF	-43	10	GO:0016646	oxidoreductase activity	
MF	9	19	GO:0016651	oxidoreductase activity	
MF	484	8	GO:0016653	oxidoreductase activity	
MF	397	5	GO:0016667	oxidoreductase activity	
MF	-512	6	GO:0016702	oxidoreductase activity	
MF	-31	12	GO:0016903	oxidoreductase activity	

MF	651	7	GO:0002039	p53 binding	0.267862
MF	156	18	GO:0004866	peptidase inhibitor activity	0.797691
MF	-398	5	GO:0034212	peptide N-acetyltransferase activity	0.638377
MF	-398	5	GO:0003755	peptidyl-prolyl cis-trans isomerase activity	0.638377
MF	-172	9	GO:0035091	phosphatidylinositol binding	0.855211
MF	728	7	GO:0052866	phosphatidylinositol phosphate phosphatase activity	0.197316
MF	1077	5	GO:0004438	phosphatidylinositol-3-phosphatase activity	0.094142
MF	-469	5	GO:0005546	phosphatidylinositol-4	
MF	597	6	GO:0001786	phosphatidylserine binding	0.383826
MF	-486	5	GO:0004623	phospholipase A2 activity	0.578732
MF	59	27	GO:0005543	phospholipid binding	0.955282
MF	692	15	GO:0008081	phosphoric diester hydrolase activity	0.058511
MF	261	84	GO:0016791	phosphoric ester hydrolase activity	0.095321
MF	-40	6	GO:0016780	phosphotransferase activity	
MF	-368	9	GO:0004659	prenyltransferase activity	0.568982
MF	-142	14	GO:0002020	protease binding	0.855211
MF	-252	7	GO:0051998	protein methyltransferase activity	0.797678
MF	251	8	GO:0004864	protein phosphatase inhibitor activity	0.772631
MF	408	4	GO:0001784	protein phosphorylated amino acid binding	0.695243
MF	-120	5	GO:0008318	protein prenyltransferase activity	0.959015
MF	566	13	GO:0004722	protein serine/threonine phosphatase activity	0.168563
MF	45	7	GO:0030674	protein-macromolecule adaptor activity	0.965643
MF	-222	16	GO:0015078	proton transmembrane transporter activity	0.638377
MF	-908	4	GO:0016857	racemase and epimerase activity	0.241343
MF	-235	89	GO:0000048	receptor ligand activity	0.125384
MF	-79	300	GO:0003723	RNA binding	0.465489
MF	51	7	GO:0000339	RNA cap binding	0.965643
MF	-540	8	GO:0008173	RNA methyltransferase activity	0.377687
MF	592	14	GO:0043175	RNA polymerase core enzyme binding	0.122102
MF	337	7	GO:0001103	RNA polymerase II-specific DNA-binding transcription factor binding	0.638377
MF	**-637**	**21**	**GO:0008757**	**S-adenosylmethionine-dependent methyltransferase activity**	**0.047308**

MF	-78	11	GO:0004867	serine-type endopeptidase inhibitor activity	0.963024
MF	-700	13	GO:0003697	single-stranded DNA binding	0.076687
MF	455	5	GO:0003727	single-stranded RNA binding	0.613139
MF	-210	21	GO:0001614	sodium:phosphate symporter activity	0.627982
MF	-252	4	GO:0015295	solute:proton symporter activity	0.855211
MF	-345	6	GO:0033764	steroid dehydrogenase activity	0.673276
MF	-84	6	GO:0005200	structural constituent of cytoskeleton	0.965643
MF	**-704**	**77**	**GO:0003735**	**structural constituent of ribosome**	**2.88E-08**
MF	420	18	GO:0004843	thiol-dependent ubiquitin-specific protease activity	0.257205
MF	-1102	6	GO:0004800	thyroxine 5'-deiodinase activity	0.058511
MF	-63	13	GO:0008483	transaminase activity	0.965643
MF	187	14	GO:0003713	transcription coactivator activity	0.777975
MF	56	44	GO:0003712	transcription coregulator activity	0.921163
MF	173	12	GO:0003714	transcription corepressor activity	0.827695
MF	81	15	GO:0008134	transcription factor binding	0.954641
MF	-466	36	GO:0008168	transferase activity	
MF	-114	41	GO:0016746	transferase activity	
MF	20	424	GO:0016758	transferase activity	
MF	-574	24	GO:0016765	transferase activity	
MF	102	4	GO:0046912	transferase activity	
MF	-358	15	GO:0046915	transition metal ion transmembrane transporter activity	0.432983
MF	-321	11	GO:0003746	translation elongation factor activity	0.580341
MF	-55	9	GO:0003743	translation initiation factor activity	0.965643
MF	-199	25	GO:0090079	translation regulator activity	
MF	37	196	GO:0008324	transmembrane transporter activity	0.855211
MF	668	7	GO:0004806	triglyceride lipase activity	0.259208
MF	-358	43	GO:0000049	tRNA binding	0.098685
MF	131	294	GO:0004518	ubiquitin-like protein transferase activity	0.138002
MF	123	146	GO:0004519	UDP-glycosyltransferase activity	0.383826
MF	531	6	GO:0005247	voltage-gated anion channel activity	0.465489

MF	-74	14	GO:0008270	zinc ion binding	0.958323
MF	-55	6	GO:0005385	zinc ion transmembrane transporter activity	0.965643

Supplementary Table C.23 Differentially expressed genes between highly tolerant individuals (high ED50) and low tolerant individuals (low ED50) in the heated treatment.

Uniprot	baseMean	L2FC	padj	Direction	Gene name	Protein Name
E7FAM5	8.06	-7.01	0.002	Down	trim71 lin41	E3 ubiquitin-protein ligase TRIM71 (EC 2.3.2.27) (Protein lin-41 homolog) (RING-type E3 ubiquitin transferase TRIM71) (Tripartite motif-containing protein 71)
F6QEU4	15.74	-4.78	0.003	Down	trim71 lin41	E3 ubiquitin-protein ligase TRIM71 (EC 2.3.2.27) (Protein lin-41 homolog) (RING-type E3 ubiquitin transferase TRIM71) (Tripartite motif-containing protein 71)
Q7RTR2	40.82	-17.79	0.015	Down	NLRC3 NOD3	NLR family CARD domain-containing protein 3 (CARD15-like protein) (Caterpiller protein 16.2) (CLR16.2) (NACHT, LRR and CARD domains-containing protein 3) (Nucleotide-binding oligomerization domain protein 3)
Q54H46	89.59	-22.87	0.000	Down	drkA rk1 vsk1 DDB_G0289791	Probable serine/threonine-protein kinase drkA (EC 2.7.11.1) (Receptor-like kinase 1) (Receptor-like kinase A) (Vesicle-associated receptor tyrosine kinase-like protein 1)
Q9M2U3	19.73	-17.51	0.008	Down	At3g55350 T22E16.10	Protein ALP1-like (EC 3.1.-.-)
P15043	55.42	21.90	0.000	Up	recQ b3822 JW5855	ATP-dependent DNA helicase RecQ (EC 3.6.4.12)
Q3URF8	114.57	9.87	0.000	Up	Kctd21	BTB/POZ domain-containing protein KCTD21 (KCASH2 protein) (Potassium channel tetramerization domain-containing protein 21)
Q6DG99	9.66	18.87	0.005	Up	kctd6 zgc:91884	BTB/POZ domain-containing protein KCTD6
P12263	125.17	21.03	0.000	Up	F8 CF8	Coagulation factor VIII (Procoagulant component)
B1VEI4	32.79	19.26	0.003	Up	mshA cu0213	D-inositol 3-phosphate glycosyltransferase (EC 2.4.1.250) (N-acetylglucosamine-inositol-phosphate N-acetylglucosaminyltransferase) (GlcNAc-Ins-P N-acetylglucosaminyltransferase)
C7Q4Y6	71.32	19.90	0.000	Up	mshA1 Caci_5074	D-inositol 3-phosphate glycosyltransferase 1 (EC 2.4.1.250) (N-acetylglucosamine-inositol-phosphate N-acetylglucosaminyltransferase 1) (GlcNAc-Ins-P N-acetylglucosaminyltransferase 1)
Q4VSN2	151.64	6.36	0.004	Up	dstyk ripk5	Dual serine/threonine and tyrosine protein kinase (EC 2.7.12.1) (Dusty protein kinase) (Dusty PK) (Receptor-interacting serine/threonine-protein kinase 5)
Q5R9T9	20.54	20.59	0.001	Up	GBP6	Guanylate-binding protein 6 (GTP-binding protein 6) (GBP-6) (Guanine nucleotide-binding protein 6)
Q0VD26	38.64	5.44	0.019	Up	MORN4	MORN repeat-containing protein 4 (Retinophilin)
P31646	38.44	21.26	0.000	Up	Slc6a13 Gabt2 Gat-2	Sodium- and chloride-dependent GABA transporter 2 (GAT-2) (Solute carrier family 6 member 13)
Q9VBW3	26.78	19.43	0.000	Up	Cad96Ca HD-14 CG10244	Tyrosine kinase receptor Cad96Ca (EC 2.7.10.1) (Cadherin-96Ca) (Tyrosine kinase receptor HD-14)

Supplementary Table C. 24 Differentially expressed genes between highly tolerant individuals (high ED50) and low tolerant individuals (low ED50) in the ambient treatment.

Uniprot	baseMean	L2FC	padj	Direction	Gene name	Protein Name
Q95P04	1878.17	-5.91	0.001	Down	NA	GFP-like non-fluorescent chromoprotein (gtCP)
Q95P04	2107.44	-6.82	0.001	Down	NA	GFP-like non-fluorescent chromoprotein (gtCP)
C0H694	14.78	-19.04	0.008	Down	NA	Small cysteine-rich protein 1 2 (Mcap-SCRiP1b) (SCRiP1b)
A6QLU6	36.42	20.94	0.001	Up	ADGRD1 GPR133	Adhesion G-protein coupled receptor D1 (G-protein coupled receptor 133)
O50224	26.14	21.18	0.001	Up	recG	ATP-dependent DNA helicase RecG (EC 3.6.4.12)
P12263	66.31	22.22	0.000	Up	F8 CF8	Coagulation factor VIII (Procoagulant component)
Q7T312	10.00	18.56	0.016	Up	ccdc25 zgc:64173	Coiled-coil domain-containing protein 25
Q9NXS3	88.15	22.42	0.000	Up	KLHL28 BTBD5	Kelch-like protein 28 (BTB/POZ domain-containing protein 5)
P31646	21.81	19.60	0.005	Up	Slc6a13 Gabt2 Gat-2	Sodium- and chloride-dependent GABA transporter 2 (GAT-2) (Solute carrier family 6 member 13)

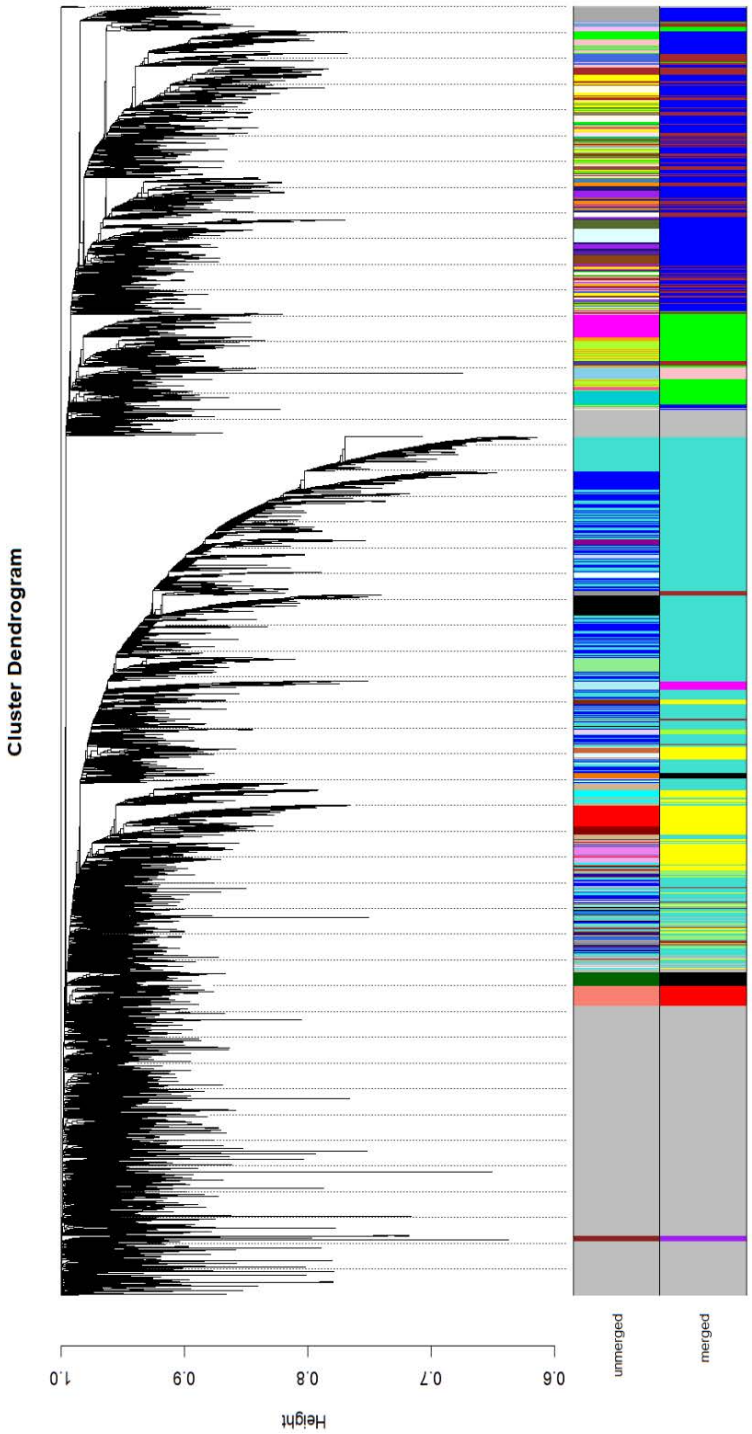

Supplementary Figure C. 25 WGCNA-assigned modules.

Supplementary Table C. 26 Number of genes per WGCNA-module. Listed by module colour name, the number of genes associated with each module, the number of associated genes with annotations, the correlation coefficient (-1 to 1) of the module eigengene to treatment, the significance level of correlation with respect to treatment, the correlation coefficient of the module eigengene to physiological maintenance and the significance level of correlation between module eigengene and physiological maintenance.

			Associated with treatment		**Associated with physiological maintenance**	
Module	**N genes**	**N genes w. annotation**	**Correlation coefficient**	**Significance level**	**Correlation coefficient**	**Significance level**
Black	170	NS	0.46		-0.01	
Blue	1953	1634	-0.7	***	-0.57	*
Brown	981	859	0.61	**	0.65	***
Green	713	616	-0.93	***	-0.21	
Green/yellow	38	NS	-0.26		0.36	
Grey	2939	NS	-0.24		0.5	*
Magenta	81	NS	0.08		-0.17	
Pink	112	89	0.75	***	-0.17	
Purple	43	NS	-0.14		-0.28	
Red	179	NS	0.24		0.19	
Turquoise	3534	NS	-0.26		0.4	
Yellow	901	841	0.54	*	-0.36	

Supplementary material C. 27 Rapid Light Curve (RLC) statistics

Ek (minimum saturating irradiance)

```
[1] "27"   "30"   "32"   "34"   "35.5"
             Df Sum Sq Mean Sq F value Pr(>F)
treatment     4 591496  147874   85.08 <2e-16 ***
Residuals   252 438005    1738
---
Signif. codes:  0 ‘***’ 0.001 ‘**’ 0.01 ‘*’ 0.05 ‘.’ 0.1 ‘ ’ 1
$emmeans
 treatment emmean   SE  df lower.CL upper.CL
 27         187.1 5.43 252      176      198
 30         174.3 5.62 252      163      185
 32         126.2 5.57 252      115      137
 34         132.6 6.29 252      120      145
 35.5        45.5 6.36 252       33       58
```

```
Confidence level used: 0.95

$contrasts
 contrast                    estimate   SE  df t.ratio p.value
 treatment27 - treatment30      12.81 7.81 252   1.639  0.4737
 treatment27 - treatment32      60.90 7.78 252   7.830  <.0001
 treatment27 - treatment34      54.44 8.30 252   6.556  <.0001
 treatment27 - treatment35.5   141.58 8.36 252  16.937  <.0001
 treatment30 - treatment32      48.09 7.91 252   6.076  <.0001
 treatment30 - treatment34      41.63 8.43 252   4.937  <.0001
 treatment30 - treatment35.5   128.77 8.49 252  15.173  <.0001
 treatment32 - treatment34      -6.46 8.40 252  -0.769  0.9392
 treatment32 - treatment35.5    80.68 8.45 252   9.544  <.0001
 treatment34 - treatment35.5    87.14 8.94 252   9.747  <.0001

P value adjustment: tukey method for comparing a family of 5 estimates

 treatment emmean   SE  df lower.CL upper.CL
 27         187.1 5.43 252      176      198
 30         174.3 5.62 252      163      185
 32         126.2 5.57 252      115      137
 34         132.6 6.29 252      120      145
 35.5        45.5 6.36 252       33       58

Confidence level used: 0.95
```

FqFm(max) (model predicted max photochemical efficiency of PSII)

```
             Df Sum Sq Mean Sq F value Pr(>F)
treatment     4  5.885   1.471   485.8 <2e-16 ***
Residuals   253  0.766   0.003
---
Signif. codes:  0 ‘***’ 0.001 ‘**’ 0.01 ‘*’ 0.05 ‘.’ 0.1 ‘ ’ 1
$emmeans
 treatment emmean      SE  df lower.CL upper.CL
 27         0.640 0.00716 253    0.626    0.654
 30         0.648 0.00742 253    0.634    0.663
 32         0.636 0.00735 253    0.622    0.651
 34         0.611 0.00830 253    0.595    0.627
 35.5       0.235 0.00830 253    0.219    0.251
```

```
Confidence level used: 0.95

$contrasts
 contrast                    estimate     SE  df t.ratio p.value
 treatment27 - treatment30   -0.00856 0.0103 253  -0.830  0.9213
 treatment27 - treatment32    0.00379 0.0103 253   0.369  0.9960
 treatment27 - treatment34    0.02884 0.0110 253   2.631  0.0679
 treatment27 - treatment35.5  0.40502 0.0110 253  36.950  <.0001
 treatment30 - treatment32    0.01235 0.0104 253   1.182  0.7617
 treatment30 - treatment34    0.03739 0.0111 253   3.359  0.0080
 treatment30 - treatment35.5  0.41357 0.0111 253  37.158  <.0001
 treatment32 - treatment34    0.02504 0.0111 253   2.259  0.1619
 treatment32 - treatment35.5  0.40123 0.0111 253  36.192  <.0001
 treatment34 - treatment35.5  0.37618 0.0117 253  32.064  <.0001

P value adjustment: tukey method for comparing a family of 5 estimates

 treatment emmean      SE  df lower.CL upper.CL
 27         0.640 0.00716 253    0.626    0.654
 30         0.648 0.00742 253    0.634    0.663
 32         0.636 0.00735 253    0.622    0.651
 34         0.611 0.00830 253    0.595    0.627
 35.5       0.235 0.00830 253    0.219    0.251

Confidence level used: 0.95
```

Supplementary material C.28 Correlations between physiological traits and ED50.

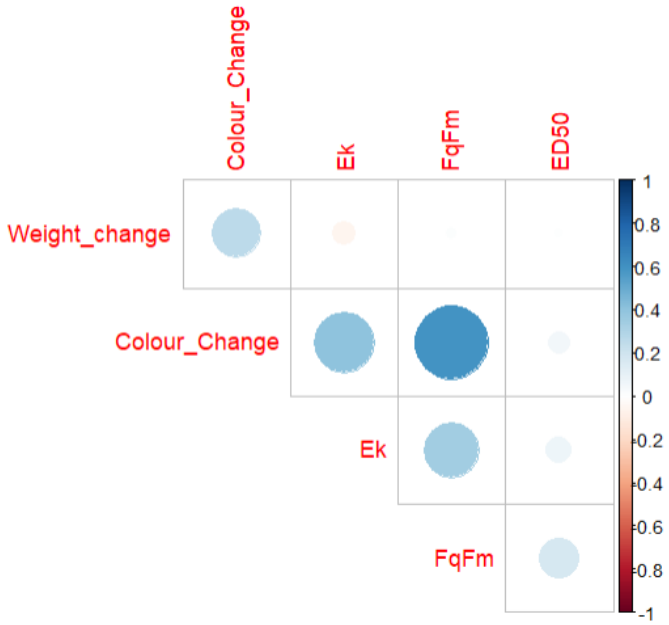

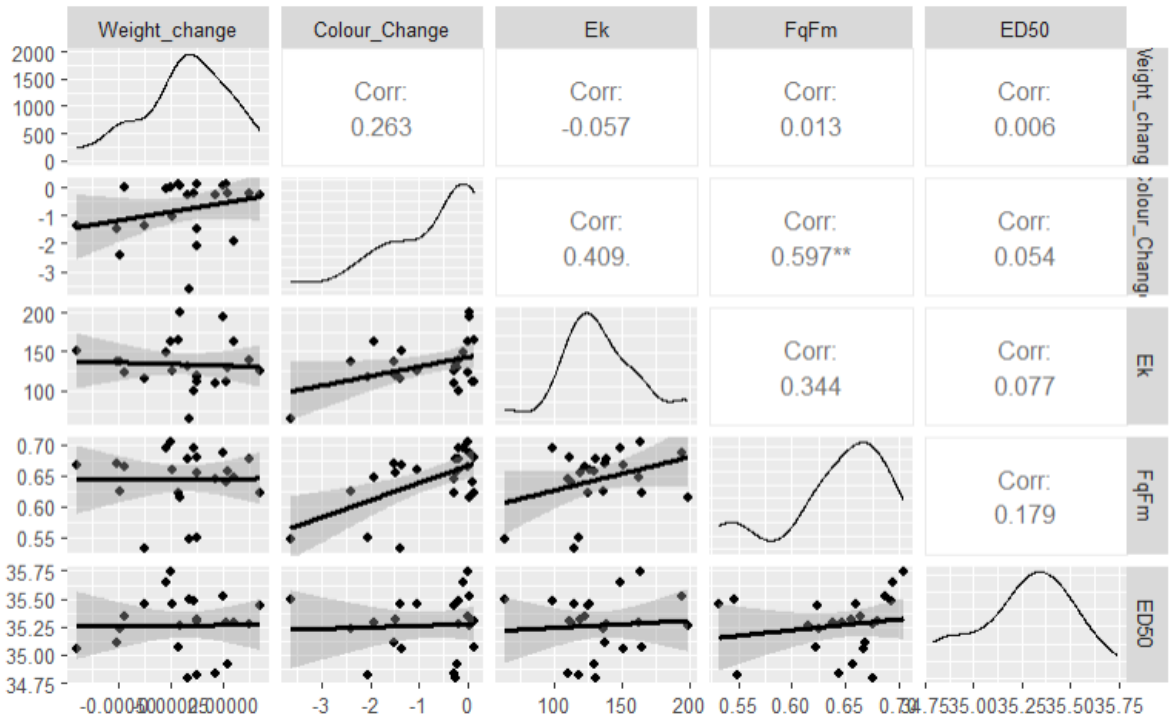

ED50 was not significantly correlated to any of the other four physiological trait rankings nor was ED50-derived colony rankings correlated to colony rankings in the other four traits.

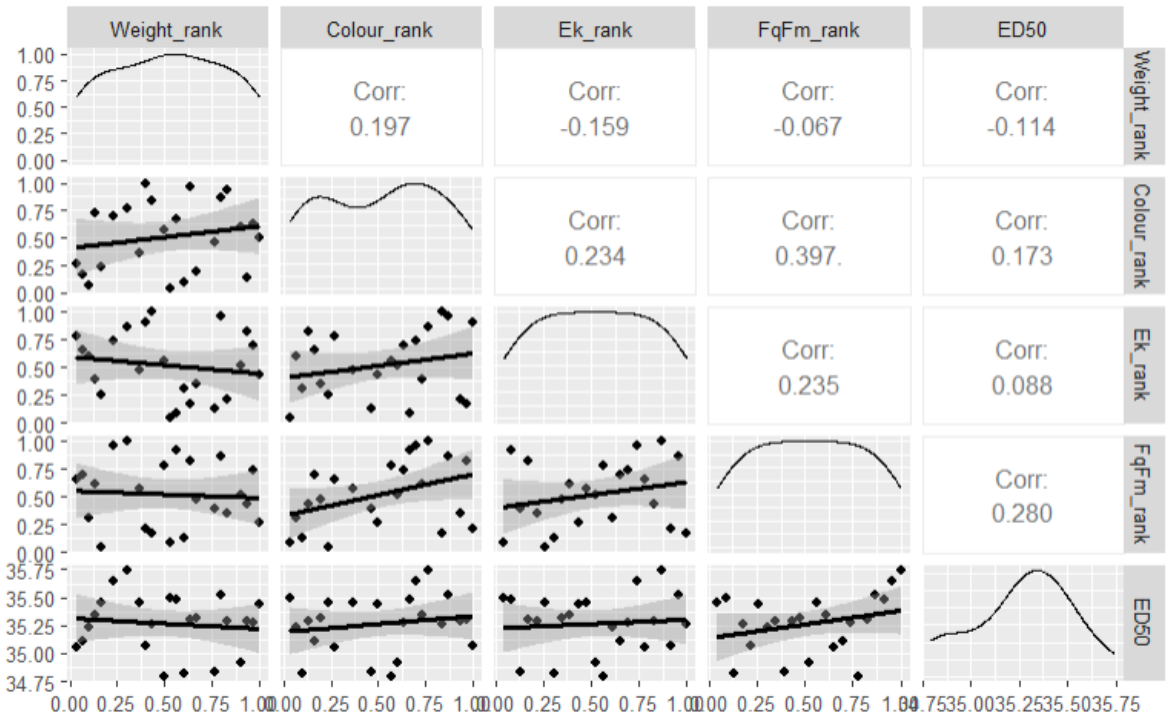
Weight_rank
Colour_rank
Ek_rank
FqFm_rank
ED50
Corr: 0.197
Corr: -0.159
Corr: -0.067
Corr: -0.114
Corr: 0.234
Corr: 0.397.
Corr: 0.173
Corr: 0.235
Corr: 0.088
Corr: 0.280

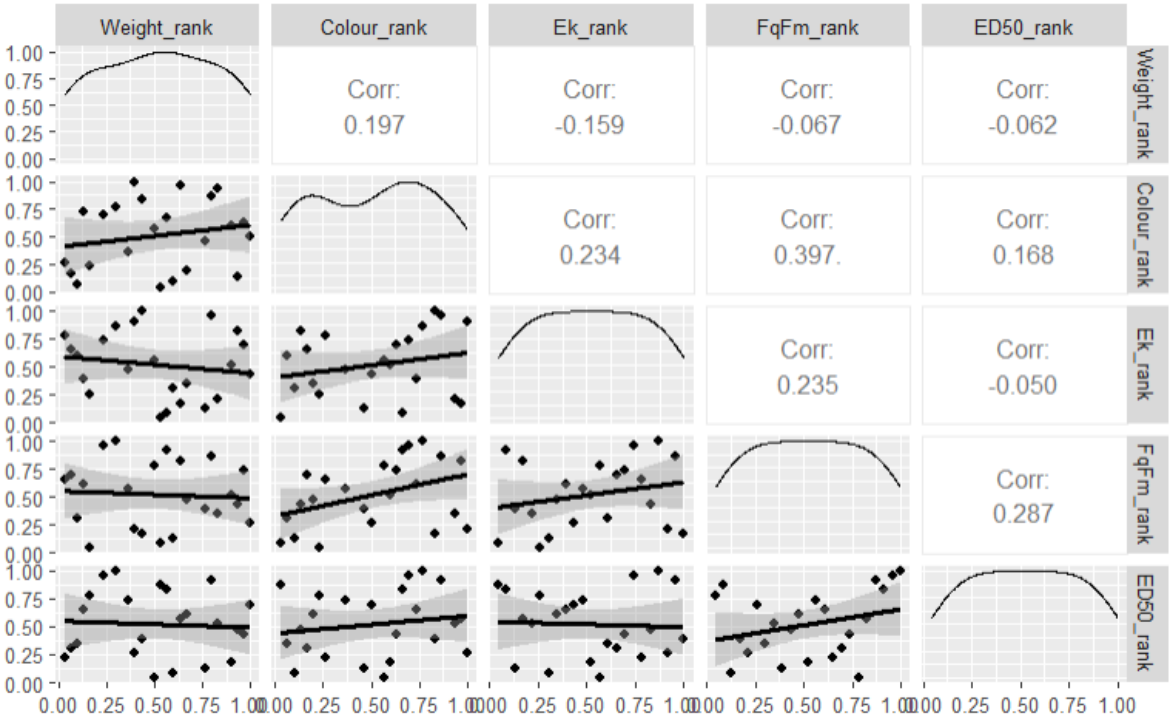
Weight_rank
Colour_rank
Ek_rank
FqFm_rank
ED50_rank
Corr: 0.197
Corr: -0.159
Corr: -0.067
Corr: -0.062
Corr: 0.234
Corr: 0.397.
Corr: 0.168
Corr: 0.235
Corr: -0.050
Corr: 0.287

Supplementary material C.29 ED50 curves by genotype. Top graph shows all genotypes together with the mean derived ED50 (35.27ºC) indicated by the vertical black line. The bottom graph shows each genotype in a separate panel.

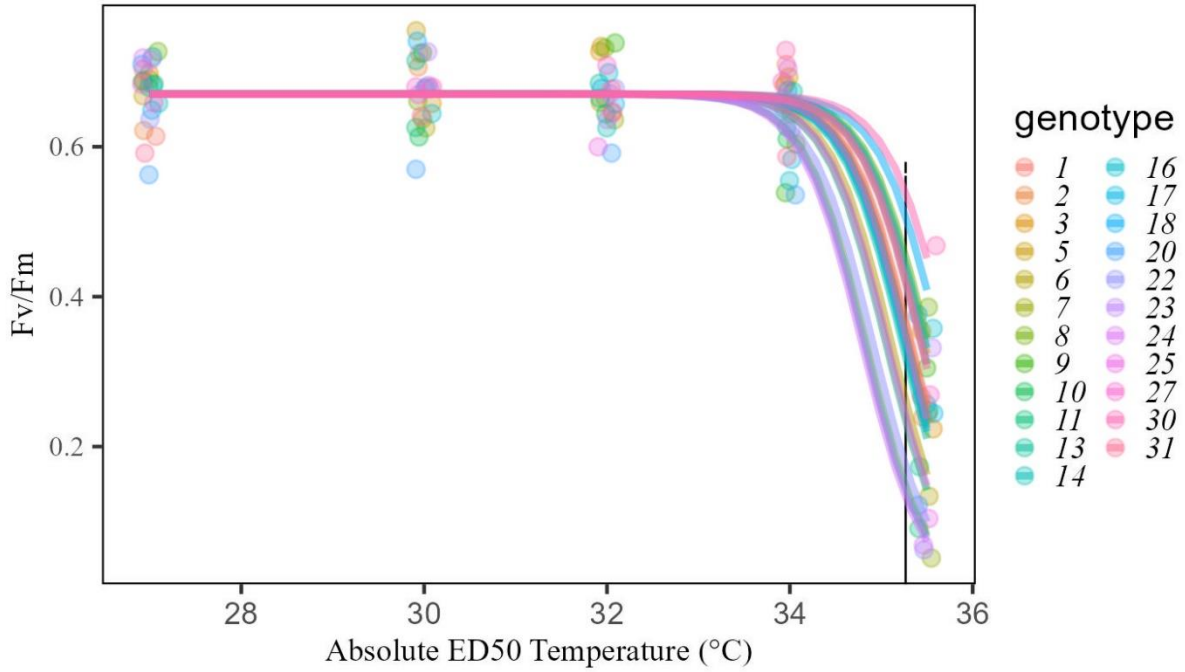

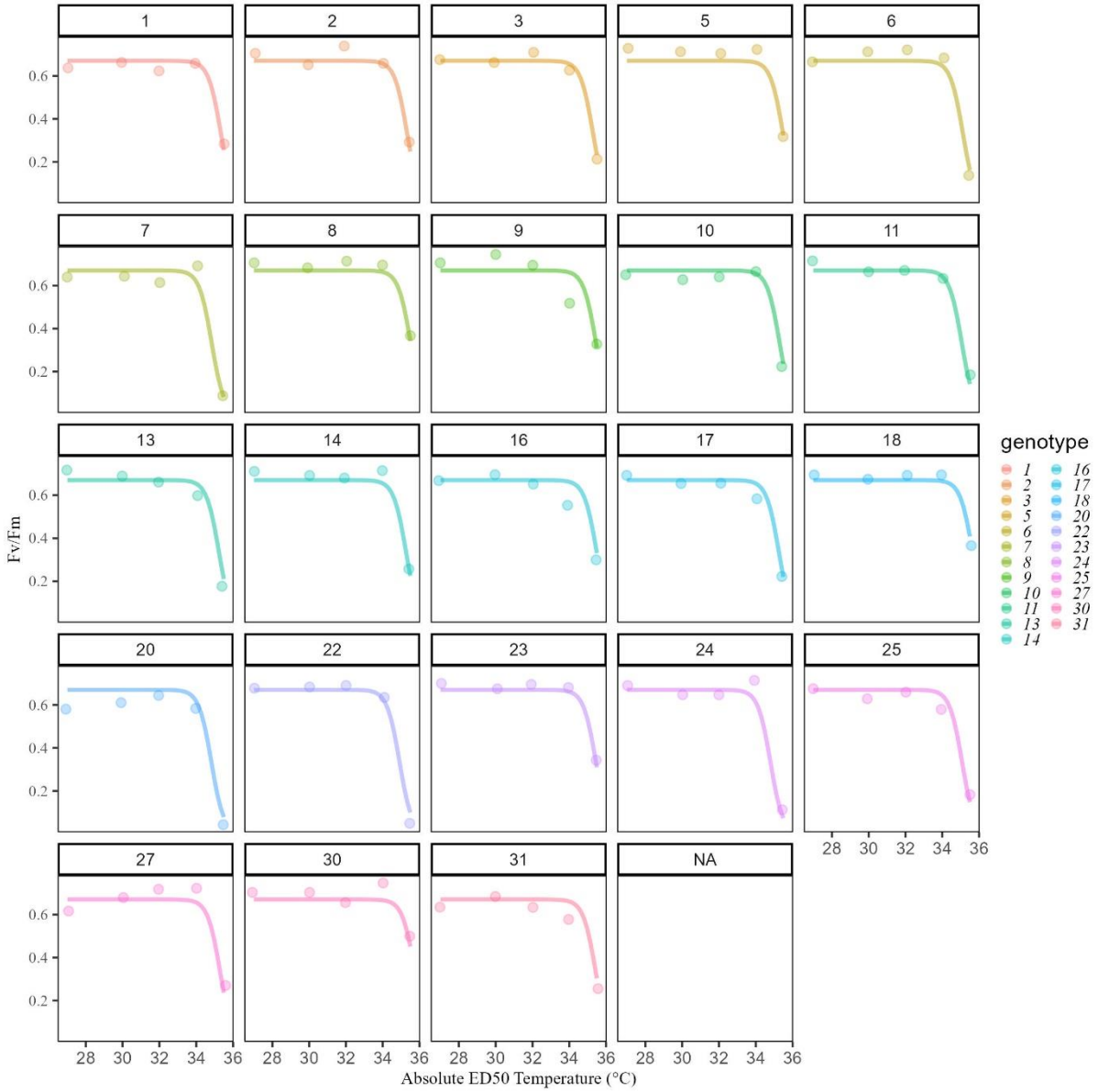
1
2
3
5
6
7
8
9
10
11
13
14
16
17
18
20
22
23
24
25
27
30
31
NA
Fv/Fm
0.6
0.4
0.2
28
30
32
34
36
Absolute ED50 Temperature (°C)
genotype
1
2
3
5
6
7
8
9
10
11
13
14
16
17
18
20
22
23
24
25
27
30
31

Supplementary material C.30 WGCNA with respect to ED50 category.

Sample G8 was identified as a significant outlying sample and therefore removed from the analysis.

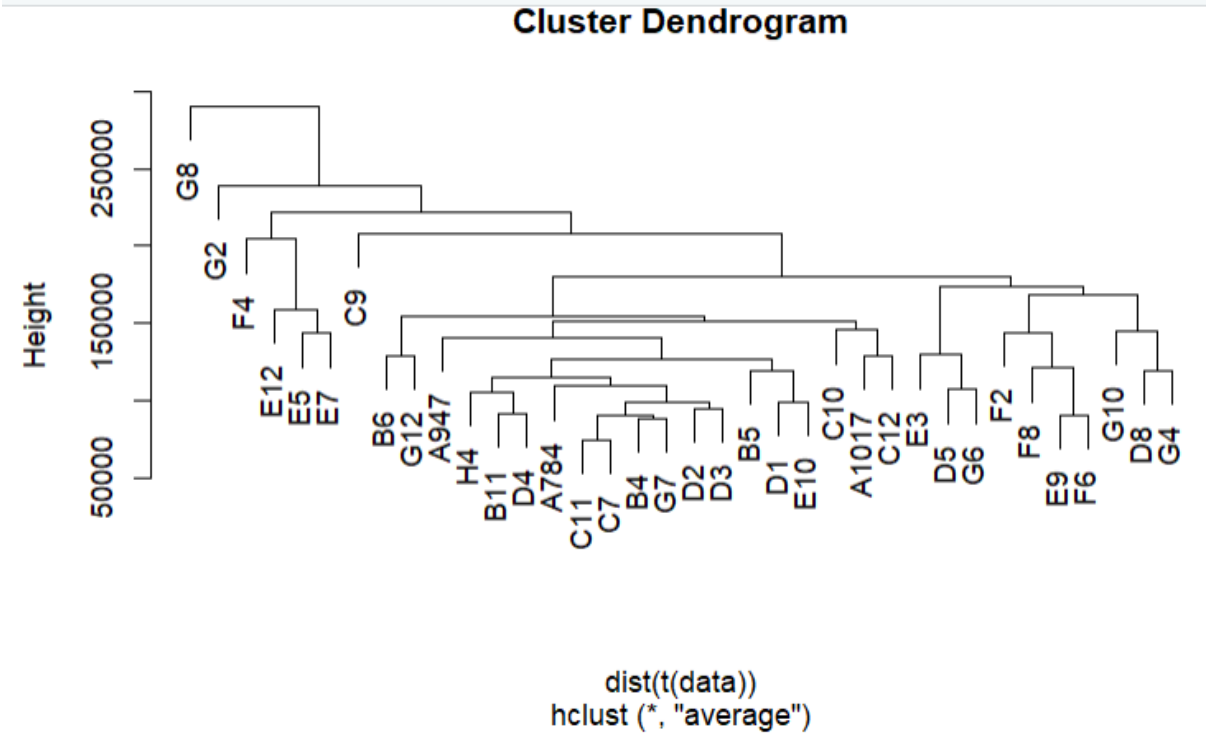

After sample exclusion:

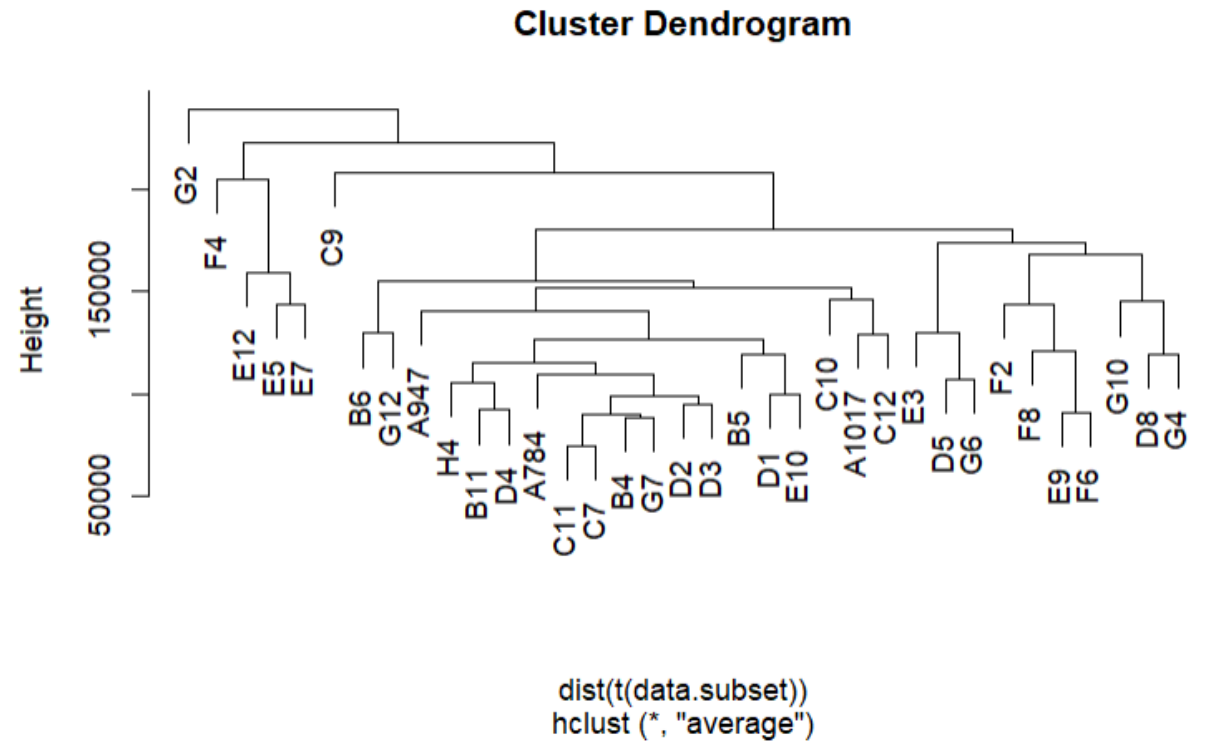

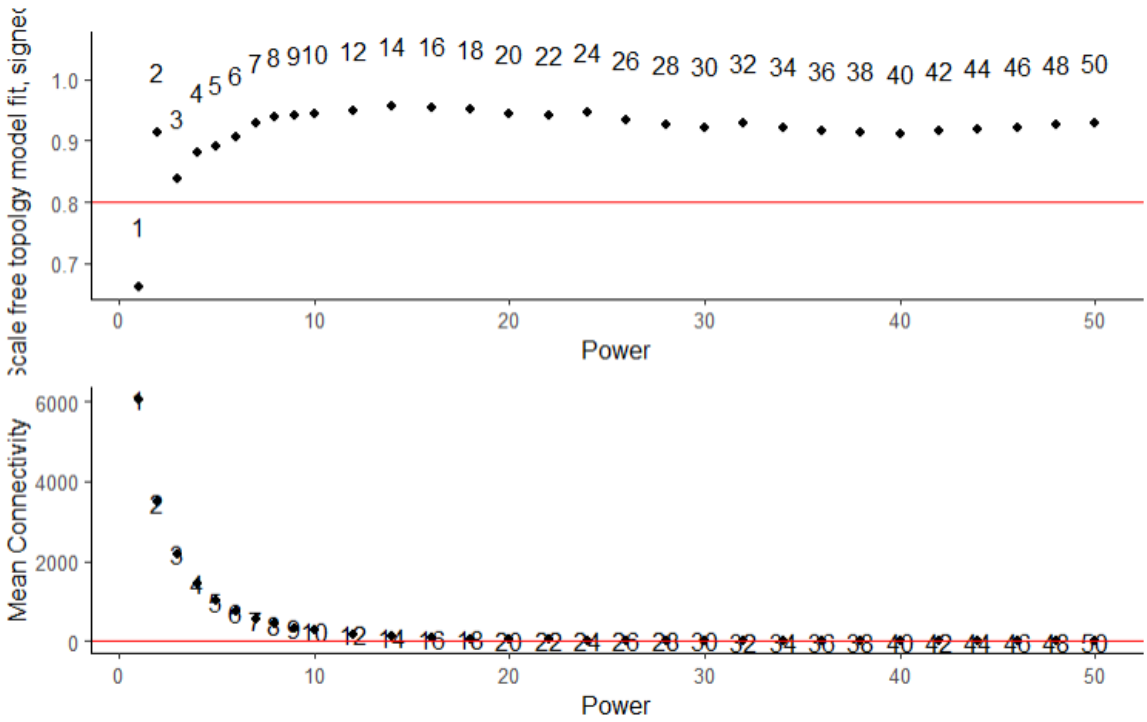
Scale free topolgy model fit, signed
1.0
0.9
0.8
0.7
0
10
20
30
40
50
Power
Mean Connectivity
6000
4000
2000
0
0
10
20
30
40
50
Power

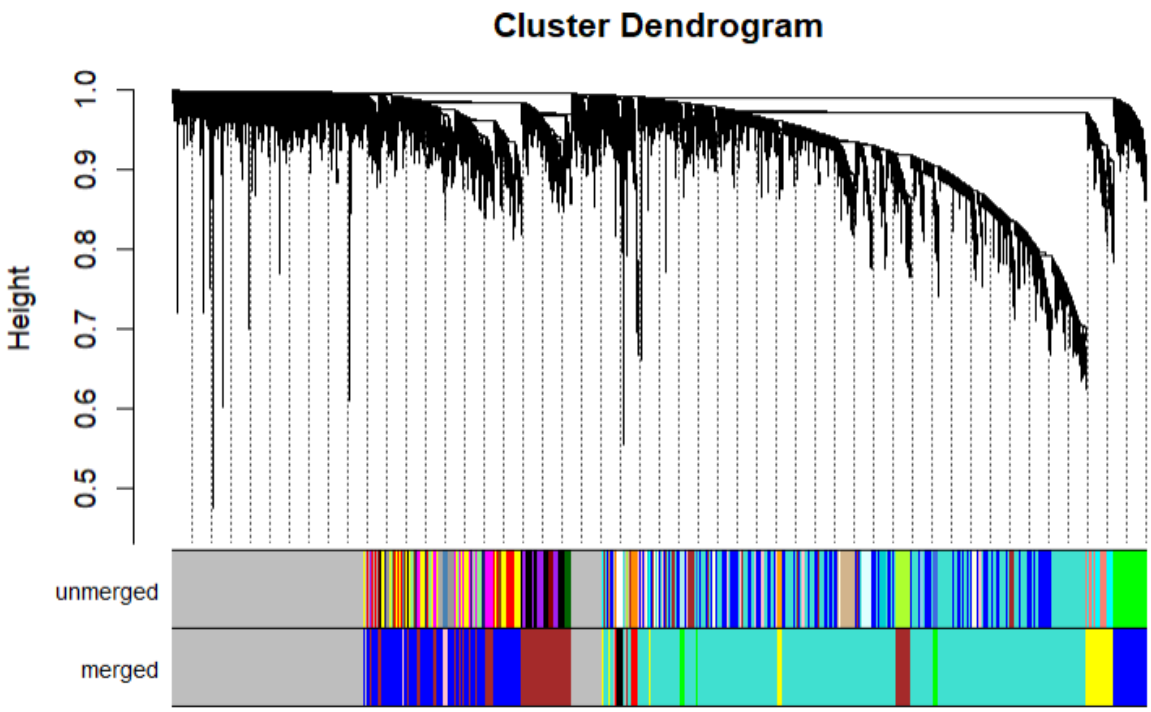

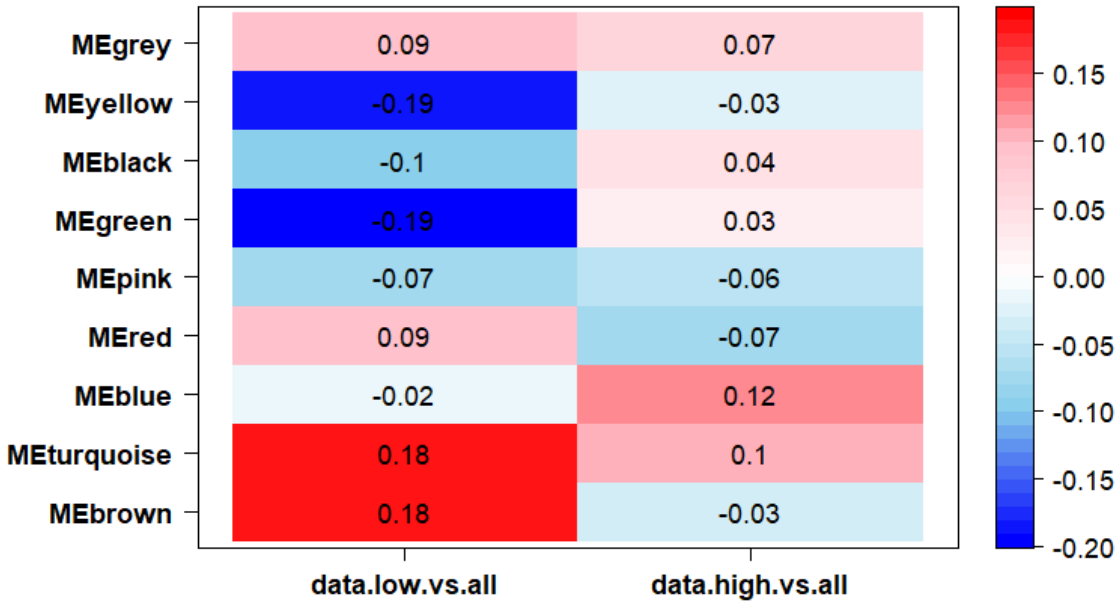

There were statistically significant co-expressed gene modules with respect to ED50 category.